

**Synthesis and Characterization of Copper Complexes
with Tridentate NNO and NNS Ligands and Their
Catalytic Applications in Oxidation and Cycloaddition
Reactions**

By

SUBRAT SETHI

CHEM11201804024

National Institute of Science Education and Research Bhubaneswar,

Odisha-752050

A thesis submitted to the

Board of Studies in Chemical Sciences

In partial fulfilment of requirements

for the Degree of

DOCTOR OF PHILOSOPHY

of

HOMI BHABHA NATIONAL INSTITUTE



May, 2023

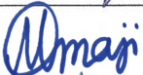
Homi Bhabha National Institute¹

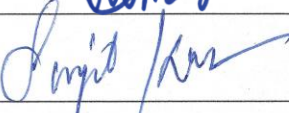
Recommendations of the Viva Voce Committee

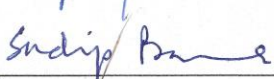
1. As members of the Viva Voce Committee, we certify that we have read the dissertation prepared by **Subrat Sethi** entitled “**Synthesis and characterization of Copper complexes with tridentate NNO and NNS ligands and their catalytic applications in oxidation and cycloaddition reactions**” and recommend that it may be accepted as fulfilling the thesis requirement for the award of Degree of Doctor of Philosophy.

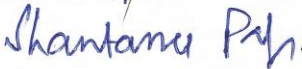
Chairman - Dr. Prasenjit Mal  Date: 05-01-2024

Guide / Convener - Dr. Bidraha Bagh  Date: 05/01/2024

Examiner – Prof. Modhu Sudan Maji  Date: 05.01.2024

Member 1- Dr. Sanjib Kar  Date: 05/01/2024

Member 2- Dr. Sudip Barman  Date: 05/01/2024,

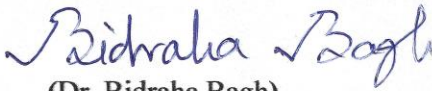
Member 3- Dr. Shantanu Pal  Date: 05/01/2024

Final approval and acceptance of this thesis is contingent upon the candidate's submission of the final copies of the thesis to HBNI.

I/We hereby certify that I/we have read this thesis prepared under my/our direction and recommend that it may be accepted as fulfilling the thesis requirement.

Date: 05/01/2024

Place: NISER


(Dr. Bidraha Bagh)

Guide

¹ This page is to be included only for final submission after successful completion of viva voce.

STATEMENT BY AUTHOR

This dissertation has been submitted in partial fulfilment of requirements for an advanced degree at Homi Bhabha National Institute (HBNI) and is deposited in the library to be made available to borrowers under rules of the HBNI.

Brief quotations from this dissertation are allowable without special permission, provided that accurate acknowledgement of source is made. Requests for permission for extended quotation from or reproduction of this manuscript in whole or in part may be granted by the Competent Authority of HBNI when in his or her judgment the proposed use of the material is in the interests of scholarship. In all other instances, however, permission must be obtained from the author.

A handwritten signature in cursive script that reads "Subrat Sethi". The signature is written in black ink on a light-colored background.

Subrat Sethi

DECLARATION

I, hereby declare that the investigation presented in the thesis has been carried out by me.

The work is original and has not been submitted earlier as a whole or in part for a degree / diploma at this or any other Institution / University.

A handwritten signature in black ink that reads "Subrat Sethi". The signature is written in a cursive style and is enclosed within a light gray rectangular border.

Subrat Sethi

List of publications arising from the thesis

Journal

- 1) Jana, N. C.; Sethi, S.; Saha, R.; Bagh, B. Aerobic oxidation of vanillyl alcohol to vanillin catalyzed by air-stable and recyclable Copper complex and TEMPO under base-free conditions. *Green Chem.* **2022**, *24*, 2542-2556.
- 2) Sethi, S.; Jana, N. C.; Behera S.; C.; Bagh, B. Azide-Alkyne Cycloaddition Catalyzed by Copper(I) Coordination Polymers in PPM Levels Using Deep Eutectic Solvents as Reusable Reaction Media: A Waste-Minimized Sustainable Approach. *ACS Omega.* **2023**, *8*, 1, 868-878.
- 3) Sethi, S.; Jana, N. C.; Panda S.; Maharana S. K.; Behera R. R.; Bagh, B. Copper(I)-catalyzed click chemistry in deep eutectic solvent for the syntheses of β -D-glucoopyranosyltriazoles. *RSC Adv.* **2023**, *13*, 10424.

Publication not includes in the thesis

- 1) Panda, S.; Saha, R.; Sethi, S.; Ghosh, R.; Bagh, B. Efficient α -Alkylation of Arylacetonitriles with Secondary Alcohols Catalyzed by a PhosphineFree Air-Stable Iridium (III) Complex. *J. Org. Chem.* **2020**, *85*, 15610–15621.
- 2) Behera, R. R.; Asish Kumar, A.; Sethi, S.; Jana, N. C.; Bagh, B. Hydrosilylation of Terminal Alkynes Catalyzed by Air-stable Manganese-NHC Complex. (Manuscript under revision).

Conferences:

- 1) **Oral Presentation (Virtual):** International conference on polymer chemistry (ICPOCL-22), Sambalpur, Odisha, India on 11th June 2022. Title: Aerobic oxidation of vanillyl alcohol to vanillin catalyzed by air-stable and recyclable Copper complex and TEMPO under base-free conditions.

- 2) **Oral Presentation (Virtual):** International conference on polymer chemistry (ICPOCL-22), Jaipur, Rajasthan, India on 26th June 2022. Title: Efficient α -Alkylation of Arylacetonitriles with Secondary Alcohols Catalyzed by a Phosphine-Free Air-Stable Iridium(III) Complex.

Dedicated to....

To my parents

&

Dr. Bidraha Bagh

ACKNOWLEDGEMENTS

This smooth journey would not be possible without the blessing of “*Lord Jagannath*”. His grace was always there for me and guided me in every perspective of life. This thesis appears in its current form due to the assistance and guidance of several people. I would therefore like to offer my sincere thanks to all of them. I am extremely thankful to my thesis supervisor Dr. Bidraha Bagh for his guidance, constant support, sincere advices, and valuable suggestions to improve the quality of work throughout my tenure. I appreciate all his contributions of valuable time, stimulating ideas, and funding to make my project experience interesting and productive. Also, I would like to express my gratitude to him for providing me the opportunity to work on this exciting project. My sincere gratitude goes to Prof. A. Srinivasan, Director (NISER), Prof. T. K. Chandrashekar, founder-Director (NISER) and Prof. Sudhakar Panda, former Director (NISER), I would like to thank my doctoral committee members, Dr. Prasenjit Mal, Dr. Sudip Barman, Dr. Sanjib Kar, and Dr. Shantanu Pal for their support and suggestions. I am also greatly privileged by the immense help of all faculty members of School of Chemical Sciences. I would like to recognize Mr. Sanjaya Mishra for their kind help in recording NMR data, Mr. Deepak Kumar Behera for his kind help in X-ray analysis and Mr. Amit Sankar Sahu and Mr. Prakash Behera for their kind help in ESI-MS analysis. This would not have been possible without the continuous, unconditional help from my lab mates Dr. Narayan h. Jana, Rahul Ghosh, Rakesh Ranjan Behera, Surajit Panda, Ratnakar Saha, my sincere thanks to my lab mates for their cooperation in the lab, which is, helped me to plan and execute the experiments meticulously. I would also like to thank my NISER friends for their valuable suggestion and help. Financial assistance (fellowship) by Council of Scientific and Industrial Research (CSIR), Govt. of India is gratefully acknowledged. I would also like to acknowledge DST-SERB, New Delhi, Govt. of India for research funding.

Finally, I would like to thank my parents, family and Rasmi who were witness to every step of the way and provided me support and confidence whenever I needed it the most. Thank you all, so much for your unconditional love and enthusiastic support.

.....*Subrat Sethi*

SYNOPSIS

1. **Name of the Student** : Mr. Subrat Sethi
 2. **Name of the Constituent Institution** : National Institute of Science Education and Research (NISER)
 3. **Enrolment No.** : CHEM11201804024
 4. **Title of the Thesis** : Synthesis and characterization of Copper complexes with tridentate NNO and NNS ligands and their catalytic applications in oxidation and cycloaddition reactions.
 5. **Board of Studies** : Chemical Sciences
-

Introduction

Global warming and anthropogenic climate change are critical challenges that must be addressed as soon as possible in order to mitigate the consequence. It is essential for our sustainable future to create "green" chemical transformation technologies that are both cost-effective and waste-free. In this strategy, chemists have paid enormous attentions in recent years to develop greener and sustainable synthetic chemical processes.¹ Green chemistry is defined by the efficient use of renewable raw resources, the reduction of waste, and the avoidance of dangerous substances. It is challenging to develop synthetic processes that is parallel to the "12 principles of green chemistry."^{2,3} However, a majority of these chemical processes are dominated by scarce, expensive, and mostly toxic noble metal catalysts. As the use of noble metal catalysts is not sustainable, earth-abundant, cheap and often less toxic base metals such as manganese, iron, cobalt, nickel, and Copper can serve as indispensable alternatives. When it comes to the synthesis of highly valuable organic compounds, transition metal catalysts are an important component since they optimize the key ideas of organic synthesis.

Copper is usually considered as a "metal of choice" in organometallic chemistry and homogeneous catalysis due to its vast applications in a wide variety of organic transformations.

Synthesized Copper complexes are mostly air stable and has various stable oxidation states (0 to +3) with dynamic geometries and a less toxic and sustainable base metal. Utilizing Copper complexes as catalysts rather than noble metals to produce agrochemicals, pharmaceuticals, and biological commodities has facilitated the creation of advanced synthetic methods within the toolbox of organic synthetic chemistry. In this regard, a lot of the phosphines-based ligands are used in synthesis of active catalysts.

However, phosphines are also very reactive on their own, especially when it comes to oxidation, and must be handled in inert environments. In addition to being extremely flammable, numerous trialkyl phosphines, including PMe_3 and PtBu_3 , are also frequently described as pyrophoric, just like elemental white phosphorus. Therefore, we turned our attention to synthesize phosphine free ligands and, we have major intensions to prepare readily assessable NNO and NNS tridentate ligand frameworks. Furthermore, a tridentate ligand with a labile bulky arm can be a potential choice in the development of catalytically active metal complexes. Hence various NNO and NNS ligand backbone were synthesized and employed for the synthesis of a wide range of Copper complexes. The catalytic efficiency of the synthesized Copper complexes has been explored and investigated in diverse organic transformations.

Scope and Organization of the Present Thesis

A simple and novel NNO and NNS based Copper complexes were prepared with an aim for the catalytic applications in different trial organic transformations (mainly oxidation and cycloaddition reactions). In very first work, selective aerobic oxidation of biomass derived monomeric phenolic compound particularly vanillyl alcohol to vanillin was demonstrated by an air stable Copper(II) complex using aerobic oxygen as sustainable oxidant. Most of the active catalytic systems for this oxidation process utilize rare and expensive noble metals or various stoichiometric oxidants such as manganese dioxide, chromium salts, activated DMSO,

peroxides, and hypervalent iodine and thus, those systems are not sustainable. Hence, we aimed to perform the oxidation reaction under green and sustainable protocols and the aerobic oxidation of vanillyl alcohol to vanillin was successfully carried out in various green solvent mixtures such as ethanol/water (1:1) and acetone/water (1:1) in presence of catalytic amount of Copper complex and TEMPO under base free conditions. In another work, the Copper azide-alkyne cycloaddition reaction (CuAAC) of terminal alkyne and different azides was performed in various green solvents such as water, ethanol, glycerol, and deep eutectic solvents (DESs) under sustainable conditions. Generally, high loading of Cu(I)-catalysts or reducing agents in case of Cu(II)-species are used for CuAAC reactions. In this context, a ppm-level catalyst loading (50 ppm) was used to achieve complete conversion in deep eutectic solvents, an emerging class of green solvents at 70 °C. Optimized protocols were successfully used to expand the substrate scope. In the final work of the thesis, CuAAC reaction was also explored for the synthesis of biologically active triazole-attached carbohydrate-containing molecular architectures, 1,4-disubstituted 1,2,3-glucopyranosyltriazoles. In literature, this glycochemistry is performed in various hazardous organic solvents such as toluene, DCM, acetonitrile, DMF and THF. Hence, we studied the potential applicability of DESs as sustainable reaction medium for the synthesis of important glycoconjugate triazoles for the first time *via* CuAAC reaction. In all cases, the green and sustainable credentials of above catalytic protocols were evaluated with the help of CHEM21 green metrics toolkit. Overall, the current thesis includes four chapters with the following contents. Chapter-wise brief discussions are given below.

CHAPTER 1

Introduction

The selective oxidation of alcohol to aldehyde is a fundamental and significant chemical transformation. Despite the fact that several techniques for the synthesis of aldehydes have been developed. In line with that, the green catalytic oxidation process utilizing air as an oxidant is the most appealing since the protocol is non-hazardous and only produce water as a byproduct.^{4,5} This chapter highlights the basic introduction to the most recent advances in peroxidative, and aerobic oxidation of primary and secondary alcohols catalyzed by Copper complexes in homogeneous conditions. Another class of Copper catalysts utilize dioxygen (or air) in the presence of a catalytic amount of the TEMPO (2,2,6,6-tetramethylpiperidine-1-oxyl) radical for alcohol oxidation. In the second part, the general introduction of various click reactions was discussed. In chemical synthesis, click chemistry is a class of simple, atom-economy reactions commonly used for joining two molecular entities of choice. In 2002, Karl B. Sharpless and Morten P. Meldal discovered an important “click reaction” in which 1,3-dipolar cycloaddition reaction between organic azides and terminal alkynes was performed.^{6,7} Later the CuAAC reaction became popular to the scientific community because of its flexible and adaptable strategies for the easy syntheses of 1,4-disubstituted 1,2,3-triazoles. In this context, some relevant literature reports on CuAAC reactions were summarized and discussed. Finally, the chapter is closed with a brief outline of the research contents of the current thesis.

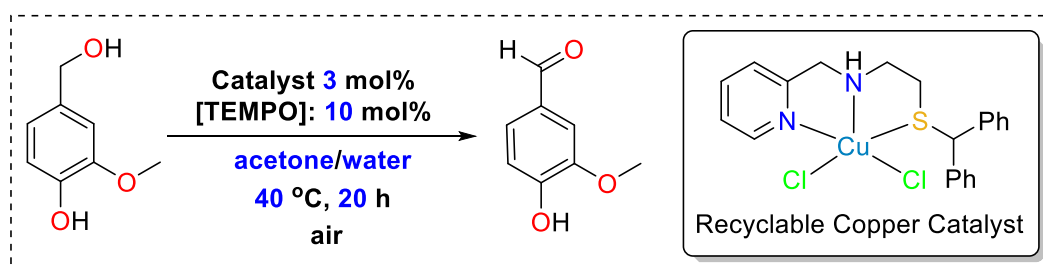
CHAPTER 2

Aerobic Oxidation of Vanillyl Alcohol to Vanillin Catalyzed by Air-Stable and Recyclable Copper Complex and TEMPO Under Base-free Conditions

The conversion of biomass for the manufacture of fine chemicals has become a significant area of research due to the need for sustainable development in the current day. The scientific

community has paid close attention to the aerobic oxidation of monomeric phenolics produced from lignin for the development of several value-added products. The aerobic oxidation of vanillyl alcohol to vanillin, an essential fragrance molecule with various uses, has attracted an enormous amount of research interests. For this, Copper(II) complexes were developed and tested for selective oxidation of vanillyl alcohol to vanillin at ambient conditions in the presence of a catalytic amount of the TEMPO radical (Scheme 1). The selective oxidation of vanillyl alcohol to vanillin was successfully carried out in various green solvent mixtures such as ethanol/water (1:1) and acetone/water (1:1). Catalyst is highly recyclable and did not show any reduction of catalytic activity after three cycles. Finally, the green and sustainable credentials of various catalytic protocols under various reaction conditions were compared with the help of CHEM21 green metrics toolkit. A plausible catalytic pathway is proposed based on the published reports and experimental evidences.

Scheme 1. Aerobic oxidation of vanillyl alcohol to vanillin catalysed by air-stable and recyclable Copper complex.



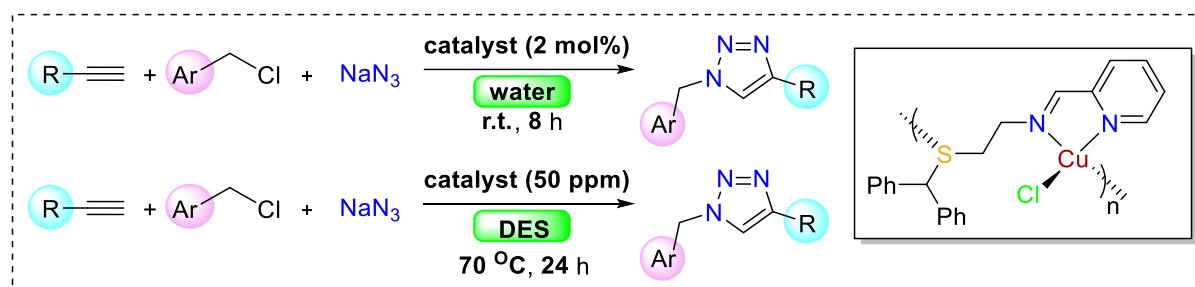
CHAPTER 3

Azide-alkyne Cycloaddition Catalyzed by Copper(I) Coordination Polymer in PPM Level Using Deep Eutectic Solvent as a Reusable Reaction Media: A Waste Minimized Sustainable Approach

Copper(I)-catalyzed 1,3-dipolar cycloaddition of organic azides and alkynes, commonly called CuAAC, is a popular, versatile and reliable strategy for the synthesis of 1,4-disubstituted 1,2,3-

triazole. This triazole (containing different functional groups) is a significant class of nitrogen-containing heterocycles that has found widespread applications in various branch of sciences. In CuAAC reactions, either Cu(I) species is generated in situ by reducing a Cu(II) salt (commonly by sodium ascorbate) or Cu(I) complexes with various ligand frameworks are directly utilized. These reactions are generally performed in a mixture of water and organic solvent, such as alcohols (*t*-BuOH, EtOH, and MeOH), dichloromethane, acetonitrile, and THF. The purification of triazole products often includes chromatographic separation, which also produces a lot of solvent waste. In the present chapter, the azide–alkyne cycloaddition reaction was successfully conducted in pure water at r.t. under aerobic conditions in absence of reducing agents (Scheme 2). Other green solvents, including ethanol and glycerol, were also effectively used. Finally, deep eutectic solvents as green and sustainable reaction media were successfully utilized. Finally, we turned our attention to DESs as an emerging class of green reaction media. Although DESs are highly underexplored for organic transformations, they may have high potential applicability in the CuAAC reaction. In deep eutectic solvents, complete conversion with excellent isolated yield was achieved in a short period of time (1 h) with low catalyst loading (1 mol%) at r.t. Full conversion could also be achieved within 24 h with ppm-level (50 ppm) catalyst loading at 70 °C. Optimized reaction conditions were used for the syntheses of a large number of 1,4-disubstituted 1,2,3-triazoles with various functionalities. Triazole products were easily isolated by simple filtration. The reaction media, such as water and deep eutectic solvents, were recovered and recycled in three consecutive runs. The limited waste production is reflected in a very low *E*-factor (0.3–2.8). Finally, the CHEM21 green metrics toolkit was employed to evaluate the green and sustainable credentials of different optimized protocols in various green solvents such as water, ethanol, glycerol, and deep eutectic solvents.

Scheme 2. Copper catalyzed three component cycloaddition reaction in green solvents following sustainable reaction conditions.

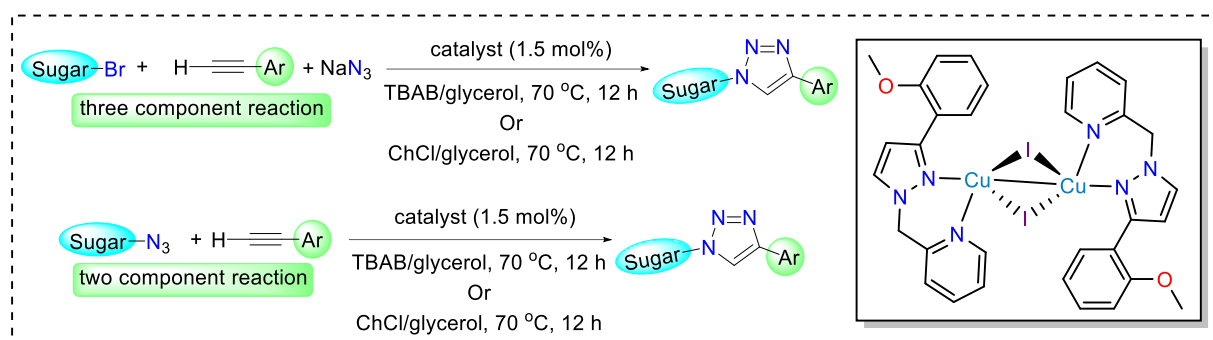


CHAPTER 4

Copper(I)-catalyzed Click Chemistry in Deep Eutectic Solvent for the Syntheses of β -D-glucopyranosyltriazoles

This work is the extensions of chapter 3. In this chapter, we showed readily accessible and well-defined Copper(I)-iodide complex with NNO ligand framework as efficient catalyst for the syntheses of various glucopyranosyltriazoles in DESs (**Scheme 3**). Facile synthesis of triazole-appended carbohydrate building blocks such as glycoconjugates, glycopolymers, glycohybrids, glycopeptides, glycoproteins, glycolipids, glycoclusters, and glycodendrimers is an emerging area of glycoscience.^{8, 9} Instead of using potentially hazardous reaction media such as DCM or toluene, the use of deep eutectic solvent (DES) is advantageous for the syntheses of triazole-glycohybrids. The present chapter shows, for the first time, the successful use of DES as a reaction medium to click various glycosides and terminal alkynes in the presence of sodium azide. Various 1,4-disubstituted 1,2,3-glucopyranosyltriazoles were synthesized either *via* three or two component reaction (**Scheme 3**) and the pure products were isolated by using a very simple work up process (filtration). The reaction media was recovered and recycled in five consecutive runs. The presented catalytic protocol generated very minimum waste as reflected by a low *E*-factor (2.21–3.12). Finally, green metrics of the optimized reaction conditions were evaluated with the help of CHEM21 green metrics toolkit.

Scheme 3. CuAAC reactions of various glycosides and terminal alkynes in deep eutectic solvents.



References

1. Anastas, P.; Eghbali, N. Green Chemistry: Principles and Practice. *Chem. Soc. Rev.* **2010**, *39*, 301-312.
2. Schmidt, F. Baerns M. (eds) The Importance of Catalysis in the Chemical and Non-Chemical Industries, In *Basic Principles in Applied Catalysis*. Springer Series in Chemical Physics, vol 75. Springer, Berlin, Heidelberg, 2004.
3. Chorkendorff, I.; Niemantsverdriet, J. W. *Concepts of Modern Catalysis and Kinetics, Second Edition. I*. WILEY-VCH Verlag GmbH&Co. KGaA, Weinheim, 2007.
4. Steves, J.E.; Stahl, S.S. Copper(I)/ABNO-catalyzed aerobic alcohol oxidation: alleviating steric and electronic constraints of Cu/TEMPO catalyst systems, *J. Am. Chem. Soc.* **2013**, *135*, 15742–15745.
5. Hoover, J.M.; Ryland, B.L.; Stahl, S.S. Mechanism of Copper(I)/TEMPO-catalyzed aerobic alcohol oxidation, *J. Am. Chem. Soc.* **2013**, *135*, 2357-2367.
6. Rostovtsev, V. V.; Green, L. G.; Fokin, V. V.; Sharpless, K. B. A Stepwise Huisgen Cycloaddition Process: Copper(I)-Catalyzed Regioselective “Ligation” of Azides and Terminal Alkynes. *Angew. Chem., Int. Ed.* **2002**, *41*, 2596-2599.

7. Tornøe, C. W.; Christensen, C.; Meldal, M. Peptidotriazoles on Solid Phase: [1,2,3]-Triazoles by Regiospecific Copper(I)-Catalyzed 1,3-Dipolar Cycloadditions of Terminal Alkynes to Azides. *J. Org. Chem.* **2002**, *67*, 3057–3064.
8. Tiwari, V. K.; Mishra, B. B.; Mishra, K. B.; Mishra, N.; Singh, A. S.; Chen, X. Cu-Catalyzed Click Reaction in Carbohydrate Chemistry. *Chem. Rev.* **2016**, *116*, 3086–3240.
9. Agrahari, A. K.; Bose, P.; Jaiswal, M. K.; Rajkhowa, S.; Singh, A. S.; Hotha, S.; Mishra, N.; Tiwari, V. K. Cu(I)-Catalyzed Click Chemistry in Glycoscience and Their Diverse Applications. *Chem. Rev.* **2021**, *121*, 7638–7956.

List of Scheme		Page No.
1	Scheme 1.1.1 Oxidation of both primary and secondary alcohol	25
2	Scheme 1.1.2 The oxidation of active and non-active alcohols	26
3	Scheme 1.1.3 Efficient aerobic oxidation of alcohols	26
4	Scheme 1.1.4 Aerobic oxidation of primary and secondary alcohols by new mononuclear Cu (II) radical catalyst	27
5	Scheme 1.1.5 The oxidation of aromatic and aliphatic alcohols by using the Cu-3 complex	28
6	Scheme 1.1.6 The application of Cu-4 and H ₂ O ₂ for the oxidation of primary and secondary alcohols at 70 °C	28
7	Scheme 1.1.7 The application of Cu-5 and H ₂ O ₂ for the oxidation of primary and secondary alcohols at 70 °C	29
8	Scheme 1.1.8 Oxidation of various alcohols with Copper (II) complex in water	30
9	Scheme 1.1.9 Complete oxidation of benzyl alcohol to benzoic acid in the presence of Cu(II) complex	30
10	Scheme 1.1.10 Cu-8/H ₂ O ₂ catalyst system for the oxidation of benzyl, cinnamyl, piperonyl alcohol at room temperature	31
11	Scheme 1.1.11 The application of Cu-9 and H ₂ O ₂ or TBHP for the oxidation of 1-phenylethanol at 70 °C	31
12	Scheme 1.1.12 The oxidation of cyclohexanol in presence of Cu-10/H ₂ O ₂ catalyst at 80 °C in 24 h	32
13	Scheme 1.1.13 The oxidation of cyclohexanol in presence of Cu-10/H ₂ O ₂ catalyst at 80 °C in 24 h	33

14	Scheme 1.1.14 Aerobic oxidation of aliphatic alcohols with reported Koskinen	34
15	Scheme 1.1.15 Aerobic oxidation of aliphatic alcohols with bpy/CuI/NMI/TEMPO reported by Stahl	35
16	Scheme 1.1.16 Oxidation of alcohol using DABCO-CuCl complex	35
17	Scheme 1.1.17 Aerobic Oxidation of Benzylic Alcohols in Water	36
18	Scheme 1.1.18. TEMPO mediated copper catalyzed allylic alcohol oxidation/conjugate addition	37
19	Scheme 1.1.19 Aerobic oxidation of primary alcohols with a Copper(I)/TEMPO catalyst	38
20	Scheme 1.1.20 Cu(I)/NMI/TEMPO catalyzed by aerobic oxidation of alcohol	38
21	Scheme 1.1.21 Copper (I) catalyst for the selective aerobic oxidation of primary alcohols	39
22	Scheme 1.2.1 Cu-catalyzed cycloaddition of azides and terminal alkynes (a) thermodynamically generated Huisgen cycloaddition vs (b) CuAAC	41
23	Scheme 1.2.2 Sharpless Copper(I)-catalysed azide-alkyne cycloaddition (CuAAC)	42
24	Scheme 1.2.3 1,3-dipolar cycloaddition of terminal alkynes to azides, regiospecific Copper(I) catalyses the formation of [1,2,3]-triazoles	42
25	Scheme 1.2.4 CuAAC on microtiter plate-bound saccharide derivatives.	43
26	Scheme 1.2.5 Indirect Coupling of the pyrazinones Scaffold with different mono and disaccharides through click chemistry	43
27	Scheme 1.2.6 Copper (I)-catalyzed azide-alkyne cycloaddition enhanced by acid and base	44

28	Scheme 1.2.7 A recoverable polymer-supported azide and CuI used in a multicomponent synthesis of 1,4-disubstituted 1,2,3-triazoles	44
29	Scheme 1.2.8 A click cycloaddition/decarboxylation process for 1-Monosubstituted 1,2,3-triazoles	45
30	Scheme 1.2.9 An efficient synthesis of 1-substituted 1,2,3-triazoles from azides and acetylene using CuI/Et ₃ N catalyzed 'Click Chemistry'	45
31	Scheme 1.2.10 Alkyne-azide cycloaddition reactions by using stoichiometric amounts of Copper(II) precatalysts in methanol	46
32	Scheme 1.2.11 Three-component cyclization of alkynes, alkyl halides, sodium azide	46
33	Scheme 1.2.12 Abnormal N-heterocyclic carbene-Copper(I) complex in click chemistry	47
34	Scheme 1.2.13 Copper-catalyzed azide-alkyne cycloaddition (CuAAC) by functionalized NHC-based polynuclear catalyst	48
35	Scheme 1.2.14 Synthesis of 1,2,3-triazoles in glycerol by using CuI as a catalyst	49
36	Scheme 1.2.15 CuAAC cycloaddition reaction in glycerol as a reaction media catalysed by CuI or combination of CuI/L(proline)	50
37	Scheme 1.2.16 Cycloaddition of azides and alkynes (AAC) in pure glycerol as solve	50
38	Scheme 1.2.17 One-pot synthesis of triazoles from alkyl halides, NaN ₃ , and alkynes	51
39	Scheme 1.2.18 Synthesis of 1,2,3-triazoles via Huisgen-click reaction in water.	51

40	Scheme 1.2.19 1,4-disubstituted 1,2,3-triazole synthesis through CuAAC reaction enhanced by visible light	51
41	Scheme 1.2.20 Preparation of 5-iodo-1,2,3-triazole derivatives from alkynes and organic azides	52
42	Scheme 1.2.21 Application of Copper complex for the synthesis of glycoconjugates/sugar-based triazoles	53
43	Scheme 1.2.22 Synthesis of 1,4-substituted 1,2,3-triazole in the D-sorbitol/urea	54
44	Scheme 1.2.23 Copper-catalyzed aryl and heteroaryl bromides click reaction in an eco-friendly deep eutectic solvent	54
45	Scheme 1.2.24 Cu-catalyzed azide-alkyne cycloadditions (CuAAC) in DES	55
46	Scheme 2.1 Catalytic oxidation of vanillyl alcohol	73
47	Scheme 2.2 Synthesis of ligands L3 and L4	77
48	Scheme 2.3. Synthesis of Copper(II) complexes complex 15a, complex 15b, complex 16a, and complex 16b (the molecular structures showing 30% ellipsoids and hydrogen atoms (except amine proton) and [ClO ₄] ⁻ counter anions are omitted for clarity).	77
49	Scheme 2.4 Catalytic aerobic oxidation of vanillyl alcohol to vanillin using different optimized reaction conditions	93
50	Scheme 2.5. Plausible mechanism for the catalytic aerobic oxidation of vanillyl alcohol to vanillin (dotted bonds indicate weak noncovalent interactions)	98
51	Scheme 3.1 CuAAC reaction in green reaction media and sustainable features of the present work	138

52	Scheme 3.2. Synthesis of Copper(I) complexes 17 and 18 (the molecular structures showing 30% ellipsoids and hydrogen atoms are omitted for clarity)	142
53	Scheme 3.3. CuAAC reaction using different optimized reaction conditions (Bn-N ₃ was synthesized in situ by reacting Bn-Cl and NaN ₃)	148
54	Scheme 3.4. CuAAC reactions of various alkynes with in situ generated organic azides using Method A and Method F	153
55	Scheme 4.1 CuAAC reaction in synthesis of triazolyl glycoconjugates and sustainable features of the present work.	199
56	Scheme 4.2 Synthesis of Copper(I) iodide 19 (the molecular structure of 19 showing 30% ellipsoids and hydrogen atoms are omitted for clarity).	201
57	Scheme 4.3. CuAAC reactions of various glycosides and terminal alkynes in TBAB/glycerol (1: 4) and ChCl/glycerol (1: 2) using optimized methods.	211

List of Figure		Page No
1	Figure 2.1 Graphical representation of the catalytic activity of 16b for the aerobic oxidation of vanillyl alcohol to vanillin in various solvents at 40 °C for 6 h	83
2	Figure 2.2 Graphical representation of the catalytic activity of 16b for the aerobic oxidation of vanillyl alcohol to vanillin in various solvent mixtures at 40 °C for 6 h	87
3	Figure 2.3 Graphical representation of the catalytic activity of 16b for the aerobic oxidation of vanillyl alcohol to vanillin at 40 °C in ethanol/water (1: 1) and acetone/water (1:1) at various times with two different catalyst	90

	loadings (16b: 5 mol %, TEMPO: 20 mol % and 16b: 3 mol %, TEMPO: 10 mol %).	
4	Figure 2.4 EPR spectra of (a) complex 2b and TEMPO radical (2b in the insert) under inert conditions, (b) complex 2b, TEMPO radical, and vanillyl alcohol (VA) under inert conditions, and (c) complex 2b, TEMPO radical, and vanillyl alcohol (VA) in air.	101
5	Figure 2.5 ¹ H NMR of 2-(benzhydrylthio)-ethanamine hydrochloride in CDCl ₃ at r.t.	112
6	Figure 2.6: ¹ H NMR of 2-(benzhydrylthio)-ethanamine in CDCl ₃ at r.t.	112
7	Figure 2.7: ¹ H NMR of N-(2-(benzhydrylthio) ethyl)-1-(pyridine-2-yl) methanimine (L3) in CDCl ₃ at r.t.	113
8	Figure 2.8 ¹³ C NMR of N-(2-(benzhydrylthio) ethyl)-1-(pyridine-2-yl) methanimine (L3) in CDCl ₃ at r.t.	113
9	Figure 2.9: ¹ H NMR of 2-(benzhydrylthio)-N-(pyridine-2-ylmethyl) ethan-1-amine (L4) in CDCl ₃ at r.t.	114
10	Figure 2.10 ¹³ C NMR of 2-(benzhydrylthio)-N-(pyridine-2-ylmethyl) ethan-1-amine (L4) in CDCl ₃	114
11	Figure 2.11 FTIR Spectrum of ligand L3 .	115
12	Figure 2.12 FTIR Spectrum of ligand L3 .	115
13	Figure 2.13 FTIR Spectrum of complex 15a .	115
14	Figure 2.14 FTIR Spectrum of complex 15b .	116
15	Figure 2.15 FTIR Spectrum of complex 16a .	116
16	Figure 2.16 FTIR Spectrum of complex 16b .	116

17	Figure 2.17 ^{13}C NMR spectrum of 4-isopropyl benzoic acid	119
18	Figure 3.1 ^1H NMR of N-(2-(benzhydrylthio) ethyl)-1-(pyridine-2-yl) methanimine (L5) in CDCl_3 at r.t.	159
19	Figure 3.2 ^{13}C NMR of N-(2-(benzhydrylthio) ethyl)-1-(pyridine-2-yl) methanimine (L5) in CDCl_3 at r.t.	159

20	Figure 3.3 ^1H NMR of 2-((3-(2-methoxyphenyl)-1H-pyrazol-1-yl) methyl) pyridine (L6) in CDCl_3 at r.t.	160
21	Figure 3.4 ^{13}C NMR of 2-((3-(2-methoxyphenyl)-1H-pyrazol-1-yl) methyl)pyridine (L6) in CDCl_3 at r.t.	160
22	Figure 3.5 ^1H NMR of complex 17 in DMSO-d_6 .	161
23	Figure 3.6 ^{13}C NMR of complex 17 in DMSO-d_6 .	161
24	Figure 3.7 ^1H NMR of complex 18 in DMSO-d_6 .	162
25	Figure 3.8 ^{13}C NMR of complex 18 in DMSO-d_6 .	162
26	Figure 3.9 FTIR Spectrum of ligand L5	163
27	Figure 3.10 FTIR Spectrum of ligand L6	163
28	Figure 3.11 FTIR Spectrum of complex 17	163
29	Figure 3.12 FTIR Spectrum of complex 18	163
30	Figure 3.13 ^1H NMR (400 MHz) spectrum of 1-benzyl-4-phenyl-1H-1,2,3-triazole (A) CDCl_3 at r.t.	178
31	Figure 3.14. ^{13}C NMR spectrum of 1-benzyl-4-phenyl-1H-1,2,3-triazole (A) in CDCl_3 at r.t.	178
32	Figure 3.15 ^1H NMR spectrum of 1-benzyl-4-(4-fluorophenyl)-1H-1,2,3-triazole (C4) in CDCl_3 at r.t.	179

33	Figure 3.16 ¹³ C NMR (101 MHz) spectrum of 1-benzyl-4-(4-fluorophenyl)-1H-1,2,3-triazole (C4) in CDCl ₃ at r.t.	179
34	Figure 3.17 1D Molecular chain of complex 17 and 18 .	182
35	Figure 4.1 Comparative catalytic performance of complex 17 in various DESs.	206
36	Figure 4.2 ¹ H NMR of 2-((3-(2-methoxyphenyl)-1H-pyrazol-1-yl)methyl)pyridine (L7) in CDCl ₃ at r.t.	215
37	Figure 4.3 ¹³ C NMR of 2-((3-(2-methoxyphenyl)-1H-pyrazol-1-yl)methyl)pyridine (L7) in CDCl ₃ at r.t.	215
38	Figure 4.4 ¹ H NMR of complex 19 in DMSO-d ₆ .	216
39	Figure 4.5 ¹³ C NMR of complex 19 in DMSO-d ₆ .	216
40	Figure 4.6 FTIR Spectrum of ligand L7 .	217
41	Figure 4.7 FTIR Spectrum of complex 19 .	217
42	Figure 4.8 ¹ H NMR (400 MHz) spectrum of (2R,3R,4S,5R,6R)-2-(acetoxymethyl)-6-(4-phenyl-1H-1,2,3-triazol-1-yl) tetrahydro-2H-pyran-3,4,5-triyl triacetate (A) CDCl ₃ at r.t.	230
43	Figure 4.9 ¹³ C NMR (101 MHz) spectrum of (2R,3R,4S,5R,6R)-2-(acetoxymethyl)-6-(4-phenyl-1H-1,2,3-triazol-1-yl)tetrahydro-2H-pyran-3,4,5-triyl triacetate (A) in CDCl ₃ at r.t.	231
44	Figure 4.10 ¹ H NMR (400 MHz) spectrum of (2R,3R,4S,5R,6R)-2-(acetoxymethyl)-6-(4-(p-tolyl)-1H-1,2,3-triazol-1-yl)tetrahydro-2H-pyran-3,4,5-triyl triacetate (B1) CDCl ₃ at r.t.	231

45	Figure 4.11 ^{13}C NMR (101 MHz) spectrum of (2R,3R,4S,5R,6R)-2-(acetoxymethyl)-6-(4-(p-tolyl)-1H-1,2,3-triazol-1-yl)tetrahydro-2H-pyran-3,4,5-triyl triacetate (B₁) in CDCl_3 at r.t.	232
46	Figure 4.12 ^1H NMR (400 MHz) spectrum of (2S,3S,4S,5R,6R)-2-(methoxycarbonyl)-6-(4-(p-tolyl)-1H-1,2,3-triazol-1-yl)tetrahydro-2H-pyran-3,4,5-triyl triacetate (C₂) DMSO at r.t	232
47	Figure 13 ^{13}C NMR (101 MHz) spectrum of (2S,3S,4S,5R,6R)-2-(methoxycarbonyl)-6-(4-(p-tolyl)-1H-1,2,3-triazol-1-yl)tetrahydro-2H-pyran-3,4,5-triyl triacetate (C₂) in DMSO at r.t.	233
48	Figure 4.14. Molecular structure of complex 19	235
List of Tables		Page No
1	Table 2.1 Catalytic performance of 16b for the aerobic oxidation of vanillyl alcohol to vanillin in different solvents with various polarities and coordination abilities (C.A.)	82
2	Table 2.2 Catalytic performance of 16b for the aerobic oxidation of vanillyl alcohol to vanillin in different solvents	84
3	Table 2.3 Catalytic performance of 16 b for the aerobic oxidation of vanillyl alcohol	88
4	Table 2.4 Comparison of the six different methods (Methods A to F) for the aerobic oxidation of vanillyl alcohol from the CHEM21 Green Metrics Toolkit calculation	95
5	Table 2.5 Catalytic performance of 16b for the aerobic oxidation of vanillyl alcohol to vanillin at different concentrations of vanillyl alcohol	102

6	Table 2.6. Crystallographic Data and Refinement Parameters for 15a, 15b, 16a, 16b and 16b (recycled).	117
7	Table 2.7. Bond lengths (Å) around the metal centre in Copper complexes.	119
8	Table 3.1. Catalytic performance of 17 and 18 for three component CuAAC reaction in pure water, ethanol, and glycerol as green solvents	144
9	Table 3.2. Catalytic performance of 17 for CuAAC reaction in deep eutectic solvents as sustainable reaction media	146
10	Table 3.3. Comparison of the six different methods (Method A to F) of CuAAC reaction	150
11	Table 3.4. Crystallographic Data and Refinement Parameters for 17 and 18 .	180
12	Table 3.5. Selected bond lengths (Å) around the metal centre in Copper complexes 17 and 18 .	181
13	Table 3.6. Selected bond angles (°) around the metal centre in Copper complexes 17 and 18 .	182
13	Table 4.1 Catalytic activity of complex 19 for CuAAC reaction in various DESs	203
14	Table 4.2 Calculation of different metrics of CuAAC reaction under optimized condition	209
15	Table 4.3. Crystallographic Data and Refinement Parameters for 19 .	234
16	Table 4.4. Selected bond lengths (Å) around the metal centre in Copper complexes 19 and 20 .	234
17	Table 4.5. Selected bond angles (Å) around the metal centre in Copper complexes	235

List of Abbreviations Used

Å	Angstrom
Anal.	Analytically
Anhyd	Anhydrous
aq	Aqueous
bp	Boiling Point
br	Broad
°C	Degree Celcius
Calcd	Calculated
cm	Centimetre
Conc	Concentrated
CuAAC	Copper catalysed azide-alkyne cycloaddition reactions
conv	Conversion
ChCl	Choline chloride
d	Doublet, Days
DES	Deep eutectic solvents
DCM	Dichloromethane
dd	Doublet of a Doublet
DMF	N,N-Dimethyl Formamide

eq	Equation
equiv	Equivalent
Et	Ethyl
g	Grams
Gly	Glycerol
h	Hours
HRMS	High-resolution Mass Spectrometry
IR	Infrared
K	Kelvin
kcal	Kilo calories
lit	Liter
m	Multiplet
M	Molar
MeCN	Acetonitrile
mp	Melting point
Me	Methyl
MHz	Mega Hertz
Min	Minutes
mL	Milliliter

mM	Millimolar
mmol	Millimole
mol	Mole
MS	Mass Spectra
N	Normal
NMR	Nuclear Magnetic Resonance
ppm	Parts per Million
rt	Room Temperature
s	Singlet, Seconds
XRD	X-Ray Diffraction
TBAB	Tetra butyl ammonium bromide
TMAC	Tetra methyl ammonium Chloride
VOCs	Volatile organic solvents

Table of Contents

Synopsis	Synthesis and characterization of Copper complexes with tridentate NNO and NNS ligands and their catalytic applications in oxidation and cycloaddition reactions	
List of Schemes		19
List of Figures		22
List of Tables		24
Chapter 1	Introduction	31
Chapter 2	Aerobic oxidation of vanillyl alcohol to vanillin catalyzed by air-stable and recyclable Copper complex and TEMPO under base-free conditions	45
	2.1 Abstract	
	2.2 Introduction	63
	2.3 Results and Discussion	65
	2.4 Conclusions	82
	2.5 Experimental Section	83
	2.6 References	102
	¹ H and ¹³ C Spectra	112
Chapter 3	Azide-alkyne cycloaddition catalyzed by Copper(I) coordination polymer in PPM level using deep eutectic solvent as a reusable reaction media: a waste minimized sustainable approach	115

3.1 Abstract	115
3.2 Introduction	115
3.3 Results and Discussion	117
3.4 Conclusions	127
3.5 Experimental Section	127
3.6 Notes and References	139
¹ H and ¹³ C Spectra	145
Chapter 4 Copper(I)-catalyzed click chemistry in deep eutectic solvent for the syntheses of β-D-glucoopyranosyltriazoles	148
4.1 Abstract	148
4.2 Introduction	148
4.3 Results and Discussion	151
4.4 Conclusions	157
4.5 Experimental Section	158
4.6 Notes and References	163
¹ H and ¹³ C Spectra	169
Chapter 5 Summary	124

Chapter-1

INTRODUCTION

Global warming and anthropogenic climate change are pressing issues that need urgently viable solutions to minimize their consequences. For our sustainable future, it is essential to develop "green" chemical transformation technologies that are both affordable and waste-free. Chemists have worked hard in recent years to create greener chemical processes in this approach.¹ The essential concept of green chemistry is the effective utilisation of renewable raw materials, waste minimization, and the avoidance of hazardous compounds. It is difficult to establish synthetic techniques that adhere to the "12 principles of green chemistry."^{2,3} Transition metal catalysts are an inseparable tool when it comes to the synthesis of high-value organic materials, as it maximizes organic synthesis' important concepts : (i) economically viable; reduces energy demand and production cost (ii) improves selectivity (iii) catalyst recycling; reduces the metal consumption, all these synthetic paradigms are very close to the views and principles of Green Chemistry.^{4,5}

As a result of growing environmental concerns, techniques that use the least amount of energy and generate the least amount of trash should be produced. Catalytic reactions stand out as vital and feasible answers in this perspective, providing them an unprecedented position to attain these goals.⁶ Catalysis techniques are including heterogeneous catalysis, homogeneous catalysis, bio catalysis, and others. The most widely acknowledged are transition metal-catalysed homogeneous and heterogeneous processes. Catalysis has several advantages, including low energy requirements, increased selectivity, and the use of catalytic amounts of chemicals rather than stoichiometric amounts or excess.⁷ A catalyst in a chemical process accelerates the reaction by lowering the activation barrier of the transition state. Substantial use of catalysis in the chemical industry displays its economic and environmental success.⁸⁻¹⁰

In recent decades, the transition metal-catalyzed reaction evolved into a strong tool in the synthesis of organic molecules, considerably contributing to the growth of chemical research and industry by finding and producing new classes of chemical compounds and helpful new synthetic methods.¹¹ Metals like palladium,¹² nickel,¹³ Copper,¹⁴ zinc,¹⁵ cobalt,¹⁶ iron,¹⁷ gold,¹⁸ manganese,¹⁹ rhodium²⁰ and ruthenium,²¹ is commonly the foundation of transition metal catalysts. The first transition metal-catalyzed reaction was the homocoupling of acetylenes which was performed in the mixture of CuCl, NH₄OH, and EtOH, which Carl Andreas Glaser reported in 1869.²² Beginning in the year 1900, palladium-catalyzed reactions were first seen, but Pd chemistry was mainly unexplored until the 1960s. Because of its strong catalytic activity, flexibility, and ability to change reaction conditions, Pd catalysis subsequently attracted considerable interest and gained pace. In the 1920s, research on alternative transition metals, including Ir, Rh and Ru as catalysts, also started. The three chemistry Nobel Prizes awarded to Richard F. Heck, Akira Suzuki, and Ei-ichi Negishi for their revolutionary discoveries in transition metal chemistry serve as further proof of the importance of this field.

Even though transition metal catalysts for diverse bond-breaking/forming processes have been well established up to this point, several significant and often surprising advances continue unabatedly. In addition to the ongoing research and usage of classic noble metals like palladium,²³ rhodium,²⁴ and ruthenium,²⁵ other inexpensive metal catalysts have lately drawn more interest due to their ease of use and unbeatable affordability. Thus, the attention shifted to far less expensive and efficient metal catalysts. Throughout the beginning of human history, mankind has used Copper, a useful transition metal. It is the second most abundant element on the planet, existing as ores and in a directly utilizable metal form. Copper is a soft orange metal found mostly in carbonate, oxide and sulphate ores. Chalcopyrite, CuFeS₂, is the most common Copper ore, accounting for more than half of global Copper resources. Further Copper-

containing minerals include a thick green ore, malachite, and red cuprite, Cu_2O , bornite, Cu_5FeS_4 , covellite, CuS , chalcocite, Cu_2S , $\text{Cu}_3(\text{CO}_3)_2(\text{OH})_2$ and azurite.²⁶ Copper was named after the Latin word *cuprum*, which means "from Cyprus," and it possesses the atomic number 29 with the mass number 63.546 and the electronic configuration $[\text{Ar}]3\text{d}^{10}4\text{s}^1$.²⁷ Copper becomes more ductile and conductive when one electron is present in the s subshell well above complete d orbital (thermal as well as electrical).

Notably, due to their scarcity within the Earth's crust, noble metals have market values that are similarly high and often quite volatile. As a result, a recent EU publication on key raw materials revealed that all first-row transition metals meet the economic relevance criterion while also having lower abundance than the supply risk level (excluding cobalt). As a result, there is a growing need to switch out expensive, scarce noble metals like Rh, Ir, Pt, and Ru (2nd and 3rd row transition metals) with far less expensive, abundant in the earth (1st row) transition metals like Mn, Fe, Co, Ni, or Cu. Utilizing Copper complexes as catalysts rather than noble metals to produce agricultural, chemical, pharmaceutical, and biological commodities has facilitated the creation of innovative synthetic methods within the toolbox of organic synthetic chemistry.²⁸ Considering the following factors, Copper has a significant potential in homogeneous catalysis. Copper is far cheaper than noble metals and the overall amount of Copper on the planet is enormous. Furthermore, Copper salts are typically less toxic. Cu-based materials may assist and undergo a wide range of reactions. Since Cu has a wide variety of readily available oxidation states (Cu^0 , Cu^{I} , Cu^{II} , and Cu^{III}), which allows reactions with ionic and radical intermediates through one and two electron routes. Curiously, despite Cu(II) being the most stable oxidation state of Copper, Cu(I)/Cu(III) are isoelectronic with Pd(0)/Pd(II). Cu(II) derivatives predominate in the coordination chemistry of Copper, Because they are (i) redox active, (ii) frequently labile, (iii) unusual in their tendency to be distorted (iv) Copper (I or II) complexes are substantially less geometrically predicted than other first-row

complexes of transition metals due to the tendency for deformed coordination geometries.^{29,30} Copper(I) mostly favours ligands with soft donor atoms, such as C, P thioether S, and aromatic amines. The majority of Cu(I) complexes are four-coordinate species that assume a tetrahedral shape, even though three coordinated trigonal configurations and two coordinated linear arrangements have been found. Cu(II) complexes, the coordination number ranges from four to six, with the most common geometries being the four coordinate square-planar (sp), six coordinate octahedral (oc) five coordinate trigonal bipyramidal (tbp) geometries. Copper's excellent capacity to interact with both hetero atoms and pi systems further increased the catalytic efficiency. Furthermore, Copper in its many oxidation states interacts well with a diverse range of functional groups via π -coordination or Lewis' acid interaction. It can produce both σ - and π -complexes by accommodating both hard and soft ligands.³¹ Copper is commonly regarded as a "metal of choice" in homogeneous catalysis and in organometallic chemistry due to its extensive applications in variety of organic transformations.³²

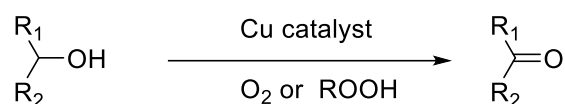
These outstanding properties of Copper have been effectively utilised in several processes, including the Ullmann-Goldberg coupling, Ullmann coupling,³³ Ullmann diaryl ether production,³⁴ Cadiot-Chodkiewicz reaction,³⁵ Ullmann-Hurtley condensation,³⁶ Chan-Lam reaction,³⁷⁻⁴⁰ and others. These reactions are supported by the creation of C-C and C-N bonds. Later studies were done on a variety of additional bonding modes, including C-S, C-O and others. Amination and etherification of aryl halides and related compounds, hydrosilylation reactions, aziridination of olefins, "click chemistry," oxidation, additions to carbonyl and, unsaturated carbonyl compounds, etc. are some examples of Copper-catalyzed reactions that are currently useful for the synthesis of organic compounds. This thesis is focusing on two reactions i) oxidation of alcohol (ii) click chemistry. I have divided my thesis introduction into two parts, in first part I will show the selective oxidation of alcohol to aldehyde, ketone and acids, in the second part I will describe the click chemistry.

Chapter-1.1

1.1 Cu-based oxidative transformation reactions

The most popular form of oxidation reaction in organic chemistry is the conversion of alcohols to ketones, aldehydes, and carboxylic acids. There are many reagents and catalysts for these reactions, but creating efficient techniques for aerobic oxidation is still challenging. Traditional oxidation processes employ stoichiometric concentrations of oxidants, such as chromium (VI), MnO₂ or the Swern reagents, Moffatt oxidants, Corey Kim oxidants, Dess-Martin periodinane are frequently hazardous which produce large quantities of byproducts.⁴¹⁻⁴³

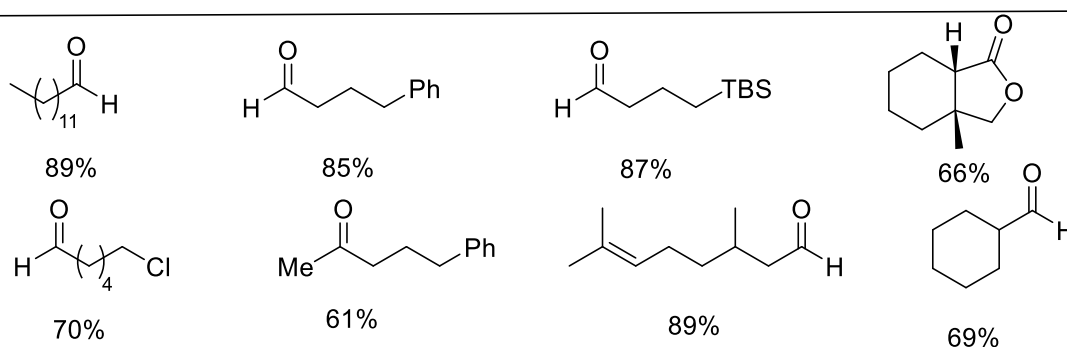
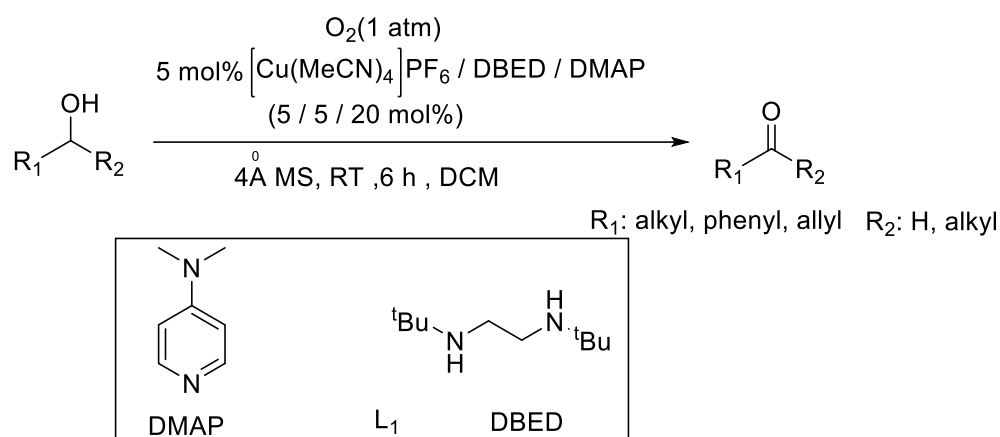
Scheme 1.1.1 Oxidation of both primary and secondary alcohol



Alcohol oxidation with molecular oxygen

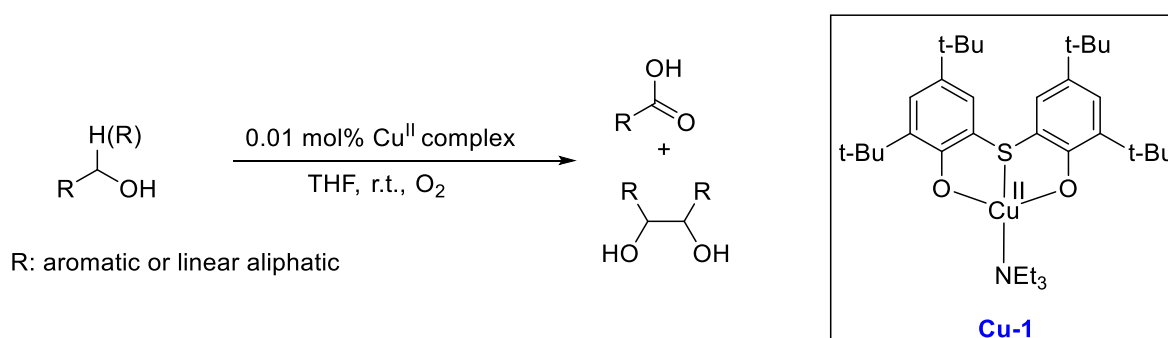
Arndtsen and colleagues described the use of tetrakis(acetonitrile)Copper(I) hexafluorophosphate and N, N-di-tert-butyl ethylenediamine in the oxidation of a wide scale of activated (1 h) and nonactivated (6 h) alcohols. Although both primary and secondary alcohols could be oxidised using the catalytic system, secondary alcohols were preferred. N-containing bases such pyridine, N-methylimidazole (NMI), and dimethyl aminopyridine (DMAP) affects the catalytic activity, DMAP was selected as the most effective base. Therefore, the Copper metal is used as catalyst, DMAP as a base in presence of air was employed to convert 1-octanol to 1-octanal having 92% conversion rate in 3 hours.⁴⁴

Scheme 1.1.2 The oxidation of active and non-active alcohols



Wieghardt and Chaudhuri developed on this catalyst system by creating a mononuclear Cu^{II} complex, [L₁Cu^{II}(NEt₃)], including doubly deprotonated triethylamine (NEt₃), 2,20-thio-bis(4,6-di-tert-butylphenol as another Goase(Galactose oxidase) mimic for both primary and secondary alcohol oxidation.⁴⁵

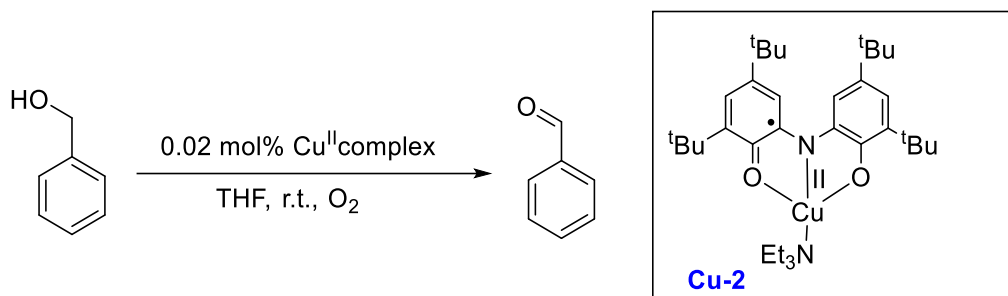
Scheme 1.1.3 Efficient aerobic oxidation of alcohols



In 1999 Wieghardt and colleagues discovered another mononuclear Cu(II)-imino emiquinone complex, [Cu^{II}L₂(NEt₃)], containing double deprotonated N,N-bis(2-hydroxy-3,5-di-tert-butylphenyl)ammonium(L₂) and NEt₃ ligands. After 20 hours at room temperature, the Cu-2

complex was tested in the O₂ mediated oxidation of ethanol and benzyl alcohol to acetaldehyde and benzaldehyde with 55% conversion⁴⁶

Scheme 1.1.4 Aerobic oxidation of primary and secondary alcohols by new mononuclear Cu (II) radical catalyst



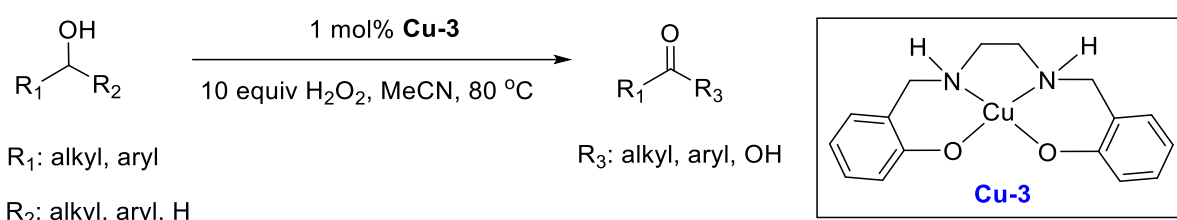
Peroxidative oxidation of alcohols

Oxidation with hydrogen peroxide(H₂O₂)

Peroxidative alcohol oxidation is the most common reactions in organic synthesis due to its relevance and accessibility; cheap, tert-butyl hydroperoxide, hydrogen peroxide oxidants and easy techniques are generally used. Because peroxides may be easily synthesized in aqueous solutions, research to enhance the sustainable development of alcohol oxidations focus on the adoption of water as reaction media. As a result, new water-soluble Copper complexes were synthesized and investigated for their catalytic activity for alcohol oxidation in aqueous media. The oxidant of choice was always hydrogen peroxide, the most ecologically friendly peroxide. In fact, hydrogen peroxide is rapidly degraded in the environment by biological and/or chemical processes, releasing oxygen and water. H₂O₂ neither evaporates nor adsorbs to soil. Punniyamurthy and colleagues published the first instance of a Cu-based catalyst system involving H₂O₂ in 2003.⁴⁷ Compound (Cu-3) was tested in conjunction with H₂O₂ (30% H₂O) for the oxidation of 4-chlorobenzyl alcohol in acetonitrile in room temperature to produce a yield of 30% that comprises mixture of 4-chlorobenzoic acid and 4-chlorobenzaldehyde (ratio of 1:2) at 60 °C. But, when the temperature was raised to 80 °C, the conversion rate soared to

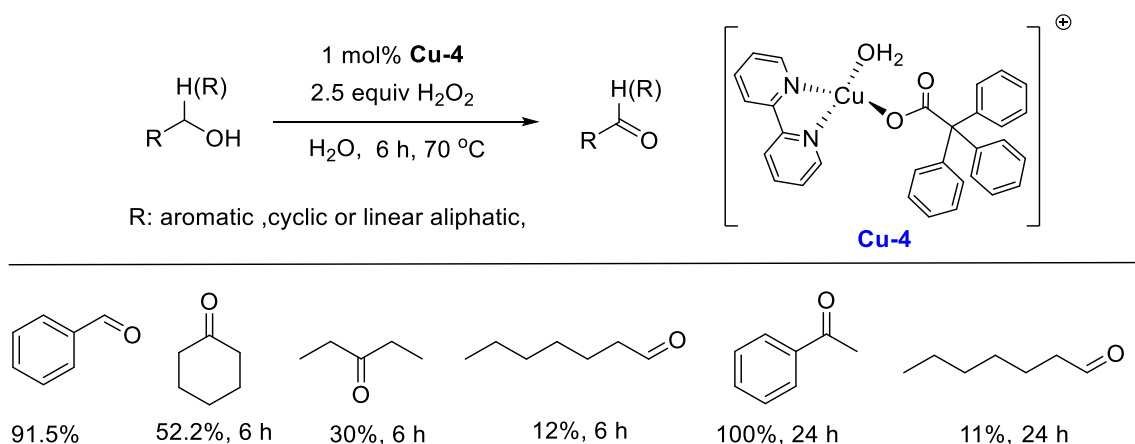
95% after 4.5 hours. When the catalyst was substituted with Cu (OAc)₂ · 2H₂O or CuII(salen), lower conversions of 30 and 65% were achieved, respectively. Additionally, when without the catalyst or when O₂ was used as the oxidant, the oxidation process did not occur. Catalytic oxidation of primary alcohols resulted in the synthesis of carboxylic acids, whereas secondary alcohols ended with the ketones.

Scheme 1.1.5 The oxidation of aromatic and aliphatic alcohols by using the Cu-3 complex



In 2017, Kani and coworkers synthesized mononuclear Cu(II) complex which is soluble in water used as catalyst for the selective oxidation of primary and secondary alcohols to corresponding carbonyl compound without forming the overoxidation product that is acid.⁴⁸ They use water and H₂O₂ as a reaction media. Aliphatic alcohol gives low yield whereas catalyst show good yield when they utilize benzyl alcohol.

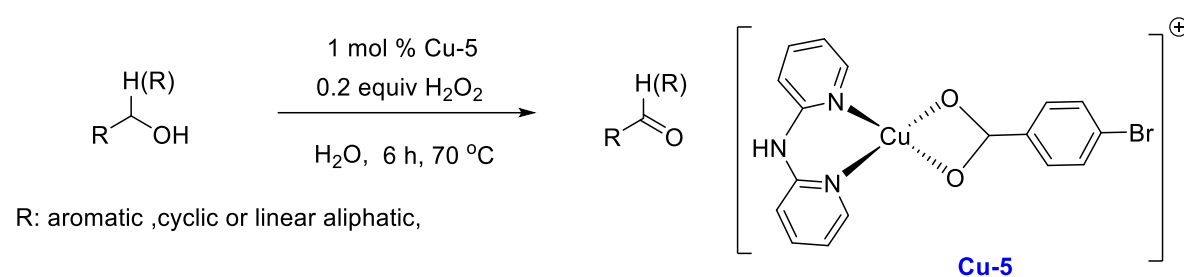
Scheme 1.1.6 The application of Cu-4 and H₂O₂ for the oxidation of primary and secondary alcohols at 70 °C



Again the same group utilize the exact reaction conditions to know the best activity of the catalyst, a new water soluble Cu(II) complex comprising 4-bromobenzoate/2,2-

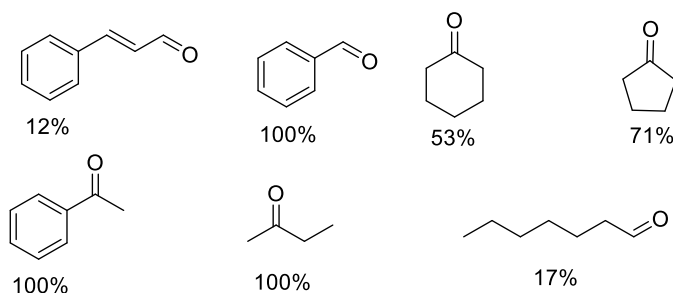
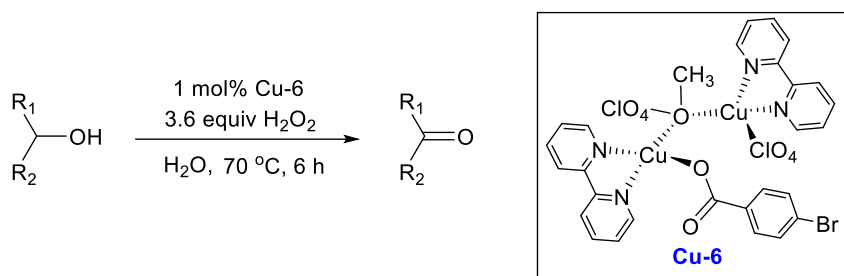
dipyridylamine for oxidation of the corresponding alcohols was introduced.⁴⁹ This complex has been used as catalyst to realize the catalytic activity. The substrate like benzyl alcohol, cinnamyl alcohol, 1-phenylethanol, cyclohexanol, 1-heptanol showing good conversion in aqueous medium. Alkene was also tested and shows very good yield. H₂O₂ is used as oxidant for alcohol oxidation while *t*-BuOOH (TBHP) is used for alkenes.

Scheme 1.1.7 The application of Cu-5 and H₂O₂ for the oxidation of primary and secondary alcohols at 70 °C



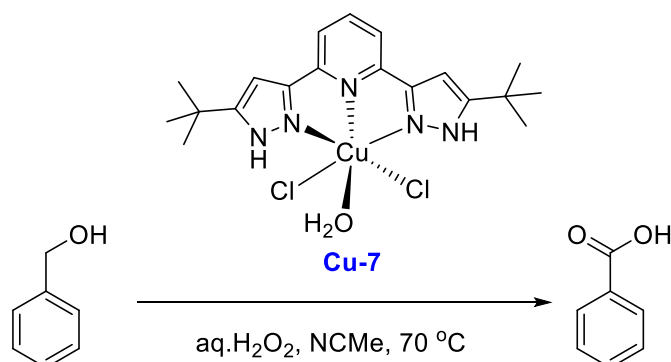
Unver and coworker showed the oxidation of primary and secondary alcohols in homogeneous medium in 2018, This reaction is performed by water soluble di-nuclear Cu (II) complex, utilizing H₂O₂ (30%) in water and air at 70 °C.⁵⁰ The appropriate aldehydes or ketones were produced using the di-nuclear complex as an active catalyst. Therefore, with simultaneous high turnover number (TON) values, 1-phenylethanol and benzyl alcohol were substantially oxidised in 6 hours. In general, it was discovered that **Complex 5** worked better as a catalyst for cyclic and benzylic alcohols. Moreover, this catalytic system's selectivity examined between primary and secondary alcohols as well as between cyclic and aliphatic alcohols. In the process of oxidising the combination of benzyl alcohol and 1-phenylethanol, 62% acetophenone and 16% benzaldehyde were produced.

Scheme 1.1.8 Oxidation of various alcohols with Copper (II) complex in water



In order to test the catalytic activity of the recently synthesized **Cu-6** complex, Hu et al. examined the oxidation of benzyl alcohol. At 70 °C, the oxidation processes were carried out using a 30% aq. solution of H₂O₂ in acetonitrile.⁵¹ Pleasingly, and in contrast to most Copper catalysts, which produce mostly benzaldehyde under light in the presence of catalyst (**Cu-6**), after 1 hour under the specified milder conditions, 97% benzoic acid (96%) was isolated from benzyl alcohol.

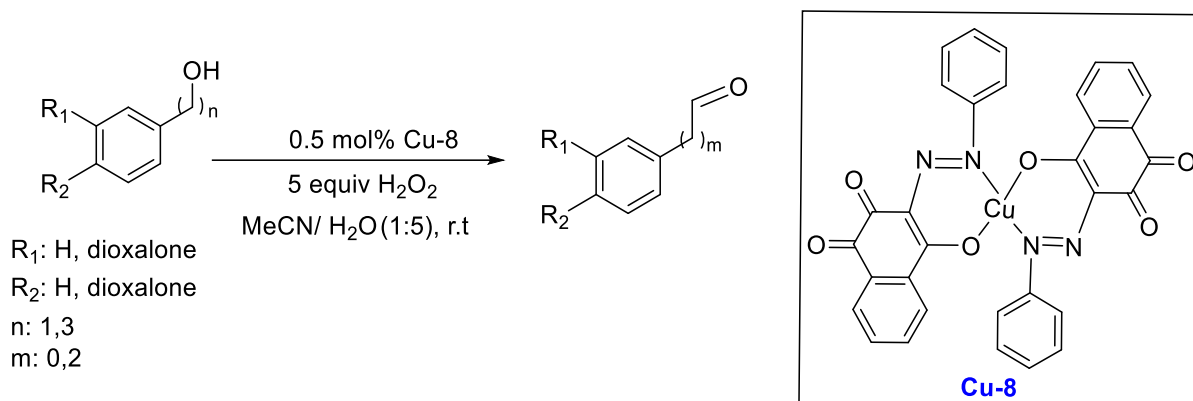
Scheme 1.1.9 Complete oxidation of benzyl alcohol to benzoic acid in the presence of Cu(II) complex



Shoair described the usage of CuII complexes with substituted 4-hydroxyl-1,2-naphthoquinone ligands in mixed with H₂O₂ towards the oxidation of benzyl alcohol (90%), and cinnamyl

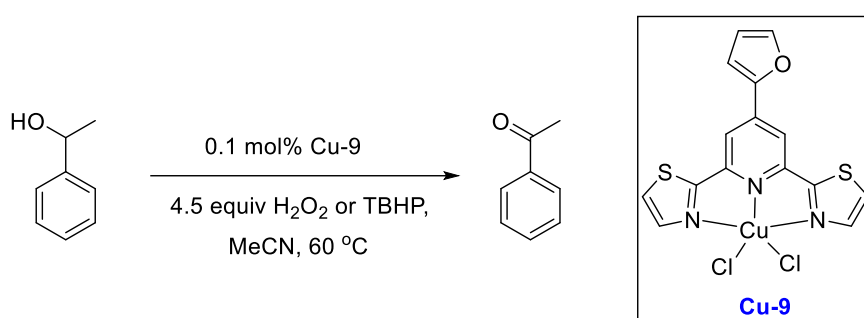
alcohol (75%), piperonyl alcohol (80%), for 2 hours at room temperature, in a MeCN/H₂O (1:5) solvent system.⁵²

Scheme 1.1.10 Cu-8/H₂O₂ catalyst system for the oxidation of benzyl, cinnamyl, piperonyl alcohol at room temperature



Shul'pin and team developed the oxidation of cyclic and secondary benzylic alcohols using CuII complexes with functionalised 2,2':6,2''-terpyridine and 2,6-di(thiazol-2-yl) pyridine ligands.⁵³ By employing TBHP or H₂O₂ (30% in H₂O) in association with [CuCl₂(R₁-dtpy)] an almost conversion of 98% with a turnover number of 630 was observed at 60 °C in 5 h.

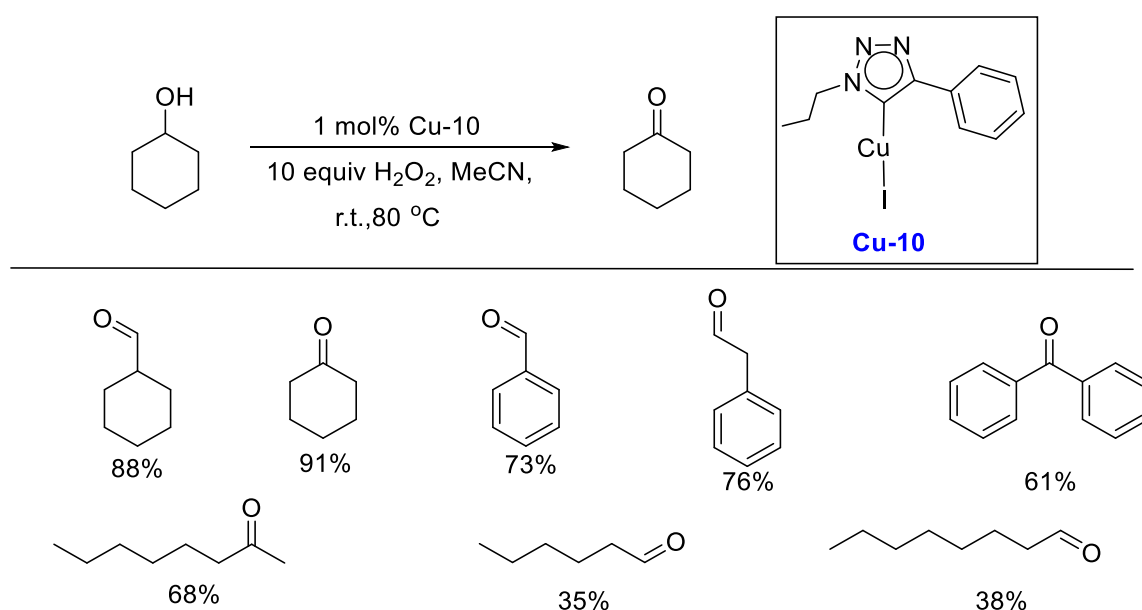
Scheme 1.1.11 The application of Cu-9 and H₂O₂ or TBHP for the oxidation of 1-phenylethanol at 70 °C



Mncube and Bala proposed the use of in situ synthesized CuI complexes including CuI in a 1:1 ratio with NHC-triazolylidene ligands and H₂O₂ on the peroxidation of cyclohexane. Under optimized reaction conditions, the oxidation of alcohol substrates has been tested.⁵⁴ The use of **complex Cu-9** and H₂O₂ as the oxidants tends to result a maximum conversion of 91% to

cyclohexanone at 80 °C in 24 h. Aliphatic alcohols were less reactive than phenolic benzylic and phenolic alcohols. Additionally, secondary aliphatic alcohols were shown to have greater catalytic activity than primary alcohols, meaning that reactions at the secondary carbon atom of aliphatic alcohols are easier to perform than reactions at either the primary or terminal carbon atoms.

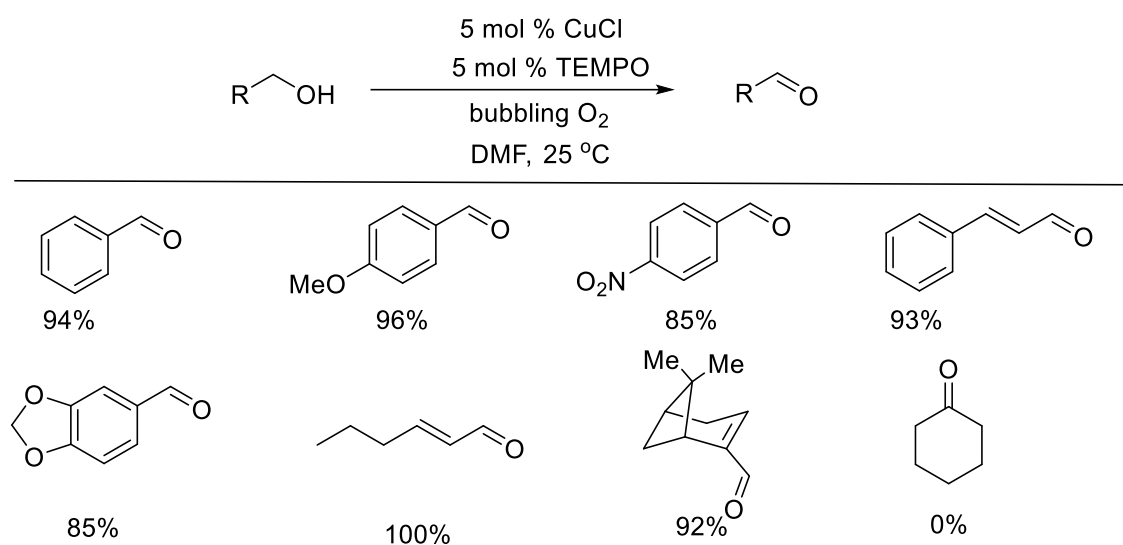
Scheme 1.1.12 The oxidation of cyclohexanol in presence of Cu-10/H₂O₂ catalyst at 80 °C in 24 h



Oxidation of alcohol with TEMPO

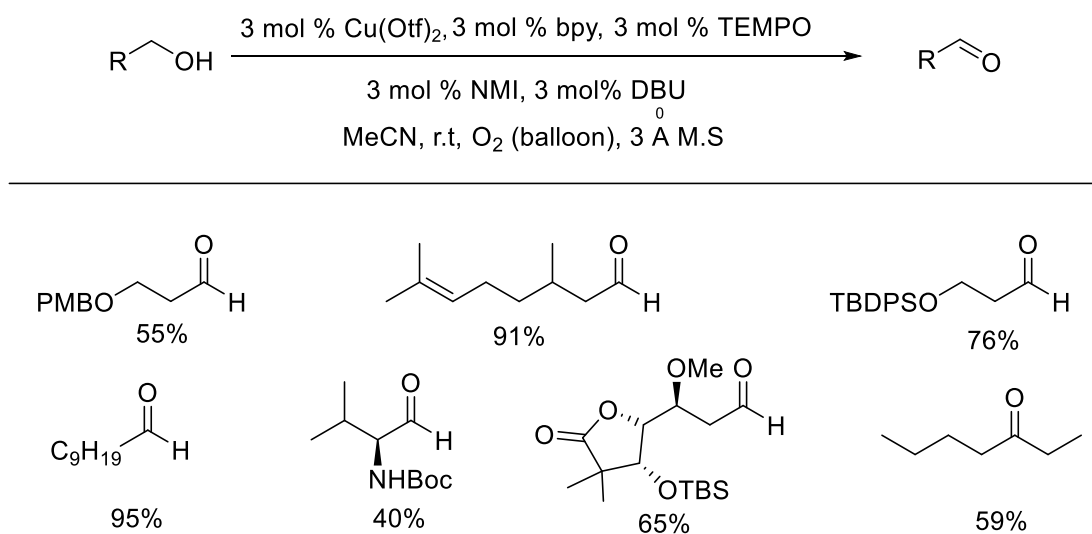
In 1984 Semmelhack published the first study of the synthesis potential of Cu/nitroxyl-catalyzed aerobic alcohol oxidation.⁵⁵ CuCl and TEMPO in dimethyl formamide facilitate the oxidation of several reactive primary alcohols (benzylic and allylic). Since aliphatic alcohols are substantially less reactive, stoichiometric amounts of Copper and TEMPO were needed to oxidized them at the observed conditions.

Scheme 1.1.13 Aerobic oxidation of activated alcohols by CuCl/TEMPO in DMF reported by Semmelhack



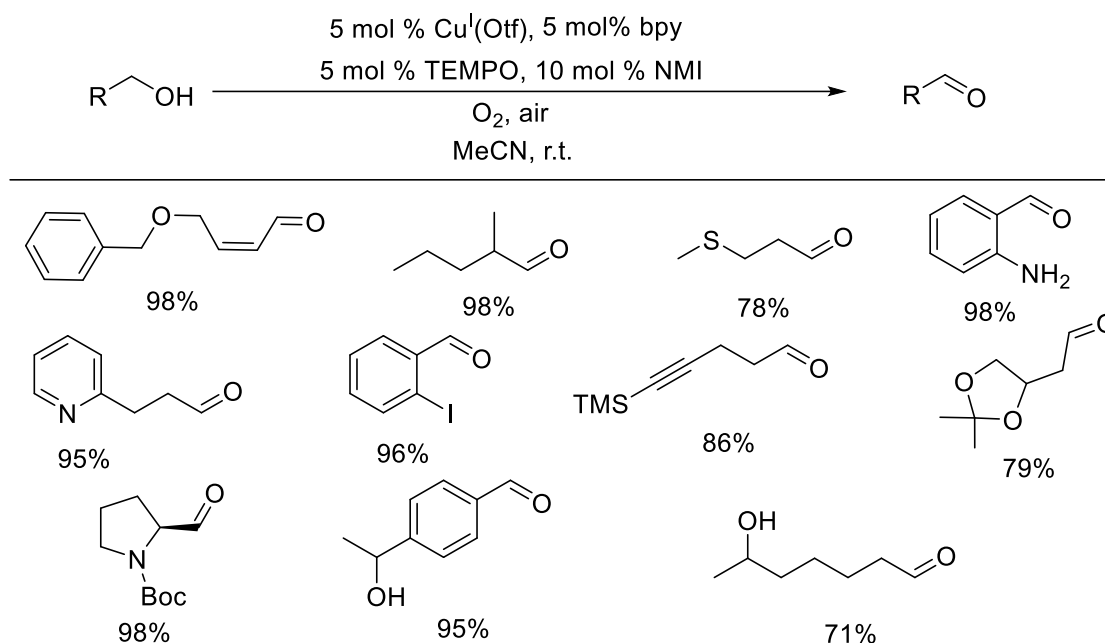
Koskinen's research groups designed two catalysts with extensive synthetic use for the oxidation of primary alcohols to aldehydes, involving aliphatic substrates.⁵⁶ Kumpulainen and Koskinen's catalytic system contains Cu(OTf)₂/bpy/TEMPO, two heterocyclic bases, 1,8-diazabicycloundec-7-ene (DBU) and N-methylimidazole (NMI) and 3 Å molecular sieves. Many aliphatic alcohols were oxidized at ambient temperature in 1-5 hours in an air of pure O₂. This reaction sustains ethers, alkenes esters, alcohol, and protected amines. This catalyst system's modifications, which differed in the identities of the organic base (among NMI, DMAP, DBU, shown outstanding activity in the aerobic oxidation of benzylic and allylic alcohols.

Scheme 1.1.14 Aerobic oxidation of aliphatic alcohols with reported Koskinen



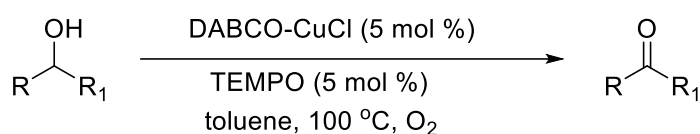
Hoover and Stahl observed a significant increase in catalytic activity when they used Copper(I) instead of Cu(II). Copper iodide salts having a non-coordinating anion (CuI, OTf) were highly efficient and the CuOTf/bpy/TEMPO/NMI catalyst was suitable for oxidation of benzylic, propargylic, allylic, and aliphatic alcohols. Almost all the reactions were carried out in ambient temperature, while several aliphatic alcohols needed heating to 50 °C for complete conversion. Several common functional groups, such as anilines, aryl halides, nitrogen and sulphides, sulphur heterocycles are well tolerated.⁵⁷

Scheme 1.1.15 Aerobic oxidation of aliphatic alcohols with bpy/CuI/NMI/TEMPO reported by Stahl



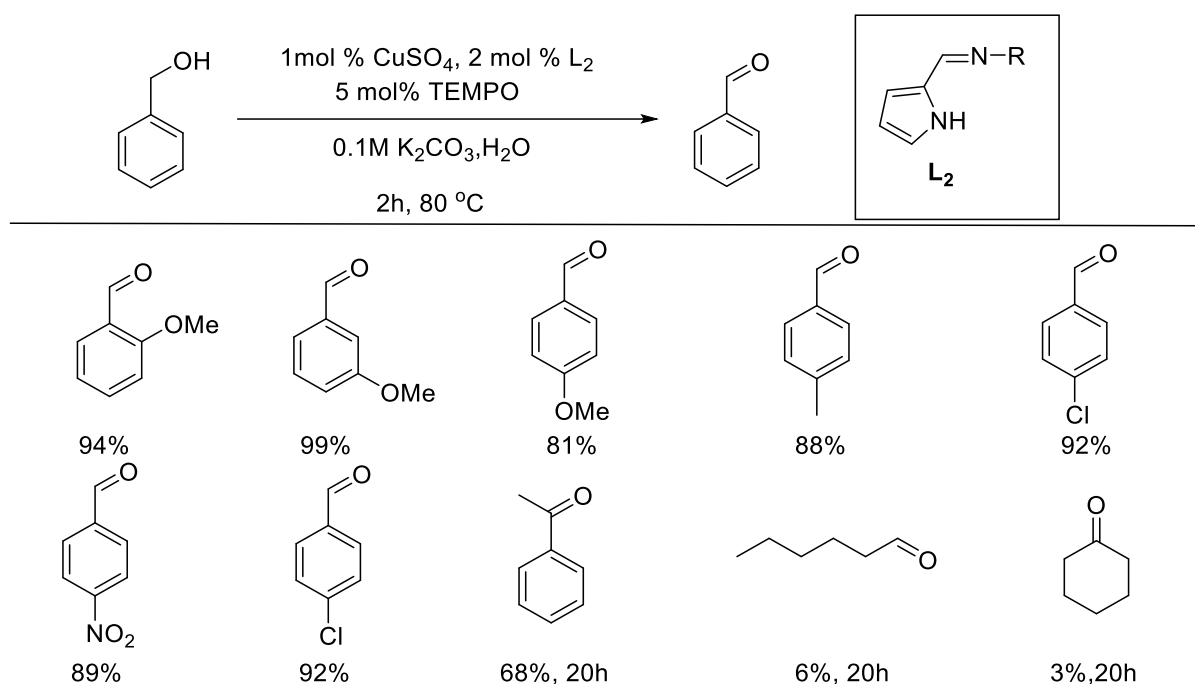
G. Seker and co-workers demonstrated the preferential oxidation of benzylic and allylic alcohols to the respective carbonyl compounds at room temp using a molecular oxygen DABCO-Copper(I) chloride complex (5 mol %) in nitromethane as a solvent as an excellent catalytic system.⁵⁸

Scheme 1.1.16 Oxidation of alcohol using DABCO-CuCl complex



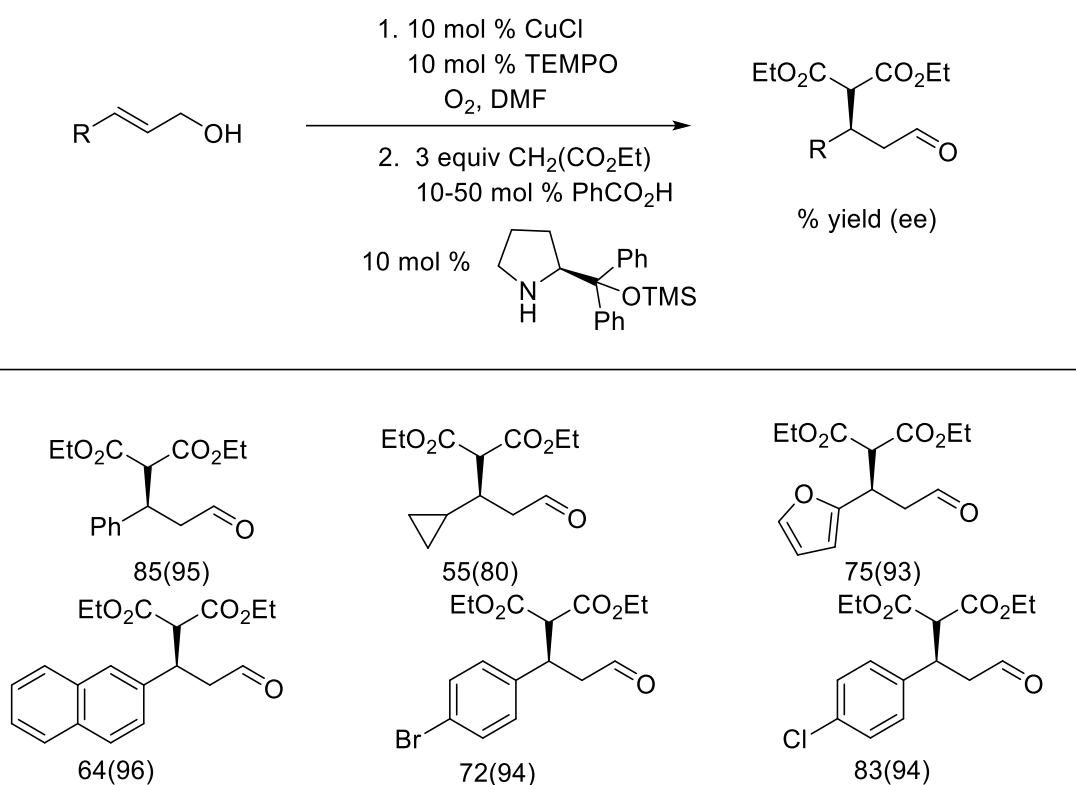
Timo Repo et al. discovered a very active catalytic system for aerobic benzylic alcohol oxidation in alkaline water solutions based on Copper 2-N-arylpyrrolicarbaldimino complexes for both catalytic systems.⁵⁹ For instance, quantitative conversion of benzyl alcohol to benzaldehyde may be accomplished in 2 hours at 80 °C with in situ produced bis[2-N-(4-fluorophenyl)-pyrrolicarbaldimide] Copper (II) catalysts.

Scheme 1.1.17 Aerobic oxidation of benzylic alcohols in water



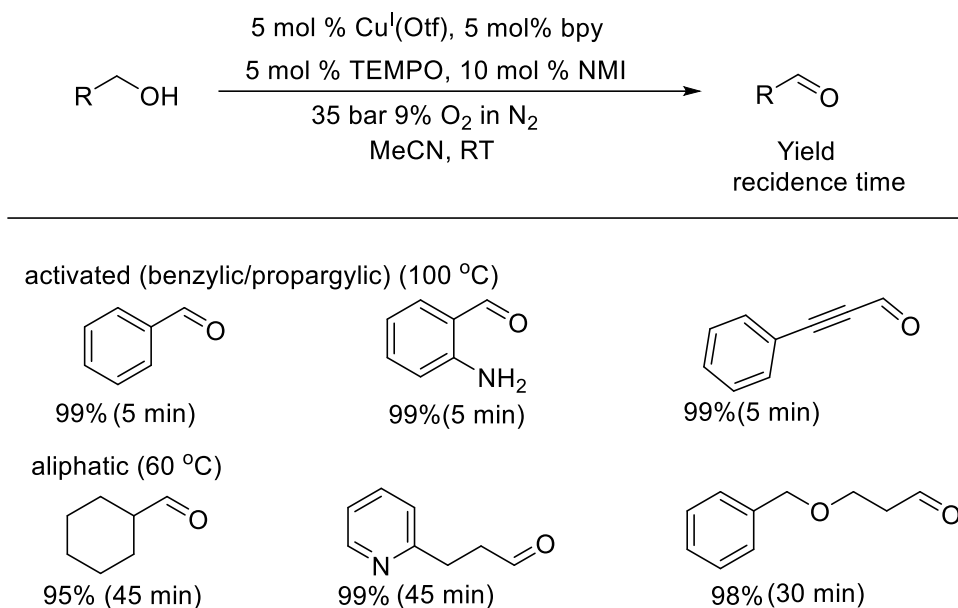
Jang et al. demonstrated Cu/TEMPO mediated oxidation of allylic alcohol may be carried out with enantioselective organocatalytic Michael additions without isolating the intermediate aldehyde.⁶⁰ Dimethyl malonate was added to oxidised cinnamyl alcohol with the use of a chiral amine catalyst, producing the necessary Michael addition product in 43% yield and 94% ee. Then, with the presence of diethyl malonate, a variety of allylic alcohols have been subjected to the reaction conditions. The process included halogen-substituted cinnamyl alcohols, which produced excellent yields and good enantioselectivities. 2-furyl- and 2-Naphthyl-substituted allylic alcohols were transformed into desirable products with a 74% yield with of 93 % and 96% e.e, respectively.

Scheme 1.1.18. TEMPO mediated copper catalyzed allylic alcohol oxidation/conjugate addition



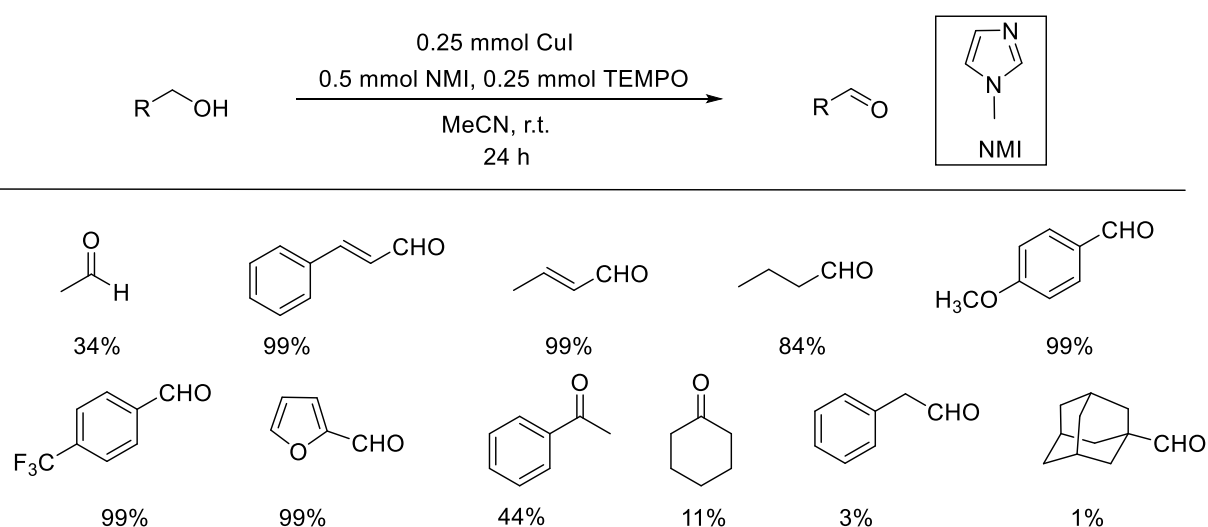
Shannon S. Stahl et al. proposed a reproducible, continuous-flow approach for implementing a homogenous CuI/TEMPO catalyst system for oxidation of primary alcohols to corresponding carbonyl compound.⁶¹ This catalyst is suitable with different types alcohols with varying functional groups. To avoid explosive oxygen/organic combinations, a dilute oxygen source (9% O₂ in N₂) is employed. The flow-based catalytic technique has substantial benefits for aerobic alcohol oxidation. This catalyst has substantially quicker. It tolerates a wide range of substituted heteroatom, including halogenated arenes, thioethers, pyridines. Primary alcohols and aliphatic substrates are both transformed with a high degree of selectivity.

Scheme 1.1.19 Aerobic Oxidation of Primary Alcohols with a Copper(I)/TEMPO Catalyst



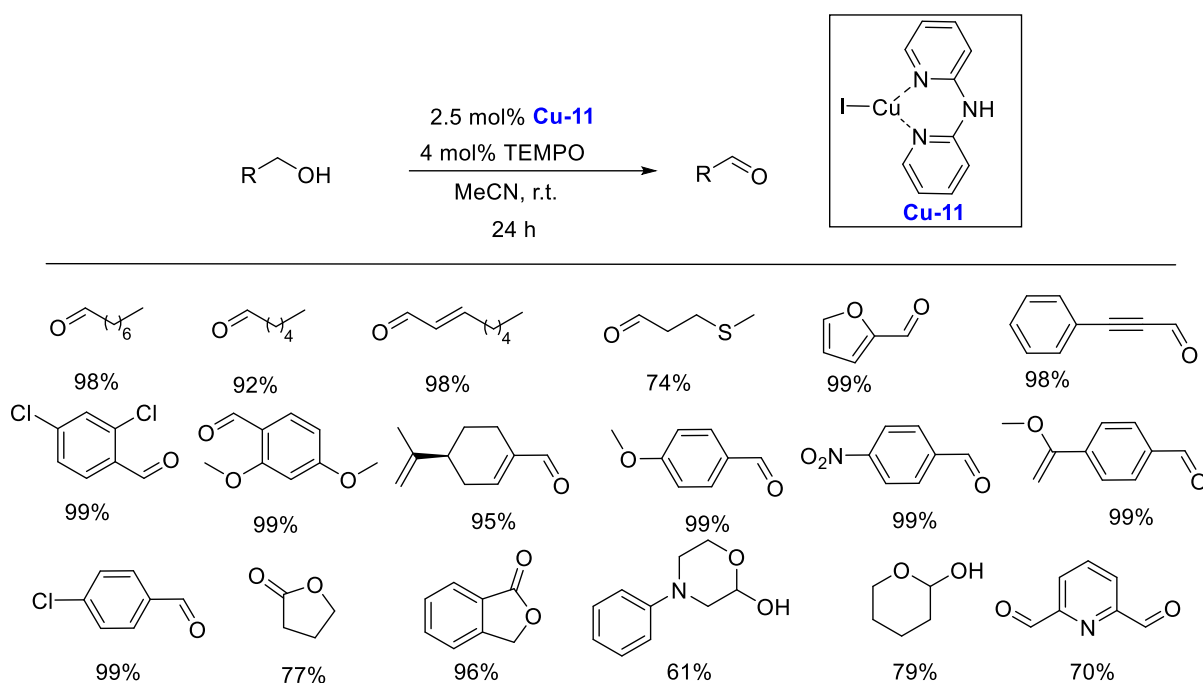
Liu et al. described a homogeneous Cu(I)/TEMPO/NMI catalyst for the aerobic oxidation of 1-octanol and other alcohols into the corresponding aldehydes in acetonitrile at ambient temperature.⁶² Cu(I) complex [CuI(NMI)(CH₃CN)₂] was discovered to be the catalytic species, with the labile solvent binding to the Copper center is necessary for alcohol and oxygen coordination.

Scheme 1.1.20 Cu(I)/NMI/TEMPO catalyzed by aerobic oxidation of alcohol



Repo et. al targeted a base-free Cu(I) catalyst for the aerobic oxidation of primary alcohols to corresponding carbonyl compound and different lactones, lactols, diols. In the presence of a Cu(I)-catalyst generated in situ that included a ligand of 2,2'-dipyridylamine (dpa) and a sustained radical of 2,2,6,6-tetramethylpiperidine-N-oxyl (TEMPO), the oxidation process takes place in true aerobic environments, at room temperature, with air as the oxidant and without base. Several primary alcohols (allylic, aliphatic, benzylic and diols) with various substitution patterns showed high catalytic activity without excess oxidation.⁶³

Scheme 1.1.21 Copper (I) catalyst for the selective aerobic oxidation of primary alcohols

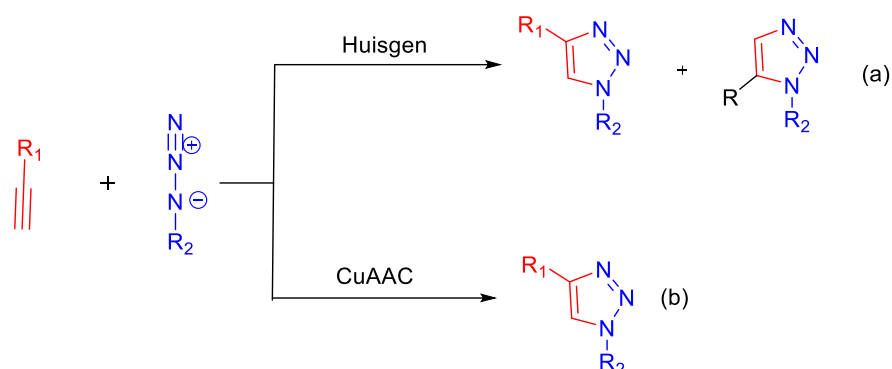


Chapter-1.2

1.2 Cycloaddition reactions by Copper catalyst

In recent years, Cu-based complex-based chemical conversions have become an essential tool. CuAAC, often known as the "click" reaction, has been shown to be extremely specific for Copper(I) complexes, where the oxidation state of the metal remains unchanged right through the process. It has been discovered that the CuAAC reaction has a wide range of applications in molecular engineering, including physiologically active compounds, functional macromolecules, nanomaterials, and the development of several therapeutic drugs, etc. in both industry and academia. In this chapter I will be focusing on Copper catalyzed azide-alkyne cycloaddition via click chemistry. The 1,3-dipolar cycloaddition reaction between terminal alkynes and organic azides, popularly known as the "click reaction," was independently discovered in 2002 by Karl. Sharpless⁶⁴ and Morten P. Meldal⁶⁵. This significant discovery is based on the previously published Huisgen cycloaddition, which is the most authentic example of this "click chemistry" principle, as a synthetically produced tool that accelerates steadily in heating condition, generating a mixture of 1,4- and 1,5-disubstituted 1,2,3-triazoles (Scheme 1.2.1a)^{65a}. By simply adding a Copper catalyst to an atom-economic 1,3-dipolar cycloaddition, Meldal and Sharpless found that the 1,4-triazole was the only product produced, meeting the principles of "click chemistry." (Scheme 1.2.2b).

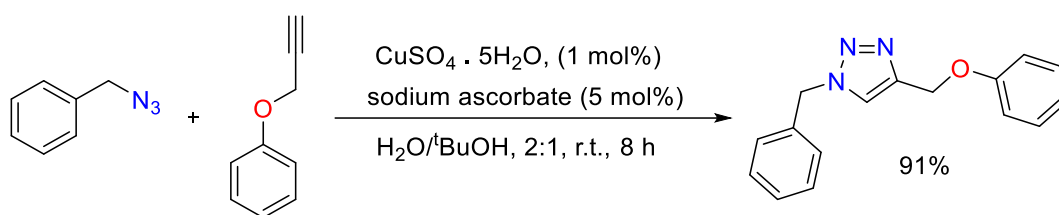
Scheme 1.2.1 Cu-catalyzed cycloaddition of azides and terminal alkynes (a) thermodynamically generated Huisgen cycloaddition vs (b) CuAAC



Later, the reaction gained widespread acceptance in the scientific community due to its adaptable and flexible strategies for the simple synthesis of 1,4-disubstituted 1,2,3-triazoles, which have numerous applications in medicine,⁶⁶⁻⁶⁸ pharmaceuticals,^{69,70} chemical and biological sciences,⁷¹⁻⁷⁵ material sciences,⁷⁶⁻⁸⁰ drug discoveries,⁸¹⁻⁸⁴ and catalysis.⁸⁵⁻⁸⁹ Karl B. Sharpless, Morten P. Meldal, and Carolyn R. Bertozzi received the 2022 Nobel Prize in Chemistry for their groundbreaking work on click and biorthogonal chemistry.

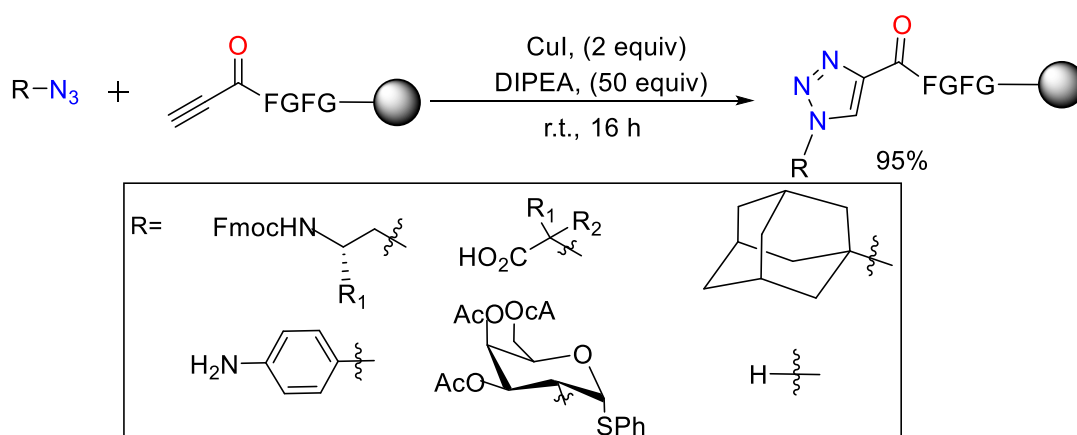
The pure technique was thoroughly examined in Sharpless' report⁶⁴ (**scheme 1.2.2**), examining the interaction of alkynes with azides on a wide range of substrates. The described conditions are air and moisture sensitive, consisting of a pre catalyst system comprising CuSO₄ (1 mol %) and sodium ascorbate (5 mol %) loading. The sodium ascorbate both produces the active Cu(I) catalyst and decreases any Copper(II) generated during the process by oxidation with air. By dissolving most of the substrates tested as well as the catalytic system, the tert-butanol/water solvent solution allowed for uniform catalysis. It would also commonly precipitate triazole from the reaction mixture.

Scheme 1.2.2 Sharpless Copper(I)-catalysed azide-alkyne cycloaddition (CuAAC)



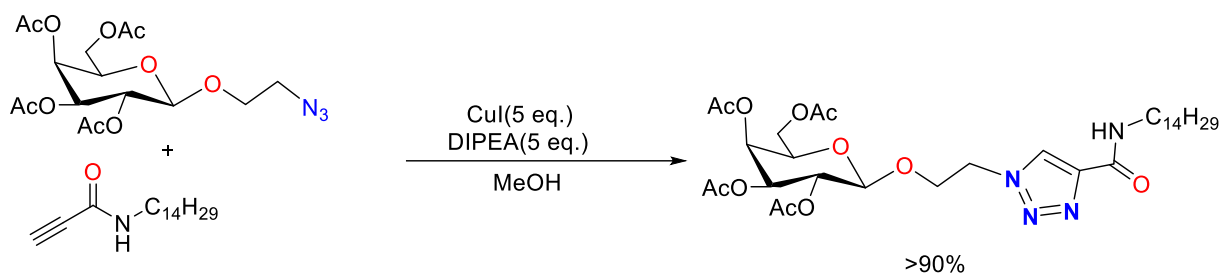
Meldal's⁶⁵ work focuses on the reaction's biochemical uses (**scheme 1.2.3**). They have utilized CuCl in stoichiometric amount, it was possible to couple resin-bound peptide chains with alkyne to organic azide. Here various 1,4-substituted [1,2,3]-triazoles in peptide backbones or side chains were produced by the Copper(I)-catalyzed cycloaddition using primary, secondary, and tertiary alkyl azides, aryl azides, and an azido sugar. Solid-phase peptide synthesis on polar supports was entirely feasible under the reaction conditions.

Scheme 1.2.3 1,3-dipolar cycloaddition of terminal alkynes to azides, regioselective Copper(I) catalyses the formation of [1,2,3]-triazoles



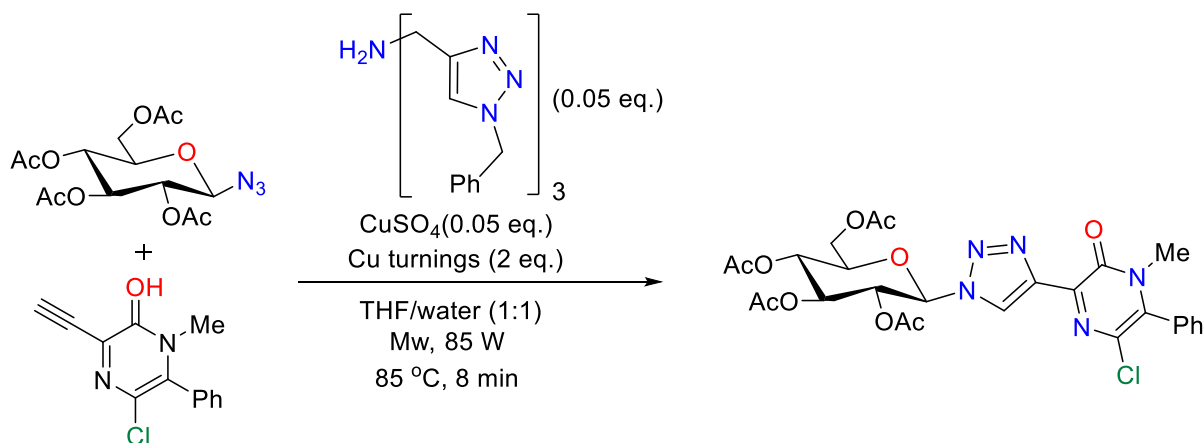
Wong⁹⁰ and colleagues made a quick discovery of the Cu(I) catalysed azide-alkyne cycloaddition process at the Scripps Research Institute, who used the process devised by Meldal's laboratory using Copper(I) iodide using DIPEA to link a propiolamide derivative linked to polystyrene microtiter plates with a series of azide-modified saccharides and oligosaccharides.

Scheme 1.2.4 CuAAC on microtiter plate-bound saccharide derivatives.



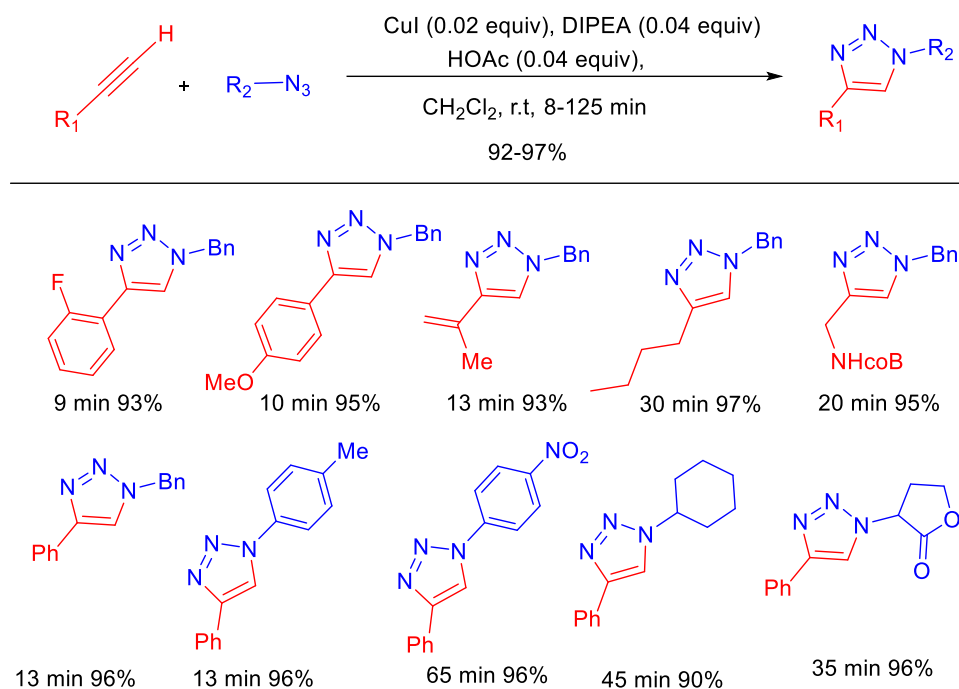
Under microwave conditions, Van der Eycken's group reported⁹¹ the indirect coupling of various mono- and disaccharides via 1,2,3 triazoles moiety to pyrazinones utilizing the activating tris(triazolyl) ligand TBTA with CuSO₄/Copper turnings as catalyst (**scheme 1.2.4**).

Scheme 1.2.5 Indirect Coupling of the pyrazinones Scaffold with different mono and disaccharides through click chemistry



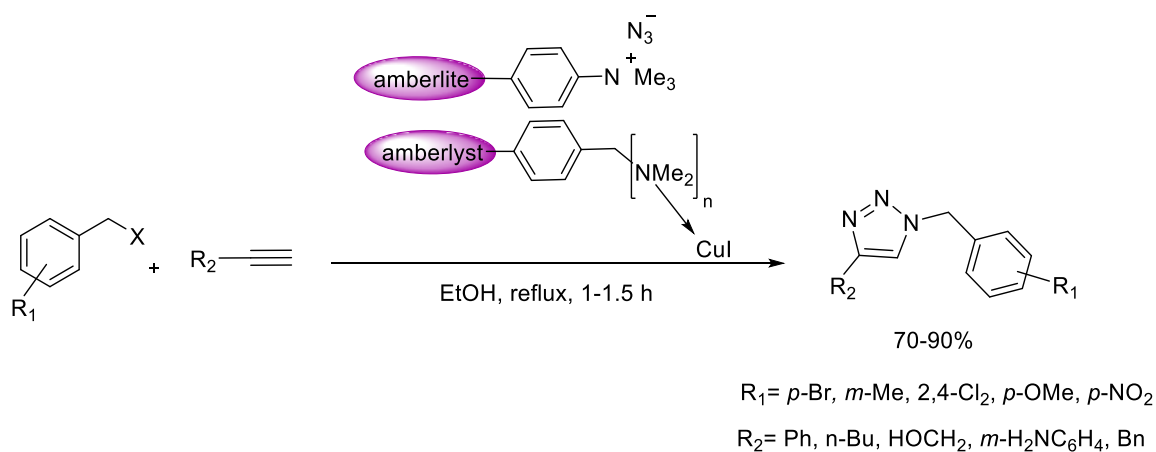
Xinyan Wang⁹² group reported acid base jointly promoted CuAAC, a highly efficient catalytic system was constructed by combining Cu/DIPEA/HOAc. HOAc and DIPEA have been ascribed roles, with HOAc being identified to enable the transformations of C-Cu bond-containing intermediates and to buffer DIPEA's basicity.

Scheme 1.2.6 Copper (I)-catalyzed azide-alkyne cycloaddition enhanced by acid and base



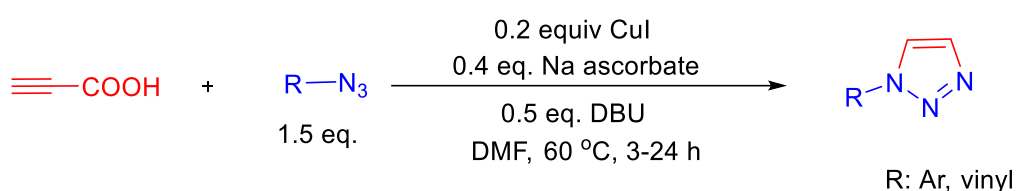
Mosadegh Keshavarz presented in 2013 a one-pot multicomponent click method for synthesising 1,4-disubstituted triazoles from benzyl halides terminal alkynes utilising polymer aided azide and CuI nanoparticles that was novel, easy, and ecologically friendly. Following green chemistry protocols, polymer (amberlyst A21)-immobilized CuI nanoparticles and a macroporous polymer (amberlite IRA-400)-supported azide reagent was employed to speed the production of 1,4-disubstituted-1,2,3-triazoles from various benzyl halides.⁹³

Scheme 1.2.7 A recoverable polymer-supported azide and CuI used in a multicomponent synthesis of 1,4-disubstituted 1,2,3-triazoles



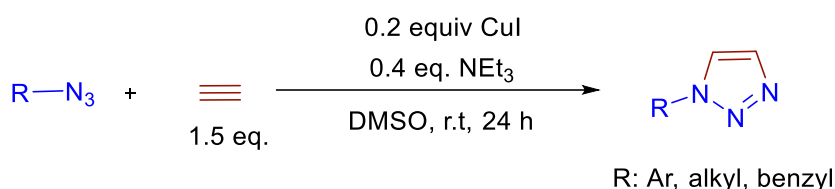
Chunxiang Kuang and teams demonstrated a simple technique for producing 1-monosubstituted 1,2,3-triazoles where propiolic acid was coupled with aryl azides by Copper-catalyzed click cycloaddition. It was readily performed in DMF at ambient temperature or 60°C with medium to good yields.⁹⁴

Scheme 1.2.8 A click cycloaddition/decarboxylation process for 1-Monosubstituted 1,2,3-triazoles



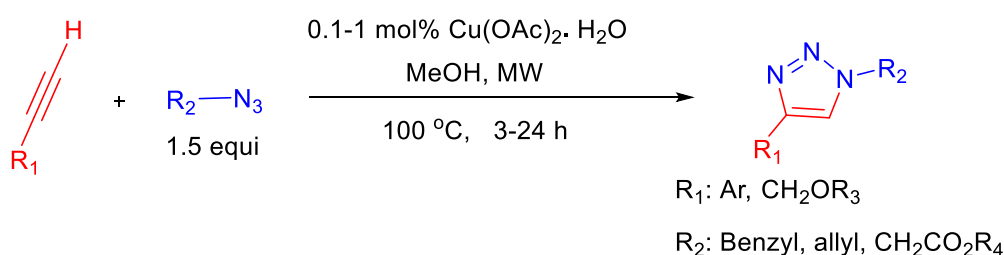
Modak et al. claimed that under moderate conditions, Copper(I)-catalyzed 'click chemistry' with acetylene was effectively investigated. The aromatic and aliphatic azides were easily converted into 1-substituted 1,2,3-triazoles.⁹⁵

Scheme 1.2.9 An efficient synthesis of 1-substituted 1,2,3-triazoles from azides and acetylene using CuI/Et₃N catalyzed 'Click Chemistry'



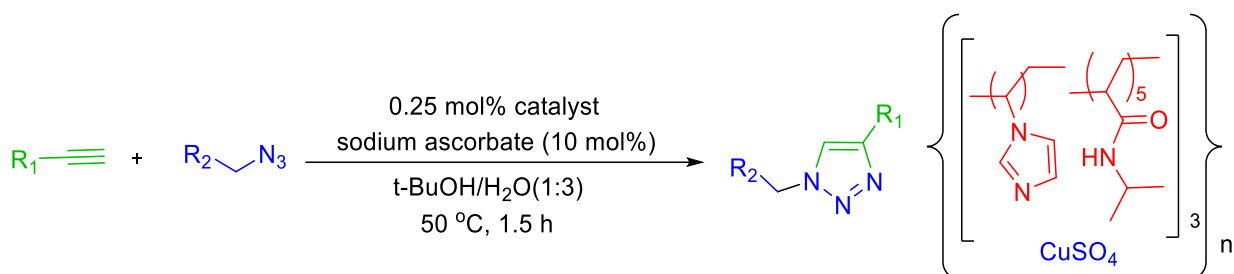
B. R. Buckley et al. demonstrated that in the presence of alkynes, methanol effectively reduces Copper (II) carboxylates, resulting in the formation of yellow alkynyl Copper(I) polymeric precatalysts which are used azides.⁹⁶

Scheme 1.2.10 Alkyne-azide cycloaddition reactions by using stoichiometric amounts of Copper(II) precatalysts in methanol



Yasuhiro Uozumi coworkers developed a unique self-assembled poly[(acrylamideimidazole)Copper] catalyst. At a TON of up to >200000, a catalyst ranging from 0.00045 mol % to 0.25 mol % successfully established the 1,3-dipolar cycloaddition of aryl azides and terminus alkynes, and This could be reused with no loss of catalytic activity or Copper leaching⁹⁷. Under identical circumstances, electron donating and electron withdrawing group substituted naphthylmethyl azides and benzyl azides interacted effectively with to give the respective triazoles in 94-97% yields. The reactions of benzyl azide and the alkyl azides and 4-tolylacetylene with 1-azidodecane 1-azido-2-phenylethane resulted in full conversion, yielding cyclized compounds in 96-97% yields. Hex-5-yn-1-ol, an aliphatic alkynol, rapidly interacted with a range of aliphatic benzylic azides to generate the matching triazoles in 97 % yields.

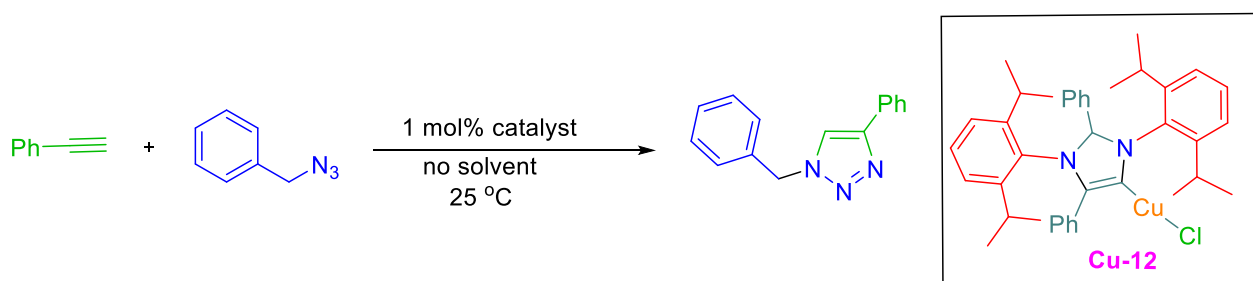
Scheme 1.2.11 Three-component cyclization of alkynes, alkyl halides, sodium azide



Mandal et al. created a flexible and extremely effective catalytic system including the N-heterocyclic carbene which is used for the azide-alkyne cycloaddition at ambient temperature. Under solvent-free circumstances, this catalysis may produce a wide variety of pure triazoles

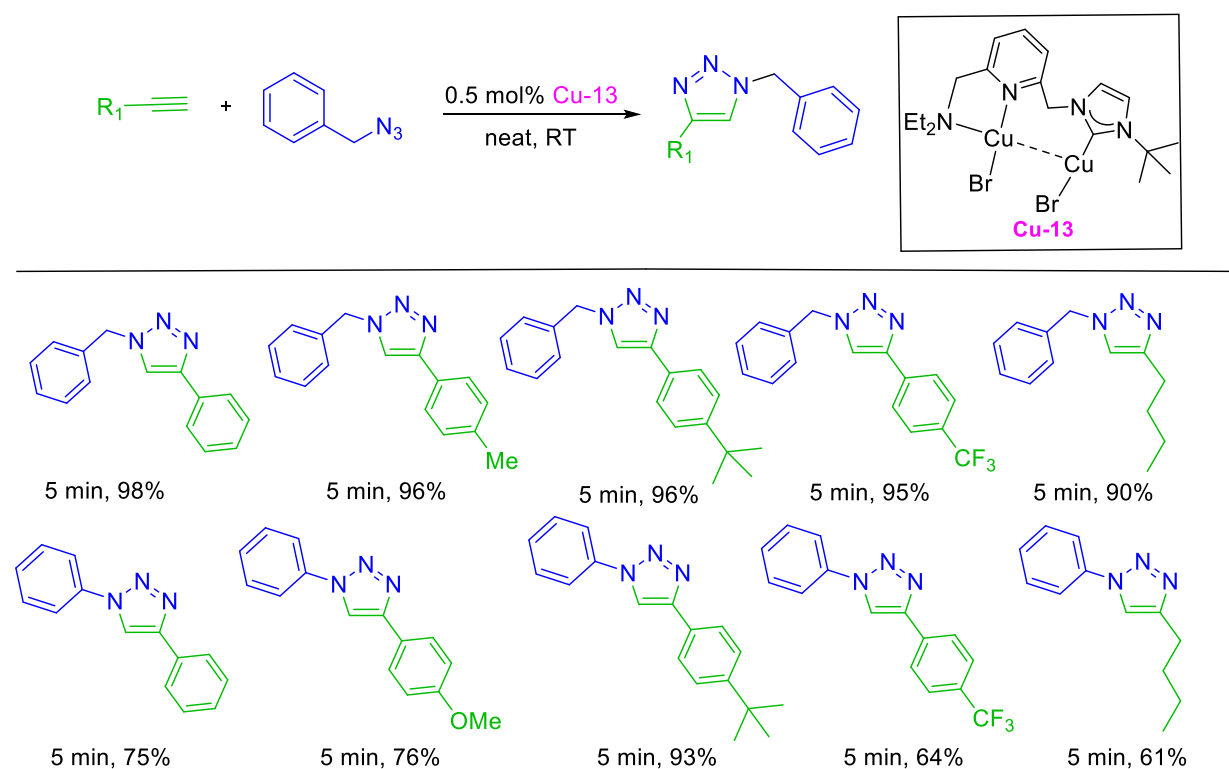
with good to excellent yields in just a brief period. This catalytic method successfully used electron-deficient, electron-rich and different functionalized alkynes and aromatic azides as well as aliphatic azides, yielding about quantifiable yield. The catalyst displayed effectiveness at exceptionally low catalytic loadings of up to 0.005 mol % at r.t., leading to significant TON value of 19,800. In solvent-free circumstances and at room temperature. The catalyst has the potential to successfully catalyse the reaction of sterically hindered azides and sterically hindered alkynes.⁹⁸

Scheme 1.2.12 Abnormal N-heterocyclic carbene-Copper(I) complex in click chemistry



In 2022 M. Victoria Jimenez and co-workers created compounds which are enabled by suitable functionalized NHC-based polydentate ligands. This reaction was carried out in a pot by treating the matching imidazolium salt with an adequate supply of Copper powder and Ag₂O. These complex catalyses the cycloaddition reactions of a variety of azides and alkynes in nitrogen environment at ambient temperature in solvent free circumstances with low catalyst loading, in a few of minutes, the appropriate 1,4-disubstituted 1,2,3-triazole molecules are quantitatively synthesised. With a catalyst loading of 20-50 ppm, the cycloaddition reaction of phenylacetylene and benzyl azide can be carried out.⁹⁹

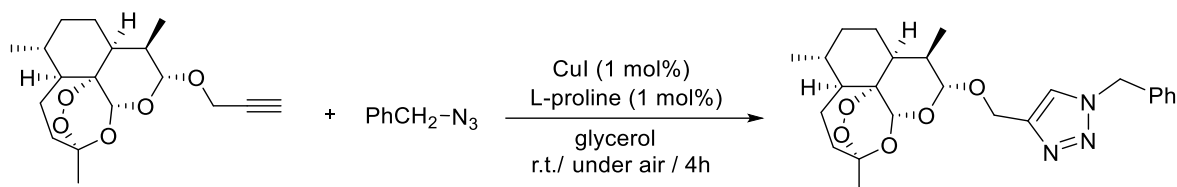
Scheme 1.2.13 Copper-catalyzed azide-alkyne cycloaddition (CuAAC) by functionalized NHC-based polynuclear catalyst



I demonstrated Copper-catalyzed cycloaddition reactions in water and organic solvents which includes alcohols (MeOH, *t*-BuOH and EtOH), THF acetonitrile. The purification of triazole compounds usually involves chromatographic separation, which generates a large amount of solvent waste. The employment of benign solvents is an important aspect in the growth of the green and sustainable process. Solvents are frequently the main cause of waste formation in organic syntheses, hence Solvent selection is therefore a common problem for chemical companies. Application of bio-based solvents for metal catalyzed organic conversion has recently gained the interest of many researchers. To function under tight "click" conditions, the optimum approach is to substitute an ecologically friendly reaction medium for traditional and toxic volatile organic solvents (VOCs). In practice, these solvents should be (i) biodegradable and bio renewable; (ii) non-toxic to both the environment and humans; (iii) cheap and widely available; (iv) capable of dissolving a wide spectrum of substances; and (v) harmless (non-

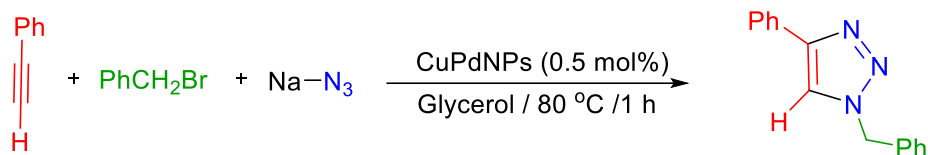
use of this technology was made in the synthesis of potential pharmacologically active heterocyclic molecules, such as those produced from propargylated dihydroartemisinin.

Scheme 1.2.15 CuAAC cycloaddition reaction in glycerol as a reaction media catalysed by CuI or combination of CuI/L(proline)



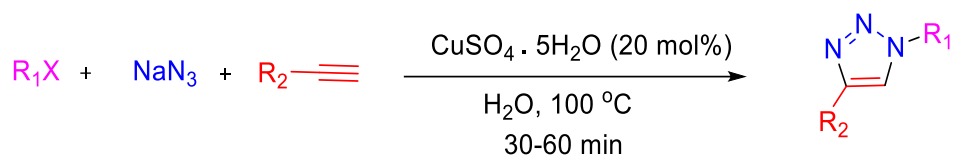
Gomez^{109b} group reported the three-component form of AAC cycloadditions by utilising a combination of $\text{PhCH}_2\text{Br}/\text{NaN}_3$ as a supplier of benzyl azide, the Gomez group has reported the three-component version of AAC cycloadditions in pure glycerol (at 80°C). The catalysts used were small, evenly dispersed, zerovalent PdCu bimetallic nanoparticles (PdCuNPs, mean diameter, ca. 34 nm), stabilised by polyvinyl (see **Scheme 1.2.16**).

Scheme 1.2.16 Cycloaddition of azides and alkynes (AAC) in pure glycerol as solve



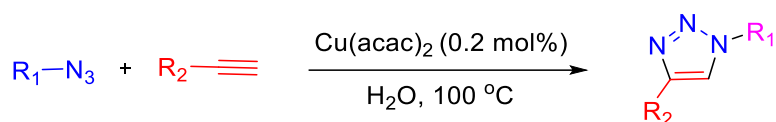
There are many benefits to using water as a reaction medium, including: (i) its lack of toxicity and flammability; (ii) its high availability and low cost (iii) its high boiling point; and (iv) its non-miscibility with organic molecules allows for easy product separation and catalyst recycling during filtration. Therefore, it is in accordance with green chemistry principles that Water appears as one of the most appealing solvents in terms of sustainability, and it is usually used as the solvent of preference when handling with CuAAC procedures. Guiqing Xu and team found a facile approach for synthesizing of 1,4-disubstituted 1,2,3-triazoles in H_2O at 100°C utilizing $\text{Cu}(\text{OAc})_2 \cdot \text{H}_2\text{O}$ (1 mol %) as the catalyst loading resulting in satisfactory yield in 1 h.¹¹⁰

Scheme 1.2.17 One-pot synthesis of triazoles from alkyl halides, NaN₃, and alkynes



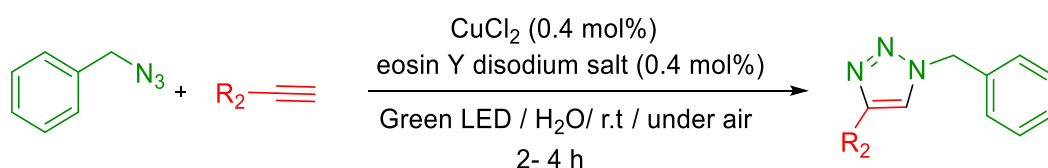
In 2017, Weiwei Zhang and colleagues created an efficient and green Cu (II) acetyl acetonate-catalyzed procedure for CuACC in H₂O at 100 °C. In addition to being suitable for the reaction between alkynes and organic azides, the method was also suitable for a one pot three component reaction combining alkynes, NaN₃ and alkyl halides.¹¹¹

Scheme 1.2.18 Synthesis of 1,2,3-triazoles via Huisgen-click reaction in water.



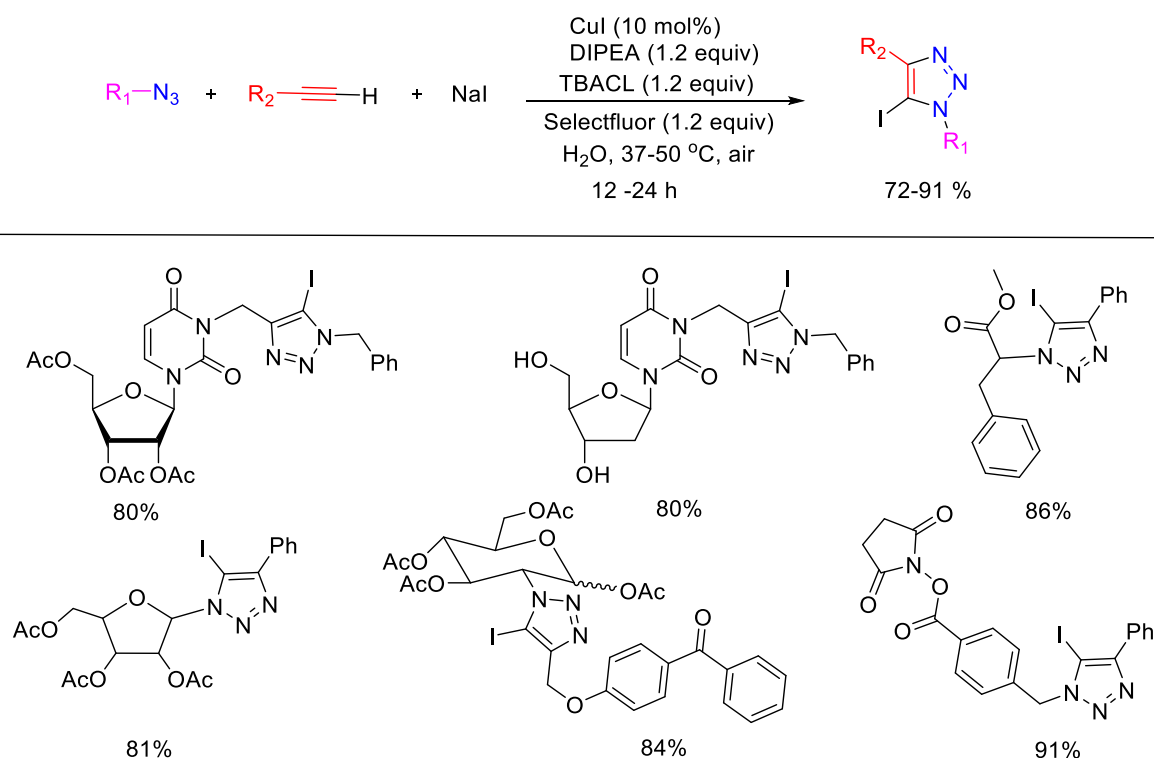
Juan E. Arguello and a coworker claimed a facile and environmentally friendly synthesis of 1,4-disubstituted 1,2,3-triazoles aided by organic dyes and promoted by visible light. Milder conditions were needed when CuCl₂ was used as a catalyst in conjunction with green LED irradiation and organic photosensitizer (eosin Y disodium salt (EY)).¹¹²

Scheme 1.2.19 1,4-disubstituted 1,2,3-triazole synthesis through CuAAC reaction enhanced by visible light



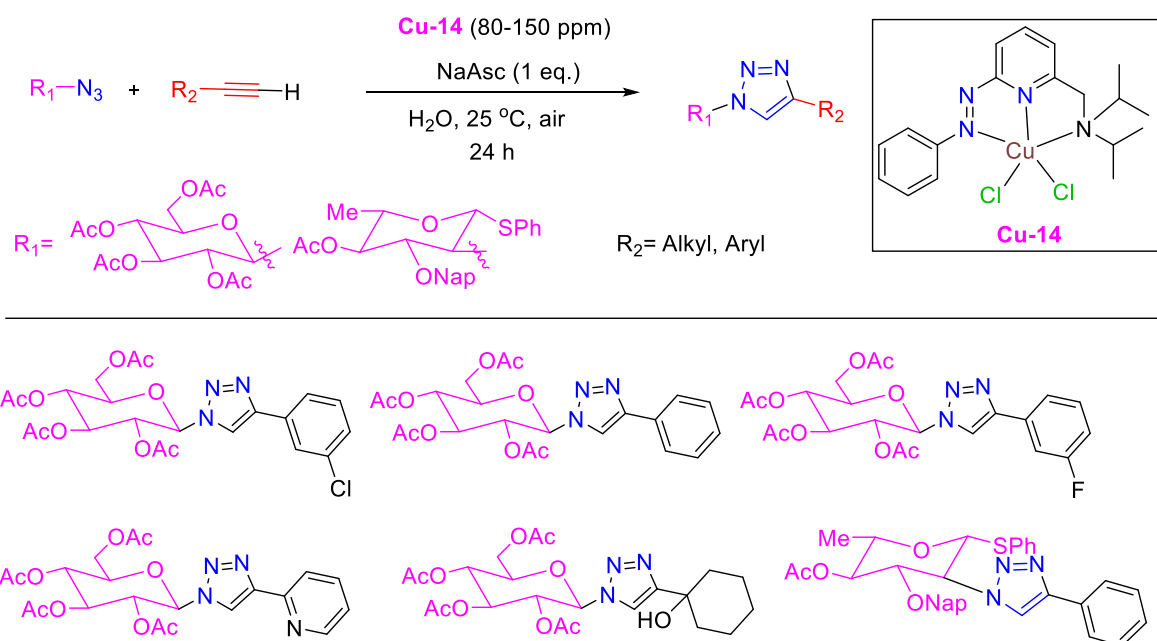
Li, Cui, and Zhang developed a process for making 5-iodo-1,2,3-triazoles in H₂O using a 3-component reaction involving NaI, organic azides and terminal alkynes.¹¹³ Then they optimize the reaction conditions with 10 mol % CuI and equimolar amounts of DIPEA, NaI (1.2 equiv.), selectfluor (1.2 equiv.), TBACl (tetrabutylammonium chloride), and slight heating. They have isolated several 5-iodo-1,2,3-triazoles with good to excellent yield.

Scheme 1.2.20 Preparation of 5-iodo-1,2,3-triazole derivatives from alkynes and organic azides



In 2021 Subhas Samanta and co-worker reported Cu(I)-catalyzed 1,3-dipolar azide-alkyne cycloaddition (CuAAC) process in water under air at ambient temperature. Complexes, on the other hand, needed 1 equiv. of sodium L-ascorbate to produce equal amount of active CuI catalyst.¹¹⁴ It was discovered that Cu(I)-complexes containing azo-based ligand are stable in air and extremely efficient for the CuAAC process. When 2,3,4,6-tetra-O-acetyl-D-glucopyranosylazide is used to treat a range of aryl acetylenes, it only takes an 80–100 ppm loading of the complex to produce 78-91% of the isolated triazole attached glycoconjugates. Triazole using different sugar was tested. The reaction of this sugar with benzyl azide was found to be remarkably smooth, yielding 76% isolated yield of its triazole product with just 100 ppm loading

Schseme 1.2.21 Application of Copper complex for the synthesis of glycoconjugates/sugar-based triazoles

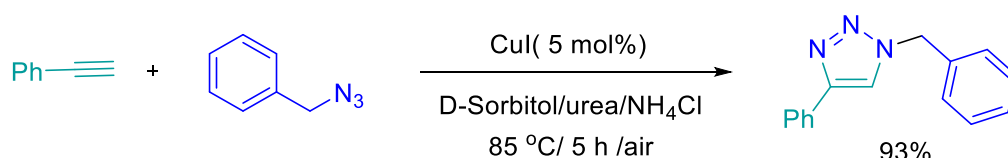


Deep Eutectic Solvents (DESs)¹¹⁵ are described as the outcome of the mixing of two (or three) compounds that can generate an entirely new eutectic mixture (having melting point lesser than that of each part) via development of a tri dimensional hydrogen-bond network.¹¹⁶ Bio renewable and biodegradable ammonium salt choline chloride is a typical component in the preparation of these eutectic combinations (ChCl, vitamin B4)¹¹⁷. When combined with various hydrogen bond donors such as i) urea,¹¹⁸ choline chloride (ChCl) (ii) bio renewable organic acids,¹¹⁹ or (iii) naturally occurring polyols (ethylene glycol, glycerol, or carbohydrates),¹²⁰ can generate liquid, sustainable eutectic mixtures that have uses across a variety of chemical disciplines.¹²¹⁻¹²³ When the concept of deep eutectic solvents reached the arena of classical organic synthesis. The Copper catalyzed azide alkyne cycloadditions were tested in these sustained solvents, as expected.

In 2009, König et al. demonstrated the CuI-catalyzed cycloaddition of benzyl azide with phenylacetylene for the synthesis of the classic 1,4-disubstituted triazoles,¹²⁴ making them the true pioneers in this field. It should be noted, that (i) high temperature (85 °C, and 5 h) was

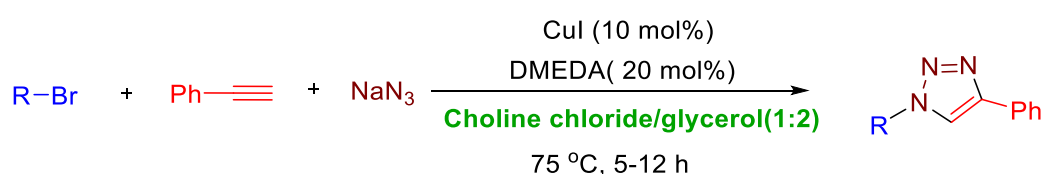
required to produce necessary triazole in an excellent yield (ii) no reports of recycling investigations of the catalyst in DESs. In comparison, the requisite triazole yield was only 84% when using a catalytic system that combined CuSO₄ with sodium ascorbate as a reducing agent (as is often used in other CuAAC processes).

Scheme 1.2.22 Synthesis of 1,4-substituted 1,2,3-triazole in the D-sorbitol/urea



Handy et al.¹²⁵ demonstrated the CuI-catalyzed cycloaddition of terminal alkynes with in-situ released aryl azides using the previously indicated ChCl/Gly (1:2) eutectic combination as a green solvent and N, N-dimethylethylenediamine (20 mol %) as a co-catalyst. Very severe reaction conditions (10 mol % CuI, 5-10 h, 75 °C) were necessary despite the solvent being recycled up to four times in a succession to get moderate excellent yields (45-89%).

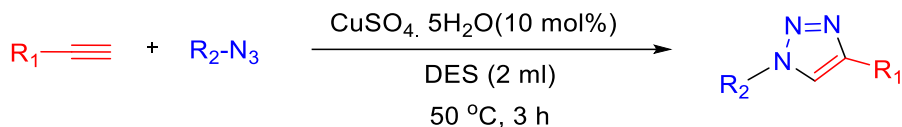
Scheme 1.2.23 Copper-catalyzed aryl and heteroaryl bromides click reaction in an eco-friendly deep eutectic solvent



In 2021 Roberto Romeo and coworkers reported 1,3-dipolar cycloadditions of terminal alkynes with organic azides were explored, utilizing traditional cycloaddition of phenyl-acetylene and benzyl azide as a model reaction.¹²⁶ Under diverse experimental conditions, the chemical role of DESs components in cycloaddition processes was investigated (time, temperature and in presence or absence of catalytic reductants). The reactions were carried out without the presence of a base, did not require extreme temperatures, tolerated a broad range of functional groups, and did not need the use of a third reducing agent and they permitted solvent recycling.

The DESGA/TMG provided best green solvent for obtaining substituted 1,2,3-triazoles with various functional groups in good yield.

Scheme 1.2.24 Cu-catalyzed azide-alkyne cycloadditions (CuAAC) in DES



REFERENCE:

- (1) Anastas, P.; Eghbali, N. Green Chemistry: Principles and practice. *Chem. Soc. Rev.* **2010**, 39, 301-312.
- (2) Schmidt, F. Baerns M. (eds) The Importance of catalysis in the chemical and non-chemical industries, In *basic Principles in Applied Catalysis*. Springer series in chemical physics, vol 75. Springer, Berlin, Heidelberg, 2004.
- (3) Chorkendorff, I.; Niemantsverdriet, J. W. *Concepts of Modern Catalysis and Kinetics, Second Edition. I*. WILEY-VCH Verlag GmbH&Co. KGaA, Weinheim, 2007
- (4) van Leeuwen, P.W.N.M. (2004). Homogeneous Catalysis: Understanding the Art. Amsterdam, the Netherlands: Kluwer Academic Publishers.
- (5) Hartwig, J.F. (2010). Organotransition Metal Chemistry: From bonding to catalysis. Sausalito, USA: University Science Books.
- (6) Shi, Z.; Zhang, C.; Tang, C.; Jiao, N. Recent advances in transition-metal catalyzed reactions using molecular oxygen as the oxidant. *Chem. Soc. Rev.* **2012**, 41, 3381-3430.
- (7) Ackermann, L.; Vicente, R.; Kapdi, A. R. Transition-metal catalyzed direct arylation of (Hetero)arenes by C-H bond cleavage. *Angew. Chem. Int. Ed.* **2009**, 48, 9792-9826.
- (8) (a) Ashenhurst, J. A. Intermolecular oxidative cross-coupling of arenes. *Chem. Soc. Rev.* **2010**, 39, 540. (b) Chinchilla, R.; Najera, C. The Sonogashira reaction: a booming methodology in synthetic organic chemistry. *Chem. Rev.* **2007**, 107, 874; (c) K. M. Gligorich, K. M.; Sigman, M. S. Recent advancements and challenges of palladium (II)

- catalyzed oxidation reactions with molecular oxygen as the sole oxidant. *Chem. Commun.* **2009**, 3854.
- (9) (a) Liu, C.; Zhang, H.; Shi, W.; Lei, A. Bond formations between two nucleophiles: transition metal catalyzed oxidative cross-coupling reactions. *Chem. Rev.* **2011**, *111*, 1780–1824. (b) Schultz, M. J.; Sigman, M. S.; Recent advances in homogeneous transition metal-catalyzed aerobic alcohol oxidations. *Tetrahedron.* **2006**, *62*, 8227.
- (10) Yoshikai, N.; Nakamura, E. Mechanisms of nucleophilic organoCopper(I) reactions. *Chem. Rev.* **2012**, *112*, 2339-2372.
- (11) Gutekunst, W. R.; Baran, P. S. C-H functionalization logic in total synthesis. *Chem. Soc. Rev.* **2011**, *40*, 1976-1991.
- (12) Phapale, V. B.; Cardenas, D. J. Nickel-catalysed negishi cross-coupling reactions: scope and mechanisms. *Chem. Soc. Rev.* **2009**, *38*, 1598-1607. (b) Muto, K.; Yamaguchi, J.; Lei, A.; Itami, K. Isolation, structure, and reactivity of an arynickel(II) pivalate complex in catalytic C-H/C-O diaryl coupling. *J. Am. Chem. Soc.* **2013**, *135*, 16384–16387.
- (13) Alexandre Alexakis; Jan-E. Bäckvall; Krause, N.; Pàmies, O.; Montserrat Dieguez. Enantioselective Copper-catalyzed conjugate addition and allylic substitution reactions. *Chemical Reviews.* **2008**, *108*, 2796-2823.
- (14) Hebrard, F.; Kalck, P. Cobalt-Catalyzed Hydroformylation of Alkenes: Generation and Recycling of the Carbonyl Species, and Catalytic Cycle. *Chem. Rev.* **2009**, *109*, 4272-4282
- (15) Murakami, K.; Yorimitsu, H.; Oshima, K. Zinc-Catalyzed nucleophilic substitution reaction of chlorosilanes with organomagnesium reagents. *J. Org. Chem.* **2009**, *74*, 1415-1417.

- (16) Correa, A.; García Mancheno, O.; Bolm, C. Iron-Catalysed Carbon-Heteroatom and Heteroatom-Heteroatom Bond Forming Processes. *Chem. Soc. Rev.* **2008**, *37*, 1108-1117.
- (17) (a) Hashmi, A. S. K. Gold-Catalyzed Organic Reactions. *Chem. Rev.* **2007**, *107*, 3180-3211. (b) Min, B. K.; Friend, C. M. Heterogeneous gold-based catalysis for green chemistry: Low-temperature CO oxidation and propene oxidation. *Chem. Rev.* **2007**, *107*, 2709-2724. (c) Li, Z.; Brouwer, C.; He, C. Gold-catalyzed organic transformations. *Chem. Rev.* **2008**, *108*, 3239-3265.
- (18) (a) Saisaha, P.; de Boer, J. W.; Browne, W. R. Mechanisms in Manganese Catalysed Oxidation of Alkenes with H₂O₂. *Chem. Soc. Rev.* **2013**, *42*, 2059-2074. (b) Zhou, B.; Chen, H.; Wang, C. Mn-Catalyzed Aromatic C-H Alkenylation with Terminal Alkynes. *J. Am. Chem. Soc.* **2013**, *135*, 1264-1267.
- (19) Fagnou, K.; Lautens, M. Rhodium-Catalyzed Carbon-Carbon Bond Forming Reactions of Organometallic Compounds. *Chem. Rev.* **2003**, *103*, 169-196. (b) Hayashi, T.; Yamasaki, K. Rhodium-Catalyzed Asymmetric 1,4-Addition and Its Related Asymmetric Reactions. *Chem. Rev.* **2003**, *103*, 2829-2844.
- (20) Maas, G. Ruthenium-Catalysed Carbenoid Cyclopropanation Reactions with Diazo Compounds. *Chem. Soc. Rev.* **2004**, *33*, 183-190. (b) Murahashi, S. I.; Zhang, D. Ruthenium Catalyzed Biomimetic Oxidation in Organic Synthesis Inspired by Cytochrome P-450. *Chem. Soc. Rev.* **2008**, *37*, 1490-1501.
- (21) (a) Zhu, C.; Falck, J. R. Alternative Pathways for Heck Intermediates: Palladium-Catalyzed Oxyarylation of Homoallylic Alcohols. *Angew. Chem. Int. Ed.* **2011**, *50*, 6626-6629. (b) Wei, Y.; Deb, I.; Yoshikai, N. Palladium-Catalyzed Aerobic Oxidative Cyclization of N-Aryl Imines: Indole Synthesis from Anilines and Ketones. *J. Am. Chem. Soc.* **2012**, *134*, 9098-9101.

- (22) Sharifi, A.; Mirzaei, M.; Reza Naimi-Jamal, M. Modified Glaser Reaction of Terminal Alkynes on KF/Alumina. *Monatsh. Chem.* **2006**, *137*, 213–217.
- (23) Zhu, C.; Falck, J. R. Alternative Pathways for Heck Intermediates: Palladium-Catalyzed Oxyarylation of Homoallylic Alcohols. *Angew. Chem. Int. Ed.* **2011**, *50*, 6626–6629.
- (24) Chan, W.-W.; Lo, S.-F.; Zhou, Z.; Yu, W.-Y. Rh-Catalyzed Intermolecular Carbenoid Functionalization of Aromatic C-H Bonds by α -Diazomalonates. *J. Am. Chem. Soc.* **2012**, *134* (33), 13565–13568
- (25) Arockiam, P. B.; Fischmeister, C.; Bruneau, C.; Dixneuf, P. H. Ruthenium Diacetate-Catalysed Oxidative Alkenylation of C–H Bonds in Air: Synthesis of Alkenyl N-Arylpyrazoles. *Green Chem.* **2011**, *13*, 3075.
- (26) Davenport, W.G.; King, C.; Schlesinger, M.; and Biswas, A.K. Extractive Metallurgy of Copper, 25. Oxford, UK: Pergamon, 2002.
- (27) Meija, J.; Coplen, T.B.; and Berglund, M. *Pure Appl. Chem.* **2016**, *88*, 265.
- (28) Anilkumar, G.; Saranya, S. *Copper Catalysis in Organic Synthesis*; John Wiley & Sons: Weinheim, Germany, **2020**.
- (29) Hathaway, B. J.; Billing, D. E. The Electronic Properties and Stereochemistry of Mono-Nuclear Complexes of the Copper(II) Ion. *Coord. Chem. Rev.* **1970**, *5*, 143-207.
- (30) Ullmann, F. Ueber Eine Neue Bildungsweise von Diphenylaminderivaten. *Ber. Dtsch. Chem. Ges.* **1903**, *36*, 2382-2384.
- (31) Allen, S. E.; Walvoord, R. R.; Padilla-Salinas, R.; Kozlowski, M. C. Aerobic Copper-Catalyzed Organic Reactions. *Chem. Rev.* **2013**, *113*, 6234–6458.
- (32) Evano, G.; Blanchard, N. *Copper-Mediated Cross-Coupling Reactions*; Wiley & Sons: New Jersey, USA, 2013.

- (33) Mairena, A.; Wackerlin, C.; Wienke, M.; Grenader, K.; Terfort, A.; Ernst, K.-H. Diastereoselective Ullmann Coupling to Bishelicenes by Surface Topochemistry. *J. Am. Chem. Soc.* **2018**, *140*, 15186-15189.
- (34) Ullmann, F. and Sponagel, P. (1905). *Ber. Dtsch. Chem. Ges.* **38**: 2211.
- (35) Stephens, R. D.; Castro, C. E. The Substitution of Aryl Iodides with Cuprous Acetylides. A Synthesis of Tolanes and Heterocyclics. *J. Org. Chem.* **1963**, *28*, 3313-3315.
- (36) Ma, D.; Cai, Q. Copper/Amino Acid Catalyzed Cross-Couplings of Aryl and Vinyl Halides with Nucleophiles. *Acc. Chem. Res.* **2008**, *41*, 1450–1460.
- (37) Chan, D. M. T.; Monaco, K. L.; Wang, R.-P.; Winters, M. P. New N- and O-Arylations with Phenylboronic Acids and Cupric Acetate. *Tetrahedron Lett.* **1998**, *39*, 2933–2936.
- (38) Evans, D. A.; Katz, J. L.; West, T. R. Synthesis of Diaryl Ethers through the Copper-Promoted Arylation of Phenols with Arylboronic Acids. An Expedient Synthesis of Thyroxine. *Tetrahedron Lett.* **1998**, *39*, 2937-2940.
- (39) Lam, P. Y. S.; Clark, C. G.; Saubern, S.; Adams, J.; Winters, M. P.; Chan, D. M. T.; Combs, A. New Aryl/Heteroaryl C-N Bond Cross-Coupling Reactions via Arylboronic Acid/Cupric Acetate Arylation. *Tetrahedron Lett.* **1998**, *39*, 2941-2944.
- (40) Arends, I.W.C.E.; Sheldon, R.A. *Modern Oxidation Methods*, 2nd ed.; Backvall, J.-E., Ed.; Wiley VCH: Weinheim, Germany, 2010; pp. 147-185.
- (41) Ege, S. N. *Organic Chemistry*; D. C. Heath Company: Lexington, MA, 1989; p 596.
- (42) Kopylovich, M.N.; Ribeiro, A.P.C.; Alegria, E.C.B.A.; Martins, N.M.R.; Martins, L.M.D.R.S.; Pombeiro, A.J.L. Catalytic oxidation of alcohols: Recent advances. *Adv. Organometal. Chem.* **2015**, *63*, 91-174.
- (43) Jiao, N.; Stahl, S.S. *Green Oxidation in Organic Synthesis*; Wiley-VCH: Weinheim, Germany, 2019.

- (44) Xu, B.; Lumb, J.-P.; Arndtsen, B. A. A TEMPO-Free Copper-Catalyzed Aerobic Oxidation of Alcohols. *Angew. Chem. Int. Ed.* **2015**, *54*, 4208–4211.
- (45) Chaudhuri, P.; Hess, M.; Flörke, U.; Wieghardt, K. From Structural Models of Galactose Oxidase to Homogeneous Catalysis: Efficient Aerobic Oxidation of Alcohols. *Angew. Chem. Int. Ed.* **1998**, *37*, 2217-2220.
- (46) Chaudhuri, P.; Hess, M.; Weyhermuller, T.; Wieghardt, K. Aerobic Oxidation of Primary Alcohols by a New Mononuclear Cu(II) -Radical Catalyst. *Angew. Chem. Int. Ed.* **1999**, *38*, 1095-1098.
- (47) Velusamy, S.; Punniyamurthy, T. Copper(II)-Catalyzed Oxidation of Alcohols to Carbonyl Compounds with Hydrogen Peroxide. *European J. Org. Chem.* **2003**, *2003*, 3913-3915.
- (48) Unver, H.; Kani, I. Homogeneous Oxidation of Alcohols in Water Catalyzed with Cu(II)-Triphenyl Acetate/Bipyridyl Complex. *Polyhedron* **2017**, *134*, 257-262.
- (49) Unver, H.; Kani, I. Homogeneous Oxidation of Alcohol and Alkene with Copper (II) Complex in Water. *J. Chem. Sci.* **2018**, *130*.
- (50) Unver, H. Crystal Structure of an Alkoxide Bridged Dinuclear Copper(II) Complex: Mild and Selective Oxidation of Primary and Secondary Alcohols in Water. *Transit. Met. Chem.* **2018**, *43*, 641-646.
- (51) Wu, C.; Liu, B.; Geng, X.; Zhang, Z.; Liu, S.; Hu, Q. Selective Catalytic Oxidation of Aromatic Substrates Employing Mononuclear Copper(II) Catalyst with H₂O₂. *Polyhedron*. **2019**, *158*, 334–341.
- (52) Shoair, A. G. F. Catalytic Activity of Some New Copper(II) Azo-Complexes. *J. Coord. Chem.* **2012**, *65*, 3511–3518.
- (53) Czerwińska, K.; Machura, B.; Kula, S.; Krompiec, S.; Erfurt, K.; Roma-Rodrigues, C.; Fernandes, A. R.; Shul'pina, L. S.; Ikonnikov, N. S.; Shul'pin, G. B. Copper(II)

- Complexes of Functionalized 2,2':6',2''-Terpyridines and 2,6-Di(Thiazol-2-Yl)Pyridine: Structure, Spectroscopy, Cytotoxicity and Catalytic Activity. *Dalton Trans.* **2017**, *46*, 9591–9604.
- (54) Mncube, S. G.; Bala, M. D. Homogeneous Oxidation Reactions Catalysed by in Situ-Generated Triazolylidene Copper(I) Complexes. *Transit. Met. Chem.* **2019**, *44*, 145–151.
- (55) Semmelhack, M. F.; Schmid, C. R.; Cortes, D. A.; Chou, C. S. Oxidation of Alcohols to Aldehydes with Oxygen and Cupric Ion, Mediated by Nitrosonium Ion. *J. Am. Chem. Soc.* **1984**, *106*, 3374–3376.
- (56) Kumpulainen, E. T. T.; Koskinen, A. M. P. Catalytic Activity Dependency on Catalyst Components in Aerobic Copper-TEMPO Oxidation. *Chemistry.* **2009**, *15*, 10901-10911.
- (57) Hoover, J. M.; Stahl, S. S. Highly Practical Copper(I)/TEMPO Catalyst System for Chemo selective Aerobic Oxidation of Primary Alcohols. *J. Am. Chem. Soc.* **2011**, *133*, 16901-16910.
- (58) Mannam, S.; Alamsetti, S. K.; Sekar, G. Aerobic, chemo selective oxidation of alcohols to carbonyl compounds catalyzed by a DABCO-Copper complex under mild conditions. *Adv. Synth. Catal.* **2007**, *349*, 2253–2258.
- (59) Figiel, P. J.; Leskelä, M.; Repo, T. TEMPO-Copper(II) Diimine-Catalysed Oxidation of Benzylic Alcohols in Aqueous Media. *Adv. Synth. Catal.* **2007**, *349*, 1173–1179
- (60) Ho, X.-H.; Oh, H.-J.; Jang, H.-Y. Multistep Organocatalysis for the Asymmetric Synthesis of Mult substituted Aldehydes from Allylic Alcohols. *European J. Org. Chem.* **2012**, *2012*, 5655–5659.
- (61) Hoover, J. M.; Ryland, B. L.; Stahl, S. S. Mechanism of Copper(I)/TEMPO-Catalyzed Aerobic Alcohol Oxidation. *J. Am. Chem. Soc.* **2013**, *135*, 2357–2367.

- (62) Liu, Z.; Shen, Z.; Zhang, N.; Zhong, W.; Liu, X. Aerobic Oxidation of Alcohols Catalysed by Cu(I)/NMI/TEMPO System and Its Mechanistic Insights. *Catal. Letters*. **2018**, *148*, 2709–2718.
- (63) Lagerspets, E.; Abba, D.; Sharratt, J.; Eronen, A.; Repo, T. Water Tolerant Base Free Copper (I) Catalyst for the Selective Aerobic Oxidation of Primary Alcohols. *Mol. Catal.* **2022**, *520*, 112-167.
- (64) Rostovtsev, V. V.; Green, L. G.; Fokin, V. V.; Sharpless, K. B., A Stepwise Huisgen Cycloaddition Process. Copper(I)-Catalyzed Regioselective “Ligation” of Azides and Terminal Alkynes. *Angew. Chem. Int. Ed.* **2002**, *41*, 2596-2599.
- (65) (a) Tornøe, C. W.; Christensen, C.; Meldal, M., Peptidotriazoles on Solid Phase: [1,2,3]-Triazoles by Regiospecific Copper(I)-Catalyzed 1,3-Dipolar Cycloadditions of Terminal Alkynes to Azides. *J. Org. Chem.* **2002**, *67*, 3057-3064 (b) Huisgen, R.; Pawda, A. (Eds.) 1,3-Dipolar Cycloaddition Chemistry; *John Wiley & Sons, Ltd.*: New York, NY, USA, 1984; Volume 1.
- (66) B. Zhang, Comprehensive review on the anti-bacterial activity of 1,2,3-triazole hybrids. *Eur. J. Med. Chem.* **2019**, *168*, 357-372.
- (67) Prasher, P.; Sharma, M. Tailored Therapeutics Based on 1,2,3-1H-Triazoles: A Mini Review. *Medchemcomm.* **2019**, *10* (8), 1302-1328.
- (68) Bonandi, E.; Christodoulou, M. S.; Fumagalli, G.; Perdicchia, D.; Rastelli, G.; Passarella, D. The 1,2,3-Triazole Ring as a Bioisostere in Medicinal Chemistry. *Drug Discov. Today*. **2017**, *22*, 1572-1581.
- (69) Kluba, C. A.; Mindt, T. L. Click-to-Chelate: Development of Technetium and Rhenium-Tricarbonyl Labeled Radiopharmaceuticals. *Molecules*. **2013**, *18*, 3206-3226.
- (70) Moses, J. E.; Moorhouse, A. D. The Growing Applications of Click Chemistry. *Chem. Soc. Rev.* **2007**, *36*, 1249–1262.

- (71) Amblard, F.; Cho, J. H.; Schinazi, R. F. Cu(I)-Catalyzed Huisgen Azide-Alkyne 1,3-Dipolar Cycloaddition Reaction in Nucleoside, Nucleotide, and Oligonucleotide Chemistry. *Chem. Rev.* **2009**, *109*, 4207-4220.
- (72) Angell, Y. L.; Burgess, K. Peptidomimetics via Copper-Catalyzed Azide-Alkyne Cycloadditions. *Chem. Soc. Rev.* **2007**, *36*, 1674-1689.
- (73) El-Sagheer, A. H.; Brown, T. Click Chemistry with DNA. *Chem. Soc. Rev.* **2010**, *39*, 1388-1405.
- (74) Saha, P.; Panda, D.; Dash, J. The Application of Click Chemistry for Targeting Quadruplex Nucleic Acids. *Chem. Commun.* **2019**, *55*, 731-750.
- (75) El-Sagheer, A. H.; Brown, T. Click Nucleic Acid Ligation: Applications in Biology and Nanotechnology. *Acc. Chem. Res.* **2012**, *45*, 1258-1267.
- (76) Akter, M.; Rupa, K.; Anbarasan, P. 1,2,3-Triazole and Its Analogues: New Surrogates for Diazo Compounds. *Chem. Rev.* **2022**, *122*, 13108-13205.
- (77) Golas, P. L.; Matyjaszewski, K. Marrying Click Chemistry with Polymerization: Expanding the Scope of Polymeric Materials. *Chem. Soc. Rev.* **2010**, *39*, 1338-1354.
- (78) Qin, A.; Lam, J. W. Y.; Tang, B. Z. Click Polymerization. *Chem. Soc. Rev.* **2010**, *39*, 2522-2544.
- (79) Nandivada, H.; Jiang, X.; Lahann, J. Click Chemistry: Versatility and Control in the Hands of Materials Scientists. *Adv. Mater.* **2007**, *19*, 2197-2208.
- (80) Aromí, G.; Barrios, L. A.; Roubeau, O.; Gamez, P. Triazoles and Tetrazoles: Prime Ligands to Generate Remarkable Coordination Materials. *Coord. Chem. Rev.* **2011**, *255*, 485-546.
- (81) Kolb, H. C.; Sharpless, K. B. The Growing Impact of Click Chemistry on Drug Discovery. *Drug Discov. Today.* **2003**, *8*, 1128-1137.

- (82) Sharpless, K. B.; Manetsch, R. In Situ Click Chemistry: A Powerful Means for Lead Discovery. *Expert Opin. Drug Discov.* **2006**, *1*, 525–538.
- (83) Thirumurugan, P.; Matosiuk, D.; Jozwiak, K. Click Chemistry for Drug Development and Diverse Chemical-Biology Applications. *Chem. Rev.* **2013**, *113*, 4905–4979.
- (84) Rani, A.; Singh, G.; Singh, A.; Maqbool, U.; Kaur, G.; Singh, J. CuAAC-Ensembled 1,2,3-Triazole-Linked Isosteres as Pharmacophores in Drug Discovery: Review. *RSC Adv.* **2020**, *10*, 5610–5635.
- (85) Huang, D.; Zhao, P.; Astruc, D. Catalysis by 1,2,3-Triazole- and Related Transition-Metal Complexes. *Coord. Chem. Rev.* **2014**, *272*, 145–165.
- (86) Ghosh, R.; Jana, N. C.; Panda, S.; Bagh, B. Transfer Hydrogenation of Aldehydes and Ketones in Air with Methanol and Ethanol by an Air-Stable Ruthenium–Triazole Complex. *ACS Sustain. Chem. Eng.* **2021**, *9*, 4903–4914.
- (87) Bagh, B.; McKinty, A. M.; Lough, A. J.; Stephan, D. W. 1,2,3-Triazolylidene Ruthenium(II)(H⁶-Arene) Complexes: Synthesis, Metallation and Reactivity. *Dalton Trans.* **2014**, *43*, 12842–12850.
- (88) Bagh, B.; McKinty, A. M.; Lough, A. J.; Stephan, D. W. 1,2,3-Triazolylidene Ruthenium(II)-Cyclometalated Complexes and Olefin Selective Hydrogenation Catalysis. *Dalton Trans.* **2015**, *44*, 2712–2723.
- (89) Bagh, B.; Stephan, D. W. Half Sandwich Ruthenium(II) Hydrides: Hydrogenation of Terminal, Internal, Cyclic and Functionalized Olefins. *Dalton Trans.* **2014**, *43*, 15638–15645.
- (90) Fazio, F.; Bryan, M. C.; Blixt, O.; Paulson, J. C.; Wong, C.-H., Synthesis of Sugar Arrays in Microtiter Plate. *J. Am. Chem. Soc.* **2002**, *124*, 14397–14402.

- (91) Ermolat'ev, D.; Dehaen, W.; Van der Eycken, E., Indirect Coupling of the 2(1H)-pyrazinone Scaffold with Various (oligo)-saccharides via “click chemistry”: en route towards Glycopeptidomimetics.) *E. QSAR Comb. Sci.* **2004**, *23*, 915- 918.
- (92) Shao, C.; Wang, X.; Zhang, Q.; Luo, S.; Zhao, J.; Hu, Y. Acid–base jointly promoted Copper (I)-catalyzed azide alkyne cycloaddition. *J. Org. Chem.* **2011**, *76*, 6832-6836.
- (93) Keshavarz, M.; Irvani, N.; Ghaedi, A.; Ahmady, A. Z.; Vafaei-Nezhad, M.; Karimi, S. Macroporous polymer supported azide and nanoCopper (I): efficient and reusable reagent and catalyst for multicomponent click synthesis of 1, 4-disubstituted-1*H*-1,2,3-triazoles from benzyl halides. *SpringerPlus.* **2013**, *2*, 1-8.
- (94) Kuang, C.; Xu, M.; Wang, Z.; Yang, Q.; Jiang, Y. A Novel Approach to 1-Monosubstituted 1,2,3-Triazoles by a Click Cycloaddition/Decarboxylation Process. *Synthesis.* **2011**, *2011*, 223–228.
- (95) Liang, Y.-M.; Wu, L.-Y.; Xie, Y.-X.; Chen, Z.-S.; Niu, Y.-N. A Convenient Synthesis of 1-Substituted 1,2,3-Triazoles via CuI/Et₃N Catalyzed ‘Click Chemistry’ from Azides and Acetylene Gas. *Synlett.* **2009**, *2009*, 1453–1456.
- (96) Heaney, H.; Buckley, B.; Figueres, M.; Khan, A. A New Simplified Protocol for Copper(I) Alkyne–Azide Cycloaddition Reactions Using Low Substoichiometric Amounts of Copper(II) Precatalysts in Methanol. *Synlett.* **2015**, *27*, 51–56.
- (97) Yamada, Y. M. A.; Sarkar, S. M.; Uozumi, Y. Amphiphilic Self-Assembled Polymeric Copper Catalyst to Parts per Million Levels: Click Chemistry. *J. Am. Chem. Soc.* **2012**, *134*, 9285–9290.
- (98) Sau, S. C.; Roy, S. R.; Sen, T. K.; Mullangi, D.; Mandal, S. K. An abnormal N-heterocyclic carbene–Copper(I) complex in click chemistry. *Adv. Synth. Catal.* **2013**, *355*, 2982–2991.

- (99) Gonzalez-Lainez, M.; Gallegos, M.; Munarriz, J.; Azpiroz, R.; Passarelli, V.; Jimenez, M.V.; Perez-Torrente, J.J. Copper-catalyzed azide-alkyne cycloaddition (CuAAC) by functionalized NHC-based polynuclear catalysts: Scope and mechanistic insights. *Organometallics*. **2022**, *41*, 2154-2169.
- (100) Zhang, W.; Cue, B. W. *Green Techniques for Organic Synthesis and Medicinal Chemistry*, 2nd ed.; Zhang, W., Cue, B. W., Eds.; John Wiley & Sons: Nashville, TN, 2018.
- (101) Ravichandiran, P.; Gu, Y.; Glycerol as eco-efficient solvent for organic transformations, in bio-based solvents; Jerome, F., Luque, R., Eds.; John Wiley & Sons: Hoboken, NJ, USA, 2017
- (102) Vaccaro, L.; Santoro, S.; Curini, M.; Lanari, D. The emerging use of γ -valerolactone as a green solvent. *Chem. Today*. **2017**, *35*, 46-48.
- (103) Pace, V.; Hoyos, P.; Castoldi, L.; Dominguez de Maria, P.; Alcantara, A.R. 2-Methyltetrahydrofuran (2-MeTHF): A biomass-derived solvent with broad application in organic chemistry. *ChemSusChem*. **2012**, *5*, 1369-1379.
- (104) Yang, J.; Tan, J.-N.; Gu, Y. Lactic acid as an invaluable bio-based solvent for organic reactions. *Green Chem*. **2012**, *14*, 3304-3317.
- (105) *Deep Eutectic Solvents: Synthesis, Properties, and Applications*; Ramón, D. J., Guillena, G., Eds.; Wiley, 2019.
- (106) Kolb, H.C.; Finn, M.G.; Sharpless, K.B. Click Chemistry: Diverse chemical function from a few good reactions. *Angew. Chem. Int. Ed*. **2001**, *40*, 2004-2021.
- (107) Horvath, I. T. Solvents from nature. *Green Chem*. **2008**, *10*, 1024-1028.
- (108) Vidal, C.; Garcia-Alvarez, J. Glycerol: A biorenewable solvent for base-free Cu(I)-catalyzed 1,3-dipolar cycloaddition of azides with terminal and 1-iodoalkynes. Highly efficient transformations and catalyst recycling. *Green Chem*. **2014**, *16*, 3515-3521.

- (109) (a) Pasupuleti, B.G.; Bez, G. CuI/L-proline catalyzed click reaction in glycerol for the synthesis of 1,2,3-triazoles. *Tetrahedron Lett.* **2019**, *60*, 142-146. (b) Chahdoura, F.; Pradel, C.; Gomez, M. Copper(I) oxide nanoparticles in glycerol: A convenient catalyst for cross-coupling and azide-alkyne cycloaddition processes. *ChemCatChem.* **2014**, *6*, 2929-2936.
- (110) Jiang, Y.; Li, X.; Li, X.; Sun, Y.; Zhao, Y.; Jia, S.; Guo, N.; Xu, G.; Zhang, W. Copper(II) Acetylacetonate: An efficient catalyst for Huisgen-Click reaction for synthesis of 1,2,3-triazoles in water. *Chin. J. Chem.* **2017**, *35*, 1239-1245.
- (111) Shi, X.-L.; Chen, Y.; Hu, Q.; Zhang, W.; Luo, C.; Duan, P. A potential industrialized fiber-supported Copper catalyst for one-pot multicomponent CuAAC reactions in water. *J. Ind. Eng. Chem.* **2017**, *53*, 134–142.
- (112) Castro-Godoy, W.D.; Heredia, A.A.; Schmidt, L.C.; Arguello, J.E. A straightforward and sustainable synthesis of 1,4-disubstituted 1,2,3-triazoles via visible-light promoted Copper-catalyzed azide–alkyne cycloaddition (CuAAC). *RSC Adv.* **2017**, *7*, 33967-33973
- (113) Li, L.; Ding, S.; Yang, Y.; Zhu, A.; Fan, X.; Cui, M.; Chen, C.; Zhang, G. Multicomponent aqueous synthesis of Iodo-1,2,3-triazoles: single-step models for dual modification of free peptide and radioactive iodo labeling. *Chem. Eur. J.* **2017**, *23*, 1166-1172.
- (114) Khatua, M.; Goswami, B.; Kamal; Samanta, S. Azide-alkyne “Click” reaction in water using parts-per-million amine-functionalized azoaromatic Cu(I) complex as catalyst: effect of the amine side arm. *Inorg. Chem.* **2021**, *60*, 17537-17554,
- (115) Garcia-Alvarez, J. Deep eutectic solvents and their applications as new green and biorenewable reaction media. In handbook of solvents, Volume 2: Use, health, and environment, 3rd ed.; Wypych, G., Ed.; ChemTec Publishing: Toronto, ON, Canada, 2019.

- (116) Hammond, O.S.; Bowron, D.T.; Edler, K.J. Liquid structure of the choline chloride-urea deep eutectic solvent (reline) from neutron diffraction and atomistic modelling. *Green Chem.* **2016**, *18*, 2736-2744.
- (117) Blusztajn, J. K. Choline, a vital amine. *Science* **1998**, *281*, 794–795.
- (118) Abbott, A.P.; Harris, R.C.; Ryder, K.S.; D’Agostino, C.; Gladden, L.F.; Mantle, M.D. Glycerol eutectics as sustainable solvent systems. *Green Chem.* **2011**, *13*, 82-90.
- (119) Abbott, A.P.; Boothby, D.; Capper, G.; Davies, D.; Rasheed, R.K. Deep eutectic solvents formed between choline chloride and carboxylic acids: Versatile alternatives to ionic liquids. *J. Am. Chem. Soc.* **2004**, *126*, 9142-9147.
- (120) Alonso, D.A.; Baeza, A.; Chinchilla, R.; Guillena, G.; Pastor, I.M.; Ramon, D.J. Deep eutectic solvents: The organic reaction medium of the century. *Eur. J. Org. Chem.* **2016**, 612-632.
- (121) Garcia-Alvarez, J. Deep Eutectic Mixtures: Promising sustainable solvents for metal-catalysed and metal-mediated organic reactions. *Eur. J. Inorg. Chem.* **2015**, 5147-5157.
- (122) Smith, E.L.; Abbott, A.P.; Ryder, K.S. Deep eutectic solvents (DESs) and their applications. *Chem. Rev.* **2014**, *114*, 11060-11082.
- (123) Zhao, J.; Li, P.; Xu, Y.; Shi, Y.; Li, F. Nickel-Catalyzed Transformation of Diazoacetates to Alkyl Radicals Using Alcohol as a Hydrogen Source. *Org. Lett.* **2019**, *21*, 9386–9390,
- (124) Illgen, F.; Konig, B. Organic reactions in low melting mixtures based on carbohydrates and l-carnitine-a comparison. *Green Chem.* **2009**, *11*, 848-854.
- (125) Kafle, A.; Handy, S.T. A one-pot, Copper-catalyzed azidation/click reaction of aryl and heteroaryl bromides in an environmentally friendly deep eutectic solvent. *Tetrahedron.* **2017**, *73*, 7024-7029.

(126) Giofre, S. V.; Tiecco, M.; Ferlazzo, A.; Romeo, R.; Ciancaleoni, G.; Germani, R.; Iannazzo, D. Base-free Copper-catalyzed azide-alkyne click cycloadditions (CuAAC) in natural deep eutectic solvents as green and catalytic reaction media. *European J. Org. Chem.* **2021**, 2021, 4777–4789.

Chapter-2

Aerobic Oxidation of Vanillyl Alcohol to Vanillin Catalyzed by Air-stable and Recyclable Copper Complex and TEMPO Under Base-Free Conditions

2.1 ABSTRACT

The need of sustainable development in the modern era has driven the transformation of biomass for the production of fine chemicals into a strong trend of research. The aerobic oxidation of lignin-derived monomeric phenolics for the synthesis of various value-added products has attracted significant attention of the scientific community. Enormous research interest has been devoted to the aerobic oxidation of vanillyl alcohol to vanillin, which is an important aroma chemical with wide applications. Four Copper(II) complexes were synthesized for this purpose. The coordination of the Schiff base **ligand L3** containing pendant thioether arm with Copper(II) perchlorate and Copper(II) chloride yielded homoleptic **complex 15a** and dinuclear **complex 16a**, respectively. Similar coordination of the NNS amine ligand **L4** with Copper(II) perchlorate and Copper(II) chloride resulted in the formation of homoleptic **complex 15b** and mononuclear **complex 16b**, respectively. All four air stable complexes were tested for the aerobic oxidation of vanillyl alcohol to vanillin at ambient conditions in the presence of a catalytic amount of the TEMPO radical. Mononuclear **complex 16b** displayed the best catalytic activity. Species **complex 16b** is highly selective for the conversion of vanillyl alcohol to vanillin in various green solvent mixtures. Catalyst **complex 16b** is highly recyclable and did not show any reduction of catalytic activity after three cycles. Finally, the green and sustainable credentials of various catalytic protocols under various reaction conditions were compared with the help of CHEM21 green metrics toolkit. A plausible catalytic pathway is proposed based on the published reports and experimental evidences.

2.2 INTRODUCTION

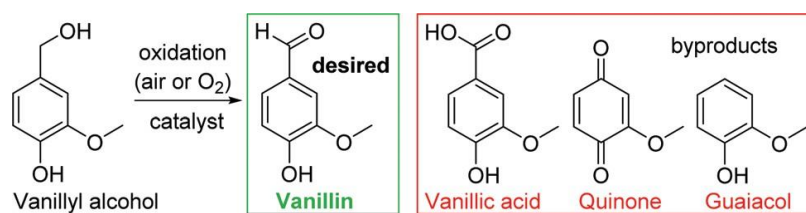
Presently, the major sources for the vast majority of organic chemicals are fossil fuels. However, the overgrowing demand mainly due to the rise of the global population and the improvement of human living standards will cause un-avoidable shortage of Petro based resources. In addition, recent trends in global warming and climate change strongly suggest that the reduction in the use of fossil fuels are necessity. Finding alternatives to non-renewable fossil fuels, which also have limited reserves, has become a vital need in our present world. In this context, the effective utilization of renewable biomass feedstock has become a top alternative and thus the use of biorefinery has started gaining significant attention.^{1,2} Most of the bio based value-added chemicals are aliphatic and often they are derived from cellulose.³ However, a wide range of important chemicals are aromatic in nature and thus the effective use of lignin in the biorefinery is essential as it contains a variety of aromatic chemicals. Various synthetic protocols have been established for the production of fine chemicals and fuel grade chemicals from lignin.^{4,5} Lignin extracted from wood and cashew nutshell liquid is the major source of important bio-based phenolic compounds such as coniferyl, p-coumaryl, p-sinapyl, veratryl, and vanillyl alcohol.⁶ A lot of attention is being devoted to the aerobic oxidation of lignin derived monomeric phenolics to synthesize functionalized compounds for the production of various fine chemicals. In this context, one of the most studied phenolics is vanillyl alcohol and the aerobic oxidation of vanillyl alcohol to vanillin(4-hydroxy-3-methoxybenzaldehyde) has attracted enormous research interest. Vanillin is a very important aroma chemical and it has found wide application in food additives, pharmaceuticals, perfumes, and cosmetics.⁷⁻¹⁰ A major demand of vanillin comes from chocolate and ice-cream manufacturers. In addition, vanillin is an interesting building block for fine chemicals as it bears two reactive groups (phenolic-OH and aldehyde), which can be functionalized.^{11,12} Hence, vanillin is a potential

candidate for renewable aromatic building block and it is not surprising that yearly more than 3000 tons of vanillin are produced from lignin biomass.¹³

In the present era, the scientific community is paying great attention to evaluate the environmental and green credentials of chemical transformation guided by “The 12 Principles of Green Chemistry”.^{14–18} The twelve principles involve the use of renewable feedstocks and the utilization of lignocellulosic biomass as a raw material is very significant in this regard. Another key factor for the development of green and sustainable process is catalysis.^{19–21} Various stoichiometric oxidants such as manganese dioxide,²² chromium salts,²³ activated DMSO,²⁴ peroxides,²⁵ and hypervalent iodines²⁶ are utilized for this purpose. However, oxygen, particularly air, is a very attractive alternative for obvious reasons, and a wide variety of homogeneous and heterogeneous catalysts of various metals such as V,²⁷ Mo,²⁸ Ru,²⁹ Os,³⁰ Co,³¹ Rh,³² Ni,³³ Pd,³⁴ Pt,³⁵ Au,³⁶ and Ce³⁷ have been synthesized. However, Copper catalysts have been recognized as the dominant force for the oxidation of alcohols, particularly in homogeneous systems.³⁸ One major class is the peroxidative oxidation of alcohols, which involves mostly hydrogen peroxide^{39–41} or tert-butyl hydroperoxide.^{42–46} Another class of Copper catalysts utilize dioxygen (or air) in the presence of a catalytic amount of the TEMPO (2,2,6,6-tetramethylpiperidine-1-oxyl) radical for alcohol oxidation.^{47–51} However, the aerobic oxidation of the lignin model compound vanillyl alcohol to vanillin is dominated by heterogeneous catalysts as the inefficient recyclability of homogeneous catalysts present a practical challenge.⁵² Simple handling, efficient separation, and recyclability of heterogeneous catalysts have established them as the major player for the aerobic oxidation of vanillyl alcohol to vanillin. However, often over-oxidation leads to the formation of vanillic acid as the byproduct; other minor byproducts such as guaiacol and benzoquinone can also be seen (**Scheme 2.1**). A wide range of metal oxides and mixed metal oxides as heterogeneous catalysts have been developed for the aerobic (or dioxygen) oxidation of vanillyl alcohol. Rode et al.

utilized mixed Co-Mn oxide nanorods, which afforded 62% conversion of vanillyl alcohol in 2 h with decent (83%) selectivity to vanillin in acetonitrile at high temperature (140 °C) and pressure (air pressure 21 bar).⁵³ The increase in the reaction time from 2 to 4 h leads to the formation of tar and the selectivity toward vanillin was decreased. They also used cobalt oxide nanoparticles, which gave 80% conversion in 6 h with excellent (98%) selectivity in the presence of high concentration of the base (NaOH) at moderate temperature (80 °C) and O₂-pressure (6.8 bar).⁵⁴

Scheme 2.1 Catalytic oxidation of vanillyl alcohol.



Cobalt oxide nanoparticles were also used at 140 °C for the same purpose by Zhang et al. The very poor selectivity (21%) to vanillin was due to the formation of a high amount of various byproducts (particularly, 2-methoxy-1,4-benzoquinone and 2-methoxyphenol).⁵⁵ Hamid et al. reported Cu–Zr oxide that gave 91% conversion of vanillyl alcohol in 2h with moderate (76%) selectivity to vanillin in acetonitrile at high temperature (120 °C) and O₂ pressure (21 bar).⁵⁶ The formation of 2-methoxy benzoquinone and guaiacol along with vanillic acid as byproducts increased with time. Reddy et al. achieved high conversion and excellent selectivity employing highly recyclable Ce-Zr mixed oxide nanoparticles; however, harsh reaction conditions (140 °C, 20 bar O₂ pressure, 5 h, acetonitrile) were used.⁵⁷ Raja et al. reported Au, Pd, and Pt nanoparticles catalyzed aerobic oxidation of vanillyl alcohol under harsh conditions (170 °C, 20 bar air pressure).⁵⁸ Platinum nanoparticles yielded the complete conversion of vanillyl alcohol in 10 h with roughly 80% selectivity toward vanillin and a large amount of 4-hydroxy-3-methoxybenzyl tert-butyl ether byproduct in tert-butanol solvent was observed. Various other metal nanoparticles immobilized on a variety of carriers such as metal organic

frameworks (MOFs), carbon, titania, and ceria have been also investigated.^{59–62} Photocatalytic oxidations of vanillyl alcohol to vanillin over Ce and Zr oxide supported on biomass templated titania were also reported by Munoz- Batista and Luque et al.⁶³ These smart materials showed excellent selectivity (99%) toward vanillin; however, the conversion of vanillyl alcohol was not great (maximum 52%). Similar photocatalytic conversion of vanillyl alcohol to vanillin under mild reaction conditions are reported by other groups.^{64,65} Though high selectivity could be achieved, these photocatalysts gave poor conversions. Several research groups targeted the oxidation of lignin model compounds for the synthesis of fine chemicals by utilizing a wide variety of homogeneous catalysts. Generally, the oxidation (by O₂ and H₂O₂) of lignin model compounds such as veratryl alcohol, 2-hydroxyethyl apocynol, isoeugenol, guaiacol, homovanillyl alcohol, isovanillyl alcohol, and vanillyl alcohol were performed by metalloporphyrins, cobalt(salen) complexes, polyoxometalates, and iron complexes with tetraamido macrocyclic ligands.⁶⁶ However, the numbers of reports that targeted the oxidation of vanillyl alcohol by homogeneous catalysts are very limited. Bozell et al. reported cobalt(salen) catalyst, which gave poor yields of vanillin (3%) and 2-methoxy-1,4-benzoquinone (12%) upon oxidation of vanillyl alcohol under ambient conditions (10 mol % catalyst, r.t., 3.5 bar O₂-pressure, 17 h) in methanol.⁶⁷ Changing the solvent from methanol to dichloromethane gave better yields of the quinone (43%). Sanjust et al. reported iron porphyrin complex catalyzed oxidation of vanillyl alcohol along with various lignin model compounds using H₂O₂.⁶⁸ Though the complete conversion of vanillyl alcohol was achieved in 3 h, the nature of the oxidation product was not mentioned. It is worth mentioning that Li et al. reported an elegant cationic cobalt (salen) catalyst, which afforded the complete conversion of 4-methyl guaiacol with 86% selectivity to vanillin in 18 h in the presence of NaOH.⁶⁹ The requirement of base and toxic organic solvents (such as acetonitrile and toluene) is another drawback to the green synthetic criteria. Though various photocatalysts operate at ambient conditions, poor

conversion of vanillyl alcohol to vanillin is a major setback. Many catalytic protocols suffer poor vanillin selectivity. Most of the active catalytic systems utilize rare and expensive noble metals; thus, those systems are not sustainable. The green credentials of these catalytic protocols are also addressed by utilizing CHEM21 green metrics toolkit.⁷⁰

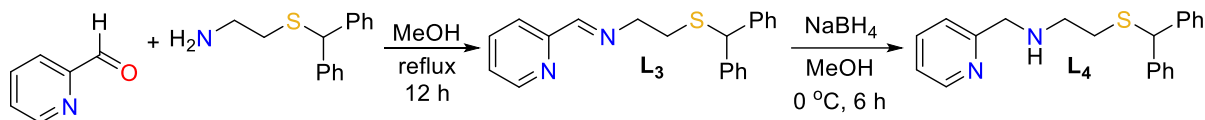
2.3 RESULTS AND DISCUSSION

Schiff base ligands are widely utilized in modern coordination chemistry due to their easy syntheses and tunable size and architectures.^{71,72} Furthermore, a tridentate ligand with a labile bulky arm can be a potential choice in the development of catalytically active metal complexes. Pincer complexes comprising tunable tridentate ligands are one of the most actively studied metal complexes for a wide range of applications.⁷³⁻⁷⁶ For the catalytic oxidation of primary alcohols, Copper bipyridines are frequently used in the presence of base or N-methylimidazole (NMI).⁷⁷⁻⁸³ NMI acts as the ligand as well as the base and plays an important role in hydrogen atom transfer from the alcohol substrate. Recently, dinuclear copper(II) complexes with bulky Schiff base ligands were utilized for alcohol oxidation.⁸⁴ Pendant hemilabile amine arms act as the internal base and play a key role in hydrogen atom transfer from alcohol. A very similar role of the oxy arms in similar Cu(II)-ONNO salen complexes was reported before.⁸⁵⁻⁸⁷ In this regard, our intention was to design a tridentate Schiff base ligand with a labile pendent thioether moiety. Such a labile arm can easily leave the metal and thus creates a vacant coordination site for substrate binding during catalysis. At the same time, the hemilabile thioether arm may act as the internal base and play a crucial role in hydrogen atom transfer from the alcohol substrate. Rose et al. smartly adjusted the ligand backbones of NNS Schiff base ligands to tune the coordination behavior.⁸⁸ The fine tuning of the ligand environments lead to the formation of metal complexes with the metal bound and free thioether arm.⁸⁸ Following the same line of thought, we began our ligand synthesis with the Schiff base condensation between 2-(benzhydrylthio)-ethanamine and pyridine-2-carboxaldehyde, which afforded the NNS Schiff

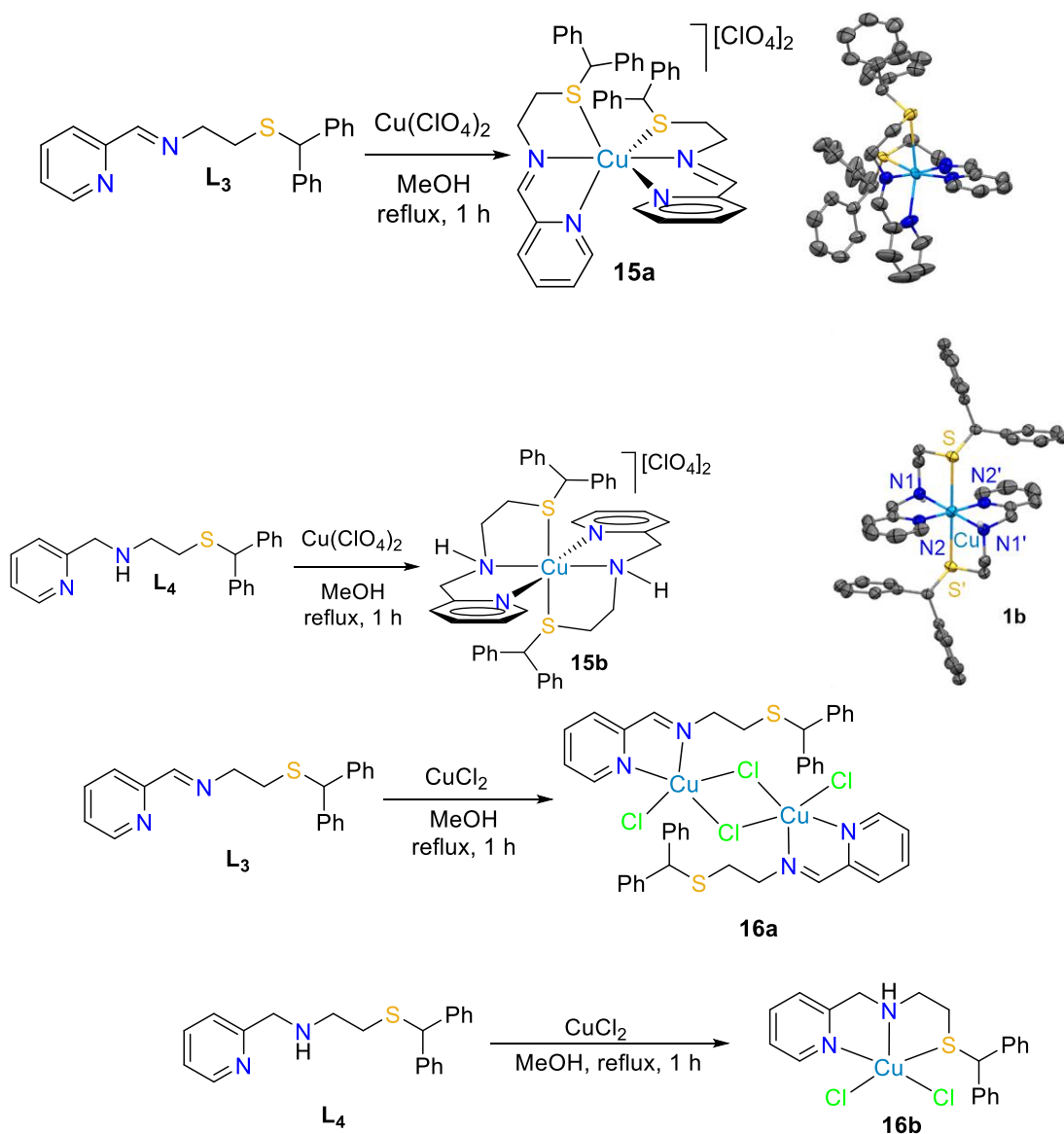
base ligand **L3** in almost quantitative yield (**Scheme 4.2**). The standard reduction of **L3** by NaBH_4 yielded the saturated version **L4** in excellent yield (**Scheme 4.2**). Ligands **L3** and **L4** were characterized by ^1H and ^{13}C NMR spectroscopy, FT-IR, mass spectrometry, and elemental analysis. The aliphatic CH_2 moieties appear as two triplets in the range of 2.50 ppm to 4.00 ppm (**L3**: 2.79 ppm and 3.83 ppm, **L4**: 2.61 ppm and 2.80 ppm) in the ^1H NMR spectra. The benzylic resonances were observed at 5.26 ppm (**L3**) and 5.18 ppm (**L4**). While the proton on the imine carbon of **L3** was found at 8.35 ppm, the respective resonance was found at 3.88 ppm for **L4**. The NH resonance of **L4** appeared as a broad singlet at 2.38 ppm. The resonances for aromatic protons of pyridine and phenyl rings were observed in the range of 7.20 ppm to 8.70 ppm. The facile coordination of **L3** and **L4** with Copper(II) perchlorate in 2:1 stoichiometric ratio resulted in the formation of homoleptic **complex 15a** and **complex 15b**, respectively, in good yields (**Scheme 4.2**). Homoleptic complexes were also formed in less yield when 1:1 metal ligand stoichiometric ratio was used. Similarly, the reaction of **L3** with CuCl_2 yielded a di nuclear **complex 16a** with free thioether arms (**Scheme 2.3**). However, **L4** reacted with CuCl_2 to form a mononuclear **complex 16b** with a coordinated thioether arm (**Scheme 2.3**). All these four air stable complexes were characterized by IR spectroscopy, mass spectrometry, and elemental analysis. In the IR spectrum of the free **ligand L3**, a sharp band was observed at 1646 cm^{-1} , which is the characteristic peak for the azomethine stretching vibration of the Schiff base.⁸⁹ The azomethine stretching bands are slightly shifted to 1650 and 1638 cm^{-1} for **complex 15a** and **complex 16a**, respectively.^{89,90} On the other hand, the stretching vibrations of the secondary amine were observed in the range of $3270\text{--}3240\text{ cm}^{-1}$ in the IR spectra of **complex 15b** and **complex 16b**.⁹¹ Amine stretching vibration was found at 3310 cm^{-1} in the free **ligand L4**. The vibrational bands in the range of $1400\text{--}1610\text{ cm}^{-1}$ are assigned to pyridyl (CvN) and phenyl (CvC) ring stretching for both the ligands and

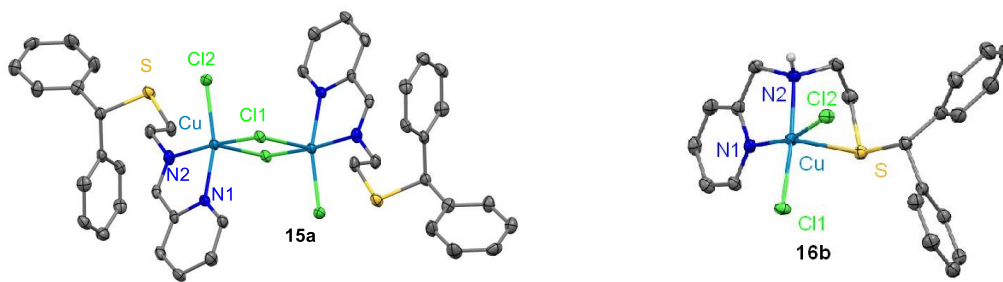
complexes.^{92,93} In addition, **complex 15a** and **complex 15b** showed strong and board absorption bands at 1080 cm^{-1} and bending vibrations

Scheme 2.2 Synthesis of ligands L3 and L4.



Scheme 2.3. Synthesis of Copper(II) complex 15a, complex 15b, complex 16a, and complex 16b (the molecular structures showing 30% ellipsoids and hydrogen atoms (except amine proton) and $[\text{ClO}_4]^-$ counter anions are omitted for clarity).





of the perchlorate counter anion.⁹⁰ The broadening of the stretching band indicates that perchlorate ions are involved in different noncovalent interactions in the solid state of **complex 15a** and **complex 15b**.⁹⁰ Complex **15a**, **15b**, **16a**, and **16b** were further characterized by single crystal X-ray analysis. X-ray crystallography reveals that **complex 15a** and **complex 15b** crystallize in the monoclinic crystal system. The asymmetric unit of **complex 15a** contains a complex cation $[\text{Cu}(\text{L}3)_2]^{2+}$ two perchlorate counter anions and half water molecule. On the other hand, two discrete crystallographically independent complex cations of general formula $[\text{Cu}(\text{L}4)_2]^{2+}$ two perchlorate counter anions, and one methanol are present in the asymmetric unit of **complex 15b**. The geometry around the metal centers in **complex 15a** and **complex 15b** is slightly distorted octahedral. However, the mode of coordination of the ligands is diverse in these complexes. The Schiff base ligand **L3** coordinates to the metal center meridionally in **complex 15a**, whereas the saturated ligand **L4** facially binds the metal center in **complex 15b**. This structural diversity arises due to the flexibility of the amine ligand **L4** compared to the rigid imine framework in ligand **L3**. The bond distances in **complex 15a** and **complex 15b** are characteristic of similar octahedral Cu(II) complexes.^{91,94} Moreover, the solid-state structures of these complexes are stabilized by $\pi \cdots \pi$ stacking interaction of the aromatic rings in **complex 15a** and strong hydrogen bonding interaction among the amine proton, solvated methanol, and perchlorate counter anion in **complex 15b**. **Complex 16a** and **complex 16b** crystallized in triclinic and monoclinic crystal systems with $P\bar{1}$ and $P21/c$ space groups, respectively. **Complex 16a** is a centrosymmetric dimer with two bridging chlorides around the metal centers while **complex 16b** is a mononuclear complex. The asymmetric unit of **complex 16a**

consists of half of the dimer. Each Cu center in **complex 16a** is coordinated by two N atoms of **L3**, two bridging chlorides, and one terminal chlorine atom. Moreover, the distance between two Copper centers is remarkably shorter (3.380 Å) than the previously reported dichloro-bridged Cu(II) complexes.⁹⁵⁻⁹⁷ It is worth noting that the pendant thioether arm of **L3** is free and far away from the metal coordination environment. On the other hand, a neutral complex unit [Cu(**L4**) Cl₄] is present in the asymmetric unit of **complex 16b**. Interestingly, the thioether arm of **L4** is coordinated to the metal center and is in the apical position while pyridine nitrogen, amine nitrogen, and two terminal chlorine atoms construct the basal plane around the metal center. The calculation of Addison parameter ($\tau=0.162$ for **complex 16a** and 0.174 for **complex 16b**) proved that the metal's surrounding geometry in both **complex 16a** and **complex 16b** can be best described as a slightly distorted square pyramidal structure.⁹⁸ The bond distances around the metal centers in **complex 16a** and **complex 16b** are consistent with similar complexes.^{94,99} Diverse hydrogen bonds (H...Cl) and $\pi\cdots\pi$ stacking interaction between the pyridine rings of two neighbouring molecules gives the solid-state stability in **complex 16a**. On the other hand, hydrogen bonding between the amine proton of one molecule and chlorine atom of the neighbouring molecule provides additional stability in the solid-state structure of **complex 16b**.

In homogeneous catalysis, the manipulation of the electronic and steric environment of the ligands has been considered very seriously for the better performance of catalysts. However, the effect of solvents in a homogeneous catalytic process often receive very trivial attention. Generally, a homogeneous catalytic reaction is performed in various solvents and the solvent with the best catalytic result is selected without further consideration of the solvent properties.¹⁰⁰⁻¹⁰⁵ The role of the solvent parameters on the outcome of the catalytic process is often ignored. In addition, solvent selection is one of the most important aspects in green chemistry research as solvents often account for a major amount of mass wasted in the synthetic

process.¹⁰⁶⁻¹⁰⁹ Though a large number of organic solvents are considered as problematic (such as acetonitrile, toluene, xylene, and DMSO) or even hazardous (such as THF, dichloromethane, chloroform, and benzene), some solvents are considered as safer and greener (water, ethanol, ethyl acetate, and acetone).⁷⁰ Moreover, Jessop et al. elegantly demonstrated how the careful selection of solvents using solvent parameters can significantly enhance the catalytic performance for homogeneous catalysis.¹¹⁰ Herein, we report the aerobic oxidation of vanillyl alcohol considering the green aspect as well as the direct role of solvent parameters.

Acetonitrile is a frequently used solvent for the aerobic oxidation of substituted benzyl alcohol.¹¹¹⁻¹¹³ Therefore, we explored the catalytic activities of four Copper(II) complexes, **complex 15a**, **complex 15b**, **complex 16a**, and **complex 16b** for the oxidation of vanillyl alcohol in air in the presence of TEMPO radical in acetonitrile. The aerobic oxidations were carried out at 40 °C for 6 h under base free conditions and 5 mol% Copper concentration was used. In the presence of a catalytic amount of the homoleptic **complex 15a** and **complex 15b**, roughly 6% vanillyl alcohol was converted to vanillin. The rest was unreacted vanillyl alcohol; the formation of vanillic acid or other byproducts was not detected by GC and NMR analysis. Compared to the homoleptic complexes, dinuclear **complex 16a** (2.5 mol % catalyst loading) gave better result with 24% conversion. The mononuclear **complex 16b** (5 mol% catalyst loading) displayed the best catalytic performance with 34% conversion. No byproduct was detected in the catalytic oxidation of vanillyl alcohol. We isolated vanillin in all catalytic oxidations (**complex 15a**: conversion 6%, yield 5%; **complex 15b**: conversion 6%, yield 5%; **complex 16a**: conversion 24%, yield 21%; **complex 16b**: conversion 34%, yield 32%) and the isolated yields were consistent with the respective conversions. The catalytic activities of **complex 15a**, **complex 15b**, **complex 16a**, and **complex 16b** were also tested in different solvents and similar activity trends were observed. Solvents might have significant effects on the outcome of aerobic oxidations of vanillyl alcohol. As the mononuclear **complex 16b**

displayed the best catalytic activity, we explored the catalytic activities of **complex 16b** in various solvents with a wide range of polarity. The aerobic oxidations in various solvents were carried out at 40 °C for 6 h in the presence of 5 mol% of **complex 16b** (**Table 2.1** and **Fig. 2.1**). Using water as a green solvent, 40% conversion of vanillyl alcohols to vanillin was observed in 6 h (entry 1). A bit reduced conversion (entry 2: 34%) was observed in acetonitrile, which is a frequently used solvent for the aerobic oxidations of substituted benzyl alcohols. Similar conversions of vanillyl alcohol were obtained in two alcoholic solvents (entry 3: ethanol, 32%; entry 4: methanol, 32%). Very similar conversion (32%) was obtained in THF (entry 7). Much reduced conversions were observed in acetone (entry 5: 16%) and ethyl acetate (entry 10: 20%). Very poor conversion (approximately 5%) of vanillyl alcohol to vanillin was also observed in DCM (entry 6), toluene (entry 9) and hexane (entry 10). Vanillin was isolated in most cases and the isolated yields were consistent with the respective conversions. The best conversion was obtained in water with very high polarity (**Table 2.1**).¹¹⁴ Similarly, highly polar organic solvents such as acetonitrile, ethanol, and methanol also gave good conversion. With decreased polarity, acetone gave reduced conversion. Very poor conversion was obtained in nonpolar solvents such as DCM, toluene, and hexane. A general trend has emerged from the data we obtained. The catalytic aerobic oxidation of vanillyl alcohol proceeds well in polar solvents and nonpolar solvents gave poor turnover. However, the nonpolar solvents ethyl acetate and THF gave decent to good conversions. As the general trend of conversion with solvent polarity is not applicable for all solvents, other solvent parameters might be more influential. In homogeneous catalysis, solvent molecules often displace a ligand site of a metal complex and later substrate binding occurs via the displacement of the solvent molecule. A very well-established reaction path of the hydrogenation of alkene by Wilkinson's catalysts involves these steps.¹¹⁵ Initially, a coordinated phosphine is replaced by a solvent molecule and later, that site is utilized for substrate coordination. In case of the present catalyst **complex 16b**,

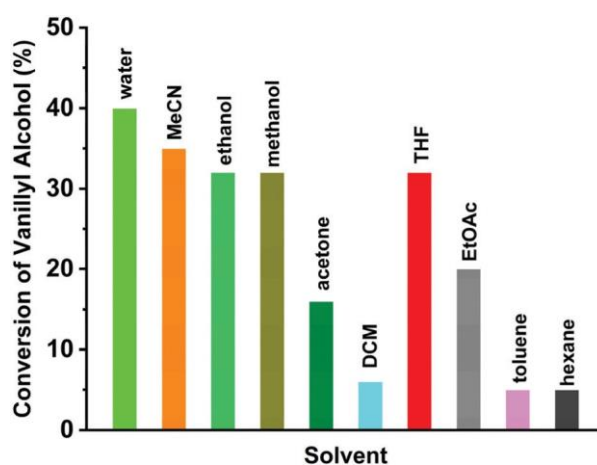
the hemilabile thioether arm can be displaced by the solvent molecule, which will be later replaced by the substrate. Hence, the coordination ability of the solvent might be a determining factor. Diaz-Torres and Alvarez developed a scale to quantify the coordination ability of solvents toward transition metals and lanthanides.¹¹⁶ The coordinating ability indices (α^{TM}) are summarized in **Table 2.1** with the highest value for water. Acetonitrile, THF, and alcoholic solvents also have good coordination ability with transition metals. Aromatic solvents (toluene), chlorocarbons (DCM), and alkanes (hexane) are considered as very weakly coordinating solvents.

Table 2.1 Catalytic performance of complex 16b for the aerobic oxidation of vanillyl alcohol to vanillin in different solvents with various polarities¹¹⁴ and coordination abilities (C.A.)^{116 a}

Ent	Solvent	Con. ^b (%)	Selectivity (%)	Isolated yield (%)	Dielectric const (ϵ)	C.A. (α^{TM})
1	Water	40	100	38	80.0	-0.1
2	MeCN	35	100	32	37.5	-0.2
3	EtOH	32	100	30	34.6	-0.5
4	MeOH	32	100	31	33.6	-0.4
5	Acetone	16	100	14	20.7	-1.0
6	DCM	<5	100	nd	8.9	-1.7
7	THF	32	100	30	7.6	-0.3
8	EtOAc	20	100	17	6.0	-0.8
9	Toluene	<5	100	nd	2.4	-1.2
10	Hexane	<5	100	nd	1.9	-1.8

^aReactions conducted for 6 h in a vial (10 mL) with 0.50 mmol of vanillyl alcohol, 5 mol % of **complex 16b** (12 mg), and 20 mol % of TEMPO (16 mg) in 2 mL of solvent at 40 °C. conversions of vanillyl alcohol to vanillin were determined by ¹H NMR spectroscopy using THF (0.50 mmol) as the external standard. nd: not determined.

Fig. 2.1 Graphical representation of the catalytic activity of complex 16b for the aerobic oxidation of vanillyl alcohol to vanillin in various solvents at 40 °C for 6 h.

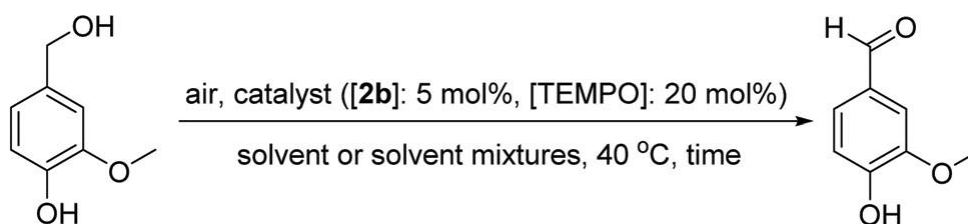


We have observed that water with the highest α^{TM} value gave the highest conversion of vanillyl alcohol to vanillin. Similarly, good coordinating organic solvents acetonitrile, THF, and alcohols gave good conversions (32-35%). Ethyl acetate and acetone as weakly coordinating solvents gave relatively poor conversion. Very poor conversions (less than 5%) were observed for very weakly coordinating solvents DCM, toluene, and hexane.

As the increasing coordination ability of the solvents toward transition metals reflected in the better transformation of vanillyl alcohol to vanillin with the best conversion in highly coordinating water, we carried out the aerobic oxidation of vanillyl alcohol in water at various times (**Table 2.2**). Using water as the green reaction media, 34% and 40% conversion of vanillyl alcohol to vanillin was observed in 3 and 6 h, respectively (entries 1 and 2). Surprisingly, increasing the reaction time to 9 and 12 h (entries 3 and 4) did not show any improvement; roughly 40% conversion was noted. In addition, black tar formation was observed. A similar observation of tar formation was reported previously in similar oxidations of lignin model compounds.⁵³ A careful observation revealed phase separation with prolonged time. A sticky and oily yellowish material separated out from the aqueous solution. The sticky material at the bottom of reaction vial prevented the spinning of the magnetic stir bar and finally formed black tar. Disappointingly, complete conversion or at least decent conversion of

vanillyl alcohol to vanillin could not be achieved in water as the green medium. As the phase separation in aqueous media pointed toward a solubility issue, we planned to use a mixture of water and organic solvent.

Table 2.2 Catalytic performance of complex 16b for the aerobic oxidation of vanillyl alcohol to vanillin in different solvents ^a



Ent	Time(h)	Solvent (ratio)	con ^b (%)	selectivity (%)	yield (%)
1	3	Water	34	100	30
2	6	Water	40	100	38
3	9	Water	42	100	nd
4	12	Water	43	100	nd
5	6	EtOH/water (1: 4)	60	100	nd
6	6	EtOH/water (1: 2)	72	100	70
7	6	EtOH/water (1: 1)	74	100	70
8	6	EtOH/water (2: 1)	69	100	nd
9	6	EtOH/water (4: 1)	62	100	nd
10	6	Acetone/water (1: 4)	56	100	nd
11	6	Acetone/water (1: 2)	70	100	nd
12	6	Acetone/water (1: 1)	81	100	80
13	6	Acetone/water (2: 1)	73	100	69
14	6	Acetone/water (4: 1)	62	100	nd
15	6	THF/water (1: 4)	60	100	nd
16	6	THF/water (1: 2)	69	100	65
17	6	THF/water (1: 1)	75	100	74
18	6	THF/water (2: 1)	58	100	nd
19	6	THF/water (4: 1)	44	100	nd
20	6	MeCN/water (1: 1)	61	100	60
21	6	MeOH/water (1: 1)	75	100	73
22	6	EtOAc/water (1: 1)	24	100	nd
23	6	DCM/water (1: 1)	14	100	nd
24	6	Toluene/water (1: 1)	12	100	nd

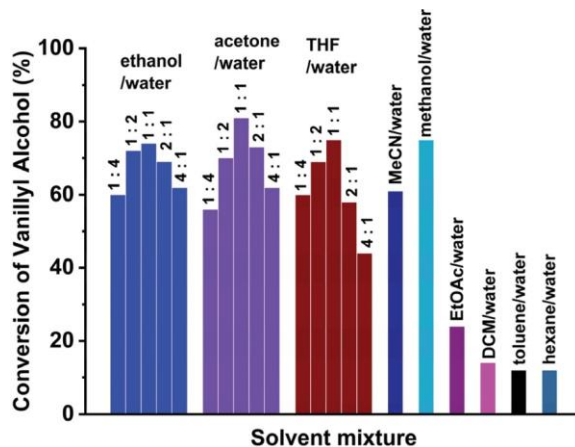
25	6	Hexane/water (1: 1)	12	100	nd
----	---	---------------------	----	-----	----

^aReactions conducted in a vial (10 mL) with 0.50 mmol of vanillyl alcohol, 5 mol % of **complex 16b** (12 mg), and 20 mol % of TEMPO (16 mg) in 2 mL of water or solvent mixtures (1: 1) at 40 °C. ^b Conversions of vanillyl alcohol to vanillin were determined by ¹H NMR spectroscopy using THF (0.50 mmol) as the standard. **nd**: not determined

9 and 12 h (entries 3 and 4) did not show any improvement; roughly 40% conversion was noted. In addition, black tar formation was observed. A similar observation of tar formation was reported previously in similar oxidations of lignin model compounds.⁵³ A careful observation revealed phase separation with prolonged time. A sticky and oily yellowish material separated out from the aqueous solution. The sticky material at the bottom of reaction vial prevented the spinning of the magnetic stir bar and finally formed black tar. Disappointingly, complete conversion or at least decent conversion of vanillyl alcohol to vanillin could not be achieved in water as the green medium. As the phase separation in aqueous media pointed toward a solubility issue, we planned to use a mixture of water and organic solvent. We first selected ethanol/water and acetone/water solvent mixtures as the reaction media (**Table 2.2**) because of the following reasons: both ethanol and acetone are considered as green solvents, they are miscible with each other, and they dissolve a wide range of organic compounds. The aerobic oxidations of vanillyl alcohol were conducted in the presence of 5 mol% **complex 16b** and 20 mol % TEMPO at 40 °C for 6 h. We noted 60, 72, 74, 69, and 62% conversions in 1:4, 1:2, 1:1, 2:1, and 4:1 mixtures of ethanol/water, respectively (entries 5-9 in **Table 2.2** and **Fig. 2.2**). Similarly, the aerobic oxidation of vanillyl alcohol was conducted in various mixtures of acetone/water (entries 10-14 in **Table 2.2**) with the best result obtained in a 1:1 mixture of acetone/water (entry 12:81%). We also utilized THF/water mixtures (entries 15-19 in **Table 2.2**) and a very similar trend was observed. Therefore, the following oxidations were carried out in a 1:1 mixture of organic solvents and water. If 1:1 mixture of acetonitrile/water (entry

20) and methanol/water (entry 21:75%) were used, 61 (entry 20) and 75% (entry 21) conversions to vanillin were obtained, respectively. In all the previous cases (entries 5-21), the organic solvents (ethanol, acetone, THF, acetonitrile, and methanol) are highly miscible with water and generally good conversions were noted. The following oxidations (entries 22-25) of vanillyl alcohol were performed in mixtures (1:1) of organic solvents (ethyl acetate, DCM, toluene, hexane), which are not miscible with water. Only 24% conversion of vanillin was obtained in a 1: 1 mixture of ethyl acetate/water (entry 22). Very poor conversions of roughly 10% were observed in 1:1 mixture of DCM/water (entry 23), toluene/water (entry 24), and hexane/water (entry 25). It was previously noted that pure ethyl acetate, DCM, toluene, and hexane also gave very poor results (entries 6, 8, 9, and 10 in Table 2.1). Therefore, the following facts can be summarized for the aerobic oxidation of vanillyl alcohol to vanillin: solvent mixtures are better media than pure solvent and the mixtures of water and water-miscible organic solvents are good reaction media. Again, no byproduct was detected in all the above catalytic oxidations We previously noted that phase separation in aqueous media resulted in tar formation with time and the complete conversion of vanillyl alcohol to vanillin in water could not be achieved. The solubility problem could be overcome using mixtures of water and water miscible organic solvents, in which good conversions of vanillyl alcohol to vanillin were achieved.

Fig. 2.2 Graphical representation of the catalytic activity of complex 16b for the aerobic oxidation of vanillyl alcohol to vanillin in various solvent mixtures at 40 °C for 6 h.



Therefore, we kept using the mixtures of water and water miscible organic solvents to further test the effect of time, temperature, and catalyst loading on the aerobic oxidation of vanillyl alcohol (Table 2.3 and Fig. 2.3). We selected 1:1 mixture of ethanol/water and acetone/water as they showed the best catalytic performances and are considered as green solvents.⁷⁰ Though the mixture of THF/water gave very similar results, we excluded the THF/water mixture as THF is not considered as a green solvent. At first, we tested how the catalytic activity of **complex 16b** in ethanol/water and acetone/water changed with time under standard reaction conditions (**complex 16b**: 5 mol%, TEMPO: 20 mol%, 40 °C). Using ethanol/water as the reaction media, 55, 74, 86, and 95% conversion of vanillyl alcohol to vanillin was observed in 3, 6, 9, and 12 h, respectively (entries 1, 2, 3, and 4). Complete conversion to vanillin in ethanol/water medium was observed in 15 h (entry 5). Slightly better conversion was observed in acetone/water as the reaction medium (entries 7, 8, 9, and 10). As compared to the ethanol/water mixture, the complete conversion of vanillyl alcohol to vanillin was observed in less time (entry 10:12 h). If the reaction times for the aerobic oxidations in ethanol/water (entry 6) and acetone/water (entry 11) were extended to 24 h, the formation of any side product was not detected. Thereafter, we reduced the catalyst loading (**complex 16b**: 3 mol% and TEMPO:

Ent	Cu (mol %)	TEMPO (mol %)	Temp. (°C)	Time (h)	Solvent (1:1)	Con.^b (%)
1	complex 16b (5)	20	40	3	E/W	55 (100 ^c)
2	complex 16b (5)	20	40	6	E/W	74 (100 ^c)
3	complex 16b (5)	20	40	9	E/W	86 (100 ^c)
4	complex 16b (5)	20	40	12	E/W	95 (100 ^c)
5	complex 16b (5)	20	40	15	E/W	100 (100 ^c , 99 ^d)
6	complex 16b (5)	20	40	24	E/W	100 (100 ^c , 100 ^d)
7	complex 16b (5)	20	40	3	A/W	62 (100 ^c)
8	complex 16b (5)	20	40	6	A/W	81 (100 ^c)
9	complex 16b (5)	20	40	9	A/W	93 (100 ^c)
10	complex 16b (5)	20	40	12	A/W	100 (100 ^c)
11	complex 16b (5)	20	40	24	A/W	100 (100 ^c)
12	complex 16b (3)	10	40	12	E/W	65 (100 ^c)
13	complex 16b (3)	10	40	24	E/W	100 (100 ^c)
14	complex 16b (3)	10	40	12	A/W	78 (100 ^c)
15	complex 16b (3)	10	40	20	A/W	100 (100 ^c)
16	complex 16b (3)	10	50	12	A/W	82 (100 ^c)
17	complex 16b (3)	10	50	18	A/W	97 (100 ^c)
18	complex 16b (3)	10	50	20	A/W	100 (100 ^c)
19	complex 16b (3)	10	25	12	A/W	62 (100 ^c)
20	complex 16b (3)	10	25	20	A/W	85 (100 ^c)
21	complex 16b (3)	10	25	30	A/W	100 (100 ^c)
22	complex 16b (5)	20	25	20	A/W	100 (100 ^c)
23	complex 16b (5)	20	25	24	E/W	100 (100 ^c)
24	complex 16b (3)	10	25	36	E/W	100 (100 ^c)
25	complex 16b (3)	10	70	12	W	42 (100 ^c)
26	complex 16b (3)	10	70	24	W	41 (100 ^c)
27	complex 16b (3)	10	70	12	E/W	84 (100 ^c)
28	complex 16b (3)	10	70	16	E/W	100 (100 ^c)
29	complex 16b (3)	10	70	24	E/W	100 (100 ^c , 99 ^d)
30	complex 16b (5)	20	100	3	E/W	71 (100 ^c , 68 ^d)
31	complex 16b (5)	20	100	6	E/W	90 (100 ^c , 88 ^d)

32	complex 16b (5)	20	100	9	E/W	100 (88 ^c , 84 ^d)
33	complex 16b (5)	20	100	12	E/W	100 (72 ^c , 68 ^d)

Table 2.3 Catalytic performance of complex 16b for the aerobic oxidation of vanillyl alcohol

^aReactions conducted in a vial (10 mL) with 0.50 mmol of vanillyl alcohol, 5/3 mol % of **complex 16b** (12/7 mg, 0.67/0.39 wt.%), and 20/10 mol % of TEMPO (16/8 mg, 0.87/0.45 wt.%) in 2 mL of water (W), 1:1 mixtures of ethanol/water (E/W), and acetone/water (A/W).

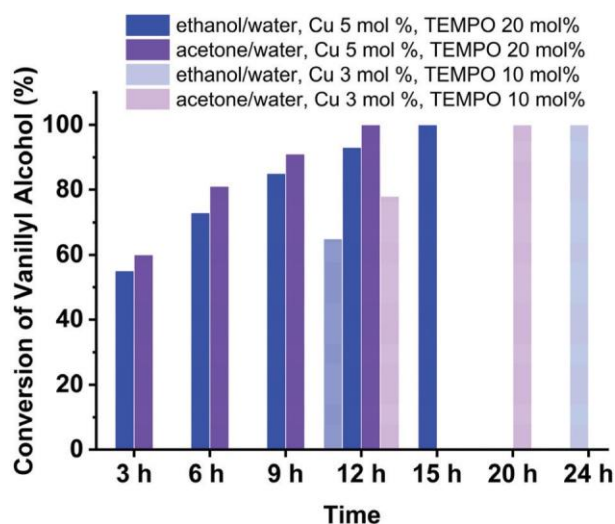
^bConversions to vanillin were determined by ¹H NMR spectroscopy using THF (0.50 mmol) as the standard. ^cSelectivity toward vanillin. ^dIsolated yields of vanillin (10 mol %).

Reduced catalyst loading lead to 65% and 78% conversion in 12 h in ethanol/water (entry 12) and acetone/water (entry 14), respectively. Under identical reaction conditions, the complete conversions of vanillyl alcohol to vanillin in ethanol/water (entry 13) and acetone/water (entry 15) were noted in 24 and 20 h, respectively. Finally, we studied the effect of temperature on the aerobic oxidation of vanillyl alcohol. The energy requirement of a chemical transformation should be minimized and ideally, the synthesis should be conducted at ambient temperature and pressure.¹⁷ Clark et al. developed the CHEM21 green metrics toolkit, which is a quantitative extension of “The 12 Principles of Green Chemistry”.⁷⁰ A chemical transformation receives a green flag if it is conducted at mild temperature, between 0 to 70 °C.

However, a synthesis gets a red flag in the temperature range of 0 to 70 °C if it is carried out at the boiling temperature of the solvent. This is because of the fact that a reaction under reflux consumes roughly six times more energy as compared to the temperature 5 °C below the boiling point of the solvent. Therefore, we carefully selected the reaction temperatures for the next set of aerobic oxidations of vanillyl alcohol at elevated temperatures. For water and ethanol/water mixture as reaction media, we selected 70 °C as the reaction temperature as it falls in the mild temperature range as well as it is more than 5 °C below the boiling point of both water and

ethanol. For the same reasons, we choose 50 °C as the reaction temperature for the oxidation of vanillyl alcohol in acetone/water reaction medium. Slightly better conversions to vanillin in acetone/ water were obtained if the reactions were carried out at 50 °C (entries 16, 17, and 18) instead of 40 °C (entries 14 and 15).

Fig. 2.3 Graphical representation of the catalytic activity of complex 16b for the aerobic oxidation of vanillyl alcohol to vanillin at 40 °C in ethanol/water (1:1) and acetone/water (1:1) at various times with two different catalyst loadings (complex 16b: 5 mol %, TEMPO: 20 mol % and complex 16b: 3 mol %, TEMPO: 10 mol %).



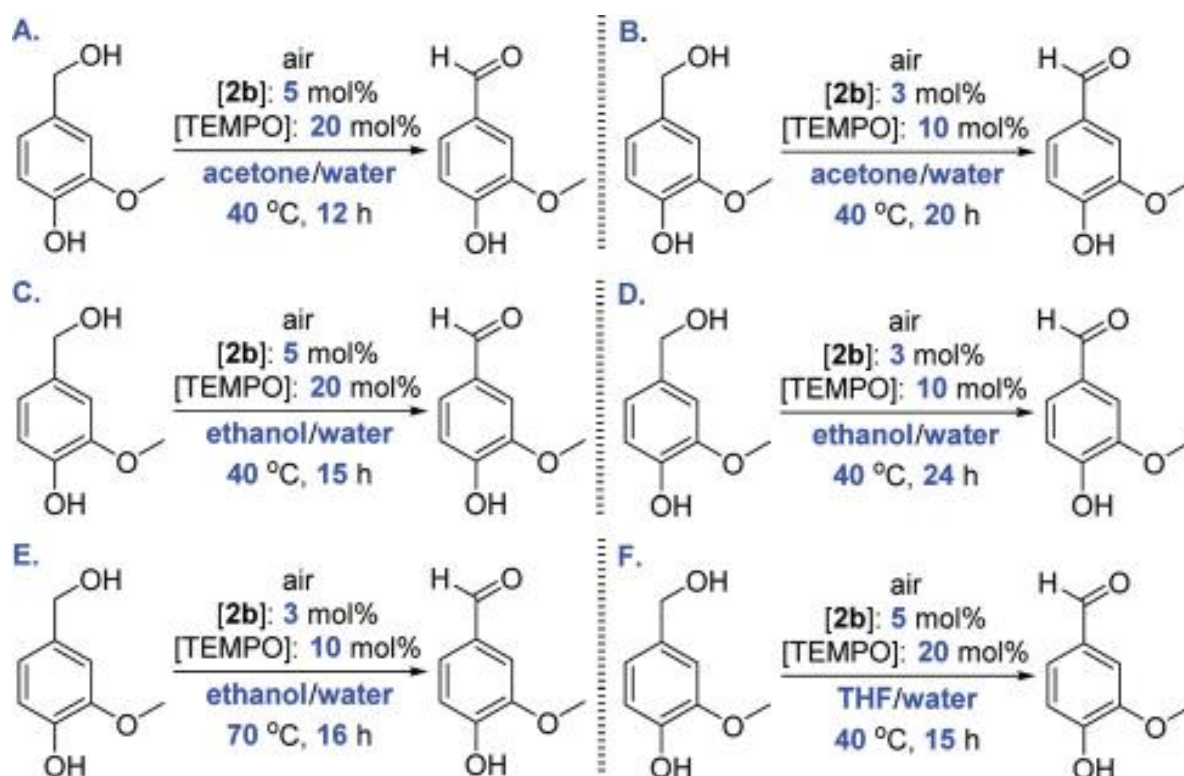
As expected, a slight increase in the reaction temperature (10 °C) was reflected at the slightly better conversion of vanillyl alcohol to vanillin. Then, we performed the aerobic oxidations of vanillyl alcohol in acetone/water and ethanol/water at r.t. (entries 19, 20, 21, 22, 23, and 24). We were pleased to see that complete conversion to vanillin could be achieved at r.t.; however, a longer time was required. Thereafter, the oxidations were done in water and ethanol/water mixture at elevated temperatures. Increasing the reaction temperature from 40 °C to 70 °C (entry 25) in water, no real improvement in the conversion of vanillyl alcohol to vanillin was observed in 12 h. Further heating at 70 °C for 24 h, very similar conversion to vanillin was obtained (entry 26) along with the formation of tar. Better conversion of vanillyl alcohol was observed if the ethanol/water reaction medium was heated to 70 °C (entries 27

and 28) instead of 40 °C (entries 12 and 13). The complete conversion of vanillyl alcohol to vanillin was obtained in 16 h at 70 °C (entry 28). If the reaction time is further extended to 24 h at 70 °C (entry 29), we did not observe the formation of any byproduct and we isolated vanillin in quantitative yield (99%). During the oxidation of vanillyl alcohol to vanillin, often overoxidation leads to the formation of vanillic acid as the byproduct. However, we did not observe any overoxidation of vanillin during the catalytic aerobic oxidations of vanillyl alcohol in the temperature range from r.t. to 70 °C (even after prolonged heating). In fact, we did not observe the formation of any byproduct. **Complex 16b** displayed remarkably good selectivity and good conversion in this temperature range. However, higher temperature might lead to the oxidation of vanillin to vanillic acid. Hence, we tested the catalytic activity of **complex 16b** at an even higher temperature (100 °C). The mixture of ethanol/water was selected for that purpose. Several catalytic aerobic oxidations of vanillyl alcohol were performed using 5 mol% of **complex 16b** and 20 mol % of TEMPO in ethanol/water mixture at 100 °C. As compared to lower temperatures, much enhanced catalytic activities were observed initially at 100 °C. Approximately 70% and 90% conversion of vanillyl alcohol to vanillin were observed in 3 and 6 h, respectively, with consistent isolated yields (entry 30: 68%, entry 31: 88%). Further extending the reaction time to 9 h lead to the complete conversion of vanillyl alcohol (entry 32). However, vanillin (84% isolated yield) was not the only product. We observed the formation of the over oxidation product vanillin acid (more than 10%). As expected, a further increase of the reaction time to 12 h (entry 33) lead to the formation of an increased amount of vanillic acid. Therefore, the selectivity of **complex 16b** was lost at 100 °C. However, **complex 16b** displayed excellent selectivity for the aerobic oxidation of vanillyl alcohol to vanillin in the milder temperature range (0 to 70 °C).

Developing a new and better synthetic method is important; however, it is more important to develop a greener and more sustainable catalytic protocol for that chemical transformation

as the need of a green and sustainable process is an unavoidable reality in our modern era. Therefore, it is necessary to assess the drawbacks and advantages of our catalytic protocol for the aerobic oxidation of vanillyl alcohol to vanillin with the green credentials based on “The 12 Principles of Green Chemistry”.^{14,17-19,117-119} First of all, we did not use external oxidant such as peroxides or pressurized dioxygen cylinder. Therefore, the selective oxidations of vanillyl alcohol to vanillin using air as a sustainable oxidant is no doubt advantageous. To further examine the green and sustainable aspects of this one step oxidation, six different optimized methods were selected using acetone/water (Methods A and B), ethanol/water (Methods C, D, and E), and THF/water (Method F) as the reaction media (**Scheme 2.4 and Table 2.4**). We evaluated the six catalytic protocols with the CHEM21 green metrics toolkit established by Clark et al.⁷⁰ This CHEM21 green metrics toolkit is a quantitative extension of “The 12 Principles of Green Chemistry” and various synthetic chemical processes were evaluated with CHEM21 green metrics toolkit.¹²⁰⁻¹²⁵

Scheme 2.4 Catalytic aerobic oxidation of vanillyl alcohol to vanillin using different optimized reaction conditions



All these show that aerobic oxidations were performed at ambient conditions except Method E, which was carried out at 70 °C. Methods B, D, and E were performed in the presence of 3 mol % of **complex 16b** and 10 mol % of the TEMPO radical. However, Methods A, C, and F were executed with higher catalyst loading (**complex 16b**: 5 mol % and TEMPO:20 mol %). Though CHEM21 green metrics toolkit involves zero pass, first pass, second pass, and third pass with increasing intricacy level, we examined Methods A to F utilizing zero pass and first pass as the second pass and third pass, which are considered as industrial toolkits and outside the scope of small-scale research in the academic laboratory. Green and red flags are assigned for promising and undesirable processes, respectively. Amber colour reflects an acceptable process with issues. The results of these analyses are summarized in Table 4. At first, we analysed the yield, conversion, and selectivity of these six methods with isolated yields of vanillin (purity check was done by ¹H NMR spectroscopy). All the six methods earn green flags for first three metrics (yield, conversion, and selectivity) as they all reach complete

conversion in a specified time. The atom economy and reaction mass efficiency for all the six methods are the same. The mass intensities for Methods A to F are more than 50. However, Method F provides slightly better mass intensity as THF is slightly lighter than acetone or ethanol. The solvent is a very important metric for the green and sustainable measure as solvents constitute roughly half of the mass intensity for all the six methods. Besides water and ethanol, acetone is also recognized as a green solvent hence, Methods A to E receive green flags. However, an amber flag is assigned for Method F as THF is considered as a problematic or a hazardous solvent.

Table 2.4 Comparison of the six different methods (Methods A to F) for the aerobic oxidation of vanillyl alcohol from the CHEM21 Green Metrics Toolkit calculation

Metric	Method A	Method B	Method C	Method D	Method E	Method F
yield	100	100	100	100	100	100
conversion	100	100	100	100	100	100
selectivity	100	100	100	100	100	100
atom economy	81.7	81.7	81.7	81.7	81.7	81.7
mass efficiency	89.4	89.4	89.4	89.4	89.4	89.4
mass intensity	55.9	55.9	55.9	55.9	55.9	57.3
solvent	acetone/ water	acetone/ water	ethanol/ water	ethanol/ water	ethanol/ water	THF/ water
catalyst	yes	yes	yes	yes	yes	yes
catalyst recovery	yes	yes	yes	yes	yes	yes
element	Cu	Cu	Cu	Cu	Cu	Cu
reactor	Batch	Batch	Batch	Batch		Batch
work up	drying	drying	drying	drying	drying	drying
energy	40 °C	40 °C	40 °C	40 °C	70 °C	40 °C
health & safety						H351

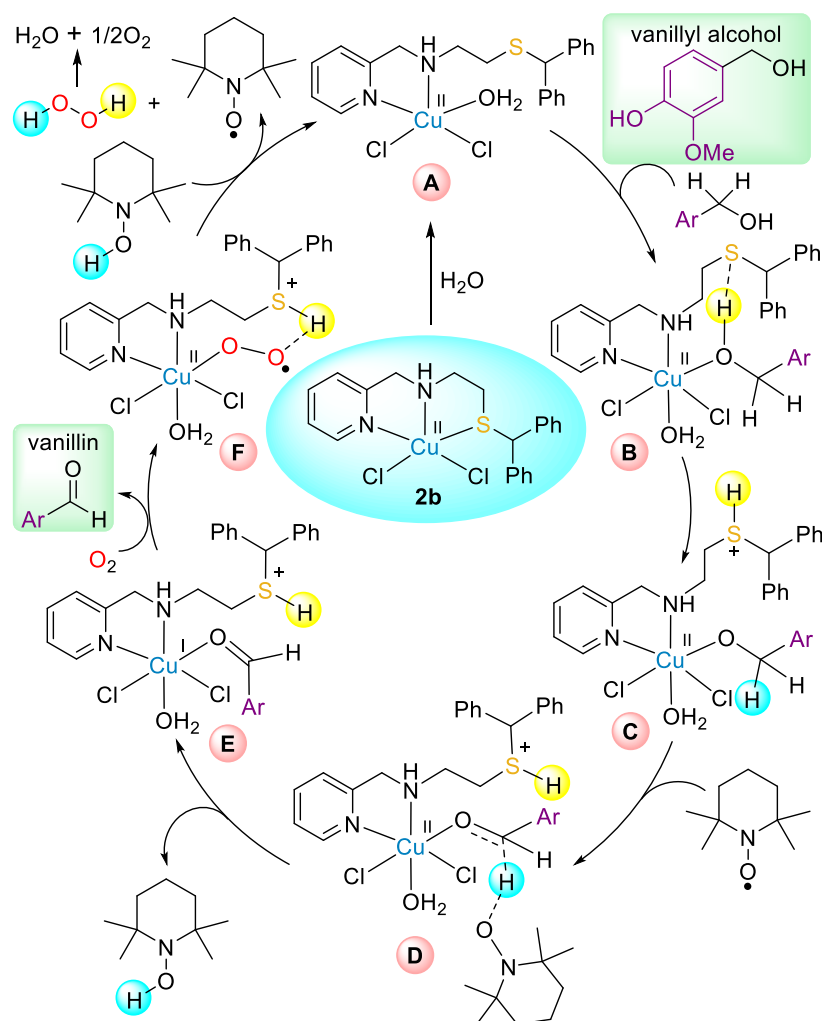
All methods utilized catalysts and catalyst recovery was also performed efficiently. Therefore, all the methods earn green flags for these two metrics. Methods A to F utilized Copper complex as the catalyst; hence, all these methods were assigned with amber flags. Though Copper is an abundant base metal on earth crust as well as in sea water, geopolitical issues may also dictate the availability of an element. However, the cost of Copper metal as catalyst component is much less compared to noble metals such as ruthenium, osmium, rhodium, iridium, palladium, platinum, silver, and gold, which are often utilized as catalysts. As we performed those

reactions in batches, Methods A to F again received amber flags; green flag is assigned for continuous flow process. As we adopted common and easy work up techniques, all methods earn green flags. Thereafter, we analyzed all six methods utilizing energy parameters. Reactions for Methods A, B, C, D, and F were carried out at ambient temperature (40 °C) and hence, they are assigned with green flags. Oxidation in Method E was performed at 70 °C, which is in the acceptable temperature range (0 to 70 °C) and more than 5 °C below the boiling point of ethanol and water. Therefore, Method E also earns a green flag irrespective of the fact that Method E was performed at elevated temperature. Finally, we evaluated all the six methods using health and safety norms. Methods A to E received green flags as no hazardous chemicals was used. However, Method F received an amber flag due to the use of THF as a potentially hazardous solvent. To test the robustness and the practical potential of this catalytic protocol, it is important to perform grayscale reactions. All the six methods under different optimized reaction conditions were performed with 10.0 mmol of vanillyl alcohol (1.54 g). All six large scale catalytic oxidation of vanillyl alcohol gave quantitative yields of vanillin and further purification of vanillin was not necessary. In summary, excellent selectivity (100%), complete conversion, and quantitative yield of vanillin could be achieved at ambient conditions (40 °C in air) using standard catalyst loading (3 to 5 mol% of **complex 16b**) in green solvent mixtures (ethanol/water and acetone/ water) without an additional base. It is worth to compare the selectivity, yield, and conversion of the present catalytic system with the existing catalytic protocols. The previously reported catalysts, which targeted the oxidation of vanillyl alcohol to vanillin, are mostly heterogeneous; only a very few homogeneous systems are known. Compared to our catalytic system, cobalt(salen) catalyst gave very poor conversions and yields (10 mol% catalyst, r.t., 3.5 bar of O₂, 17 h: 3% in methanol).⁶⁷ The selectivity of the cobalt(salen) catalyst system was also very poor as a large amount of 2-methoxy-1,4-benzoquinone was formed. The iron porphyrin complex gave much faster oxidation of vanillyl

alcohol (complete conversion in 3 h) in the presence of additional oxidant H₂O₂; however, no information on the selectivity was provided.⁶⁸ Metal oxides and mixed metal oxides were heavily used for the oxidation of vanillyl alcohol. Compared to the ambient conditions used in our catalytic system (40 °C and atmospheric pressure of air), high temperatures (120 to 140 °C) and pressures (ca. 20 bar of O₂ mostly or air) were used for most of the metal oxide catalysts.^{53,55-57} Although Ce-Zr mixed oxides gave high conversion and selectivity under harsh conditions,⁵⁷ most metal oxides gave moderate to good conversions (ca. 60 to 90%) of vanillyl alcohol with poor to moderate selectivity toward vanillin (ca. 20-70%). Various byproducts such as vanillic acid, benzoquinone derivatives, and guaiacol were identified. Cobalt oxide catalyst gave good conversion (80%) with excellent selectivity (98%) under milder conditions (80 °C, 7 bar of O₂).⁵⁴ In contrast to our base-free aerobic condition, high concentration of base and pressurized O₂ was used for the cobalt oxide catalyst. Similarly, excellent selectivity could not be achieved using metal nanoparticles.⁵⁸⁻⁶² Although high selectivity could be achieved using photocatalysts,⁶³⁻⁶⁵ poor conversion was a major issue in contrast to complete conversion achieved with the present catalyst. Hence, we can conclude that we have developed a significantly improved catalytic protocols as compared to the existing catalytic system for the aerobic oxidation of vanillyl alcohol to vanillin. In contrast to the existing catalytic systems, our catalytic protocol operates under ambient and base free conditions in green solvents with complete conversion, quantitative yield, and excellent selectivity.

Based on the previous reports and supported by experimental evidences, we propose a plausible mechanism for the aerobic oxidation of vanillyl alcohol to vanillin catalyzed by Copper **complex 16b** and TEMPO radical (**Scheme 2.5**). It is generally accepted that alcohol coordinates to the Cu(II) metal center and the TEMPO radical abstracts the β -hydrogen from the coordinated alcohol to generate TEMPOH, proton, and Cu(I) species with coordinated carbonyl.

Scheme 2.5. Plausible mechanism for the catalytic aerobic oxidation of vanillyl alcohol to vanillin (dotted bonds indicate weak noncovalent interactions).



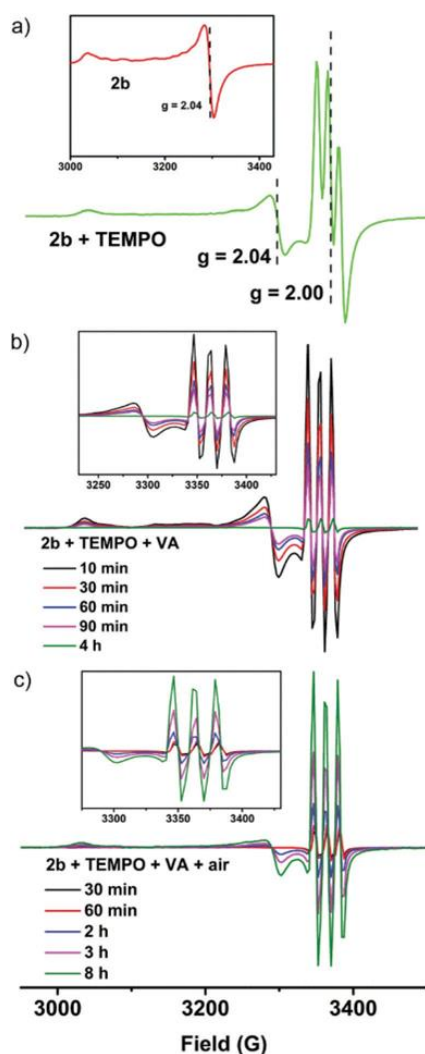
Several paths have been proposed for β -hydrogen transfer from coordinated alcohol to TEMPO such as bimolecular hydrogen atom transfer,¹²⁷ hydrogen atom transfer to η^2 -nitroxyl,¹²⁸ and hydrogen atom or hydride transfer to η^1 -nitroxyl.⁸³ By performing detailed experimental and computational analyses, Stahl et al. suggested that bimolecular hydrogen atom transfer and hydrogen atom transfer to η^2 -nitroxyl are not favored as compared to hydrogen atom or hydride transfer to η^1 -nitroxyl involving a six membered transition state for concerted hydrogen transfer (Oppenauer oxidation like pathway).⁸³ Similarly, we propose the present catalytic cycle and the prominent role of solvent coordination is emphasized with

mass analysis. As the best catalytic performances were obtained in the presence of water (either as a pure solvent or as a mixture with water miscible organic solvents) and since water has a very good coordination ability with transition metals, we propose that water coordinates with the five coordinated precatalyst **complex 16b** to give species A in the first step. In this step, water coordination results in the decoordination of the hemilabile thioether arm. In the following steps, vanillyl alcohol coordinates to the relatively open Cu center to form the six-coordinated species B with weak noncovalent interaction between the alcoholic proton and the thioether arm of the ligand framework, followed by the formation of the Cu(II) alkoxy species C with protonated thioether moiety. The coordination flexibility of this type of thioether moiety in similar ligands has been demonstrated previously.⁸⁸ The formulation of either species B or C is supported by the presence of a mass peak with m/z of 605.1961 ($[M_B-Cl]^+$ or $[M_C-Cl]^+$ for $C_{29}H_{34}ClCuN_2O_4S$). Thereafter, TEMPO radical participates to abstract the β -hydrogen from the coordinated alkoxy moiety and the formation of species D is proposed. This path involves β -hydrogen transfer to the TEMPO radical to form TEMPOH and EPR-inactive Cu(I) species E is proposed to form. The formulation of D is supported by mass analysis (m/z 782.1995 $[M_D-Cl+Na]^+$ for $C_{38}H_{51}ClCuN_3NaO_5S$). Thereafter, dioxygen interacts with the metal center with the release of carbonyl product, followed by the oxidation of Cu(I) to Cu(II). The oxidation of Cu(I) to Cu(II) takes place by transferring one electron from Cu(I) to dioxygen, resulting in Cu(II) with coordinated $O_2^{\bullet-}$.¹²⁹ This Cu(II)- $O_2^{\bullet-}$ species F is expected to be EPR silent due to the magnetic interaction between Cu(II) and $O_2^{\bullet-}$.^{129,130} Mass analysis (m/z 448.0450 $[M_F-2Cl]^+$ for $C_{21}H_{24}CuN_2O_3S$) supported the formulation of the Cu(II)- O_2 species F. $O_2^{\bullet-}$ is regarded as highly reactive for proton abstraction and in the last step, we propose that coordinated $O_2^{\bullet-}$ accepts the proton from the protonated thioether arm. Finally, TEMPOH reacts to release the starting catalyst A, TEMPO radical, and H_2O_2 . We performed EPR measurements to shed light on the proposed reaction

pathway (**Fig. 4**). At first, we measured the EPR spectrum of **complex 16b** under inert conditions (**Fig. 4a** insert). After adding two equivalents of the TEMPO radical under inert conditions, the EPR spectrum was recorded again and the EPR signals of both **complex 16b** and TEMPO were clearly detected (**Fig. 4a**). Thereafter ten equivalents of vanillyl alcohol (10 mol % **complex 16b** w.r.t. substrate) were added under an inert atmosphere and the EPR spectra were measured at regular time intervals (**Fig. 4b**). The intensities of the EPR signals of **complex 16b** and TEMPO decreased with time. Finally, the EPR signals of **complex 16b** completely disappeared, which indicates the formation of EPR inactive Cu(I) species (F). Four hours later, the reaction mixture was opened to air and the EPR spectra were recorded at regular time intervals (**Fig. 4c**). Roughly one hour later, the EPR signal of **complex 16b** reappeared and the EPR signals of **complex 16b** and TEMPO increased with time. The increased intensities of the EPR signals suggested the aerobic oxidation of EPR silent Cu(I) to EPR active Cu(II), followed by the reaction with TEMPOH to release **complex 16b**, TEMPO radical, and H₂O₂. We also analyzed the reaction mixture to identify H₂O₂ by the well-established procedure to detect the formation of H₂O₂ in the catalytic reactions.^{131,132} We were pleased to identify H₂O₂ in the reaction mixture, which provided additional support for the proposed reaction pathway.

Recyclability is an important feature for the sustainable development of a catalytic process. After using **complex 16b** as the catalyst for the aerobic oxidation of vanillyl alcohol, the used catalyst was recovered and reused. We did not see any change in the catalytic activity in the second cycle. The same catalyst was recovered and reused twice without any visible change in the catalytic conversion and selectivity. Therefore, **complex 16b** was successfully recycled three times. It is worth mentioning that we also examined the nature of the catalytic species (**complex 16b**) after the aerobic oxidation was performed.

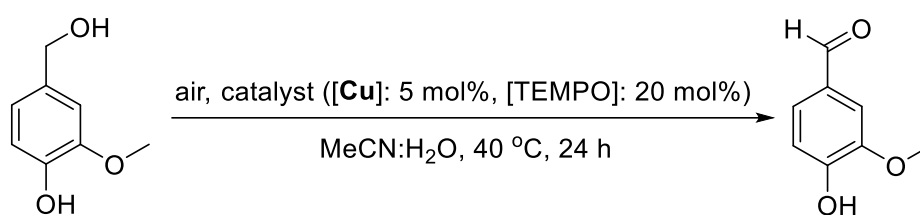
Fig. 2.4 EPR spectra of (a) complex 16b and TEMPO radical (complex 16b in the insert) under inert conditions, (b) complex 16b, TEMPO radical, and vanillyl alcohol (VA) under inert conditions, and (c) complex 16b, TEMPO radical, and vanillyl alcohol (VA) in air.



The recycled catalyst was crystallized in organic solvents and analyzed with single crystal X-ray analysis, and it was confirmed that the identity of **complex 16b** did not change after the catalytic cycle. We also verified if the concentration (particularly high concentrations) of vanillyl alcohol influences the catalytic activity of **complex 16b**. We used 0.250 M solutions of vanillyl alcohol in all the above catalytic aerobic oxidations. In addition, various concentrations of vanillyl alcohol were tested using conditions of Method B (**Table 2.5**) Under the stated conditions, complete conversions were obtained with 0.125 and 0.250 M solutions

of vanillyl alcohol. At higher concentrations, full conversions were not achieved in 20 h and the lowest conversion of 43% was observed with 1.000 M solution. Hence, the catalytic reactivity fell steadily with the increasing concentration of vanillyl alcohol. However, no byproduct was formed and the reactions at high concentrations were also 100% selective. As a final note, we discuss the possible effects of two slightly different ligands (**L3** and **L4**) and the resultant four Copper(II) complexes (**complex 15a**, **complex 15b**, **complex 16a**, and **complex 16b**) with distinct structural features on the catalytic activities for the aerobic oxidation of vanillyl alcohol.

Table 2.5 Catalytic performance of complex 16b for the aerobic oxidation of vanillyl alcohol to vanillin at different concentrations of vanillyl alcohol^a



Ent	[VA] (M)	Con.b (%)	Selectivity (%)	Isolated yield (%)
1	0.125	100	100	98
2	0.250	100	100	99
3	0.375	89	100	86
4	0.500	77	100	75
5	0.625	65	100	65
6	0.750	56	100	53
7	1.000	43	100	40

^aReactions conducted in a 10 mL vial in 2 mL of acetone/water (1:1) at 40 °C for 20 h. conversions of vanillyl alcohol (VA) to vanillin was determined by ¹H NMR spectroscopy using THF (0.50 mmol) as the standard.

The reaction of Copper(II) perchlorate with Schiff base ligand **L3** and the saturated version **L4** resulted in similar homoleptic **complex 15a** and **complex 15b**, where NNS ligands surround the Copper centers octahedrally. Both **complex 15a** and **complex 15b** showed very poor catalytic activity. A coordination number higher than six for Copper is very unlikely. However, thioether arms are hemilabile and the substrate could bind to the metal center. At the same time, substrate binding to metal faces competition from nearby perchlorate counter anions and solvent molecules. Therefore, it is not surprising that homoleptic metal complexes are either catalytically inactive or poorly active. On reaction with CuCl_2 , the Schiff base ligand **L3** yielded a dinuclear **complex 16a** with a five-coordinated metal center and a free thioether arm. The saturated ligand **L4** reacted with CuCl_2 and formed a mononuclear **complex 16b** with a five-coordinated metal center and a coordinated thioether arm. Both complexes, **complex 16a** and **complex 16b** have vacant sites for substrate coordination and both displayed good catalytic activities. However, mononuclear **complex 16b** showed slightly better catalytic activity. Mononuclear **complex 16b** already has a vacant site and in addition, another binding site may well be created by the decoordination of the hemilabile thioether moiety. In contrast, the vacant site of the five-coordinated Copper center in **complex 16a** is sterically hindered by the free dangling thioether arm. Thus, substrate coordination is expected to be better in **complex 16b** compared to **complex 16a** and the better catalytic activity for mononuclear **complex 16b** is justified.

2.4 CONCLUSION

The facile coordination of the pendant thioether-appended Schiff base ligand **L3** and the corresponding saturated version **L4** with Copper(II) perchlorate yielded similar homoleptic complexes **complex 15a** and **complex 15b**, respectively. However, the coordination of **L3** and **L4** with Copper(II) chloride resulted in the formation of dinuclear **complex 16a** with a free thioether arm and mononuclear **complex 16b** with a coordinated thioether arm, respectively.

All these air stable **complex 15a**, **complex 15b**, **complex 16a**, and **complex 16b** are active for the aerobic oxidation of vanillyl alcohol to valuable aroma molecule vanillin, with the best activity displayed by the mononuclear **complex 16b**. Using Copper complex as a catalyst is advantageous as this first-row transition metal is abundant on the earth's crust and sea water. Instead of using peroxides or dioxygen cylinder as frequently used oxidants, utilizing air as the oxidant is sustainable. In addition, the present oxidation does not require the addition of stoichiometric or catalytic amounts of the base. **Complex 16b** is highly selective toward vanillin production in a mild temperature range (r.t. to 70 °C). The selective oxidation of vanillyl alcohol to vanillin is advantageous as it reduces the wastage of valuable feedstock. The nature of solvents in sustainable chemical syntheses is crucial as solvents commonly constitute high mass intensity in chemical processes. The aerobic oxidation of vanillyl alcohol to vanillin was successfully carried out in various green solvent mixtures such as ethanol/water (1: 1) and acetone/water (1: 1). However, water could not be used as the reaction media due to the formation of tar as the decomposed material. This robust catalytic system was successfully applied for the gram-scale synthesis of vanillin. Finally, CHEM21 green metrics toolkit was utilized to analyze six optimized catalytic protocols (Methods A, B, C, D, E, and F). Method D is concluded as the most favorable catalytic procedure as it operates at ambient conditions with low catalyst loading using green, abundant, ecologically benign, and sustainable ethanol/water mixture as the solvent. The catalyst (**complex 16b**) was highly recyclable without the loss of catalytic activity. Based on the published reports and supported by experimental evidences, we propose a plausible mechanism for the aerobic oxidation of vanillyl alcohol, which involves a six six-membered η^1 -nitroxyl-Cu adduct (Oppenauer oxidation-like pathway). The nature of the recycled catalyst was also established through crystallization and further single crystal X-ray analysis, which showed no change in the complex identity. This robust catalytic protocol might be realistic for possible future application as this efficient

catalyst is cheap, readily available, air stable, highly recyclable, and sustainable, and this procedure uses only air as the oxidant and operates in green solvents under ambient conditions in the absence of a base.

2.5 EXPERIMENTAL SECTIONS

2.5.1 General experimental

All experiments were performed in air unless noted otherwise. All solvents (acetonitrile, dichloromethane, diethyl ether, THF, ethyl acetate, acetone, methanol, and ethanol) and chemicals (diphenylmethanol, cysteamine hydrochloride, boron trifluoride diethyl ether, Copper (II) chloride, Copper (II) perchlorate hexahydrate, sodium borohydride, pyridine-2-carboxaldehyde, TEMPO and vanillyl alcohol) were purchased from commercial suppliers and used without further purification. For recording NMR spectra, CDCl₃ was purchased from Sigma-Aldrich and used without further purification. ¹H and ¹³C NMR spectra were recorded at Bruker AV-400 and JEOL-400 spectrometer (¹H at 400 MHz and ¹³C at 101 MHz). ¹H NMR chemical shifts are referenced in parts per million (ppm) with respect to tetramethylsilane (δ 0.00 ppm) and ¹³C{¹H} NMR chemical shifts are referenced in ppm with respect to CDCl₃ (δ 77.16 ppm). The coupling constants (J) are reported in hertz (Hz). The following abbreviations are used to describe multiplicity: bs = broad signal, s = singlet, d = doublet, t = triplet, q = quadrate, m = multiplate.

Synthesis of 2-(benzhydrylthio)-ethanamine. 2-(benzhydrylthio)-ethanamine was synthesized by adopting a literature method with slight modification.⁷¹

Diphenylmethanol (1.842 g, 10.00 mmol) was dissolved in acetic acid (40 mL) under N₂ atmosphere. Cysteamine hydrochloride (1.128 g, 10.00 mmol) and BF₃.OEt₂ (1.402 g, 12.00 mmol) were added separately to the above solution under N₂ atmosphere. The resultant mixture was then stirred at 95°C for 1 hour on a preheated oil bath under N₂ atmosphere. The following

manipulations were done in air. The reaction mixture was cooled down to r.t. and diethyl ether was added which yielded white precipitate. The white solid was filtered, dried and kept over NaOH pellets for three days yielded 2-(benzhydrylthio)-ethanamine hydrochloride (2.744 g, 98%) as white solid. ^1H NMR (400 MHz, CDCl_3) δ 7.41 (d, $J = 7.5$ Hz, 4H), 7.25–7.22 (m, 4H), 7.15 (t, $J = 7.3$ Hz, 2H), 5.23 (s, 1H), 2.94 (t, $J = 6.2$ Hz, 2H), 2.53 (t, $J = 6.2$ Hz, 2H).

In the following step, HCl was removed from 2-(benzhydrylthio)-ethanamine hydrochloride. 2-(Benzhydrylthio)-ethanamine hydrochloride (2.798 g) was dissolve in saturated NaHCO_3 solution (100 mL) and extracted with chloroform (3 x 20 mL). The organic phase was dried over Na_2SO_4 . All volatiles were evaporated under high vacuum to yield 2-(benzhydrylthio)-ethanamine (2.381 g, 98%) as light-yellow oil. ^1H NMR (400 MHz, CDCl_3) δ 7.47-7.40 (m, 4H), 7.35-7.27 (m, 4H), 7.26-7.18 (m, 2H), 5.16 (s, 1H), 2.81 (t, $J = 6.3$ Hz, 2H), 2.51 (t, $J = 6.3$ Hz, 2H), 1.64 (bs, 2H).

Synthesis of N-(2-(benzhydrylthio) ethyl)-1-(pyridine-2-yl) methanimine (L3). A solution of 2-(benzhydrylthio)-ethanamine (0.972 g, 4.00 mmol) in methanol (20 mL) was added to a solution of pyridine-2-carboxaldehyde (0.428 g, 4.00 mmol) in methanol (10 mL) with continuous stirring. The resultant mixture was refluxed for 10 hours in a preheated oil bath. The solution was then cooled down to r.t. and all volatiles were removed under high vacuum to yield L3 (1.297 g, 98%) as a reddish-brown oil. ^1H NMR (400 MHz, CDCl_3) δ 8.65 (d, $J = 4.4$ Hz, 1H), 8.35 (s, 1H), 7.97 (d, $J = 7.9$ Hz, 1H), 7.75–7.71 (m, 1H), 7.44–7.42 (m, 4H), 7.33–7.27 (m, 5H), 7.24–7.19 (m, 2H), 5.26 (s, 1H), 3.83 (t, $J = 6.3$ Hz, 2H), 2.79 (t, $J = 6.9$ Hz, 2H). ^{13}C NMR (101 MHz, CDCl_3) δ 163.05, 154.36, 149.59, 141.41, 136.64, 128.63, 128.44, 127.28, 124.91, 121.52, 60.95, 54.48, 32.91. HRMS (ESI-TOF) m/z : $[\text{M} + \text{H}]^+$ Calcd. for $\text{C}_{21}\text{H}_{21}\text{N}_2\text{S}$ 333.1425, Found 333.1417. Anal. Calcd. for $\text{C}_{21}\text{H}_{21}\text{N}_2\text{S}$ (332.46): C, 75.87; H, 6.06; N, 8.34; S, 9.64. Found: C, 75.71; H, 6.03; N, 8.10; S, 9.53. FTIR ν_{max} (cm^{-1}): 2800–3100 (C–H), 1646 (CH=N), 1410–1600 (C=N, py; C=C, ph), 600–710 (C–S).

Synthesis of 2-(benzhydrylthio)-N-(pyridine-2-ylmethyl) ethan-1-amine (L4). A solution of **L3** (1.328 g, 4.00 mmol) in methanol (30 mL) was cooled down to 0 °C in an ice-bath. Solid NaBH₄ (0.341 g, 9.00 mmol) was then added in small quantity to the solution at 0 °C under vigorous stirring. The resultant reaction mixture was stirred at 0 °C for another 10 minutes. Then the reaction mixture was warmed up to r.t. and stirred at r.t. for another 6 hours. Water (20 mL) was added to the reaction mixture and the mixture was extracted with dichloromethane (3 x 20 mL). Combined organic phase was dried over Na₂SO₄ and dried under high vacuum to get **L4** (1.321 g, 99%) as brown oil. ¹H NMR (400 MHz, CDCl₃) δ 8.56–8.54 (m, 1H), 7.65–7.61 (m, 1H), 7.43–7.40 (m, 4H), 7.32–7.26 (m, 5H), 7.19–7.23 (m, 2H), 7.18–7.14 (m, 1H), 5.18 (s, 1H), 3.88 (s, 2H), 2.80 (t, *J* = 6.6 Hz, 2H), 2.61 (t, *J* = 6.6 Hz, 2H), 2.38 (bs, 1H). ¹³C NMR (101 MHz, CDCl₃) δ 159.68, 149.38, 141.43, 136.64, 128.66, 128.41, 127.30, 122.34, 122.11, 54.75, 53.96, 47.88, 32.60. HRMS (ESI-TOF) *m/z*: [M + H]⁺ Calcd. for C₂₁H₂₃N₂S 335.1582, Found 335.1577. Anal. Calcd. for C₂₁H₂₂N₂S (334.48): C, 75.41; H, 6.63; N, 8.38; S, 9.58. Found: C, 75.28; H, 6.63; N, 8.40; S, 9.48. FTIR *V*_{max} (cm⁻¹): 3310 (N–H), 2750–3110 (C–H), 1405–1610 (C=N, py; C=C, ph), 600–720 (C–S).

Synthesis of 15a. A solution of Cu(ClO₄)₂·6H₂O (0.093 g, 0.25 mmol) in methanol (10 mL) was added dropwise to a solution of **L3** (0.166 g 0.50 mmol) in methanol (10 mL) at r.t. The mixture was stirred at r.t. for 10 min. Then the resulting mixture was refluxed for additional 1 h yielded a green solution. After cooling to r.t, the solution was collected after filtration. Slow evaporation of the solution at ambient conditions for two days gave green crystalline blocks. The crystals were collected after filtration, washed with cold methanol/ether (1:2) mixture and dried under high vacuum to give pure **15a** (0.206 g, 85%) as green solid. Note: Metal precursor and ligand stoichiometric ratio of 1:1 also gave complex **15a**. HRMS (ESI-TOF) *m/z*: Calcd. for [C₄₂H₄₁CuN₄S₂]⁺ [M]⁺ 728.2069, Found 728.2097. Anal. Calcd. for C₄₂H₄₁Cl₄CuN₄O₈.S₂ (937.37): C, 53.87; H, 4.41; N, 5.98; S, 6.85. Found: C, 53.58; H, 4.52; N, 6.80; S, 6.71. FTIR

V_{\max} (cm^{-1}): 2880–3120 (C–H), 1650 (CH = N), 1405–1610 (C=N, py; C=C, ph), 1080 and 620 (ClO_4^-), 680–790 (C–S).

Synthesis of 15b. A solution of $\text{Cu}(\text{ClO}_4)_2 \cdot 6\text{H}_2\text{O}$ (0.093 g, 0.25 mmol) in methanol (10 mL) was added dropwise to a solution of **L4** (0.167 g 0.50 mmol) in methanol (10 mL) at r.t. The mixture was stirred at r.t. for 10 min. Then the resulting mixture was refluxed for additional 30 mins. The greenish-blue solution was filtered and cooled down to r.t. The solution was allowed to stand at r.t. for a day and light blue plates were obtained. The crystals were collected after filtration, washed with cold methanol/ether (1:2) and dried under high vacuum to give pure **15b** (0.186 g, 80%) as light blue solid. The light blue plates were suitable for single crystal X-ray analysis. Note: Metal precursor and ligand stoichiometric ratio of 1:1 also gave complex 15b. HRMS (ESI-TOF) m/z : Calcd. for $[\text{C}_{42}\text{H}_{43}\text{CuN}_4\text{S}_2]^+ [\text{M}]^+$ 732.2382, Found 732.2353. Anal. Calcd for $\text{C}_{43}\text{H}_{48}\text{Cl}_4\text{CuN}_4\text{O}_9\text{S}_2$ (963.44): C, 53.61; H, 5.02; N, 5.82; S, 6.66. Found: C, 53.53; H, 5.07; N, 5.82; S, 6.75. FTIR V_{\max} (cm^{-1}): 3182 and 3270 (N–H), 2820–3100 (C–H), 1400–1610 (C=N, py; C=C, ph), 1079 and 620 (ClO_4^-), 675–780 (C–S).

Synthesis of 16a. A solution of CuCl_4 (0.033 g, 0.25 mmol) in methanol (10 mL) was added dropwise to a solution of **L3** (0.083 g 0.25 mmol) in methanol (10 mL) at r.t. The mixture was stirred at r.t. for 10 min. Then the resulting mixture was refluxed for additional 1 h during which the colour of the solution changed to apple green and green crystalline precipitate appeared. After cooling to r.t, the solid was collected after filtration and dried under high vacuum. The solid was dissolved in DMF (1.0 mL) and slow diffusion of diethyl ether into the DMF solution gave green crystalline plates. The crystals were collected after filtration, washed with cold methanol/ether (1:2) mixture and dried under high vacuum to give pure **16a** (0.100 g, 86%) as green solid. The green plates were suitable for single crystal X-ray analysis. HRMS (ESI-TOF) m/z : Calcd for $[\text{C}_{21}\text{H}_{20}\text{CuN}_2\text{S}]^+ [\text{M}-2\text{Cl}]^+$ 395.0643, Found 395.0617. Anal. Calcd. for $\text{C}_{42}\text{H}_{40}\text{Cl}_4\text{Cu}_2\text{N}_4\text{S}_2$ (933.82): C, 54.02; H, 4.32; N, 6.00; S, 6.87. Found: C, 53.97; H, 4.30;

N, 6.03; S, 6.89. FTIR V_{\max} (cm^{-1}): 2885–3110 (C–H), 1638 (CH=N), 1410–1610 (C=N, py; C=C, ph), 680–785 (C–S).

Synthesis of 16b. A solution of CuL4 (0.033 g, 0.25 mmol) in methanol (10 mL) was added dropwise to a solution of **L4** (0.084 g 0.25 mmol) in methanol (10 mL) at r.t. The mixture was stirred at r.t. for 10 min. Then the resulting mixture was refluxed for additional 30 mins. The solution was filtered and cooled down to r.t. The solution was allowed to stand at r.t. for 16 h and bluish-green block-shaped crystals were obtained. The crystals were collected after filtration, washed with cold methanol/ether (1:2) and dried under high vacuum to give pure **16b** (0.096 g, 82%) as bluish-green solid. The bluish-green blocks were suitable for single crystal X-ray analysis. HRMS (ESI-TOF) m/z : Calcd. for $[\text{C}_{21}\text{H}_{22}\text{ClCuN}_2\text{S}]^+ [\text{M}-\text{Cl}]^+$ 432.0488, Found 432.0493. Anal. Calculated. for $\text{C}_{21}\text{H}_{22}\text{Cl}_4\text{CuN}_2\text{S}$ (468.93): C, 53.79; H, 4.73; N, 5.97; S, 6.84. Found: C, 53.93; H, 4.85; N, 6.09; S, 6.91. FTIR V_{\max} (cm^{-1}): 3244 (N–H), 2875–3120 (C–H), 1400–1620 (C=N, py; C=C, ph), 675–785 (C–S).

2.4.2 General conditions for the catalytic oxidation of vanillyl alcohol to vanillin. All manipulations were performed in air. Vanillyl alcohol (0.039 g, 0.25 mmol), Copper complex **15a/ 15b/ 16a/ 16b** (5/ 3 mol %) and TEMPO radical (20/ 10 mol %) were weighed and placed in a vial (10 mL). Thereafter, 2 mL pure solvent/ solvent mixture was added. The resultant mixture was heated at appropriate temperature (40/ 50/ 60/ 70 °C) in a preheated oil bath for appropriate time (3/ 6/ 9/ 12/ 16/ 24 h). Thereafter, the mixture was cooled down to r.t. (and occasionally GC was measured from the mixture). The mixture was dried under vacuum (using rotary evaporator). Ethyl acetate (5 mL) was added and the mixture was passed through a short bed of silica gel. The resultant solution was dried under high vacuum and the product was dissolved in CDCl_3 (0.5 mL). The solution was transferred in NMR tube. Required amount of THF (20.3 mL, 0.25 mmol) as external standard was added to the CDCl_3 solution and ^1H NMR spectrum was recorded. Occasionally the CDCl_3 solution was dried under high and the product

vanillin was purified by column chromatography. Note: In case of complete conversion of vanillyl alcohol, further purification using column chromatography was not required.

2.5.3 General conditions for gram scale synthesis of vanillin from vanillyl alcohol. A

mixture of vanillyl alcohol (1.541 g, 10.00 mmol), Copper **complex 16b** (3/ 5 mol%) and TEMPO radical (10/ 20 mol %) in 1:1 mixture of solvents (40 mL) was heated at 40/ 70 °C in a preheated oil bath for appropriate time. Following reaction conditions were used for six methods: Method A: **16b**, 5 mol %, TEMPO, 20 mol %, acetone/water (1:1), 40 °C, 12 h; Method B: **16b**, 3 mol %, TEMPO, 10 mol %, acetone/water (1:1), 40 °C, 20 h; Method C: **16b**, 5 mol %, TEMPO, 20 mol %, ethanol/water (1:1), 40 °C, 15 h; Method D: **16b**, 3 mol %, TEMPO, 10 mol %, ethanol/water (1:1), 40 °C, 24 h; Method E: **16b**, 3 mol %, TEMPO, 10 mol %, ethanol/water (1:1), 70 °C, 16 h; Method F: **16b**, 5 mol %, TEMPO, 20 mol %, THF/water (1:1), 40 °C, 15 h. The resultant reaction mixture was cooled down to room temperature and dried under high vacuum followed by the addition of water (30 mL). The mixture was extracted with ethyl acetate (3 x 10 mL). The combined organic phase was dried over Na₂SO₄. The solution was dried under high vacuum to give pure vanillin (**A**. 1.518 g, 100%, **B**. 1.520 g, 100%; **C**. 1.521 g, 100%; **D**. 1.516 g, 100%; **E**. 1.518 g, 100% and **F**. 1.515 g, 100%). Pure vanillin was characterized by ¹H and ¹³C NMR spectroscopy. ¹H NMR (400 MHz, CDCl₃) δ 9.80 (s, 1H), 7.46–7.37 (m, 2H), 7.06–6.99 (m, 1H), 6.49 (s, 1H), 3.93 (s, 3H). ¹³C NMR (101 MHz, CDCl₃) δ 191.12, 151.90, 147.32, 129.92, 127.65, 114.56, 108.97, 56.20.

General conditions for catalyst recycle. A mixture of vanillyl alcohol (1.541 g, 10.00 mmol), Copper complex **16b** (3/5 mol%) and TEMPO radical (10/ 20 mol%) in 1:1 mixture of solvents (40 mL) was heated at 40/70 °C in a preheated oil bath for appropriate time. Following reaction conditions were used for six methods: Method A: **16b**, 5 mol%, TEMPO, 20 mol%, acetone/water (1:1), 40 °C, 12 h; Method B: **16b**, 3 mol%, TEMPO, 10 mol%, acetone/water (1:1), 40 °C, 20 h; Method C: **16b**, 5 mol%, TEMPO, 20 mol%, ethanol/water (1:1), 40 °C, 15

h; Method D: **16b**, 3 mol%, TEMPO, 10 mol%, ethanol/water (1:1), 40 °C, 24 h; Method E: **16b**, 3 mol%, TEMPO, 10 mol%, ethanol/water (1:1), 70 °C, 16 h; Method F: **16b**, 5 mol%, TEMPO, 20 mol%, THF/water (1:1), 40 °C, 15 h. The resultant reaction mixture was cooled down to room temperature and dried under high vacuum followed by the addition of water (30 mL). The organic product was extracted with ethyl acetate (3 x 10 mL). The catalysts **16b** stays in water phase. The combined organic phase was dried over Na₂SO₄. The solution was dried under high vacuum to give pure vanillin. Thereafter, the volume of the aqueous phase was reduced to 20 mL followed by the addition of vanillyl alcohol (1.541 g, 10.00 mmol), TEMPO radical (10/ 20 mol%) and solvent (acetone/ ethanol/ THF: 20 mL). The mixture was heated at 40/ 70 °C in a preheated oil bath for appropriate time. The resultant reaction mixture was cooled down to room temperature and dried under high vacuum followed by the addition of water (30 mL). The organic was extracted with ethyl acetate (3 x 10 mL). The combined organic phase was dried over Na₂SO₄. The solution was dried under high vacuum to give pure vanillin. The entire process was repeated twice. Thus, **complex 16b** was recycled three times and no change in catalytic activity was observed.

Note: Recycled catalyst **16b** was dried and dissolved in minimum amount of CHCl₃. Slow evaporation of the CHCl₃ solution gave crystals which were analysed by single crystal X-ray analysis. And it confirmed the unaltered identity of **16b**.

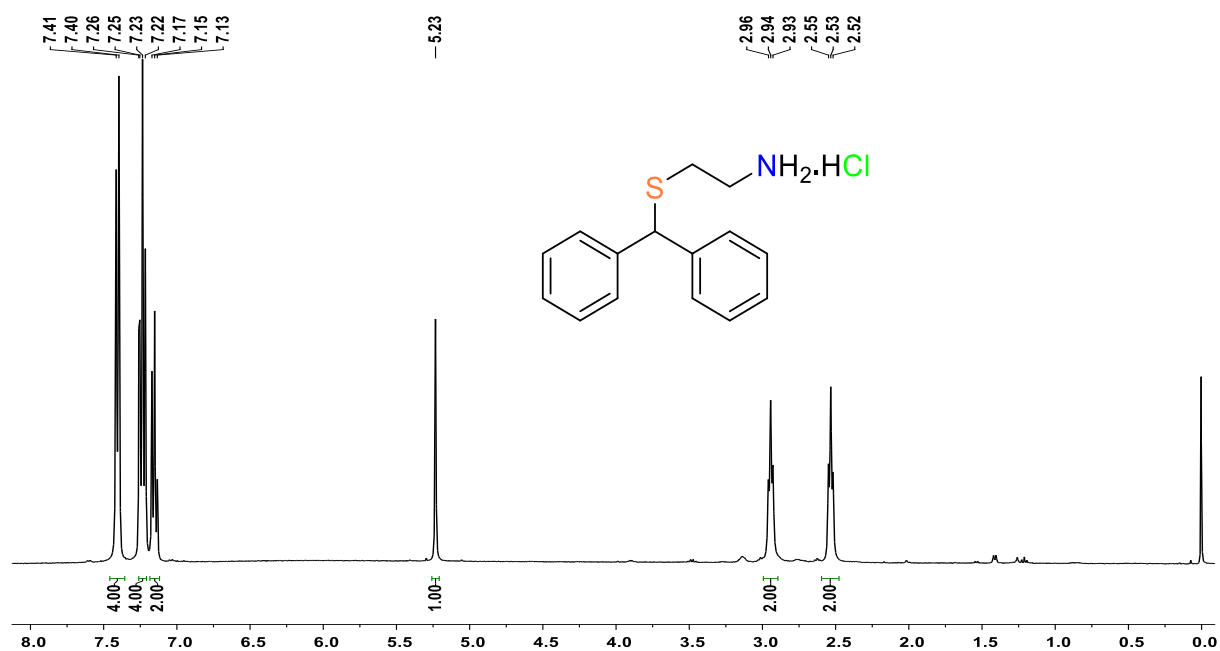


Figure 2.5. ¹H NMR of 2-(benzhydrylthio)-ethanamine hydrochloride in CDCl₃ at r.t.

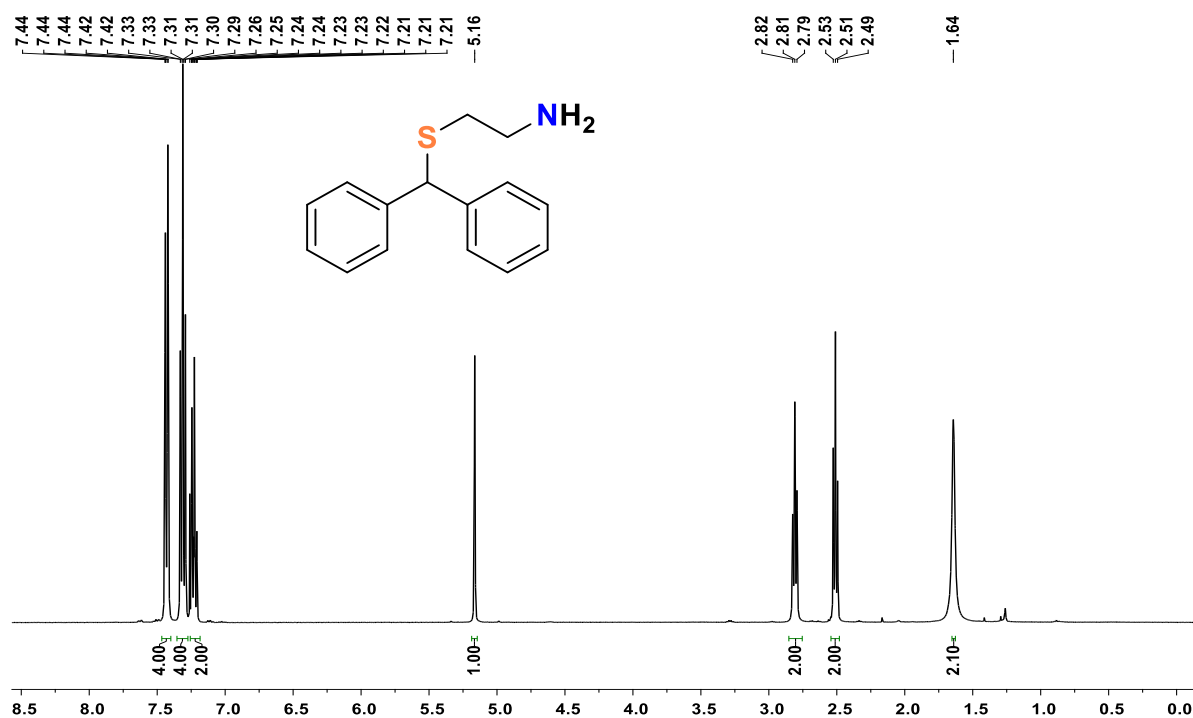


Figure 2.6: ¹H NMR of 2-(benzhydrylthio)-ethanamine in CDCl₃ at r.t.

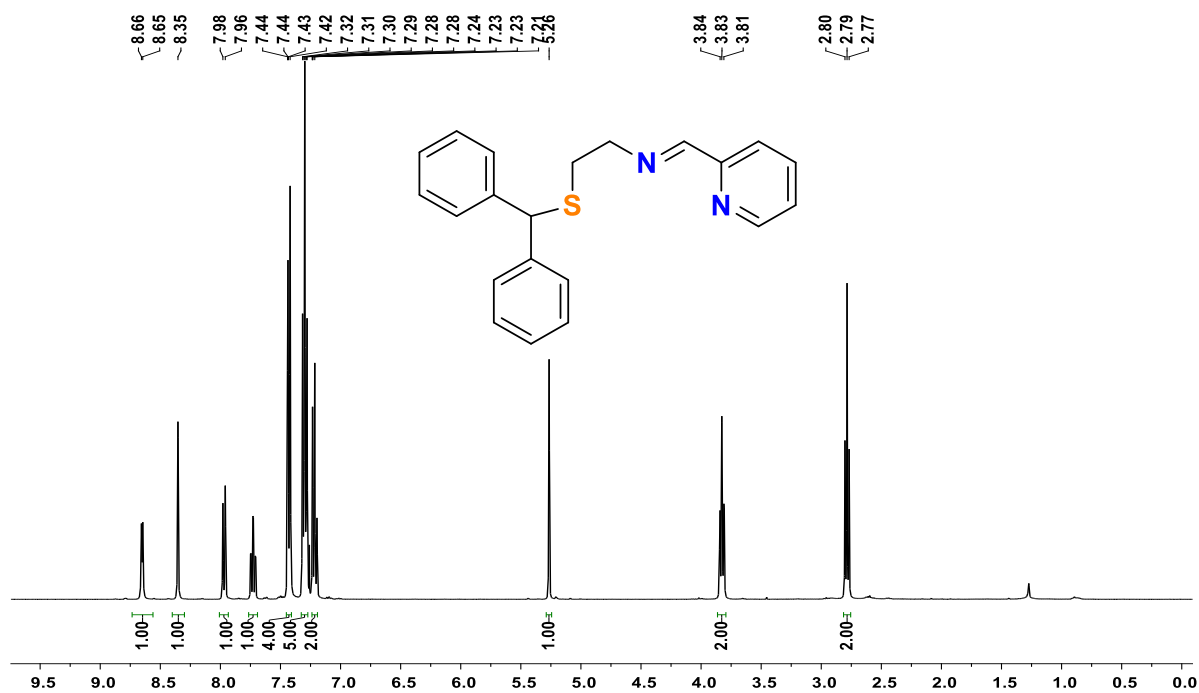


Figure 2.7: ^1H NMR of N-(2-(benzhydrylthio) ethyl)-1-(pyridine-2-yl) methanimine (**L3**) in CDCl_3 at r.t.

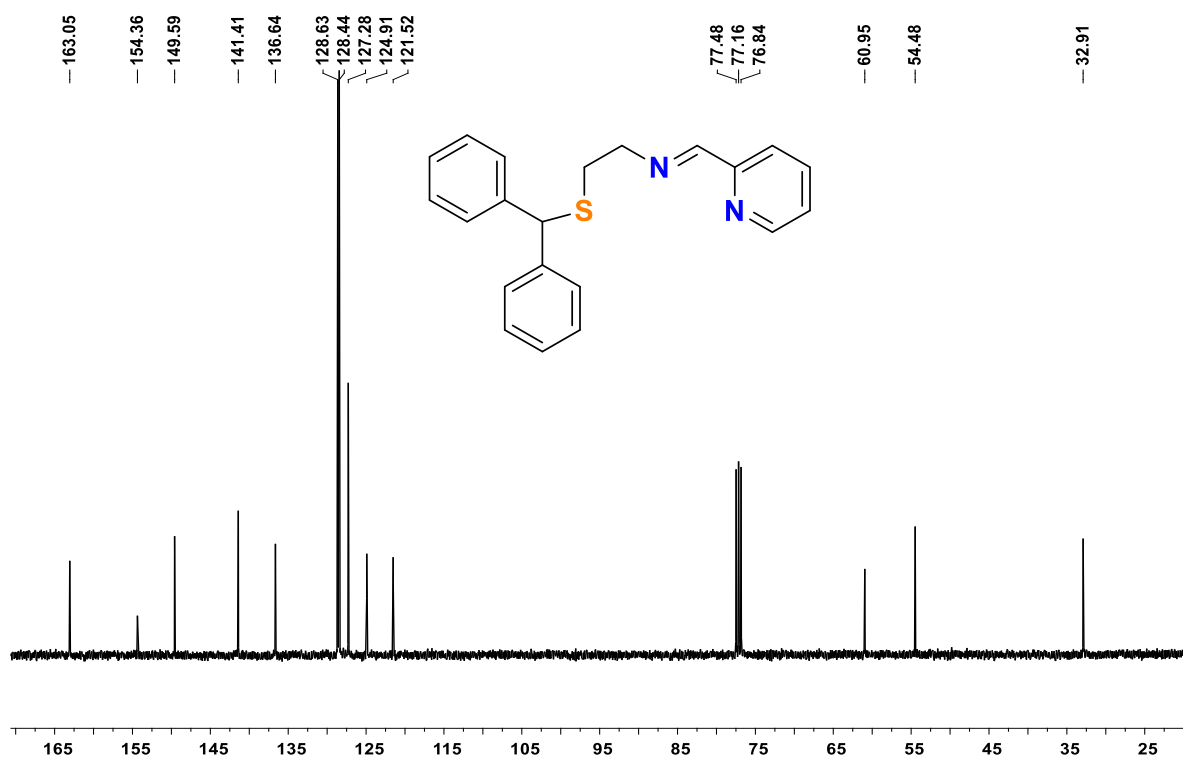


Figure 2.8: ^{13}C NMR of N-(2-(benzhydrylthio) ethyl)-1-(pyridine-2-yl) methanimine (**L3**) in CDCl_3 at r.t.

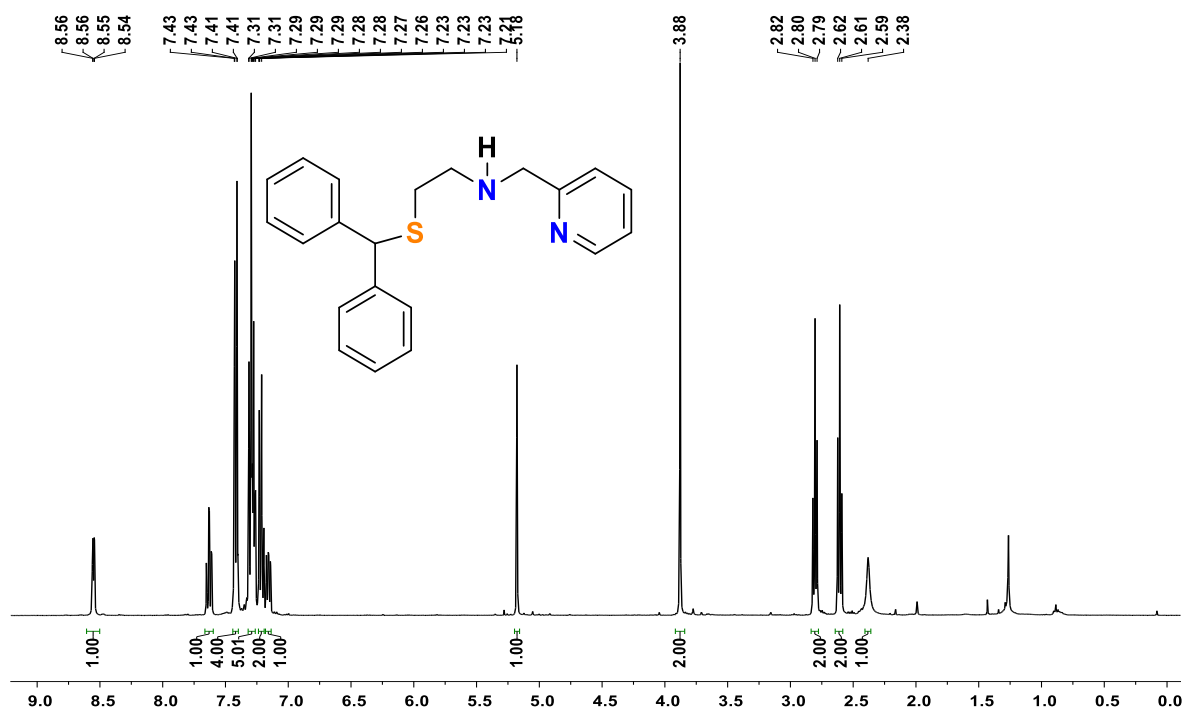


Figure 2.9: ¹H NMR of 2-(benzhydrylthio)-N-(pyridine-2-ylmethyl) ethan-1-amine (**L4**) in CDCl₃ at r.t.

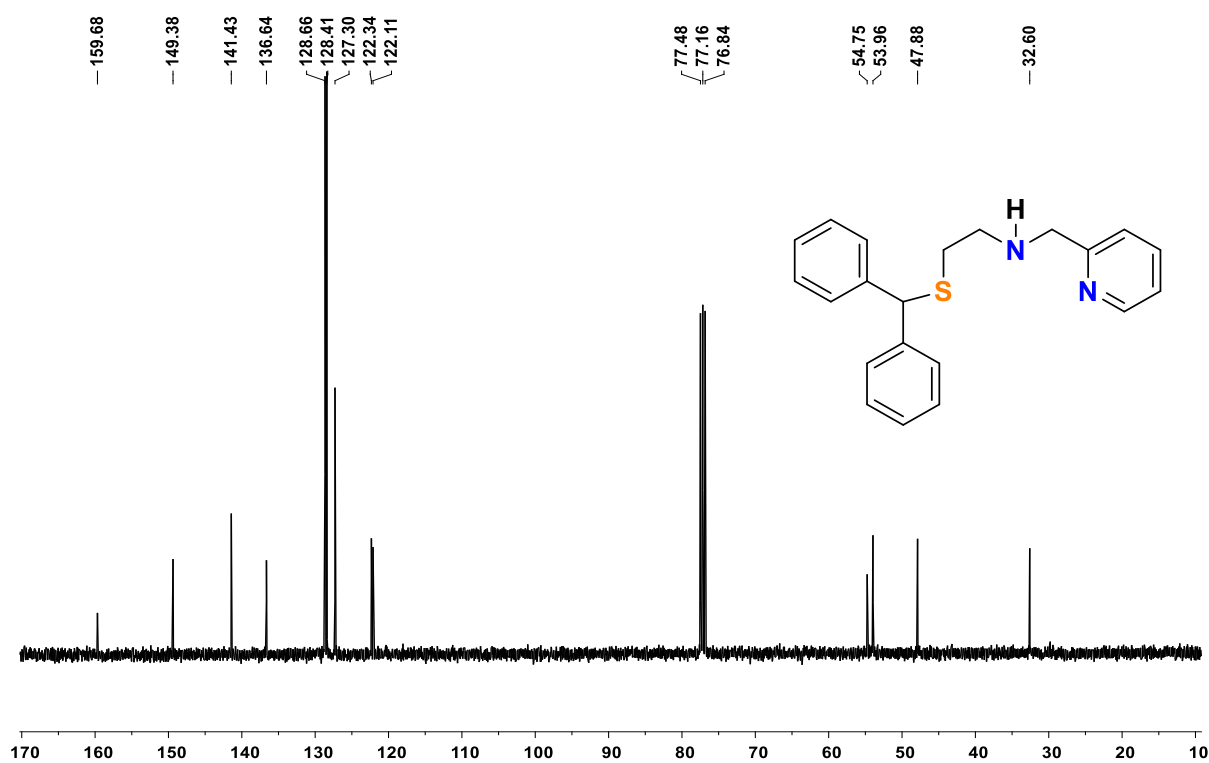


Figure 2.10: ¹³C NMR of 2-(benzhydrylthio)-N-(pyridine-2-ylmethyl) ethan-1-amine (**L4**) in CDCl₃

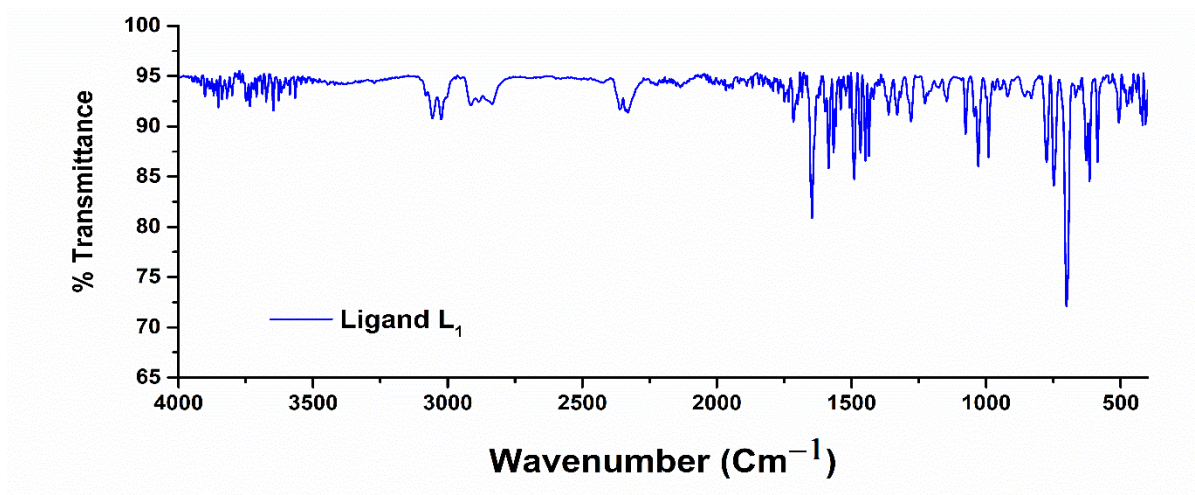


Figure 2.11: FTIR Spectrum of ligand **L3**.

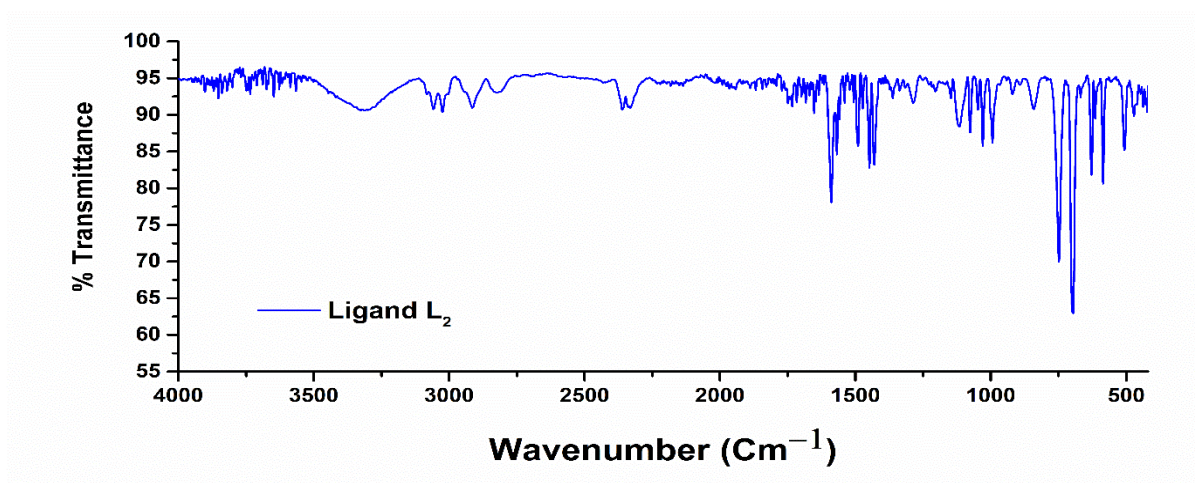


Figure 2.12: FTIR Spectrum of ligand **L4**.

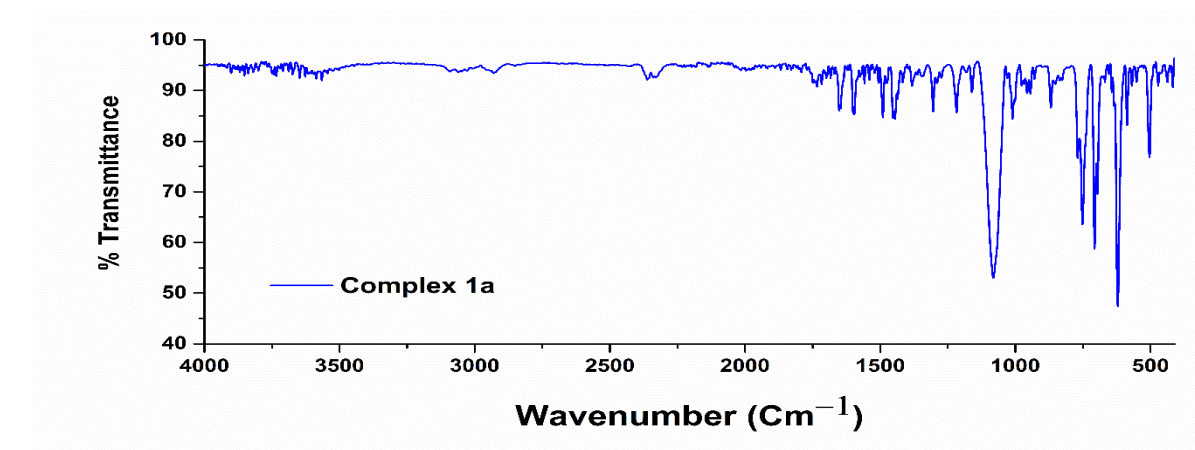


Figure 2.13: FTIR Spectrum of **Complex 15a**.

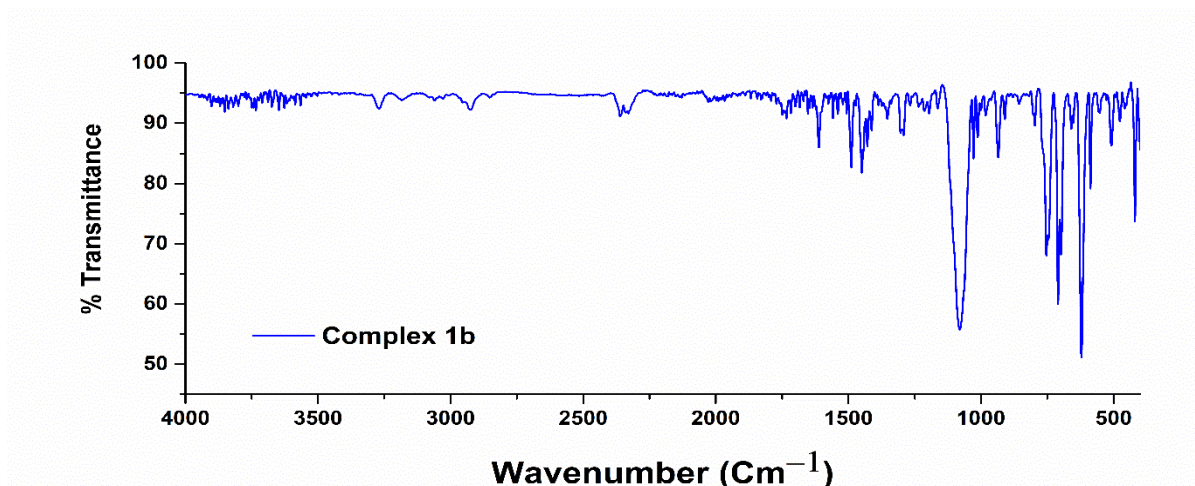


Figure 2.14: FTIR Spectrum of Complex 15b.

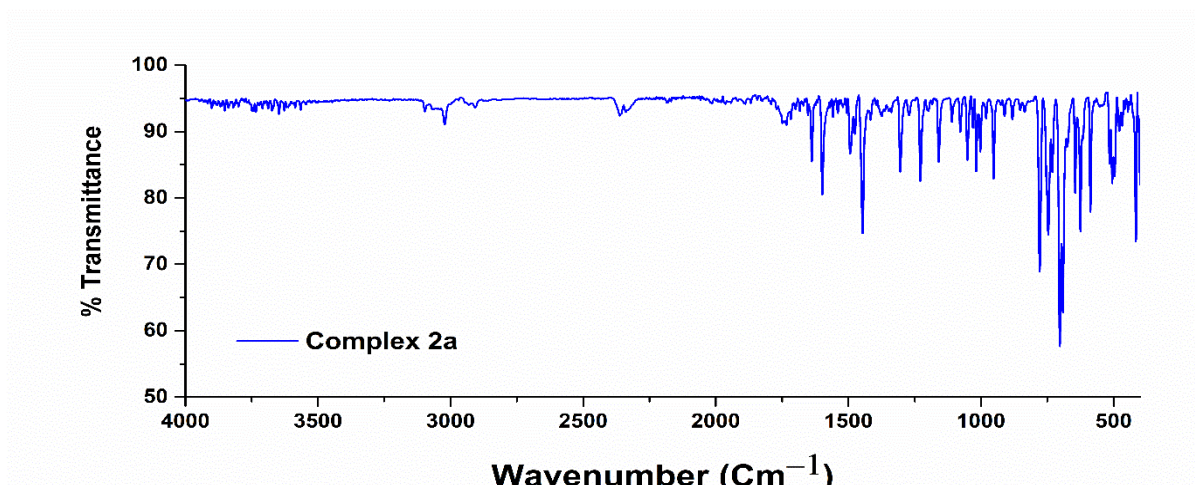


Figure 2.15: FTIR Spectrum of Complex 16a.

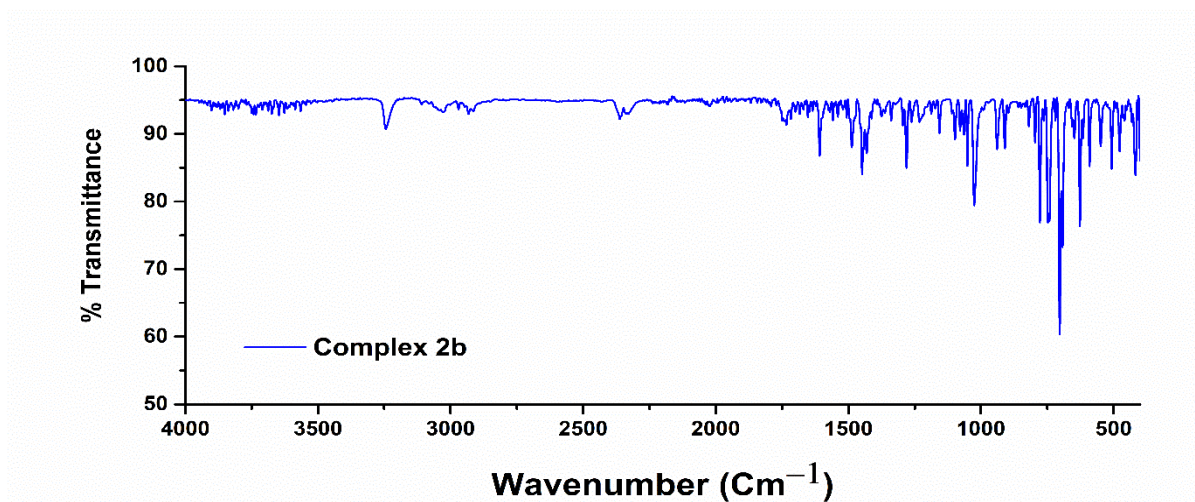


Figure 2.16: FTIR Spectrum of complex 16b.

2.5.4 Molecular structure determination by single crystal X-ray crystallography

A crystal of complex **15a**, **15b**, **16a**, **16b** and **16b** (recycled) with accession code CCDC 2088325, 2088326, 2088327, 2088328 and 2088330 were mounted in air at ambient conditions. All measurements were made on an *Oxford Diffraction SuperNova* area-detector diffractometer using mirror optics monochromatic Mo $K\alpha$ radiation ($\lambda = 0.71073 \text{ \AA}$) and Al filtered. The unit cell constants and an orientation matrix for data collection were obtained from a least-squares refinement of the setting angles of reflections in the range $2.1 < \theta < 26.4^\circ$. A total of 1090 frames were collected using ω scans, with 30+30 seconds exposure time, a rotation angle of 1.0° per frame, a crystal-detector distance of 65.0 mm, at $T = 123(2) \text{ K}$. Data reduction was performed using the *CrysAlisPro* program. The intensities were corrected for Lorentz and polarization effects, and an absorption correction based on the multi-scan method using SCALE3 ABSPACK in *CrysAlisPro* was applied. Data collection and refinement parameters are given in **Table 1**. The structure was solved by direct methods using *SHELXT*, which revealed the positions of all non-hydrogen atoms of the title compound. The non-hydrogen atoms were refined anisotropically. All H-atoms were placed in geometrically calculated positions and refined using a riding model where each H-atom was assigned a fixed isotropic displacement parameter with a value equal to $1.2U_{eq}$ of its parent atom.

Refinement of the structure was carried out on F using full-matrix least-squares procedures, which minimized the function $\Sigma w(F_o^2 - F_c^2)$. The weighting scheme was based on counting statistics and included a factor to down weight the intense reflections. All calculations were performed using the *SHELXL-2014/7* program.

Table 2.6. Crystallographic Data and Refinement Parameters for **15a**, **15b**, **16a**, **16b** and **16b** (recycled).

	15a	15b	16a	16b	16b (recycled)
Empirical formula	C ₄₂ H ₄₀ Cl ₄ CuN ₄ O _{8.5} S ₂	C ₄₃ H ₄₈ Cl ₄ CuN ₄ O ₉ S ₂	C ₄₂ H ₄₀ Cl ₄ Cu ₂ N ₄ S ₂	C ₂₁ H ₂₂ Cl ₄ CuN ₂ S	C ₂₂ H ₂₃ Cl ₅ CuN ₂ S
CCDC	2088325	2088326	2088327	2088328	2088330
Formula weight (g mol ⁻¹)	935.34	963.41	933.78	468.90	588.27
Temperature	297(2)	293(2)	100.00(10)	293(2)	100(10)
Wavelength	1.54184	1.54184	1.54184	1.54184	1.54184
Crystal system	Monoclinic	Monoclinic	Triclinic	Monoclinic	Orthorhombic
Space group	<i>I</i> 2/a	<i>P</i> 2 ₁ /c	<i>P</i> $\bar{1}$	<i>P</i> 2 ₁ /c	<i>P</i> bca
<i>a</i> (Å)	21.1362(6)	15.46340(11)	8.7543(2)	17.0171(3)	19.10688(11)
<i>b</i> (Å)	11.2833(2)	16.54964(10)	8.91433(17)	9.22230(10)	9.75754(6)
<i>c</i> (Å)	38.192(2)	18.85843(14)	14.2328(6)	13.3042(2)	26.37158(16)
α (deg)	90	90	92.973(3)	90	90
β (deg)	104.463(4)	111.1946(8)	97.234(3)	96.124(2)	90
γ (deg)	90	90	113.730(2)	90	90
volume (Å ³)	8819.7(6)	4499.68(6)	1002.26(6)	2076.00(5)	4916.61(5)
Z	1	4	2	4	8
<i>D</i> _{calc} (g cm ⁻³)	1.407	1.422	1.547	1.500	1.589
μ (mm ⁻¹)	3.172	3.130	5.022	4.849	7.156
<i>F</i> (000)	3856	2004	478	964	2392
Crystal Size	0.3 × 0.2 × 0.1 mm ³	0.4 × 0.3 × 0.2 mm ³	0.12 × 0.11 × 0.1 mm ³	0.3 × 0.2 × 0.1 mm ³	0.2 × 0.1 × 0.1 mm ³
θ Range (deg)	4.096–68.248	3.668–68.247	5.456–68.249	5.228–68.232	3.352–68.250
Index Ranges	-24 ≤ <i>h</i> ≤ 25, -12 ≤ <i>k</i> ≤ 13, -45 ≤ <i>l</i> ≤ 46	-18 ≤ <i>h</i> ≤ 15, -19 ≤ <i>k</i> ≤ 19, -21 ≤ <i>l</i> ≤ 22	-10 ≤ <i>h</i> ≤ 10, -10 ≤ <i>k</i> ≤ 8, -17 ≤ <i>l</i> ≤ 17	-20 ≤ <i>h</i> ≤ 19, -11 ≤ <i>k</i> ≤ 11, -16 ≤ <i>l</i> ≤ 16	-23 ≤ <i>h</i> ≤ 23, -10 ≤ <i>k</i> ≤ 11, -31 ≤ <i>l</i> ≤ 28
Reflections collected	60471	66480	14701	29160	83189
Independent reflections (<i>R</i> _{int})	8076 (0.1078)	8238 (0.0439)	3667(0.0485)	3790(0.0828)	4495(0.1195)
Completeness to $\theta = 66.97^\circ$	99.94	99.96	99.93	99.95	99.96
Refinement method	Full-matrix least-squares on <i>F</i> ²	Full-matrix least-squares on <i>F</i> ²	Full-matrix least-squares on <i>F</i> ²	Full-matrix least-squares on <i>F</i> ²	Full-matrix least-squares on <i>F</i> ²
Data/Restraints/parameters	8076/0/575	8238/2/557	3667/0/244	3790/0/244	4495/0/280
Goodness-of-fit on <i>F</i> ²	1.058	1.083	1.194	1.042	1.098
Final <i>R</i> indices [<i>I</i> > 2 σ (<i>I</i>)]	<i>R</i> ₁ = 0.1106, <i>wR</i> ₂ = 0.2839	<i>R</i> ₁ = 0.0734, <i>wR</i> ₂ = 0.2103	<i>R</i> ₁ = 0.0853, <i>wR</i> ₂ = 0.2628	<i>R</i> ₁ = 0.0406, <i>wR</i> ₂ = 0.1082	<i>R</i> ₁ = 0.0513, <i>wR</i> ₂ = 0.0988
<i>R</i> indices (all data)	<i>R</i> ₁ = 0.1247, <i>wR</i> ₂ = 0.2952	<i>R</i> ₁ = 0.0764, <i>wR</i> ₂ = 0.2132	<i>R</i> ₁ = 0.0873, <i>wR</i> ₂ = 0.2633	<i>R</i> ₁ = 0.0423, <i>wR</i> ₂ = 0.1098	<i>R</i> ₁ = 0.0539, <i>wR</i> ₂ = 0.1001
Largest diff. peak/hole (e Å ⁻³)	0.877/-0.549	2.00/-2.44	2.45/-0.79	0.97/-0.84	1.05/-0.67

Table 2.7. Bond lengths (Å) around the metal centre in Copper complexes.

Bonds	15a	15b	16a	16b	16b·CHCl ₃
Cu–N (pyridine)	2.078(6) 2.257(8)	2.016(3) 2.012(3)	2.035(8)	2.0166(19)	2.023(3)
Cu–N (imine)	1.941(7) 2.004(7)	–	2.025(8)	–	–
Cu–N (secondary amine)	–	2.059(3) 2.040(3)	–	2.0345(18)	2.040(2)
Cu–S (thioether)	2.410(8) 2.943(8)	2.8099(8)	–	2.7991(6)	2.829(8)
Cu–Cl (bridge)	–	–	2.590(3) 2.288(3)	–	–
Cu–Cl (terminal)	–	–	2.251(3)	2.2567(6) 2.2622(6)	2.2818(8) 2.2637(8)

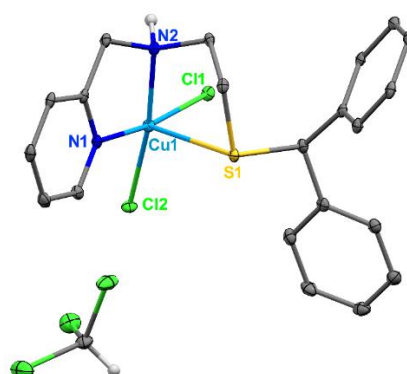


Figure 2.17. Molecular structure of **16b** (recycled) showing 30% thermal ellipsoid. Hydrogen atoms are removed for clarity except the chloroform and amine protons.

2.6 REFERENCES

- (1) Kamm, B.; Gruber P. R.; and Kamm, M.; in *Biorefineries–Industrial Processes and Products, Status Quo and Future Directions*, Wiley-VCH Verlag GmbH, Weinheim, 2006, vol. 1.
- (2) Clark, J. H.; Luque, R.; Matharu, A. S. *Green Chemistry, Biofuels, and Biorefinery. Annu. Rev. Chem. Biomol. Eng.* **2012**, *3*, 183–207.

- (3) Belgacem, M. N.; and Gandini, A.; Monomers, polymers and composites from renewable resources, Elsevier, **2011**.
- (4) Sudarsanam, P.; Zhong, R.; Van den Bosch, S.; Coman, S. M.; Parvulescu, V. I.; Sels, B. F. Functionalised Heterogeneous Catalysts for Sustainable Biomass Valorisation. *Chem. Soc. Rev.* **2018**, *47*, 8349–8402.
- (5) Deng, W.; Zhang, H.; Wu, X.; Li, R.; Zhang, Q.; Wang, Y. Oxidative Conversion of Lignin and Lignin Model Compounds Catalyzed by CeO₂-Supported Pd Nanoparticles. *Green Chem.* **2015**, *17*, 5009–5018.
- (6) Behling, R.; Valange, S.; Chatel, G. Heterogeneous Catalytic Oxidation for Lignin Valorization into Valuable Chemicals: What Results? What Limitations? What Trends? *Green Chem.* **2016**, *18*, 1839–1854.
- (7) Fitzgerald, D. J.; Stratford, M.; Narbad, A. Analysis of the Inhibition of Food Spoilage Yeasts by Vanillin. *Int. J. Food Microbiol.* **2003**, *86*, 113–122.
- (8) Walton, N. J.; Mayer, M. J.; Narbad, A. Vanillin. *Phytochemistry* **2003**, *63*, 505–515.
- (9) Bythrow, J. D. Vanilla as a Medicinal Plant. *Semin. Integr. Med.* **2005**, *3*, 129–131.
- (10) Esposito, L.; Formanek, K.; Kientz, G.; Maugeri, F.; Maureaux, V.; Robert, G.; and Truchet, F.; Kirk-Othmer Encyclopedia of Chemical Technology, 4th edn, **1997**, *24*, pp. 812–825.
- (11) Bjørsvik, H.-R.; Minisci, F. Fine Chemicals from Lignosulfonates. 1. Synthesis of Vanillin by Oxidation of Lignosulfonates. *Org. Process Res. Dev.* **1999**, *3*, 330–340.
- (12) Fache, M.; Boutevin, B.; Caillol, S. Vanillin Production from Lignin and Its Use as a Renewable Chemical. *ACS Sustain. Chem. Eng.* **2016**, *4*, 35–46.
- (13) Silva, E. A. B. da; Zabkova, M.; Araújo, J. D.; Cateto, C. A.; Barreiro, M. F.; Belgacem, M. N.; Rodrigues, A. E. An Integrated Process to Produce Vanillin and Lignin-Based Polyurethanes from Kraft Lignin. *Chem. Eng. Res. Des.* **2009**, *87*, 1276–1292.

- (14) Anastas, P. T.; Warner, J. C. Principles of Green Chemistry. In *Green Chemistry: Theory and Practice*; Oxford University Press, 1998; pp 29–56.
- (15) Anastas, P. T.; Heine, L. G.; Williamson, T. C. *Green Chemical Syntheses and Processes*; American Chemical Society: Washington, DC, 2000.
- (16) Anastas, P. T.; Kirchhoff, M. M. Origins, Current Status, and Future Challenges of Green Chemistry. *Acc. Chem. Res.* **2002**, *35*, 686–694.
- (17) Anastas, P.; Eghbali, N. Green chemistry: Principles and practice. *Chem. Soc. Rev.* **2010**, *39*, 301–312.
- (18) Sheldon, R. A. Fundamentals of green chemistry: efficiency in reaction design. *Chem. Soc. Rev.* **2012**, *41*, 1437–1451.
- (19) Prat, D.; Hayler, J.; Wells, A. A survey of solvent selection guides. *Green Chem.* **2014**, *16*, 4546–4551.
- (20) Rodríguez-Padrón, D.; Puente-Santiago, A. R.; Balu, A. M.; Muñoz-Batista, M. J.; Luque, R. Environmental Catalysis: Present and Future. *ChemCatChem.* **2019**, *11*, 18–38.
- (21) Polshettiwar, V.; Varma, R. S. Green chemistry by nano-catalysis. *Green Chem.* **2010**, *12*, 743–754.
- (22) Blackburn, L.; Taylor, R. J. In Situ Oxidation-Imine Formation-Reduction Routes from Alcohols to Amines. *Org. Lett.* **2001**, *3*, 1637–1639.
- (23) Cainelli, G.; Cardillo, G. *Chromium Oxidations in Organic Chemistry*; Springer Berlin Heidelberg: Berlin, Heidelberg, 1984. pp. 118–216.
- (24) Tidwell, T. T. Oxidation of Alcohols by Activated Dimethyl Sulfoxide and Related Reactions: An Update. *Synthesis*, **1990**, *1990*, 857–870.

- (25) Behling, R.; Chatel, G.; Valange, S. Sonochemical Oxidation of Vanillyl Alcohol to Vanillin in the Presence of a Cobalt Oxide Catalyst under Mild Conditions. *Ultrason. Sonochem.* **2017**, *36*, 27–35.
- (26) Ren, Q.-G.; Chen, S.-Y.; Zhou, X.-T.; Ji, H.-B. Highly Efficient Controllable Oxidation of Alcohols to Aldehydes and Acids with Sodium Periodate Catalyzed by Water-Soluble Metalloporphyrins as Biomimetic Catalyst. *Bioorg. Med. Chem.* **2010**, *18*, 8144–8149.
- (27) Zhang, W.; Innocenti, G.; Oulego, P.; Gitis, V.; Wu, H.; Ensing, B.; Cavani, F.; Rothenberg, G.; Shiju, N. R. Highly Selective Oxidation of Ethyl Lactate to Ethyl Pyruvate Catalyzed by Mesoporous Vanadia–Titania. *ACS Catal.* **2018**, *8*, 2365–2374.
- (28) Gao, Q.; Giordano, C.; Antonietti, M. Biomimetic Oxygen Activation by MoS₂/Ta₃N₅ Nanocomposites for Selective Aerobic Oxidation. *Angew. Chem. Int.* **2012**, *51*, 11740–11744.
- (29) Ray, R.; Chandra, S.; Maiti, D.; Lahiri, G. K. Simple and Efficient Ruthenium-Catalyzed Oxidation of Primary Alcohols with Molecular Oxygen. *Chemistry.* **2016**, *22*, 8814–8822.
- (30) Devari, S.; Deshidi, R.; Kumar, M.; Kumar, A.; Sharma, S.; Rizvi, M.; Kushwaha, M.; Gupta, A. P.; Shah, B. A. Osmium (VI) Catalyzed Chemoselective Oxidation of Allylic and Benzylic Alcohols. *Tetrahedron Lett.* **2013**, *54*, 6407–6410.
- (31) Su, H.; Zhang, K.-X.; Zhang, B.; Wang, H.-H.; Yu, Q.-Y.; Li, X.-H.; Antonietti, M.; Chen, J.-S. Activating Cobalt Nanoparticles via the Mott-Schottky Effect in Nitrogen-Rich Carbon Shells for Base-Free Aerobic Oxidation of Alcohols to Esters. *J. Am. Chem. Soc.* **2017**, *139*, 811–818.
- (32) Wu, Z.; Hull, K. L. Rhodium-Catalyzed Oxidative Amidation of Allylic Alcohols and Aldehydes: Effective Conversion of Amines and Anilines into Amides. *Chem. Sci.* **2016**, *7*, 969–975.

- (33) Weiss, C. J.; Das, P.; Miller, D. L.; Helm, M. L.; Appel, A. M. Catalytic Oxidation of Alcohol via Nickel Phosphine Complexes with Pendant Amines. *ACS Catal.* **2014**, *4*, 2951–2958.
- (34) Jaworski, J. N.; McCann, S. D.; Guzei, I. A.; Stahl, S. S. Detection of Palladium(I) in Aerobic Oxidation Catalysis. *Angew. Chem.* **2017**, *129*, 3659–3664.
- (35) Ning, X.; Li, Y.; Yu, H.; Peng, F.; Wang, H.; Yang, Y. Promoting Role of Bismuth and Antimony on Pt Catalysts for the Selective Oxidation of Glycerol to Dihydroxyacetone. *J. Catal.* **2016**, *335*, 95–104.
- (36) Li, H.; Qin, F.; Yang, Z.; Cui, X.; Wang, J.; Zhang, L. New Reaction Pathway Induced by Plasmon for Selective Benzyl Alcohol Oxidation on BiOCl Possessing Oxygen Vacancies. *J. Am. Chem. Soc.* **2017**, *139*, 3513–3521.
- (37) Zhu, J.; Zhao, Y.; Tang, D.; Zhao, Z.; Carabineiro, S. A. C. Aerobic Selective Oxidation of Alcohols Using La₁-Ce CoO₃ Perovskite Catalysts. *J. Catal.* **2016**, *340*, 41–48.
- (38) Silva, T. F. S.; Martins, L. M. D. R. S. Recent Advances in Copper Catalyzed Alcohol Oxidation in Homogeneous Medium. *Molecules* **2020**, *25*, 748.
- (39) Unver, H.; Kani, I. Homogeneous Oxidation of Alcohols in Water Catalyzed with Cu(II)-Triphenyl Acetate/Bipyridyl Complex. *Polyhedron* **2017**, *134*, 257–262.
- (40) Unver, H.; Kani, I. Homogeneous Oxidation of Alcohol and Alkene with Copper (II) Complex in Water. *J. Chem. Sci.* **2018**, *130*, 1–9.
- (41) Shchapin, I. Y.; Nekhaev, A. I.; Ramazanov, D. N.; Al-Yusufi, M.; Samoilov, V. O.; Maximov, A. L. Hydrocarbon Oxidation Depth: H₂O₂/Cu₂Cl₄·2DMG/CH₃CN System. *Catalysts*. **2022**, *12*, 409.
- (42) Kulakova, A. N.; Bilyachenko, A. N.; Levitsky, M. M.; Khrustalev, V. N.; Korlyukov, A. A.; Zubavichus, Y. V.; Dorovatovskii, P. V.; Lamaty, F.; Bantreil, X.; Villemejeanne, B.; Martinez, J.; Shul'pina, L. S.; Shubina, E. S.; Gutsul, E. I.; Mikhailov, I. A.;

- Ikonnikov, N. S.; Tsareva, U. S.; Shul'pin, G. B. $\text{Si}_{10}\text{Cu}_6\text{N}_4$ Cage HexaCoppersilsesquioxanes Containing N Ligands: Synthesis, Structure, and High Catalytic Activity in Peroxide Oxidations. *Inorg. Chem.* **2017**, *56*, 15026–15040.
- (43) Hazra, S.; Martins, L. M. D. R. S.; Guedes da Silva, M. F. C.; Pombeiro, A. J. L. Sulfonated Schiff Base Copper(II) Complexes as Efficient and Selective Catalysts in Alcohol Oxidation: Syntheses and Crystal Structures. *RSC Adv.* **2015**, *5*, 90079–90088.
- (44) Frija, L. M. T.; Alegria, E. C. B. A.; Sutradhar, M.; Cristiano, M. L. S.; Ismael, A.; Kopylovich, M. N.; Pombeiro, A. J. L. Copper(II) and Cobalt(II) Tetrazole-Saccharinate Complexes as Effective Catalysts for Oxidation of Secondary Alcohols. *J. Mol. Catal. A Chem.* **2016**, *425*, 283–290.
- (45) Sutradhar, M.; Roy Barman, T.; Pombeiro, A. J. L.; Martins, L. M. D. R. S. Cu(II) and Fe(III) Complexes Derived from N-Acetylpyrazine-2-Carbohydrazide as Efficient Catalysts towards Neat Microwave Assisted Oxidation of Alcohols. *Catalysts.* **2019**, *9*, 1053-1067.
- (46) Ma, Z.; Wang, Q.; C. B. A. Alegria, E.; C. Guedes da Silva, M. F.; M. D. R. S. Martins, L.; Telo, J. P.; Correia, I.; J. L. Pombeiro, A. Synthesis and Structure of Copper Complexes of a N6O4 Macrocyclic Ligand and Catalytic Application in Alcohol Oxidation. *Catalysts* **2019**, *9*, 424-446.
- (47) Zhang, G.; Liu, E.; Yang, C.; Li, L.; Golen, J. A.; Rheingold, A. L. Copper(II) Complexes of 2,2':6',2''-terpyridine Derivatives for Catalytic Aerobic Alcohol Oxidations—Observation of Mixed-valence Cu(I) Cu(II) Assemblies: Copper(II) Complexes of 2,2':6',2''-Terpyridine Derivatives. *Eur. J. Inorg. Chem.* **2015**, *2015*, 939–947.
- (48) Guedes da Silva, M. de F. C.; Mahmoud, A. G.; Śliwa, E. I.; Smoleński, P.; Kuznetsov, M. L.; Pombeiro, A. J. L. Cu(II) and Na(I) Complexes Based on 3,7-Diacetyl-1,3,7-

- Triaza-5-Phosphabicyclo[3.3.1]Nonane-5-Oxide(DAPTAO): Synthesis, Characterization and Catalytic Activity. *Chem. Asian J.* **2018**, *13*, 2868–2880.
- (49) Lagerspets, E.; Lagerblom, K.; Heliövaara, E.; Hiltunen, O.-M.; Moslova, K.; Nieger, M.; Repo, T. Schiff Base Cu(I) Catalyst for Aerobic Oxidation of Primary Alcohols. *Mol. Catal.* **2019**, *468*, 75–79.
- (50) Marais, L.; Burés, J.; Jordaan, J. H. L.; Mapolie, S.; Swarts, A. J. A Bis(Pyridyl)-N-Alkylamine/Cu(I) Catalyst System for Aerobic Alcohol Oxidation. *Org. Biomol. Chem.* **2017**, *15*, 6926–6933.
- (51) Ochen, A.; Whitten, R.; Aylott, H. E.; Ruffell, K.; Williams, G. D.; Slater, F.; Roberts, A.; Evans, P.; Steves, J. E.; Sanganee, M. J. Development of a Large-Scale Copper(I)/TEMPO-Catalyzed Aerobic Alcohol Oxidation for the Synthesis of LSD1 Inhibitor GSK2879552. *Organometallics.* **2019**, *38*, 176–184.
- (52) Ma, R.; Xu, Y.; Zhang, X. Catalytic Oxidation of Biorefinery Lignin to Value-Added Chemicals to Support Sustainable Biofuel Production. *ChemSusChem.* **2015**, *8*, 24–51.
- (53) Jha, A.; Patil, K. R.; Rode, C. V. Mixed Co-Mn Oxide-Catalysed Selective Aerobic Oxidation of Vanillyl Alcohol to Vanillin in Base-Free Conditions. *ChemPlusChem.* **2013**, *78*, 1384–1392.
- (54) Jha, A.; Rode, C. V. Highly Selective Liquid-Phase Aerobic Oxidation of Vanillyl Alcohol to Vanillin on Cobalt Oxide (Co₃O₄) Nanoparticles. *New J Chem.* **2013**, *37*, 2669–2674.
- (55) Zhang, J.; Zhang, F.; Guo, S.; Zhang, J. Three-Dimensional Composite of Co₃O₄ Nanoparticles and Nitrogen-Doped Reduced Graphene Oxide for Lignin Model Compound Oxidation. *New J Chem.* **2018**, *42*, 11117–11123.
- (56) Saha, S.; Abd Hamid, S. B. CuZrO₃ nanoparticles Catalyst in Aerobic Oxidation of Vanillyl Alcohol. *RSC Adv.* **2017**, *7*, 9914–9925.

- (57) Reddy, P. R. G. N.; Rao, B. G.; Rao, T. V.; Reddy, B. M. Selective Aerobic Oxidation of Vanillyl Alcohol to Vanillin Catalysed by Nanostructured Ce-Zr-O Solid Solutions. *Catal. Letters* **2019**, *149*, 533–543.
- (58) Hinde, C. S.; Ansovini, D.; Wells, P. P.; Collins, G.; Van Aswegen, S.; Holmes, J. D.; Hor, T. S. A.; Raja, R. Elucidating Structure–Property Relationships in the Design of Metal Nanoparticle Catalysts for the Activation of Molecular Oxygen. *ACS Catal.* **2015**, *5*, 3807–3816.
- (59) Baguc, I. B.; Celebi, M.; Karakas, K.; Ertas, I. E.; Keles, M. N.; Kaya, M.; Zahmakiran, M. Nanohydroxalcalite Supported Ruthenium Nanoparticles: Highly Efficient Heterogeneous Catalyst for the Oxidative Valorization of Lignin Model Compounds. *ChemistrySelect.* **2017**, *2*, 10191–10198.
- (60) Ramana, S.; Rao, B. G.; Venkataswamy, P.; Rangaswamy, A.; Reddy, B. M. Nanostructured Mn-Doped Ceria Solid Solutions for Efficient Oxidation of Vanillyl Alcohol. *J. Mol. Catal. A Chem.* **2016**, *415*, 113–121.
- (61) Yang, L.; Ma, R.; Zeng, H.; Rui, Z.; Li, Y. MOF-Templated Core-Shell Co(II/III)@ZnO Hexagonal Prisms for Selective Oxidation of Vanillyl Alcohol. *Catal. Today.* **2020**, *355*, 280–285.
- (62) Sun, W.; Wu, S.; Lu, Y.; Wang, Y.; Cao, Q.; Fang, W. Effective Control of Particle Size and Electron Density of Pd/C and Sn-Pd/C Nanocatalysts for Vanillin Production via Base-Free Oxidation. *ACS Catal.* **2020**, *10*, 7699–7709.
- (63) Martín-Perales, A. I.; Rodríguez-Padrón, D.; García Coletto, A.; Len, C.; de Miguel, G.; Muñoz-Batista, M. J.; Luque, R. Photocatalytic Production of Vanillin over CeO_x and ZrO₂ Modified Biomass-Templated Titania. *Ind. Eng. Chem. Res.* **2020**, *59*, 17085–17093.

- (64) Sampaio, M. J.; Benyounes, A.; Serp, P.; Faria, J. L.; Silva, C. G. Photocatalytic Synthesis of Vanillin Using N-Doped Carbon Nanotubes/ZnO Catalysts under UV-LED Irradiation. *Appl. Catal. A Gen.* **2018**, *551*, 71–78.
- (65) Wu, M.; Pang, J.-H.; Song, P.-P.; Peng, J.-J.; Xu, F.; Li, Q.; Zhang, X.-M. Visible Light-Driven Oxidation of Vanillyl Alcohol in Air with Au–Pd Bimetallic Nanoparticles on Phosphorylated Hydrotalcite. *New J Chem.* **2019**, *43*, 1964–1971.
- (66) Zakzeski, J.; Bruijninx, P. C. A.; Jongerius, A. L.; Weckhuysen, B. M. The Catalytic Valorization of Lignin for the Production of Renewable Chemicals. *Chem. Rev.* **2010**, *110*, 3552–3599.
- (67) Bozell, J. J.; Hames, B. R.; Dimmel, D. R. Cobalt-Schiff Base Complex Catalyzed Oxidation of Para-Substituted Phenolics. Preparation of Benzoquinones. *J. Org. Chem.* **1995**, *60*, 2398–2404.
- (68) Zucca, P.; Sollai, F.; Garau, A.; Rescigno, A.; Sanjust, E. Fe(III)-5,10,15,20-Tetrakis(Pentafluorophenyl)Porphine Supported on Pyridyl-Functionalized, Crosslinked Poly(Vinyl Alcohol) as a Biomimetic Versatile-Peroxidase-like Catalyst. *J. Mol. Catal. A Chem.* **2009**, *306*, 89–96.
- (69) Hu, J.; Hu, Y.; Mao, J.; Yao, J.; Chen, Z.; Li, H. A Cobalt Schiff Base with Ionic Substituents on the Ligand as an Efficient Catalyst for the Oxidation of 4-Methyl Guaiacol to Vanillin. *Green Chem.* **2012**, *14*, 2894–2898.
- (70) McElroy, C. R.; Constantinou, A.; Jones, L. C.; Summerton, L.; Clark, J. H. Towards a Holistic Approach to Metrics for the 21st Century Pharmaceutical Industry. *Green Chem.* **2015**, *17*, 3111–3121.
- (71) Segura, J. L.; Mancheño, M. J.; Zamora, F. Covalent Organic Frameworks Based on Schiff-Base Chemistry: Synthesis, Properties and Potential Applications. *Chem. Soc. Rev.* **2016**, *45*, 5635–5671.

- (72) Liu, X.; Manzur, C.; Novoa, N.; Celedón, S.; Carrillo, D.; Hamon, J.-R. Multidentate Unsymmetrically-Substituted Schiff Bases and Their Metal Complexes: Synthesis, Functional Materials Properties, and Applications to Catalysis. *Coord. Chem. Rev.* **2018**, *357*, 144–172.
- (73) Peris, E.; Crabtree, R. H. Key Factors in Pincer Ligand Design. *Chem. Soc. Rev.* **2018**, *47*, 1959–1968.
- (74) Gunanathan, C.; Milstein, D. Applications of Acceptorless Dehydrogenation and Related Transformations in Chemical Synthesis. *Science*. **2013**, *341*, 1229712-1229723
- (75) Koten, G.; Hollis, T. K.; Morales-Morales, D. Pincer Chemistry and Catalysis. *Eur. J. Inorg. Chem.* **2020**, *2020*, 4416–4417.
- (76) Shimbayashi, T.; Fujita, K.-I. Recent Advances in Homogeneous Catalysis via Metal–Ligand Cooperation Involving Aromatization and Dearomatization. *Catalysts*. **2020**, *10*, 635.
- (77) Gamez, P.; Arends, I. W. C. E.; Reedijk, J.; Sheldon, R. A. Copper(II)-Catalysed Aerobic Oxidation of Primary Alcohols to Aldehydes. *Chem. Commun.* **2003**, *2003*, 2414–2415.
- (78) Gamez, P.; Arends, I. W. C. E.; Sheldon, R. A.; Reedijk, J. Room Temperature Aerobic Copper–Catalysed Selective Oxidation of Primary Alcohols to Aldehydes. *Adv. Synth. Catal.* **2004**, *346*, 805–811.
- (79) Kumpulainen, E. T. T.; Koskinen, A. M. P. Catalytic Activity Dependency on Catalyst Components in Aerobic Copper-TEMPO Oxidation. *Chemistry*. **2009**, *15*, 10901–10911.
- (80) Hoover, J. M.; Stahl, S. S. Highly Practical Copper(I)/TEMPO Catalyst System for Chemoselective Aerobic Oxidation of Primary Alcohols. *J. Am. Chem. Soc.* **2011**, *133*, 16901–16910.

- (81) Hoover, J. M.; Steves, J. E.; Stahl, S. S. Copper(I)/TEMPO-Catalyzed Aerobic Oxidation of Primary Alcohols to Aldehydes with Ambient Air. *Nat. Protoc.* **2012**, *7*, 1161–1166.
- (82) Air Oxidation of Primary Alcohols Catalyzed by Copper(I)/TEMPO. Preparation of 2-Amino-5-Bromo-Benzaldehyde. *Organic Synth.* **2013**, *90*, 240-250.
- (83) Ryland, B. L.; McCann, S. D.; Brunold, T. C.; Stahl, S. S. Mechanism of Alcohol Oxidation Mediated by Copper(II) and Nitroxyl Radicals. *J. Am. Chem. Soc.* **2014**, *136*, 12166–12173.
- (84) Jana, N. C.; Ghorai, P.; Brandão, P.; Jaglicic, Z.; Panja, A. Proton Controlled Synthesis of Two DiCopper(II) Complexes and Their Magnetic and Biomimetic Catalytic Studies Together with Probing the Binding Mode of the Substrate to the Metal Center. *Dalton Trans.* **2021**, *50*, 15233–15247.
- (85) Chaudhuri, P.; Hess, M.; Müller, J.; Hildenbrand, K.; Bill, E.; Weyhermüller, T.; Wieghardt, K. Aerobic Oxidation of Primary Alcohols (Including Methanol) by Copper(II)–and Zinc(II)–Phenoxy Radical Catalysts. *J. Am. Chem. Soc.* **1999**, *121*, 9599–9610.
- (86) Velusamy, S.; Srinivasan, A.; Punniyamurthy, T. Copper(II) Catalyzed Selective Oxidation of Primary Alcohols to Aldehydes with Atmospheric Oxygen. *Tetrahedron Lett.* **2006**, *47* (6), 923–926.
- (87) Cheng, L.; Wang, J.; Wang, M.; Wu, Z. Theoretical Studies on the Reaction Mechanism of Oxidation of Primary Alcohols by Zn/Cu(II)-Phenoxy Radical Catalyst. *Dalton Trans.* **2009**, *2009*, 3286–3297.
- (88) Lumsden, S. E. A.; Durgaprasad, G.; Thomas Muthiah, K. A.; Rose, M. J. Tuning Coordination Modes of Pyridine/Thioether Schiff Base (NNS) Ligands to Mononuclear Manganese Carbonyls. *Dalton Trans.* **2014**, *43*, 10725–10738.

- (89) Turner, S. A.; Remillard, Z. D.; Gijima, D. T.; Gao, E.; Pike, R. D.; Goh, C. Syntheses and Structures of Closely Related Copper(I) Complexes of Tridentate (2-Pyridylmethyl) Imine and (2-Pyridylmethyl) Amine Ligands and Their Use in Mediating Atom Transfer Radical Polymerizations. *Inorg. Chem.* **2012**, *51*, 10762–10773.
- (90) Jana, N. C.; Brandão, P.; Frontera, A.; Panja, A. A Facile Biomimetic Catalytic Activity through Hydrogen Atom Abstraction by the Secondary Coordination Sphere in Manganese(III) Complexes. *Dalton Trans.* **2020**, *49*, 14216–14230.
- (91) Sharma, M.; Ganeshpandian, M.; Majumder, M.; Tamilarasan, A.; Sharma, M.; Mukhopadhyay, R.; Islam, N. S.; Palaniandavar, M. Octahedral Copper(II)-Diimine Complexes of Triethylenetetramine: Effect of Stereochemical Fluxionality and Ligand Hydrophobicity on CuII/CuI Redox, DNA Binding and Cleavage, Cytotoxicity and Apoptosis-Inducing Ability. *Dalton Trans.* **2020**, *49*, 8282–8297.
- (92) Bu, X. H.; Du, M.; Shang, Z. L.; Zhang, L.; Zhao, Q. H.; Zhang, R. H.; Shionoya, M. Novel Diazamesocyclic Ligands Functionalized with Pyridyl Donor Group(s)- Synthesis, Crystal Structures, and Properties of Their Copper(II) Complexes. *Eur. J. Inorg. Chem.* **2001**, *2001*, 1551–1558.
- (93) Motalebi, M.; Golchoubian, H.; Rezaee, E. Structural and Chromotropism Properties of Copper(II) Complexes Containing a Tridentate Ligand. *Chem. Pap.* **2020**, *74*, 4075–4087.
- (94) Anwar, M. U.; Al-Harrasi, A.; Rawson, J. M. Structures, Properties and Applications of Cu(II) Complexes with Tridentate Donor Ligands. *Dalton Trans.* **2021**, *50*, 5099–5108.
- (95) Banerjee, I.; Samanta, P. N.; Das, K. K.; Ababei, R.; Kalisz, M.; Girard, A.; Mathonière, C.; Nethaji, M.; Clérac, R.; Ali, M. Air Oxygenation Chemistry of 4-TBC Catalyzed by Chloro Bridged Dinuclear Copper(II) Complexes of Pyrazole Based Tridentate Ligands:

- Synthesis, Structure, Magnetic and Computational Studies. *Dalton Trans.* **2013**, *42*, 1879–1892.
- (96) Lumb, I.; Hundal, M. S.; Corbella, M.; Gómez, V.; Hundal, G. Copper(II) Complexes of N, N-diisopropylpicolinamide–Solvatochromic and Thermochromic Phase Change of a Monomeric Complex to a Ferromagnetically Coupled Dimeric Complex. *Eur. J. Inorg. Chem.* **2013**, *2013*, 4799–4811.
- (97) Choubey, S.; Roy, S.; Chattopadhyay, S.; Bhar, K.; Ribas, J.; Monfort, M.; Ghosh, B. K. Synthesis, Structure and Magnetic Property of an Asymmetric Chlorido Bridged Dinuclear Copper(II) Complex Containing a Didentate Schiff Base. *Polyhedron*. **2015**, *89*, 39–44.
- (98) Addison, A. W.; Rao, T. N.; Reedijk, J.; van Rijn, J.; Verschoor, G. C. Synthesis, Structure, and Spectroscopic Properties of Copper(II) Compounds Containing Nitrogen–Sulphur Donor Ligands; the Crystal and Molecular Structure of Aqua[1,7-Bis(N-Methylbenzimidazol-2'-yl)-2,6-Dithiaheptane]Copper(II) Perchlorate. *J. Chem. Soc., Dalton Trans.* **1984**, 1349–1356.
- (99) Durigon, D. C.; Maragno Peterle, M.; Bortoluzzi, A. J.; Ribeiro, R. R.; Braga, A. L.; Peralta, R. A.; Neves, A. Cu(II) Complexes with Tridentate Sulfur and Selenium Ligands: Catecholase and Hydrolysis Activity. *New J Chem* **2020**, *44*, 15698–15707.
- (100) Ding, C.; Ren, Y.; Sun, C.; Long, J.; Yin, G. Regio- and Stereoselective Alkylboration of Endocyclic Olefins Enabled by Nickel Catalysis. *J. Am. Chem. Soc.* **2021**, *143*, 20027–20034.
- (101) Chen, P.-F.; Zhou, B.; Wu, P.; Wang, B.; Ye, L.-W. Brønsted Acid Catalyzed Dearomatization by Intramolecular Hydroalkoxylation/Claisen Rearrangement: Diastereo- and Enantioselective Synthesis of Spirolactams. *Angew. Chem. Int. Ed.* **2021**, *60*, 27164–27170.

- (102) Talbot, F. J. T.; Zhang, S.; Satpathi, B.; Howell, G. P.; Perry, G. J. P.; Crisenza, G. E. M.; Procter, D. J. Modular Synthesis of Stereodefined Benzocyclobutene Derivatives via Sequential Cu- and Pd-Catalysis. *ACS Catal.* **2021**, *11*, 14448–14455.
- (103) Maticic, M.; Gredicak, M. Enantioselective Construction of a Tetrasubstituted Stereocenter in Isoindolinones via an Organocatalyzed Reaction between Ketones and 3-Hydroxyisoindolinones. *Chem. Commun.* **2021**, *57*, 13546–13549.
- (104) Li, M.; Wang, D.-H. Copper-Catalyzed 3-Positional Amination of 2-Azulenols with O-Benzoylhydroxylamines. *Org. Lett.* **2021**, *23*, 6638–6641.
- (105) Fazekas, E.; Jenkins, D. T.; Forbes, A. A.; Gallagher, B.; Rosair, G. M.; McIntosh, R. D. Amino Acid-Derived Bisphenolate Palladium Complexes as C-C Coupling Catalysts. *Dalton Trans.* **2021**, *50*, 17625–17634.
- (106) DeSimone, J. M. Practical Approaches to Green Solvents. *Science.* **2002**, *297*, 799–803.
- (107) Curzons, A. D.; Mortimer, D. N.; Constable, D. J. C.; Cunningham, V. L. So, You Think Your Process Is Green, How Do You Know? -Using Principles of Sustainability to Determine What Is Green - a Corporate Perspective. *Green Chem.* **2001**, *3*, 1–6.
- (108) Constable, D. J. C.; Curzons, A. D.; Cunningham, V. L. Metrics to 'Green' Chemistry- Which Are the Best? *Green Chem.* **2002**, *4*, 521–527.
- (109) Sheldon, R. A. Green Solvents for Sustainable Organic Synthesis: State of the Art. *Green Chem.* **2005**, *7*, 267–278.
- (110) Dyson, P. J.; Jessop, P. G. Solvent Effects in Catalysis: Rational Improvements of Catalysts via Manipulation of Solvent Interactions. *Catal. Sci. Technol.* **2016**, *6*, 3302–3316.

- (111) Zhao, X.; Wang, D.; Xiang, C.; Zhang, F.; Liu, L.; Zhou, X.; Zhang, H. Facile Synthesis of Boron Organic Polymers for Efficient Removal and Separation of Methylene Blue, Rhodamine B, and Rhodamine 6G. *ACS Sustain. Chem. Eng.* **2018**, *6*, 16777–16787.
- (112) Sheriff Shah, S.; Pradeep Singh, N. D. Pseudohalide Assisted Aerobic Oxidation of Alcohols in the Presence of Visible-Light. *Tetrahedron Lett.* **2018**, *59*, 247–251.
- (113) Kongkaew, M.; Sitthisuwannakul, K.; Nakarajouyphon, V.; Pornsuwan, S.; Kongsaree, P.; Sangtrirutnugul, P. Benzimidazole-Triazole Ligands with Pendent Triazole Functionality: Unexpected Formation and Effects on Copper-Catalyzed Aerobic Alcohol Oxidation. *Dalton Trans.* **2016**, *45*, 16810–16819.
- (114) Griffiths, T. R.; Pugh, D. C. Correlations among Solvent Polarity Scales, Dielectric Constant and Dipole Moment, and a Means to Reliable Predictions of Polarity Scale Values from Cu. *Coord. Chem. Rev.* **1979**, *29*, 129–211.
- (115) Van Leeuwen, P. W. N. M.; Homogeneous Catalysis – Understanding the Art, Kluwer Academic Publishers, Dordrecht, The Netherlands, 2004.
- (116) Díaz-Torres, R.; Alvarez, S. Coordinating Ability of Anions and Solvents towards Transition Metals and Lanthanides. *Dalton Trans.* **2011**, *40*, 10742–10750.
- (117) Prat, D.; Wells, A.; Hayler, J.; Sneddon, H.; McElroy, C. R.; Abou-Shehada, S.; Dunn, P. J. CHEM21 Selection Guide of Classical- and Less Classical-Solvents. *Green Chem.* **2016**, *18*, 288–296.
- (118) Allen, D. T.; Gathergood, N.; Licence, P.; Subramaniam, B. Expectations for Manuscripts Contributing to the Field of Solvents in ACS Sustainable Chemistry & Engineering. *ACS Sustainable Chem. Eng.* **2020**, *8*, 14627–14629.
- (119) Kuok (Mimi) Hii, K.; Moores, A.; Pradeep, T.; Sels, B.; Allen, D. T.; Licence, P.; Subramaniam, B. Expectations for Manuscripts on Catalysis in ACS Sustainable Chemistry & Engineering. *ACS Sustain. Chem. Eng.* **2020**, *8*, 4995–4996.

- (120) Allen, D. T.; Carrier, D. J.; Gong, J.; Hwang, B.-J.; Licence, P.; Moores, A.; Pradeep, T.; Sels, B.; Subramaniam, B.; Tam, M. K. C.; Zhang, L.; Williams, R. M. Advancing the Use of Sustainability Metrics in ACS Sustainable Chemistry & Engineering. *ACS Sustainable Chem. Eng.* **2018**, *6*, 1.
- (121) Droesbeke, M. A.; Du Prez, F. E. Sustainable Synthesis of Renewable Terpenoid-Based (Meth)acrylates Using the CHEM21 Green Metrics Toolkit. *ACS Sustainable Chem. Eng.* **2019**, *7*, 11633–11639.
- (122) Prieschl, M.; Garcia-Lacuna, J.; Munday, R.; Leslie, K.; O’Kearney-McMullan, A.; Hone, C. A.; Kappe, C. O. Optimization and sustainability assessment of a continuous flow Ru-catalyzed ester hydrogenation for an important precursor of a β 2-adrenergic receptor agonist. *Green Chem.* **2020**, *22*, 5762–5770.
- (123) Dalidovich, T.; Mishra, K. A.; Shalima, T.; Kudrjasova, M.; Kananovich, D. G.; Aav, R. Mechanochemical Synthesis of Amides with Uronium-Based Coupling Reagents: A Method for Hexaamidation of Biotin [6]uril. *ACS Sustainable Chem. Eng.* **2020**, *8*, 15703–15715.
- (124) Zhu, Z.; Wang, Z.; Jian, Y.; Sun, H.; Zhang, G.; Lynam, J. M.; McElroy, C. R.; Burden, T. J.; Inight, R. L.; Fairlamb, I. J. S.; Zhang, W.; Gao, Z. Pd-Catalysed carbonylative Suzuki-Miyaura crosscouplings using $\text{Fe}(\text{CO})_5$ under mild conditions: generation of a highly active, recyclable and scalable ‘Pd–Fe’ nanocatalyst. *Green Chem.* **2021**, *23*, 920–926.
- (125) Ghosh, R.; Jana, N. C.; Panda, S.; Bagh, B. Transfer Hydrogenation of Aldehydes and Ketones in Air with Methanol and Ethanol by an Air-Stable Ruthenium–Triazole Complex. *ACS Sustainable Chem. Eng.* **2021**, *9*, 4903–4914.

- (126) Ryland, B. L.; Stahl, S. S. Practical Aerobic Oxidations of Alcohols and Amines with Homogeneous Copper/TEMPO and Related Catalyst Systems. *Angew. Chem. Int. Ed.* **2014**, *53*, 8824–8838.
- (127) Brackman, W.; Gaasbeek, C. J. Studies in Homogeneous Catalysis.: Radicals of the Type as Catalysts for the Oxidation of Methanol by Cupric Complexes and as Promoters for Variou. *Recl. Trav. Chim. Pays Bas.* **2010**, *85*, 221–241.
- (128) Dijkstra, A.; Arends, I. W. C. E.; Sheldon, R. A. Cu(II)-Nitroxyl Radicals as Catalytic Galactose Oxidase Mimics. *Org. Biomol. Chem.* **2003**, *1*, 3232–3237.
- (129) Rabeah, J.; Bentrup, U.; Stöber, R.; Brückner, A. Selective Alcohol Oxidation by a Copper TEMPO Catalyst: Mechanistic Insights by Simultaneously Coupled Operando EPR/UV-Vis/ATR-IR Spectroscopy. *Angew. Chem. Int. Ed.* **2015**, *54*, 1791–11794.
- (130) Kitajima, N.; Moro-oka, Y. Copper-Dioxygen Complexes. Inorganic and Bioinorganic Perspectives. *Chem. Rev.* **1994**, *94*, 737–757.
- (131) Monzani, E.; Quinti, L.; Perotti, A.; Casella, L.; Gullotti, M.; Randaccio, L.; Geremia, S.; Nardin, G.; Faleschini, P.; Tabbi, G. Tyrosinase Models. Synthesis, Structure, Catechol Oxidase Activity, and Phenol Monooxygenase Activity of a Dinuclear Copper Complex Derived from a Triamino Pentabenzimidazole Ligand. *Inorg. Chem.* **1998**, *37*, 553–562.
- (132) Mandal, A.; Sarkar, A.; Adhikary, A.; Samanta, D.; Das, D. Structure and Synthesis of Copper-Based Schiff Base and Reduced Schiff Base Complexes: A Combined Experimental and Theoretical Investigation of Biomimetic Catalytic Activity. *Dalton Trans.* **2020**, *49*, 15461–15472.

Chapter-3

Azide-Alkyne Cycloaddition Catalyzed by Copper(I) Coordination Polymer in PPM Level Using Deep Eutectic Solvent as a Reusable Reaction Media: A Waste Minimized Sustainable Approach

3.1 ABSTRACT

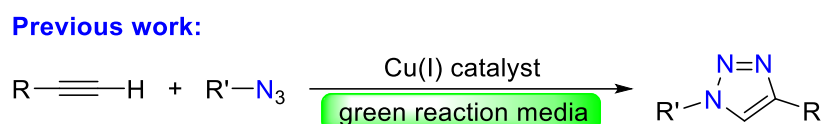
Two air-stable Copper(I)-halide coordination polymers 1 and 2 with NNS and NNO ligand frameworks were synthesized and successfully utilized as efficient catalysts in an important organic reaction, namely Copper catalysed azide-alkyne cycloaddition which is generally conducted in a mixture of water and organic solvents. The azide-alkyne “click” reaction was successfully conducted in pure water at r.t. under aerobic condition. Other green solvents ethanol and glycerol were also effectively used. Finally, deep eutectic solvent as a green and sustainable reaction media was successfully utilized. In deep eutectic solvent, complete conversion with excellent isolated yield was achieved in short period of time (1 h) with low catalyst loading (1 mol%) at r.t. Full conversion could also be achieved within 24 h with ppm level (50 ppm) catalyst loading at 70 °C. The optimized reaction condition was used for the syntheses of a large number of 1,4-disubstituted 1,2,3-triazoles with various functionalities. Triazole products were easily isolated by simple filtration. The reaction media such as water and deep eutectic solvent were recovered and recycled in three consecutive runs. The limited waste production is reflected in very low *E*-factor (0.3 to 2.8). Finally, CHEM21 green metrics toolkit was employed to evaluate the sustainable credentials of different optimized protocols in various green solvents such as water, ethanol, glycerol, and deep eutectic solvent.

3.2 INTRODUCTION

Sustainable chemical transformations for the syntheses of useful chemicals are highly essential in present era and the scientific community is keen to evaluate the environmental and green aspects of a chemical process led by “The 12 Principles of Green Chemistry”.¹⁻⁵ These twelve principles involve catalysis as one of the strategic factor⁶⁻⁸ At least one (often more) catalytic reaction step is involved in most of the significant chemical reactions for the production of valuable chemicals and catalysts play crucial roles in most of the industrial processes impacting economy significantly. However, a majority of those chemical processes are dominated by scarce, expensive and mostly toxic noble metal catalysts. As the use of noble metal catalysts is not sustainable, earth abundant, and cheap (and often less toxic) base metals such as manganese, iron, cobalt, nickel and Copper can serve indispensable alternatives. Employing Copper complexes as catalysts over the use of noble metals for the production of agrochemical and pharmaceutical commodities indeed acknowledged the discovery of new synthetic methodologies within the toolbox of organic synthetic chemistry.⁹ Copper has high potential in homogeneous catalysis because of the following reasons: (i) Copper is earth-abundant and cheap; (ii) it has various stable oxidation states (0 to +3) with dynamic geometries (linear, trigonal planar, square planar, tetrahedral, square pyramidal, trigonal bipyramidal and octahedral); (iii) it accommodates both hard or soft ligands and forms both σ - and π -complexes and (iv) it is less-toxic sustainable base metal. Copper is usually considered as a “metal of choice” in organometallic chemistry and homogeneous catalysis due to its vast application in a wide variety of organic transformations.¹⁰⁻²³ One important example is the Copper(I)-catalyzed 1,3-dipolar cycloaddition of organic azides and alkynes, commonly called CuAAC, which is one of the most versatile and reliable strategies for the synthesis of 1,4-disubstituted 1,2,3-triazole. This triazole (containing different functional groups) is a significant class of nitrogen-containing heterocycle which has found widespread applications in pharmaceutical,^{24,}

²⁵ biological^{6, 27} and material sciences (dyes, corrosion inhibitors, photo stabilizers etc.).^{25, 28–31} Moreover, they are used as ligands^{32, 33} or precursor of an important class of NHCs^{34–38} for the syntheses of metal complexes. In CuAAC reactions, either Cu(I) species is generated in situ by reducing a Cu(II) salt (commonly by sodium ascorbate)^{39, 40} or Cu(I) complexes with various ligand frameworks are directly utilized.^{19, 41–55} These reactions are generally performed in a mixture of water and organic solvent, such as alcohols (*t*-BuOH, EtOH and MeOH), dichloromethane, acetonitrile and THF.^{41–55} The purification of triazole products often include chromatographic separation which also produce a lot of solvent waste.

Scheme 3.1. CuAAC reaction in green reaction media and sustainable features of the present work



Vaccaro et al. (*Green Chem.*, 2016, **18**, 6380)

Catalyst: CuSO₄·5H₂O (2 mol%), Na-ascorbate (10 mol%), Imidazole ligand (20 mol%)

Reaction media: Furfuryl alcohol/water azotrope

Temperature & time: 30 °C, 3 to 24 h

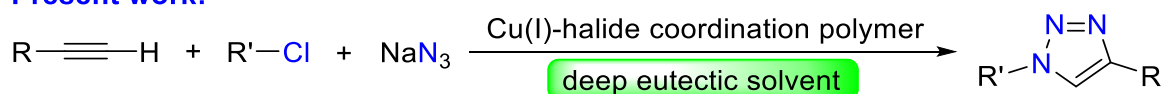
Vaccaro et al. (*Green Chem.*, 2018, **20**, 183)

Catalyst: CuSO₄·5H₂O (2 mol%), Na-ascorbate (10 mol%)

Reaction media: Polar clean/water (4:1)

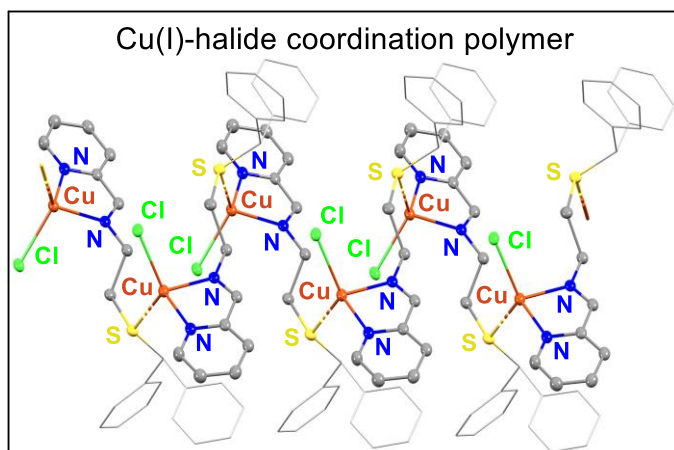
Temperature & time: 50 °C, 24 h

Present work:



Reaction condition A: Cu(I)-catalyst (1 mol%), deep eutactic solvent, r.t., 1 h

Reaction condition B: Cu(I)-catalyst (50 ppm), deep eutactic solvent, 70 °C, 24 h



- Three component one pot reaction
- Air-stable well defined Cu(I)-catalyst
- Very low (ppm level) catalyst loading
- Ambient conditions (in air at r.t.)
- Green and sustainable medium
- Easy product isolation (filtration only)
- Reaction media recycled 3 times
- Wide substrate scope
- Excellent isolated yields of products

A key factor for the advancement of green and sustainable process is the use of benign solvents.⁵⁶⁻⁶² Solvents are commonly the major sources of waste generation in vast majority of organic syntheses and thus in present era, chemical industries are often concerned in selecting solvents. The use of bio-based solvents for metal-catalyzed organic transformation has attracted a significant attention at the present time.⁶³⁻⁶⁹ The utilization of green and reusable solvents as reaction media for CuAAC reaction is very important and some important advancements in this regard have been reported by Vaccaro et al. (**Scheme 3.1**). They utilized an azeotropic mixture of water and biomass-derived furfuryl alcohol as an effective solvent.⁷⁰ In recent past, Vaccaro et al. utilized a mixture of water and Polar clean as a safe, reusable, and sustainable reaction medium.⁷¹ With the aim of using green and sustainable reaction media, we searched for other potential alternatives for sustainable development in synthetic chemistry. We focused our attention on deep eutectic solvent (DES), an emerging class of green media which can balance the major disadvantages of ionic liquids such as high cost, complex synthesis and purification, high toxicity and non-biodegradability.⁷²⁻⁷⁶ Although the use of DES in organic synthesis is limited as compared to common organic solvents, current research interest has grown significantly.⁷⁷ DES has found many applications in various field of material chemistry such as solvent for electrochemically conducting polymers,⁷⁸ recognition of analytes (e.g. Li^+ , Na^+) in analytical devices,⁷⁹ lubrication of metal contacts,⁸⁰ production of carbon

electrode for capacitors,⁸¹ as electrolyte for dye-sensitized solar cell,^{81, 82} and synthesis of drug solubilization vehicles.^{83, 84} With our specific goal of exploring the potential applicability of DES as sustainable reaction medium in important chemical transformations, we decided to investigate CuAAC reaction using DES as solvent.

Herein, we report readily accessible and air-stable Copper(I)-halide coordination polymers with NNO and NNS ligand moieties as very efficient and sustainable catalyst for CuAAC reaction in green solvents such as water, glycerol, and DES (**Scheme 3.1**). The green and sustainable features of the optimized catalytic protocols are also evaluated by utilizing CHEM21 green metrics toolkit.⁵⁶

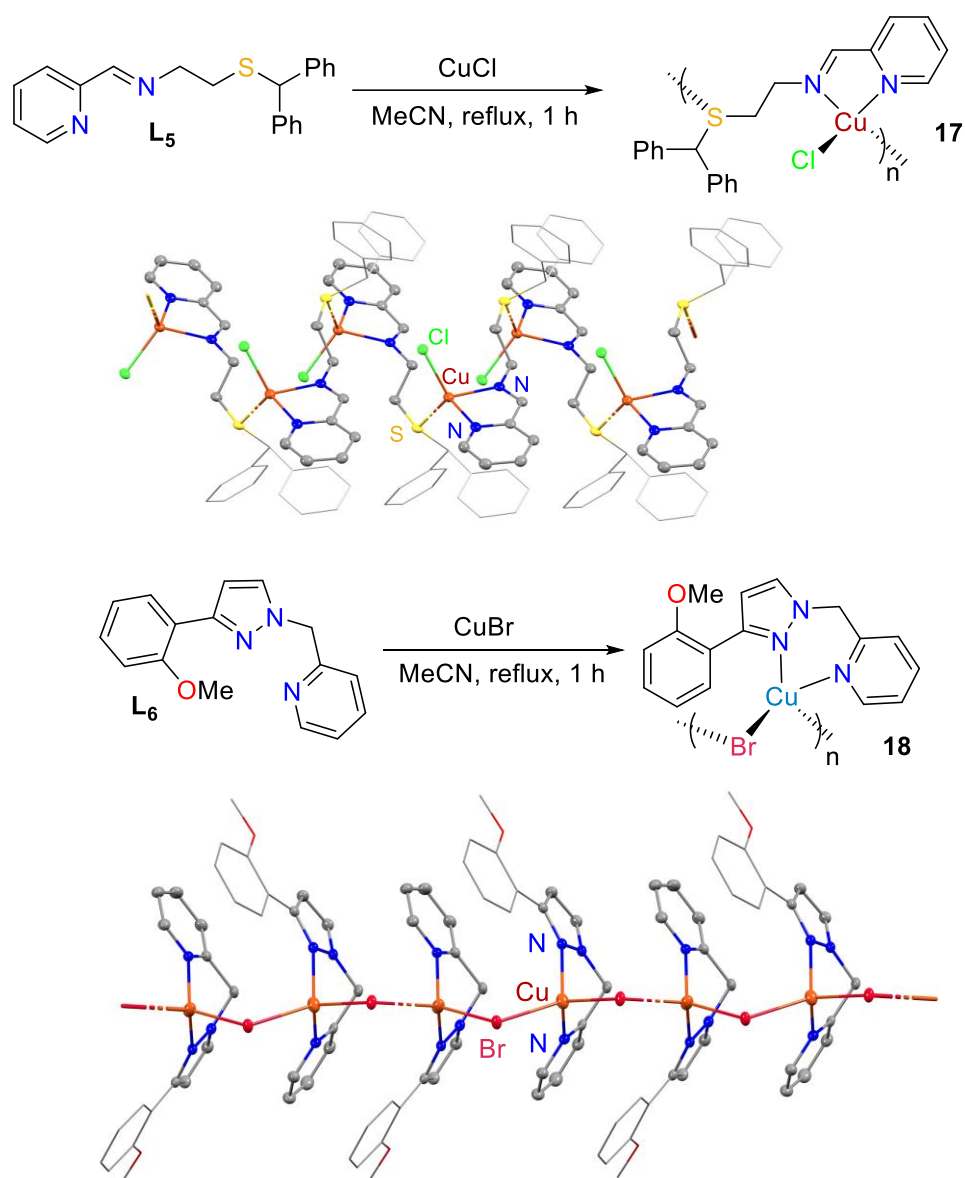
3.3 RESULTS AND DISCUSSION

Generally, Cu(I)-halides (often CuI) are used for CuAAC reactions. However, the instability and insolubility of simple Copper(I) salts in most of the reaction media (particularly organic) are the main setbacks. Alternatively, the active species are often generated in situ from a Copper(II) salt in presence of a reducing agent such as sodium ascorbate. But such in situ generated Cu(I) species are often unstable and have a tendency to disproportionate into Cu(0) and Cu(II) or may get oxidized to Cu(II) species under aerobic conditions. Hence, often a large amount of Copper salt is required for the desired yield. However, the removal of Copper from the product is a problem particularly when triazoles find applications in electronics and pharmaceuticals.⁸⁵⁻⁸⁷ To get avoid this situation, stable and highly active (very low catalyst loading) Cu(I) complexes with appropriate ligands are essential. Therefore, synthetic catalytic community of present days is expected to pay attention in designing new Copper catalyst decorated with ancillary ligands for the CuAAC reaction in sustainable organic synthesis. Yamada and Uozumi et al. reported polymeric Copper(II)-catalysts with poly-(imidazole-acrylamide) ligand framework as a very active catalyst (0.25 mol %) for CuAAC reaction in presence of sodium ascorbate (10 mol %) in *t*-BuOH/water mixture.⁸⁸ Zimmerman et al. used

Copper-cross-linked single chain metal organic framework as a highly efficient Cu(II)-catalyst (ppm level) for the same purpose in water in presence of reducing agent. Such bulky ligand frameworks not only protected in situ generated Cu(I) centre from further oxidation, but also significantly improved the catalytic activity (ppm level).⁸⁹ However, the above catalysts are heterogeneous in nature and the use of reducing agent to reduce Cu(II) to active Cu(I) species is necessary. Furthermore, use of polymeric Copper entities is limited due to its slow rate of dissociation to form active monomeric or dimeric Cu(I) species. In this regard, stable Cu(I) polymers equipped with ancillary ligands having pendant labile ligand arms are more beneficial. The labile arm can easily decoordinate the metal center which helps substrate binding (alkyne coordination). Hence, careful attention for the development of suitable ancillary ligand system is necessary to create favourable coordination linkage around the metal centre. In this regard, we have developed a NNS ligand (**L5**) with bulky labile and soft thioether arm (**Scheme 3.2**). We previously demonstrated the hemilabile nature of this type of NNS ligands.⁹⁰ To get a useful comparison, we have also used a NNO ligand (**L5**) with a harder ether arm (**Scheme 3.2**). Facile coordination of **L5** with CuCl resulted in the formation of **complex 17** (**Scheme 3.2**). Similarly, reaction of **L6** with CuBr yielded **complex 18** (**Scheme 3.2**). Both **17** and **18** were characterized by ¹H and ¹³C NMR spectroscopy, IR spectroscopy and elemental analysis. NNS and NNO ligand frameworks were clearly visible in the ¹H NMR spectra of **complex 17** and **18**, respectively. In the ¹H NMR spectra, the aromatic protons were observed as multiples in the range of 8.74-7.18 ppm and 8.28-6.68 ppm for **complex 17** and **18**, respectively. Resonance for the benzylic proton in **complex 17** was observed as singlet at 5.27 ppm. The methylene moieties in **complex 17** were found as two triplets at 3.86 ppm and 2.50 ppm, whereas a singlet was observed at 5.47 ppm for the methylene protons in **complex 18**. In the ¹H NMR spectrum of **complex 18**, the methoxy protons was appeared as singlet at 3.70 ppm. In the IR spectrum of free ligand **L5**, a sharp band was observed at 1646 cm⁻¹ which

is the characteristic peak for the azomethine stretching vibration. The azomethine stretching band is slightly shifted to 1651 cm^{-1} in **complex 17**. In the IR spectrum of free ligand **L6**, the pyrazole mixed stretching vibration of C=N and C=C bonds was observed at 1504 cm^{-1} which is slightly shifted to 1517 cm^{-1} in **complex 18**. Medium intense bands in the range 3000 to 2800 cm^{-1} were assigned as symmetric and asymmetric stretching vibrations of C(sp³)-H bonds for both **17** and **18**. The vibrational bands in the range of 1400 to 1610 cm^{-1} were assigned for pyridyl (C=N) and phenyl (C=C) stretching vibrations.

Scheme 3.2. Synthesis of Copper(I) complexes 17 and 18 (the molecular structures showing 30% ellipsoids and hydrogen atoms are omitted for clarity)



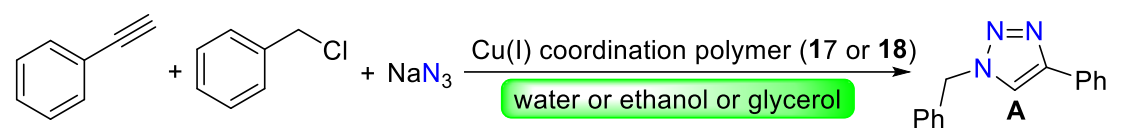
The identity of **17** and **18** was further confirmed by single crystal X-ray diffractometry (**Scheme 3.2**). XRD reveal that **17** crystallized in monoclinic system with space group $P2_1/c$, while **18** crystallize in triclinic system with space group $P1$. The asymmetric unit of **1** consist of a Copper, a chloride and a NNS ligand whereas double units of Copper, bromide and NNO ligand are present in the asymmetric unit of **18**. The geometry around Cu(I) centre in **17** and **18** can be described as distorted tetrahedral. Both **17** and **18** are 1D coordination polymers of general formula $[Cu(L)X]_n$ (**L**: **L5/L6**, **X**: Cl/Br); however, they are very different from each other. In species **17**, the pendent thioether arm of NNS ligand propagate the structure in 1D chain. On the other hand, bromide ion acts as the bridging unit in **18**; the ether arm of NNO ligand remains uncoordinated and located roughly opposite to the metal coordination environment. This is probably because soft Cu(I) center is likely to bind soft sulphur donor and avoids harder oxygen donor. The intra-chain Cu–Cu distance is 5.988 and 4.101 Å in **17** and **18**, respectively. The Cu–N bond lengths vary from 2.063(5) to 2.259(5) Å in **17** and **18**. Cu–S (2.2440(13) Å), Cu–Cl (2.2786(13) Å) and Cu–Br (2.4352(π)–2.5276(10) Å) bond lengths fall in the expected range consistent with tetrahedral Cu(I) complexes.^{91–93} Mostly C–H \cdots π and $\pi\cdots\pi$ stacking interaction gives the solid-state stability in **17** and **18**. It is worth to mention that both coordination polymers **17** and **18** are air and moisture stable.

In homogeneous catalysis, a significant attention goes to the manipulation of the ligand environment (electronic and steric factors) for the development of better performing catalysts. However, the selection of solvents for sustainable catalysis is often ignored. A major aspect in green chemistry is the selection of environmentally benign and sustainable solvents as solvents often produce the major amount of waste mass in a synthetic process.^{57–60} Various organic solvents often used in organic syntheses are considered as problematic or even hazardous such as acetonitrile, toluene, xylene, DMSO, THF, dichloromethane, chloroform and benzene.⁵⁶ Although acetonitrile, dichloromethane and THF are frequently used as solvents

in CuAAC reactions catalyzed by well-defined organometallic Cu(I) complexes.^{44–46, 50–55}

Herein, we report the utilization of various green solvents for CuAAC reaction catalyzed by well-defined Cu(I) coordination polymers **17** and **18**.

Table 3.1. Catalytic performance of 17 and 18 for three component CuAAC reaction in pure water, ethanol, and glycerol as green solvents^a



Ent.	Cat. (mol %)	Solvent	Temp. (°C)	Time (h)	Yield (%) ^b
1	17 (5)	water	r.t.	12, 8, 6	>99
2	18 (5)	water	r.t.	12, 8, 6	>99
3	17 (2)	water	r.t.	6	77
4	18 (2)	water	r.t.	6	48
3	17 (2)	water	r.t.	12	>99
4	18 (2)	water	r.t.	12	88
5	17 (2)	water	r.t.	10, 8	>99
6	17 (2)	water	70	6, 5	>99
7	17 (2)	water	70	4	80
8	17 (2)	water	100	5, 4	>99
9	17 (2)	water	100	3	85
10	17 (2)	ethanol	r.t.	8	30
11	17 (2)	ethanol	70	12, 8, 6	>99
12	17 (2)	ethanol	70	5	86
13	17 (2)	glycerol	r.t.	8, 6	>99
14	17 (2)	glycerol	r.t.	5	88

^aReactions conducted in a vial (10 mL) with 0.50 mmol of benzyl chloride, 0,50 mmol of phenyl acetylene, 1.25 mmol of sodium azide, 5/2 mol% of **1/2** in 2 mL of water/ethanol/glycerol at r.t./70/100 °C. ^bIsolated yields of triazole product.

We started testing the catalytic activities of two Cu(I)-halide coordination polymers **17** and **18** using pure water as a green solvent (**Table 1**) under aerobic condition at r.t. Using 5 mol % catalyst loading, both **17** and **18** gave quantitative yield of triazole product **A** in 6 h (entry 1 and 2). Reducing the catalyst loading to 2 mol %, **17** and **18** provided 77 (entry 3) and 48% (entry 4) yields of product, respectively. The Cu(I)-chloride coordination polymer with NNS backbone (**17**) displayed better catalytic performance as compared to Cu(I)-bromide coordination polymer with NNO backbone (**18**). Species **17** with 2 mol % loading also gave full conversion to product in 8 h at r.t. (entry 5), which was taken as optimized condition at r.t. (depicted in green in Table 3.1). Thereafter, we explored the performance of **17** at elevated temperatures. Using same catalyst loading of 2 mol%, quantitative yield of triazole **A** was obtained in 5 h at 70 °C (entry 6). Further raising the reaction temperature to 100 °C, complete conversion to product was obtained in 4 h (entry 8). Therefore, reaction time was reduced to half at 100 °C as compared to the reaction at r.t. Thereafter, we shifted our focus on ethanol. Ethanol is an attractive candidate in the context of sustainable chemistry as it is bio-abundant, cheap, and environmentally benign. We started with the previously optimized condition for water (entry 5); however, 30% yield of product was noted with 2 mol % loading of **17** in 8 h at r.t. (entry 10). Hence, the reaction temperature was raised to 70 °C (below the boiling point of ethanol) to achieve better yield of product. The following condition was accepted as the optimized condition in ethanol: 2 mol % of **17**, 70 °C, 6 h (entry 11, depicted in green in **Table 3.1**). Thereafter, we utilized glycerol, a waste produced by biodiesel industry, which is considered as a valuable green solvent. Again, we started with the previously optimized condition for water (entry 5) and complete conversion to triazole product **A** was obtained in 8 h. The best condition of CuAAC reaction in glycerol is the following: 2 mol % of **17**, r.t., 6 h (entry 13, depicted in green in **Table 3.1**).

Table 3.2. Catalytic performance of 17 for CuAAC reaction in deep eutectic solvents as sustainable reaction media^a

c1ccccc1C#C + c1ccc(cc1)CCl + [Na][N-]=[N+]=[N]
 $\xrightarrow[\text{deep eutectic solvent}]{\text{Cu(I) coordination polymer 17}}$
c1ccc(cc1)C1=CN=C(N1)c2ccccc2

A

Ent	Cat. 1 (mol %)	Solvent mixture (ratio)	Temp. (°C)	Time (h)	Yield (%) ^b
1	2	ChCl/glycerol (1:2)	r.t.	8/4/2	>99
2	1	ChCl/glycerol (1:2)	r.t.	2/1	>99
3	1	ChCl/glycerol (1:2)	r.t.	0.5	66
4	0.1	ChCl/glycerol (1:2)	r.t.	24	>99
5	0.1	ChCl/glycerol (1:2)	r.t.	18	87
6	0.05	ChCl/glycerol (1:2)	r.t.	24	75
7	0.05	ChCl/glycerol (1:2)	70	24	>99
8	0.05	ChCl/glycerol (1:2)	70	18	82

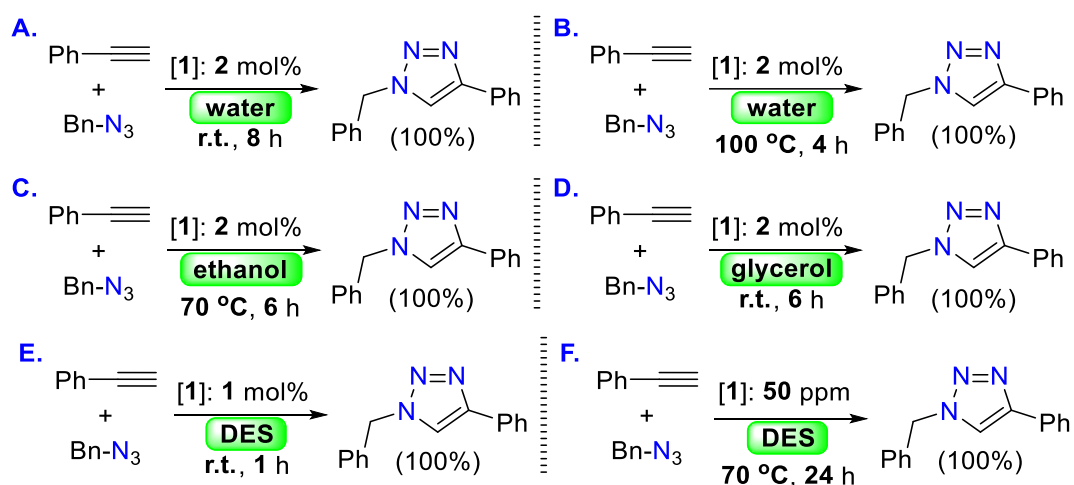
^aReactions conducted in a vial (10 mL) with 0.50 mmol of benzyl chloride, 0,50 mmol of phenyl acetylene, 1.25 mmol of sodium azide, 2 to 0.05 mol% **17** in 1 mL of ChCl/glycerol (1:2) at r.t. ^bIsolated yields of triazole product. ChCl stands for choline chloride.

Finally, we turned our attention to DES as an emerging class of green reaction medium. Although DES is very much under explored for organic transformations, it may have a high potential applicability in CuAAC reaction. Previously, few groups reported CuAAC reactions in DES as reaction media.^{66, 74, 76, 94, 95} A mixture of choline chloride and glycerol (1:2) is a commonly used DES. It is a type-III DES which does not contain metal ions with probable toxicity.⁷²⁻⁷⁶ Therefore, we choose choline chloride and glycerol mixture (1:2) as the reaction media for the following CuAAC tests (Table 3.2). We started with the previously optimized condition for water (entry 5 in **Table 1**). Using 2 mol % loading of **complex 17**, quantitative yield of triazole product **A** was obtained in 8 h at r.t. (entry 1 in Table 3.2). Complete conversion to product **A** was also obtained in 2 h (entry 1). Reducing the catalyst loading to 1

mol %, we observed quantitative yield of triazole product in just 1 h (entry 2) and this condition was considered as one of the optimized conditions using DES as reaction medium. Under identical reaction conditions, roughly 70% yield of product was obtained in half an hour (entry 3). Further reduction of catalyst loading to 0.1 mol%, full conversion of substrates to desired triazole product **A** was noted in 24 h at r.t. (entry 4). Encouraged by this result, we further reduced the catalyst loading to 50 ppm level. However, complete conversion to product (isolated yield 75%) could not be achieved in 24 h at r.t. (entry 6). Therefore, the reaction temperature was raised to 70 °C and quantitative yield was achieved in 24 h with ppm level catalyst loading (entry 7). Hence, the second optimized condition in choline chloride and glycerol mixture (1:2) is as follows: 0.05 mol% of **17**, 70 °C, 24 h (entry 7, depicted in green in **Table 3.2**).

Developing a highly efficient catalyst for an organic transformation is important; however, more importance should be given for the development of a more sustainable catalytic process for that chemical transformation as green and sustainable protocols are essential in our present era. Hence, we feel the necessity to evaluate the drawbacks and benefits of our optimized catalytic protocol for CuAAC reaction with the green credentials based on “The 12 Principles of Green Chemistry”.^{1,4-6, 96-98} To begin with, we did not use Copper(II) salt and reducing agent to generate Cu(I) active catalyst. The use of well-defined and air-stable organometallic Cu(I) catalyst for three component CuAAC reaction (in situ generated organic azides) is no doubt advantageous. We selected six previously optimized catalytic protocols for CuAAC reaction and further examined the green and sustainable aspects of those processes in various green reaction media such as water (Method A and B), ethanol (Method C), glycerol (Method D) and DES (Method E and F) (**Scheme 3.3**).

Scheme 3.3. CuAAC reaction using different optimized reaction conditions (Bn-N₃ was synthesized in situ by reacting Bn-Cl and NaN₃)



Above six catalytic protocols (Method A, B, C, D, E and F) for CuAAC reaction was evaluated with the CHEM21 green metrics toolkit which is a quantifiable extension of “The 12 Principles of Green Chemistry” (summarized in **Table 3.3**).⁵⁶ CHEM21 green metrics toolkit was previously utilized to evaluate various catalytic organic transformations.^{36, 91, 99–103} Method A to F were examined by utilizing only zero pass and first pass of CHEM21 green metrics toolkit as the second pass and third pass of CHEM21 green metrics toolkit are considered as industrial toolkits. Favourable and undesirable processes are flagged by green and red colours, respectively. Amber flag presents an acceptable process with concerns. Method A to F were analysed by various metrics starting with yield, conversion, and selectivity. All six methods gave quantitative conversions and yields in specified time with excellent selectivity and thus, all six protocols for CuAAC reaction receive green flags for yield, conversion, and selectivity. The atom economy, reaction mass efficiency and optimum efficiency for Method A to F are also good. Like most of the homogeneous catalytic process, solvents constitute most of the mass intensity for all six methods and hence, solvent is a crucial metric for the measure of sustainability. All methods from Method A to E earn green flags as the solvents used for the six processes (water, ethanol, glycerol, and DES) are green solvents. Then, the following

metrics was used one by one: catalyst, catalyst recovery, element, reactor and work-up. All methods are catalytic protocols and they receive green flags for using catalyst. Catalyst could not be recovered. In CuAAC reactions triazole product binds with Copper center and the catalyst is lost with the product. The reaction media were Copper-free and the Copper catalyst could not be recycled. Thus, using ppm level catalyst loading (in Method F) is very beneficial. All those methods earn red flags for catalyst recovery. However, recovery of reaction media was performed very easily (just filtration of product) when water was used as reaction medium (Method A and B). Similarly, reaction media were also recovered (dilution with water and filtration) in Method D (glycerol) and Method E and F (DES). The recovered reaction media in Method A, B, D, E and F were also reused. The reaction medium in Method C was ethanol in which triazole product was soluble. The product was isolated by evaporating the reaction media and thus, reaction medium could not be recovered in Method C. Copper catalyst was used in all method from A to F and hence, all methods receive amber flags for element. Copper is an earth-abundant and very cheap base metal (in earth crust and sea water). However, geopolitical issues often decide the availability of a metal worldwide. Continuous flow process is generally desirable and receives green flags. However, we performed all six CuAAC reactions in batches; therefore, amber flags were again assigned for reactors in Method A to F. Then the work-up processes were considered. Method A and B involved only filtration as a quick work-up process. Ethanol was just evaporated under vacuum in Method C. Method D, E and F involve dilution of reaction media with water followed by filtration. Therefore, we utilized very common and easy work up techniques such as filtration, evaporation, and dilution and all six methods are assigned with green flags. Thereafter, all six methods were analyzed by using energy parameters. CuAAC reactions of Method A, D and E were performed at ambient temperature (r.t.) and hence, they are favourable processes and receive green flags. Method C and F were carried out at 70 °C. The acceptable temperature range for a favourable process is

0 to 70 °C. In addition, the reaction temperature of a desirable process should be 5 °C (or more) below the boiling point of the used reaction medium. As boiling points of glycerol and used DES was much higher than 70 °C, both Method C and F were assigned with green flags (though the reactions were performed at elevated temperature). Method B was performed at 100 °C and it receive red flag indicative of an unfavourable process as the boiling point of water is also 100 °C. For Method A, B, C and D, CuAAC reactions were performed in presence of same catalyst loading (2 mol%) either at ambient temperature or elevated temperature (70 or 100 °C) in water, ethanol, and glycerol. Among these four methods, Method A is most sustainable due to the use of water at r.t. DES as a sustainable solvent was used in Method E and F. Though

Metric	Method A	Method B	Method C	Method D	Method E	Method F
Yield	100	100	100	100	100	100
Conversion	100	100	100	100	100	100
Selectivity	100	100	100	100	100	100
Atom economy	80.1	80.1	80.1	80.1	80.1	80.1
Reaction mass efficiency	60.1	60.1	60.1	60.1	60.1	60.1
Optimum efficiency	75.1	75.1	75.1	75.1	75.1	75.1
Process mass intensity	18.7	18.7	16.1	15.6	15.3	15.2
Solvent	water	water	EtOH	gly	DES	DES
Catalyst	Yes	Yes	Yes	Yes	Yes	Yes
Catalyst recovery	No	No	No	No	No	No
Media recovery	Yes	Yes	No	Yes	Yes	Yes
Element	Cu	Cu	Cu	Cu	Cu	Cu

Reactor	Batch		Batch		Batch		Batch		Batch		Batch	
Work up	Filter		Filter		Drying		Filter		Filter		Filter	
Energy	r.t.		r.t.		70 °C		r.t.		r.t.		70 °C	

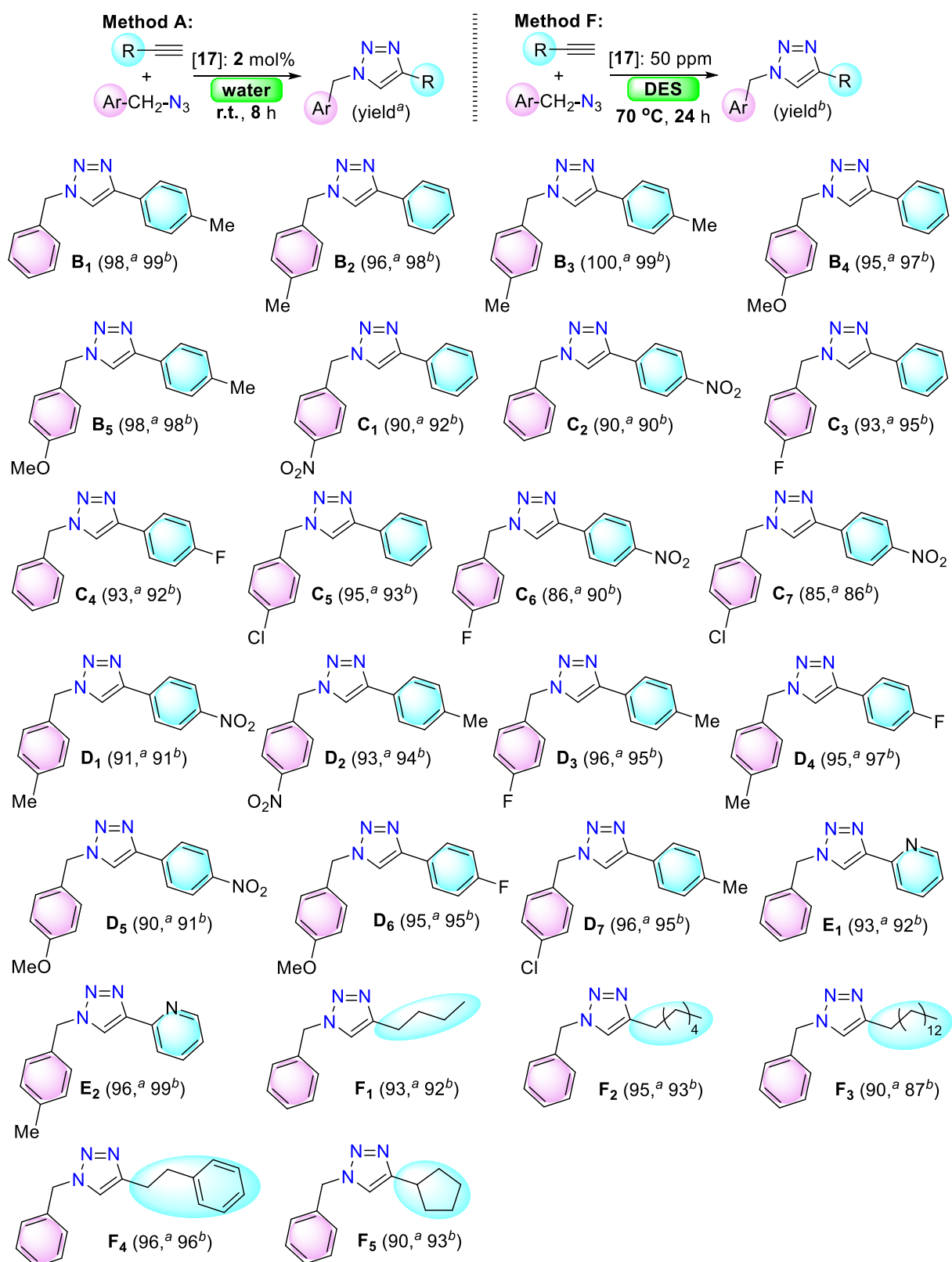
Table 3.3. Comparison of the six different methods (Method A to F) of CuAAC reaction

CuAAC reaction in Method F was performed at elevated temperature, it is still in the acceptable temperature range. In addition, ppm level catalyst loading in Method F is also attractive. Therefore, we considered Method A and F as the two most favourite processes. To establish the practical utility and robustness of these two catalytic protocols (Method A and F), gram-scale (10 mmol) reactions were successfully conducted. In addition, reaction media were successfully recovered and reused five times for Method A and F.

For the green and sustainable development, it is crucial to quantitatively evaluate the waste (leftover reactants, by-products, unrecovered catalysts, and catalyst supports, solvent losses etc.) generated in the process and thus, *E*-factor is an important parameter for sustainability.^{70, 71, 104, 105} We calculated *E*-factor of large-scale reactions for Method A (water as solvent) and F (DES as solvent) for a single run and for three consecutive runs (see ESI for details). The *E*-factor for Method A is in the range of 0.3 to 0.7. Method F involved slightly higher *E*-factor (2.4 to 2.8) as water was used for washing and it was not recovered. The overall range of *E*-factor for Method A and F is very low (0.3 to 2.8) and it is lower than the previous reports by Vaccaro et al.^{70, 71} However, Vaccaro et al. recovered the used catalyst and we failed to do so. We could recover the reaction media only. Encouraged by high catalytic activity of **complex 17**, we focused our attention in exploring various aromatic and aliphatic alkynes and organic azides (in situ generated by reacting sodium azide and corresponding organic chlorides) to expand the substrate scope (**Scheme 3.4**). Organic azides and alkynes with various arene moieties containing electron donating and electron withdrawing functionalities were tested utilized previously optimized protocols Method A and Method F (**Scheme 3.4**).

Substituted benzyl azides and aromatic alkynes with electron donating groups such as methyl and methoxy were tested and both methods (Method A and F) produced the corresponding triazoles (**B**₁, **B**₂, **B**₃, **B**₄ and **B**₅) in almost quantitative yields. Strong and weak electron withdrawing groups such as nitro, fluoro and chloro were also used and we obtain excellent isolated yields of triazole products (**C**₁, **C**₂, **C**₃, **C**₄, **C**₅, **C**₆ and **C**₇). We also combined substituted benzyl azides and aromatic alkynes with either electron donating or withdrawing groups and CuAAC reactions under both methods smoothly produced the expected triazoles (**D**₁, **D**₂, **D**₃, **D**₄, **D**₅, **D**₆ and **D**₇). We also successfully synthesized pyridyl 1,2,3-triazoles (**E**₁ and **E**₂) by using 2-ethynylpyridine. Finally, several aliphatic alkynes such as 1-hexyne, 1-octyne, 1-hexadecyne, but-3-yn-1-ylbenzene and ethynylcyclopentane were tested and the corresponding triazole products (**F**₁, **F**₂, **F**₃, **F**₄ and **F**₅) were isolated in excellent yields.

Scheme 3.4. CuAAC reactions of various alkynes with in situ generated organic azides using Method A and Method F



However, we did not explore the use of aryl azide due to their high explosive nature. Therefore, various alkynes and azides smoothly reacted to yield the expected triazole products in excellent yields irrespective of the nature of substituents. Present catalytic protocols are not limited to phenyl acetylene and benzyl azide; various electron donating and electron withdrawing groups were tolerated. Synthesized triazoles may be directly used as a monodentate or bidentate (such as triazoles **E**₁ and **E**₂ with pyridyl arm) ligands or can be served as precursors to NHCs (triazolylidenes) with electron donating and withdrawing substituents.

3.4 CONCLUSION

The facile coordination of the tridentate NNS (**L5**) and NNO ligand (**L6**) with Copper(I) halide yielded coordination polymers **17** and **18**, respectively. The pendant ether arm of NNO ligand in **18** remains uncoordinated and bromide acts as the bridging unit. In contrast, the thioether arm of NNS ligand in **17** propagate the 1D chain structure. Both **17** and **18** are air-stable and displayed efficient catalytic activities for CuAAC reactions. However, **17** displayed better catalytic activity. Using air-stable and well-defined Copper(I) complex is advantageous. The nature of solvents for the sustainable development of chemical syntheses is crucial as solvents commonly produce most of the waste. The CuAAC reactions were performed in various green and sustainable solvents such as water, ethanol, glycerol and DES. Several catalytic methods for CuAAC reaction were optimized (Method A, B, C, D, E and F). CHEM21 green metrics toolkit was utilized to analyze the advantages and setbacks of six optimized catalytic protocols (Method A, B, C, D, E and F). One of the favoured protocols (Method A) involved the reaction in water at r.t. in presence of 2 mol % of catalyst loading. However, DES proved to be a much better reaction medium. Just 1 mol % of catalyst loading gave complete conversion of substrates to desired triazole product in 1 h at r.t. (Method E). In addition, ppm level catalyst loading (50 ppm) for complete conversion was achieved in DES at 70 °C (Method F). Present robust catalytic system (Method A and F) was successfully utilized for the gram-scale synthesis

of triazole. Finally, Method A and F were successfully used to expand the substrate scope (21 additional substrates with various functionalities). The catalyst could not be recovered and the reaction media were highly recyclable. The calculated *E*-factor is very low (in the range of 0.3 to 2.8) and this reflects a process with very low waste generation. The present robust and air-stable catalytic system might be realistic for possible large-scale application.

3.5 EXPERIMENTAL SECTIONS

3.5.1 General experimental

All experiments were performed in air unless noted otherwise. Copper (I) chloride, Copper (I) bromide, phenyl acetonitrile, benzyl chloride and sodium azide were purchased from Sigma-Aldrich while other chemicals including choline chloride and glycerol were purchased from commercial suppliers. Solvents, purchased from commercial suppliers were dried prior to synthesis of Copper complexes. Copper catalysed azide alkyne cycloaddition reaction (CuAAC) were performed under aerobic condition while deep eutectic solvents were prepared inside the globe box. Deuterated solvents DMSO- d_6 and $CDCl_3$ were purchased from Sigma-Aldrich and used without further purification for recording NMR spectra. 1H and ^{13}C NMR spectra were recorded at Bruker AV-400 and 700 spectrometers (1H at 400 MHz and ^{13}C at 101 MHz). 1H NMR chemical shifts are referenced in parts per million (ppm) with respect to tetramethyl silane (δ 0.00 ppm) and $^{13}C\{^1H\}$ NMR chemical shifts are referenced in ppm with respect to DMSO- d_6 (δ 77.16 ppm) and $CDCl_3$ (δ 77.16 ppm). The coupling constants (*J*) are reported in hertz (Hz). The following abbreviations are used to describe multiplicity: bs = broad signal, s = singlet, d = doublet, t = triplet, q = quadruplet, m = multiplet. High resolution mass spectra were recorded on a Bruker microTOF-Q II Spectrometer. Elemental analysis was carried out on a EuroEA Elemental Analyser. Crystal data were collected with Rigaku Oxford diffractometer and with INCOATEC micro source (Mo- $K\alpha$ radiation, $\lambda = 0.71073 \text{ \AA}$, multilayer optics) at 100 K.

3.5.2 Synthesis of L5, L6 and Copper(I) complexes

Synthesis of L5: The ligands N-(2-(benzhydrylthio) ethyl)-1-(pyridine-2-yl) methenamine (**L5**) was prepared according to our reported procedure. ^1H NMR (400 MHz, CDCl_3) δ 8.65 (d, $J = 4.4$ Hz, 1H), 8.35 (s, 1H), 7.97 (d, $J = 7.9$ Hz, 1H), 7.75–7.71 (m, 1H), 7.44–7.42 (m, 4H), 7.33–7.27 (m, 5H), 7.24–7.19 (m, 2H), 5.26 (s, 1H), 3.83 (t, $J = 6.3$ Hz, 2H), 2.79 (t, $J = 6.9$ Hz, 2H). ^{13}C NMR (101 MHz, CDCl_3) δ 163.0, 154.3, 149.5, 141.4, 136.6, 128.6, 128.4, 127.2, 124.9, 121.5, 60.9, 54.4, 32.9. HRMS (ESI-TOF) m/z : $[\text{M}+\text{H}]^+$ Calcd. for $\text{C}_{21}\text{H}_{21}\text{N}_2\text{S}$ 333.1425; Found 333.1417. Anal. Calcd. for $\text{C}_{21}\text{H}_{20}\text{N}_2\text{S}$ (332.46): C, 75.87; H, 6.06; N, 8.34; S, 9.64. Found: C, 75.71; H, 6.03; N, 8.10; S, 9.53. FTIR ν_{max} (cm^{-1}): 2800–3100 (C–H), 1646 (CH=N), 1410–1600 (C=N, py; C=C, ph), 600–710 (C–S).

Synthesis of L6: Compound 3-(2-methoxyphenyl)-1H-pyrazole is a known compound and was synthesized using following procedure. A solution of 2-Methoxy acetophenone (1.50 g, 10.0 mmol) in a 1:1 mixture of DMF-DMA (15 mL) was reflux for 3 days under inert condition to give an orange brown solution. Removal of solvents under vacuum gave a brown oil. Thereafter, ethanol (20 mL) and hydrazine hydrate (1.28 g, 40.0 mmol) were added and the reaction mixture was refluxed for 2 hours. The resulting yellow solution was cooled to room temperature and cold water (15 mL) was added giving an off-white precipitate. The mixture was kept at 0–4 °C overnight to allow complete precipitation and the solid was collected after filtration. The solid was washed with cold water (3 x 20 mL) to give a white solid as pure product (1.67 g, 96%). ^1H NMR (CDCl_3): δ 12.50 (br, 1H), 7.73 (m, 1H), 7.69 (s, 1H), 7.09 (m, 2H), 6.67 (s, 1H), 4.02 (s, 3H). In a pressure tube, 3-(2-methoxyphenyl)-1H-pyrazole (1.74 g, 10.0 mmol), 2-(chloromethyl) pyridine hydrochloride (1.64 g, 10.0 mmol), NaOH solution (40%, 5 mL) and toluene (15 mL) were added and the reaction mixture was stirred at r.t. for 15 mins. Then tert-butylammonium hydroxide (4 mL) was added and the reaction mixture was stirred at 130 °C temperature for 24 h. The resulting red mixture was cooled down to r.t. and

extracted with ethyl acetate (3 x 50 mL). All volatiles were removed under high vacuum to give 2-((3-(2-methoxyphenyl)-1H-pyrazol-1-yl) methyl) pyridine (**L6**) as pure product (2.27 g, 73%). ¹H NMR (CDCl₃): δ 8.58 (s, 1H), 8.0 (d, *J* = 6.0 Hz, 1H), 7.6 (t, *J* = 8.0 Hz, 3H), 7.31–7.09 (m, 2H), 7.03–6.9 (m, 3H), 6.88 (s, 1H), 5.54 (s, 1H), 3.92 (s, 3H). ¹³C{¹H} NMR (CDCl₃): 155.2, 148.2, 147.3, 134.7, 130.1, 129.3, 123.4, 121.2, 122.2, 122.7, 121.7, 121.2, 113.7, 56.1, 55.2. HRMS (ESI-TOF) *m/z*: [M + H]⁺ calcd for C₁₆H₁₆N₃O 266.1293; found 266.1289. Anal. Calcd for C₁₆H₁₅N₃O (265.12): C, 72.43; H, 5.70; N, 15.84. Found: C, 72.29; H, 5.58; N, 15.67. FTIR *V*_{max} (cm⁻¹): 2800–3100 (C–H), 1504 (N–N), 1410–1600 (C=N, py; C=C, ph).

Synthesis of complex [Cu(L5)Cl]_n (**17**).

The reaction was carried out inside the glovebox. The ligand **L5** (0.083g, 0.25 mmol) was dissolved in 5 mL CH₃CN in a Schlenk tube. A suspension of CuCl (0.025 g, 0.25 mmol) in CH₃CN was then added to the ligand solution with continuous stirring. The light brown ligand solution turned into deep brown colour and the stirring was continued for 24 hours. The reaction mixture was then dried in high vacuum and the NMR of the crude solid was recorded in DMSO-d₆. The solid compound was then dissolved in CH₃CN and filtered it into a 5 mL vial. The crystallization was carried out by diffusing pure hexane solution into acetonitrile solution of the complex. Block shape light brown colour crystals suitable for X-ray crystallography were grown at the bottom of the vial after few days. Yield: (0.095 g, 88 %). ¹H NMR (700 MHz, DMSO-d₆) δ 8.74 (s, 1H), 8.42 (s, 1H), 8.17 (d, *J* = 6.9 Hz, 1H), 8.00 (d, *J* = 6.5 Hz, 1H), 7.71 (s, 1H), 7.31–7.18 (m, 10H), 5.27 (s, 1H), 3.86 (s, 2H), 2.50 (s, 2H). ¹³C NMR (176 MHz, DMSO-d₆) δ 162.8, 150.5, 149.5, 141.7, 139.0, 128.9, 128.8, 128.2, 127.7, 127.6, 58.1, 52.8, 32.8. Anal. Calcd. for C₂₁H₂₀ClCuN₂S (430.0332): C, 58.46; H, 4.67; N, 6.49; Found: C, 58.29; H, 4.48; N, 6.35. FTIR *V*_{max} (cm⁻¹): 2800–3100 (C–H), 1651 (CH=N), 1410–1610 (C=N, py; C=C, ph), 600–710 (C–S).

Synthesis of complex [Cu(L6)Br]_n (18).

The ligand **L6** (0.066 g, 0.25 mmol) was dissolved in 5 mL CH₃CN in a Schlenk tube inside the glovebox. CuBr (0.036 g, 0.25 mmol) suspension in acetonitrile was then added to the ligand solution with continuous stirring. The reaction mixture turned into yellowish colour solution and the stirring was continued for 24 hours. The reaction mixture was then dried in high vacuum and the NMR of the crude solid was recorded in DMSO-d₆. The crude solid was then dissolved in DCM and taken into a 5 mL vial. The crystallization was carried out by diffusing with diethyl ether. Block shape pale yellow crystals suitable for X-ray crystallography were grown at the bottom of the vial after two days. Yield: (0.080 g, 78 %). ¹H NMR (400 MHz, DMSO-d₆) δ 8.28 (s, 1H), 8.05 (s, 1H), 7.95 (t, *J* = 7.6 Hz, 1H), 7.64 (d, *J* = 7.5 Hz, 2H), 7.38 (s, 1H), 7.28 – 7.23 (m, 1H), 6.98 (d, *J* = 8.3 Hz, 1H), 6.77 (t, *J* = 7.4 Hz, 1H), 6.68 (s, 1H), 5.47 (s, 2H), 3.70 (s, 3H). ¹³C NMR (101 MHz, DMSO-d₆) δ 156.9, 149.9, 133.0, 130.2, 129.9, 124.8, 121.3, 112.0, 55.8, 55.3. Anal. Calcd. for C₁₆H₁₅BrCuN₃O (406.9695): C, 47.01; H, 3.70; N, 10.28; Found: C, 46.82; H, 3.57; N, 10.10. FTIR V_{max} (cm⁻¹): 2800–3100 (C–H), 1517 (N–N), 1400–1600 (C=N, py; C=C, ph).

3.5.3 Characteristic spectra of ligands and complexes

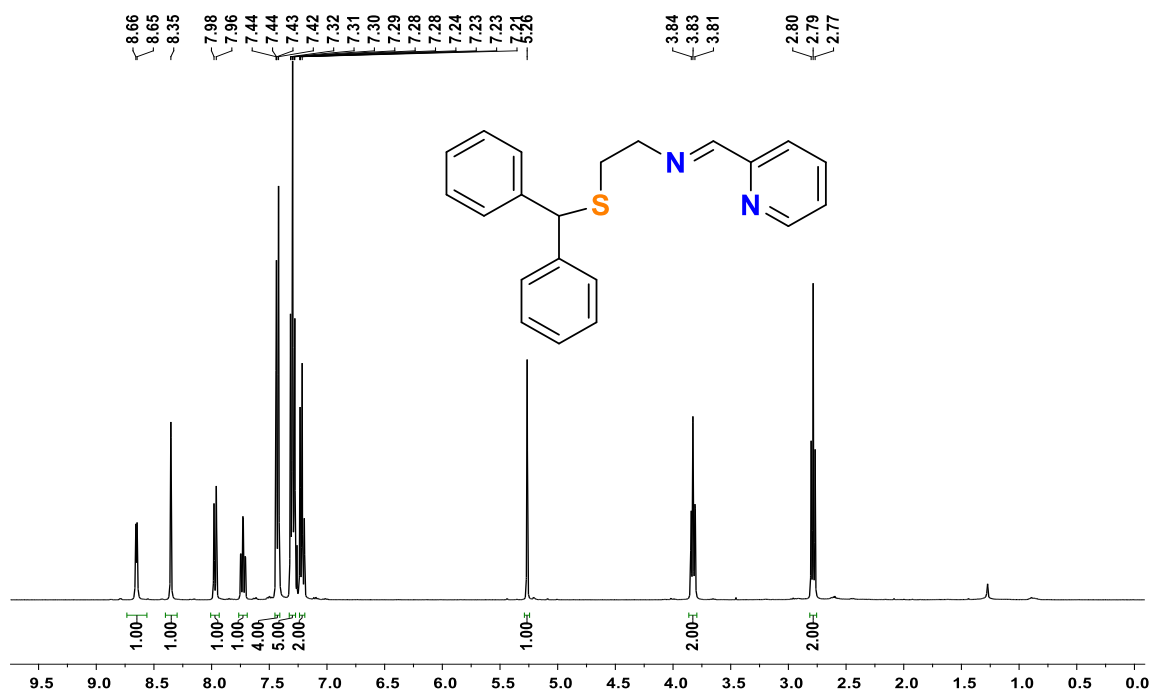


Figure 3.1: ^1H NMR of N-(2-(benzhydrylthio)ethyl)-1-(pyridine-2-yl) methanimine (L5) in CDCl_3 at r.t.

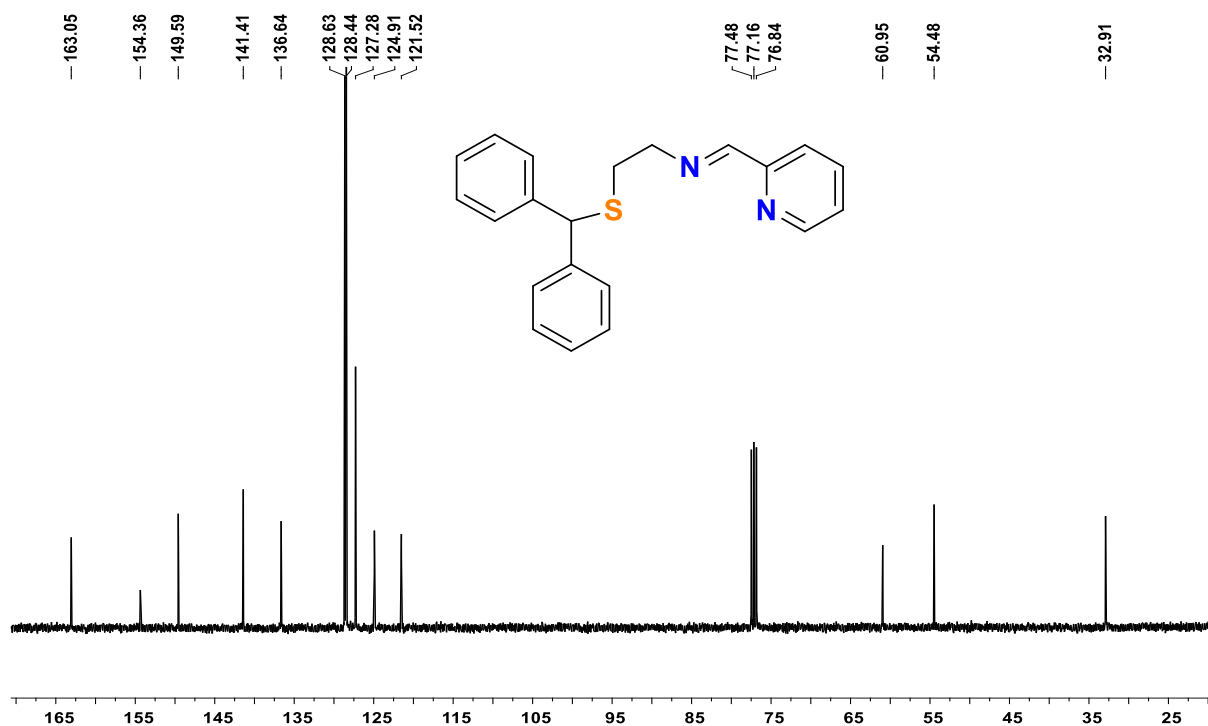


Figure 3.2: ^{13}C NMR of N-(2-(benzhydrylthio)ethyl)-1-(pyridine-2-yl) methanimine (L5) in CDCl_3 at r.t.

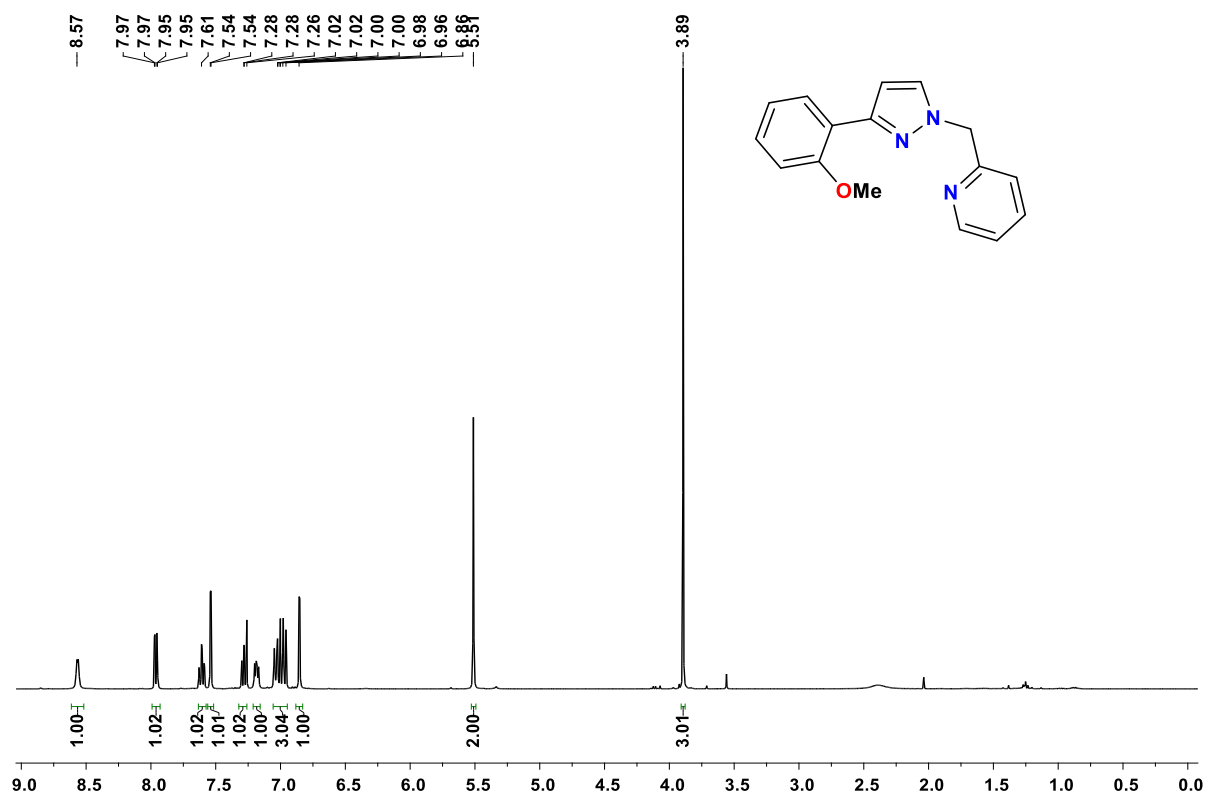


Figure 3.3. ^1H NMR of 2-((3-(2-methoxyphenyl)-1H-pyrazol-1-yl) methyl)pyridine (**L6**) in CDCl_3 at r.t.

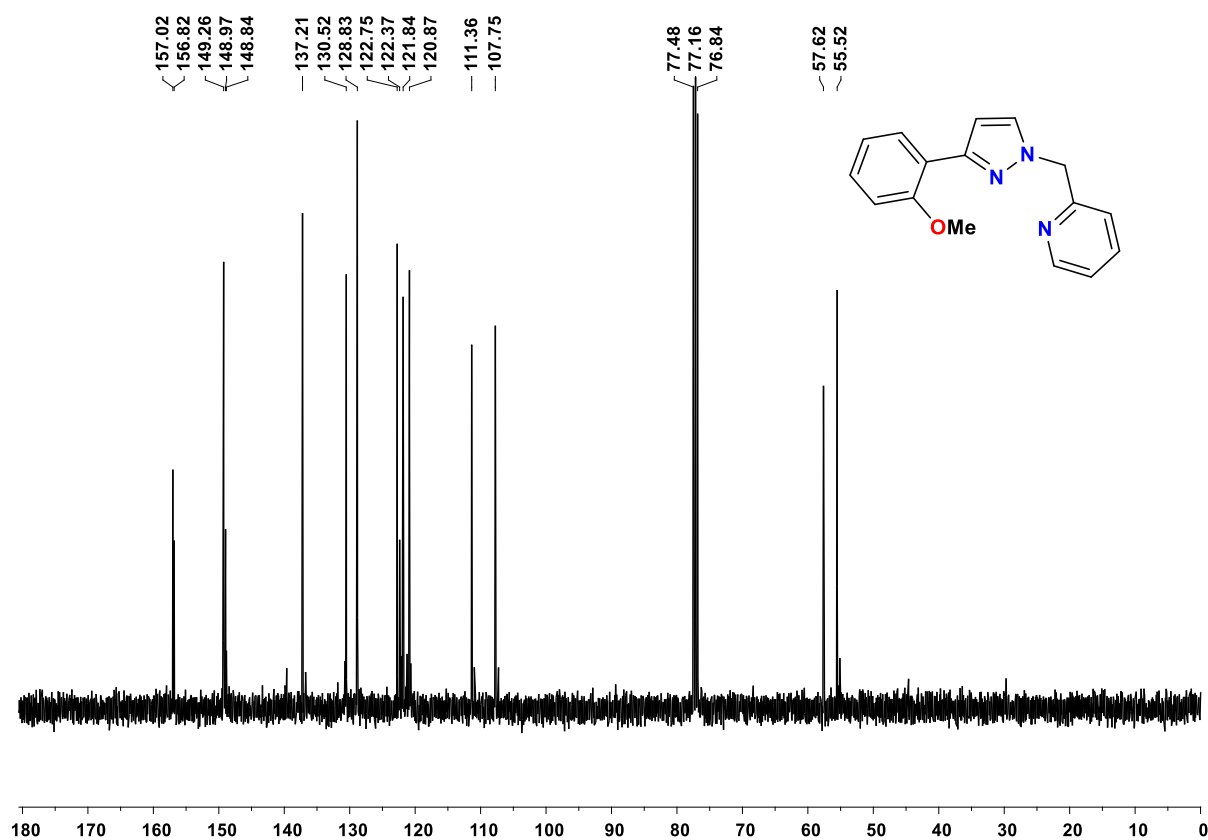


Figure 3.4. ^{13}C NMR of 2-((3-(2-methoxyphenyl)-1H-pyrazol-1-yl) methyl)pyridine (**L6**) in CDCl_3 at r.t.

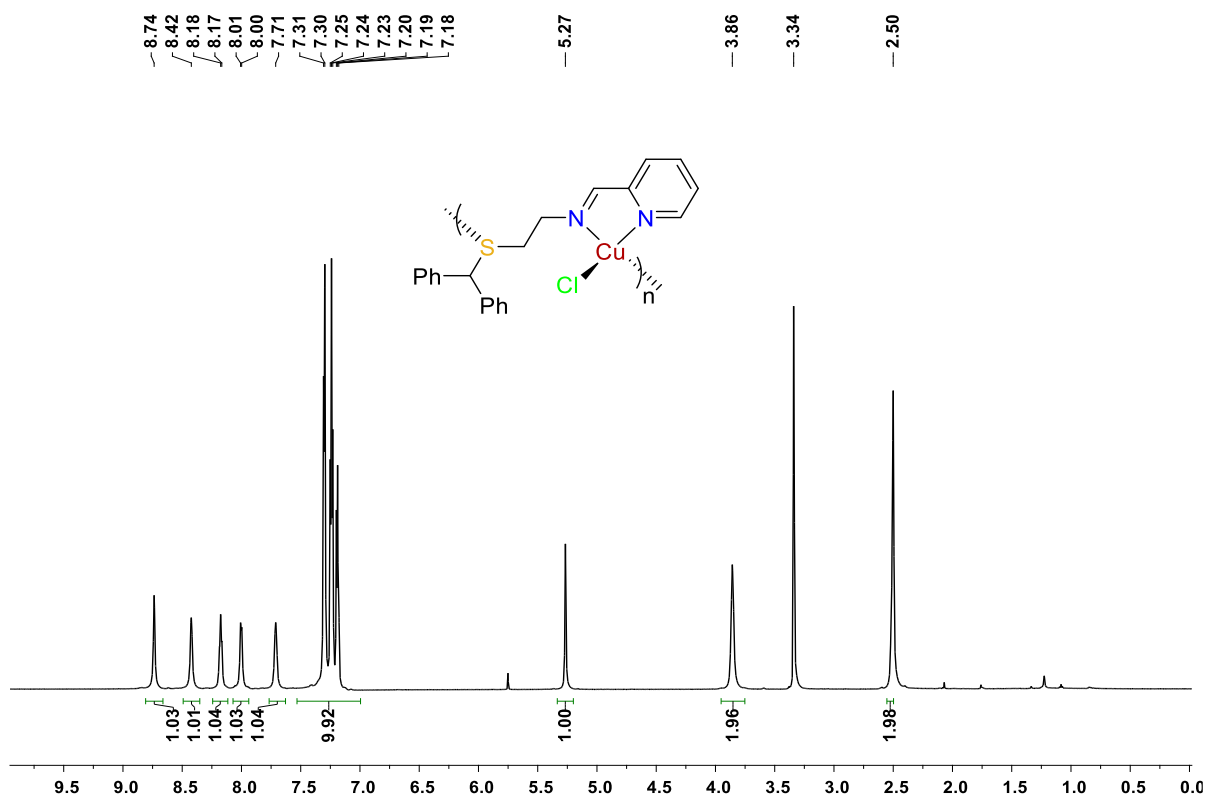


Figure 3.5: ^1H NMR of complex **17** in DMSO-d_6 .

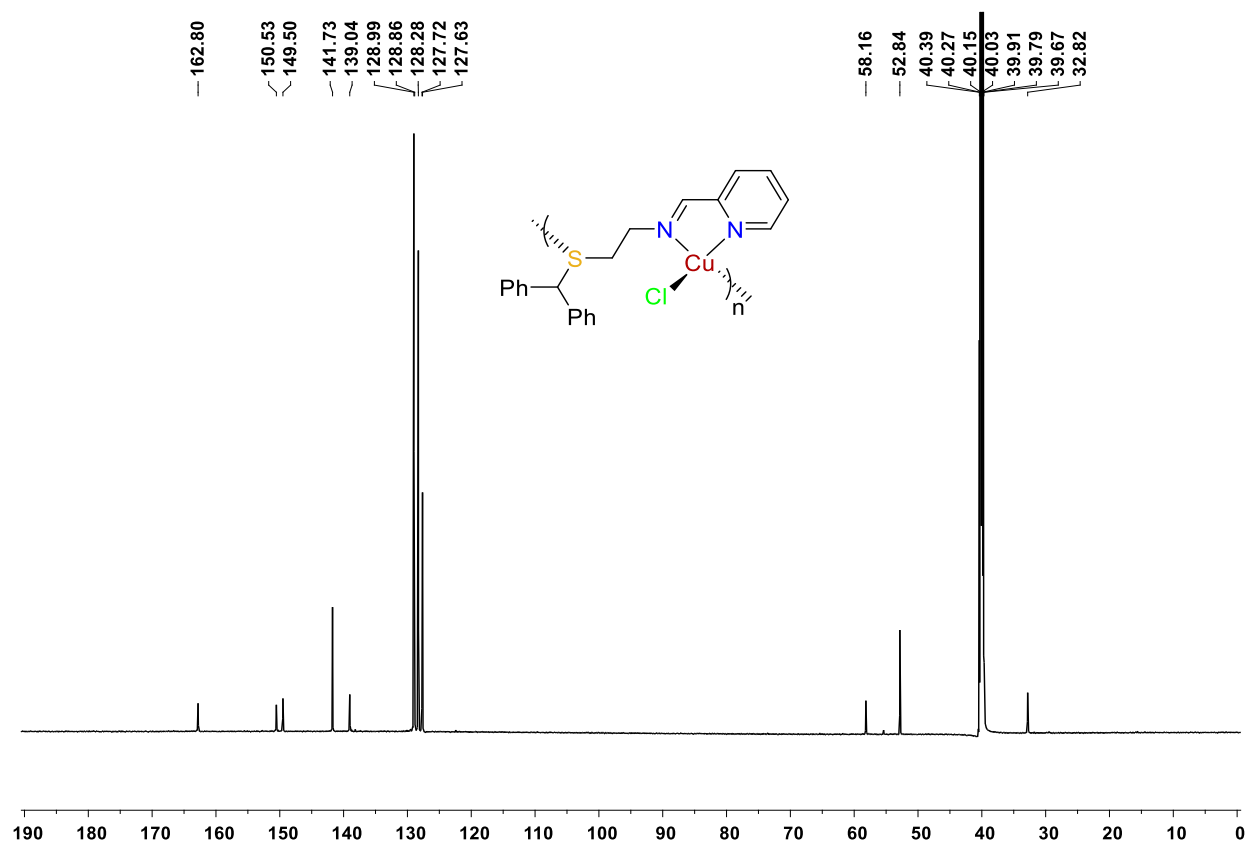


Figure 3.6: ^{13}C NMR of complex **17** in DMSO-d_6 .

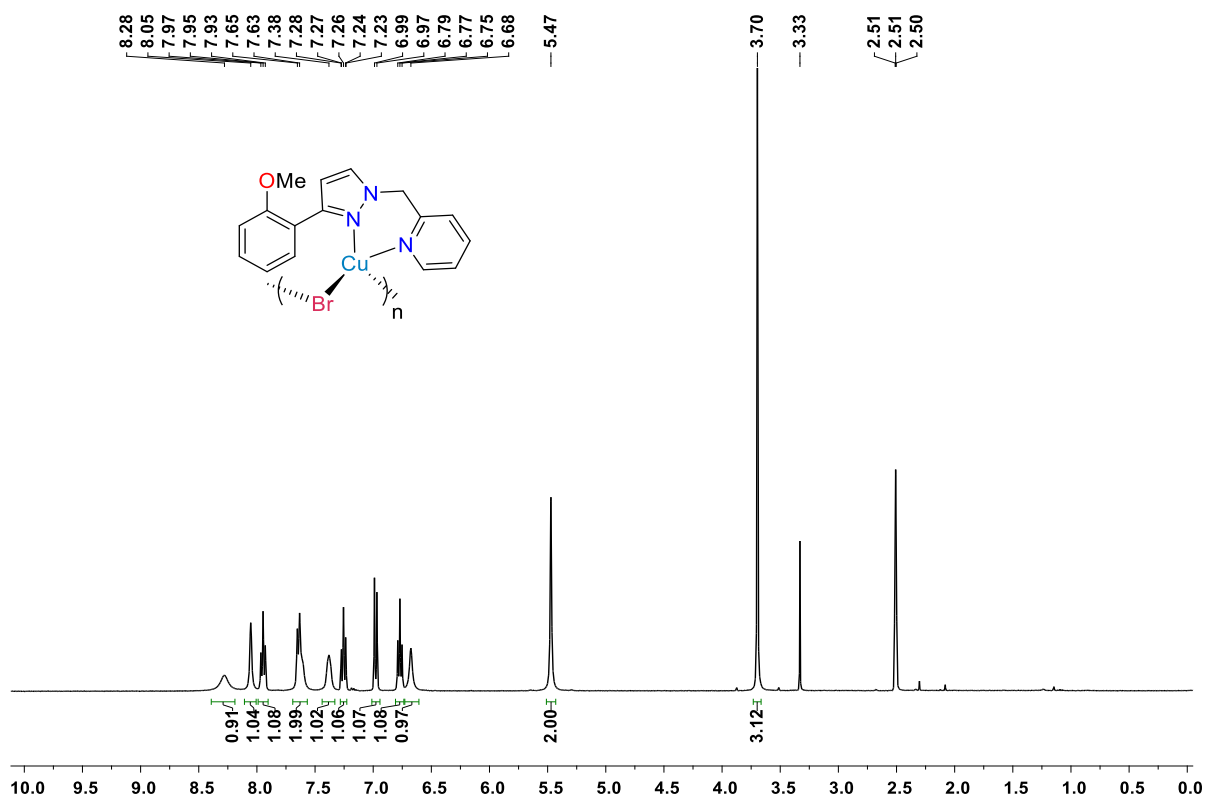


Figure 3.7: ¹H NMR of complex 18 in DMSO-d₆.

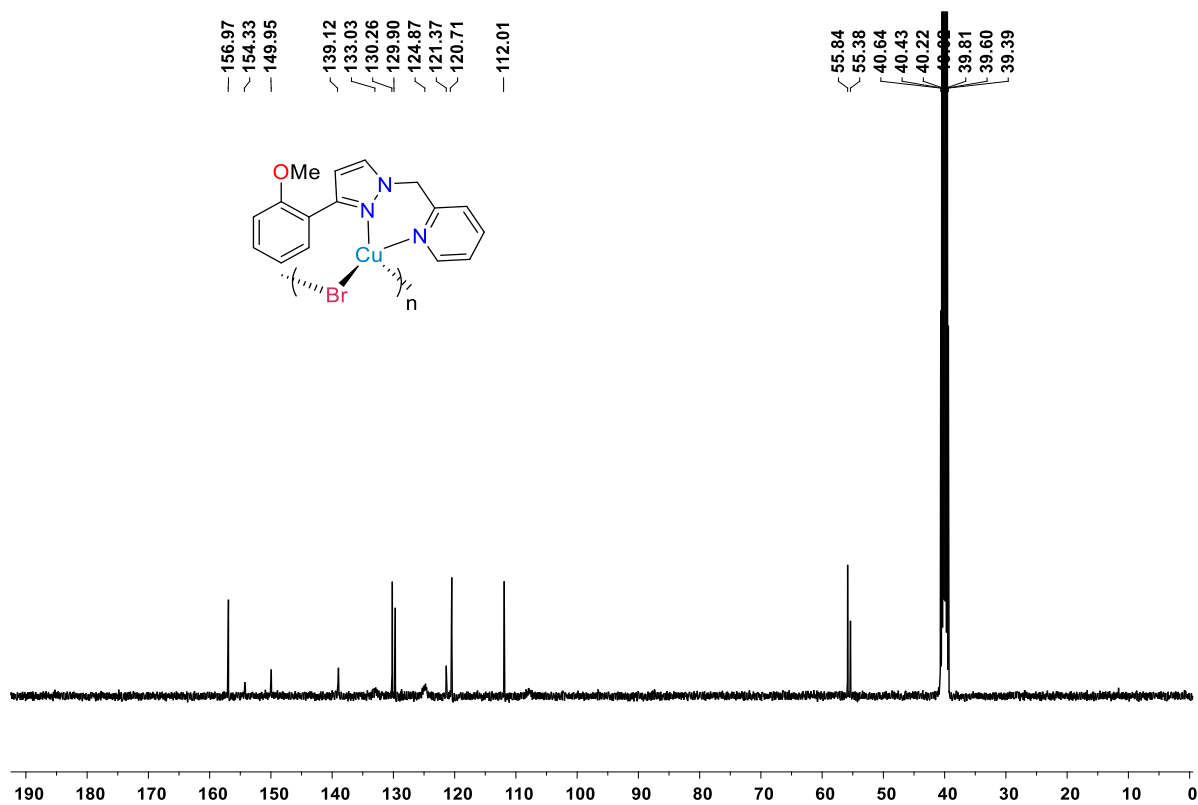


Figure 3.8: ¹³C NMR of complex 18 in DMSO-d₆.

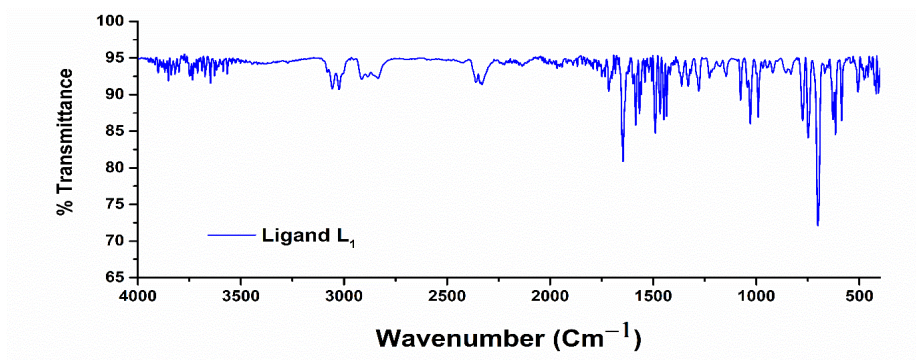


Figure 3.9: FTIR Spectrum of ligand L5.

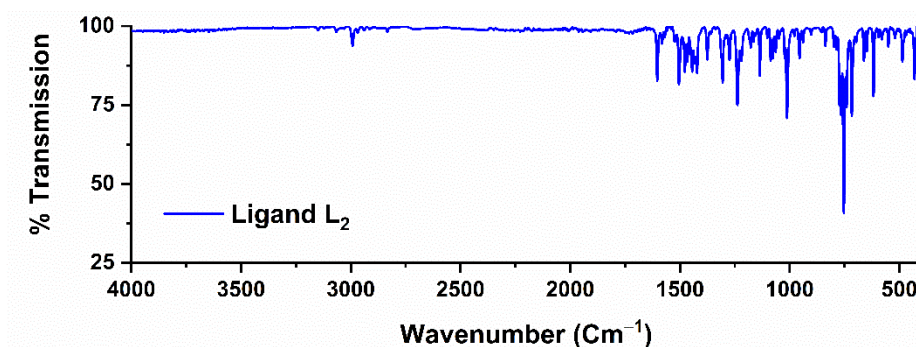


Figure 3.10: FTIR Spectrum of ligand L6.

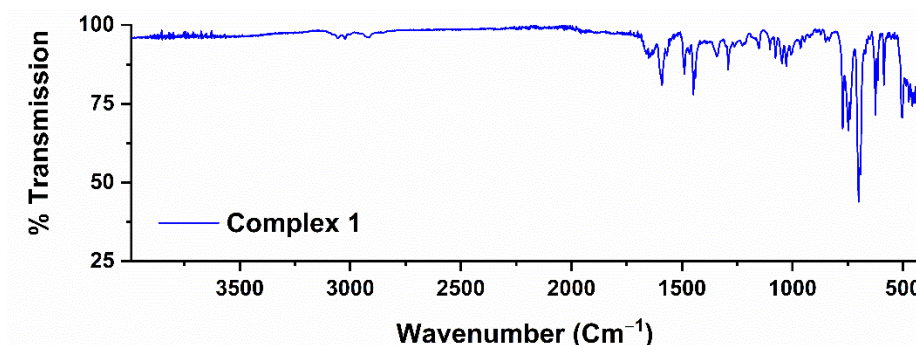


Figure 3.11: FTIR Spectrum of complex 17.

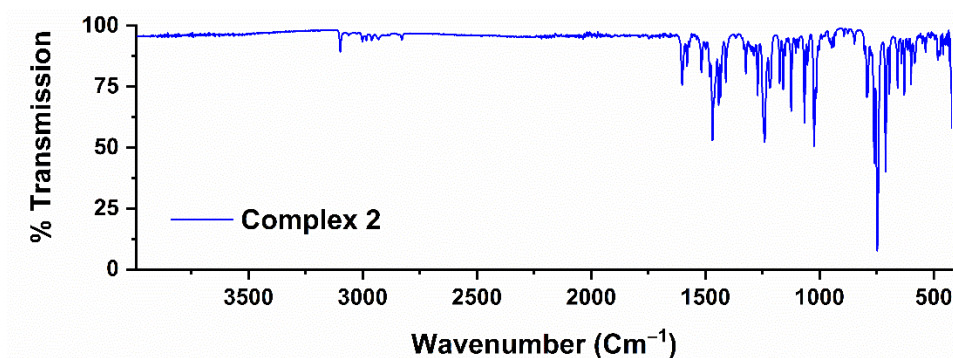


Figure 3.12: FTIR Spectrum of complex 18.

3.5.4 General experiments of CuAAC reactions in green solvents

General procedure for CuAAC reactions (for reaction optimisation). All the CuAAC reactions were performed in air. Benzyl chloride (0.6329 g, 0.5 mmol), phenyl acetylene (0.5106 g, 0.5 mmol), NaN₃ (0.0812 g, 1.25 mmol), and Copper complex **17/ 18** (2 mol %), were weighed in a vial (10 mL). Thereafter, 2 mL of water/ ethanol or 1 mL of glycerol/ DES was added to it. The resultant mixture was heated at appropriate temperature (r.t./ 70 °C/ 100 °C) for an appropriate time with stirring. Formation of solid crude was observed after the desired reaction time. The crude solid product was then filtered and washed with additional 1 mL of water. The compound was then dried under vacuum and white crude solid compound was isolated as pure form. In case of ethanol the resultant solvent mixture was dried and dissolved in ethyl acetate (2 mL) and passed through a short silica column to remove metal complex. All volatile was removed under high vacuum to give crude product. The product was dissolved in CDCl₃ and ¹H NMR spectrum was recorded.

General procedure for CuAAC reactions under different optimized catalytic protocols

For Method A: Benzyl chloride (0.6329 g, 0.5 mmol), phenyl acetylene (0.5106 g, 0.5 mmol), NaN₃ (0.0812 g, 1.25 mmol), and Copper **complex 17/ 18** (2 mol %), were weighed in a vial (10 mL). Thereafter, 2 mL of water was added to it. The resultant mixture was heated at r.t for an appropriate time with stirring. Formation of solid crude was observed after the desired reaction time. The crude solid product was then filtered and washed with additional 2 mL of water. The compound was then dried under vacuum and white crude solid compound was isolated as pure form. The product was dissolved in CDCl₃ and ¹H NMR spectrum was recorded.

For Method B: Benzyl chloride (0.6329 g, 0.5 mmol), phenyl acetylene (0.5106 g, 0.5 mmol), NaN₃ (0.0812 g, 1.25 mmol), and Copper **complex 17** (2 mol %), were weighed in a vial (10 mL). Thereafter, 2 mL of water was added to it. The resultant mixture was heated at 100 °C in

a preheated oil bath for an appropriate time with stirring. Then the mixture was cooled down to room temperature. The crude solid product was filtered and washed with additional 2 mL of water. The compound was then dried under vacuum and white crude solid compound was isolated as pure form. The product was dissolved in CDCl_3 and ^1H NMR spectrum was recorded.

For Method C: Benzyl chloride (0.6329 g, 0.5 mmol), phenyl acetylene (0.5106 g, 0.5 mmol), NaN_3 (0.0812 g, 1.25 mmol), and Copper complex 17 (2 mol%), were weighed in a vial (10 mL). Thereafter, 2 mL of ethanol was added to it. The resultant mixture was heated at 70 °C in a preheated oil bath for an appropriate time with stirring. Then the mixture was cooled down to room temperature. Thereafter, reaction solvent was dried and organic product was extracted with ethyl acetate. The organic mixture was collected and solvent was removed using rotary evaporator. The compound was then dried under vacuum and white crude solid compound was isolated as pure form. The product was dissolved in CDCl_3 and ^1H NMR spectrum was recorded.

For Method D: Benzyl chloride (0.6329 g, 0.5 mmol), phenyl acetylene (0.5106 g, 0.5 mmol), NaN_3 (0.0812 g, 1.25 mmol), and Copper **complex 17** (2 mol%), were weighed in a vial (10 mL). Thereafter, 2 mL of glycerol was added to it. The resultant mixture was stirred at r.t. for an appropriate time. Then the mixture was diluted with 1 mL of water. The crude solid product was filtered and washed with additional 1 mL of water. The compound was then dried under vacuum and white crude solid compound was isolated as pure form. The product was dissolved in CDCl_3 and ^1H NMR spectrum was recorded.

For Method E: Deep eutectic solvent, glyceline [choline chloride: glycerol (1:2)] were prepared inside the globe box in a vial. Thereafter benzyl chloride (0.6329 g, 0.5 mmol), phenyl acetylene (0.5106 g, 0.5 mmol), NaN_3 (0.0812 g, 1.25 mmol), and Copper **complex 17** (1 mol %), were weighed in the vial (10 mL) under aerobic condition. The resultant mixture was stirred

at r.t. for an appropriate time. Then the mixture was diluted with 1 mL of water. The crude solid product was filtered and washed with additional 1 mL of water. The compound was then dried under vacuum and white crude solid compound was isolated as pure form. The product was dissolved in CDCl_3 and ^1H NMR spectrum was recorded.

For Method F: Deep eutectic solvent, glyceline [choline chloride: glycerol (1:2)] were prepared inside the globe box in a vial. Thereafter benzyl chloride (1.266 g, 10 mmol), phenyl acetylene (1.021 g, 10 mmol), NaN_3 (1.625 g, 25 mmol), and Copper **complex 17** (0.05 mol %), were added to it under aerobic condition. The resultant mixture was heated at 70 °C in a preheated oil bath for an appropriate time with stirring. Then the mixture was diluted with 5 mL of water. The crude solid product was filtered and washed with additional 5 mL of water. The compound was then dried under vacuum and white crude solid compound was isolated as pure form. The product was dissolved in CDCl_3 and ^1H NMR spectrum was recorded.

General procedure for gram-scale CuAAC reactions:

Two catalytic protocols (Method A and F) were selected for gram-scale (10 mmol) CuAAC reactions. For this purpose, benzyl chloride (1.266 g, 10 mmol), phenyl acetylene (1.021 g, 10 mmol), NaN_3 (1.625 g, 25 mmol), and Copper **complex 17** (2/ 0.05 mol %), were added either in water (Method A) or in DES glyceline (Method F). In cases of method A after the desired reaction time the crude solid product was filtered and washed with additional 20 mL of water. For Method F, the mixture was diluted with 10 mL of water. Thereafter the crude solid product was filtered and washed with additional 10 mL of water. Both cases, the compound was then dried under vacuum and white crude solid compound was isolated as pure form. The product was then dissolved in CDCl_3 and ^1H NMR spectrum was recorded.

General procedure for substrate scope:

Again, the best two methods (Method A and Method F) were also utilized for the synthesis of 1,4-disubstituted 1,2,3-triazole. In this regard, derivatives of benzyl chloride (0.5 mmol), and

alkynes (0.5 mmol) were combined with sodium azide (0.0812 g, 1.25 mmol) and Copper **complex 17** (2 mol % for Method A and 0.05 mol % for Method F) in a vial (10 mL). Thereafter, solvents water (2 mL) or DES glyceline (1 mL) was added to it. The reaction mixture was stirred at optimized reaction conditions. After that, the reaction mixture was simply filtered (for Method A) or diluted with water followed by filtered and washed with water in case of Method F to get desire triazole product. Both cases, the compound was then dried under vacuum and white crude solid compound was isolated as pure form. Occasionally the crude product was purified by column chromatography using silica as stationary phase and ethyl acetate-hexane mixture (1:9) as eluent. The product was then dissolved in CDCl₃ and NMR (¹H and ¹³C) spectrum was recorded.

General procedure for the recycling of the reaction medium:

The reaction medium of methods A and F were recycled as follows:

Method A: For this purpose, reaction protocol was conducted with benzyl chloride (1.266 g, 10 mmol), phenyl acetylene (1.021 g, 10 mmol), NaN₃ (1.625 g, 25 mmol), and Copper **complex 17** (2 mol %), using 40 mL of water as reaction medium. The solid product was filtered with a Büchner funnel, washed with water (5 mL) and dried under vacuum. Thereafter, the volume of the aqueous phase was reduced to 40 mL and placed in the reaction vial equipped with a magnetic stirring bar. Benzyl chloride (1.266 g, 10 mmol), phenyl acetylene (1.021 g, 10 mmol), NaN₃ (0.650 g, 10 mmol), and Copper **complex 17** (2 mol %), were added and the reaction was stirring for 8 h at room temperature. The entire process was repeated twice. Thus, the reaction medium was recycled three times and no change in catalytic activity was observed. The triazole product **A** was obtained in 99% isolated yield in all reaction runs (1st run: 2.351 gm; 2nd run: 2.348 gm; 3rd run: 2.350 gm)

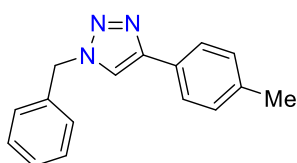
Method F: The reaction protocol was conducted with benzyl chloride (1.266 g, 10 mmol), phenyl acetylene (1.021 g, 10 mmol), NaN₃ (1.625 g, 25 mmol), and Copper **complex 17** (0.05

mol%), using 20 mL of DES glyceline as reaction medium. The product was filtered with a Büchner funnel. Additional 5 mL water was used to wash the product. Thereafter, the aqueous phase was removed under reduced pressure and the remaining DES was placed in a vial equipped with a magnetic stirring bar. Benzyl chloride (1.266 g, 10 mmol), phenyl acetylene (1.021 g, 10 mmol), NaN₃ (0.650 g, 10 mmol), and Copper **complex 17** (0.05 mol %), were added and the reaction was stirring for 24 h at 70 °C. The entire process was repeated twice. Thus, the reaction medium was recycled three times and no change in catalytic activity was observed. The triazole product **A** was obtained in 99% isolated yield in all reaction runs (1st run: 2.351 gm; 2nd run: 2.349 gm; 3rd run: 2.48 gm)

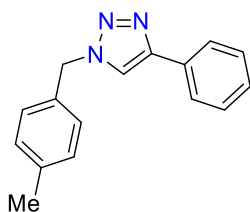
3.5.5 NMR data of the Products:



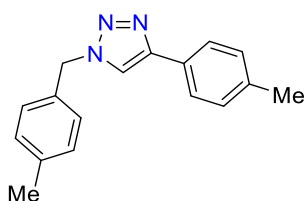
1-benzyl-4-phenyl-1H-1,2,3-triazole (A): Isolated as white solid (Method A: 115 mg, 98%; Method F: 116 mg, 99%). ¹H NMR (400 MHz, CDCl₃) δ 7.83 – 7.75 (m, 2H), 7.68 (s, 1H), 7.43 – 7.33 (m, 5H), 7.33 – 7.25 (m, 3H), 5.53 (s, 2H). ¹³C NMR (101 MHz, CDCl₃) δ 148.1, 134.7, 130.5, 129.1, 128.8, 128.7, 128.1, 128.0, 125.7, 119.6, 54.1.



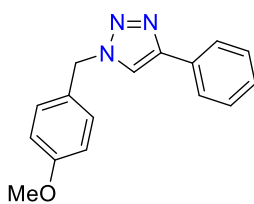
1-benzyl-4-(p-tolyl)-1H-1,2,3-triazole (B₁): Isolated as white solid (Method A: 122 mg, 98%; Method F: 123 mg, 92%). ¹H NMR (400 MHz, CDCl₃) δ 8.18 (d, *J* = 8.7 Hz, 2H), 7.74 (s, 1H), 7.68 (d, *J* = 8.1 Hz, 2H), 7.41 (d, *J* = 8.8 Hz, 2H), 7.20 (d, *J* = 7.9 Hz, 2H), 5.66 (s, 2H), 2.35 (s, 3H). ¹³C NMR (101 MHz, CDCl₃) δ 148.7, 148.0, 141.9, 138.4, 129.6, 128.6, 127.3, 125.7, 124.3, 119.6, 53.1, 21.3.



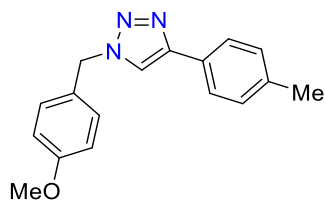
1-(4-(methylbenzyl)-4-phenyl-1H-1,2,3-triazole (B₂): Isolated as white solid (Method A: 119 mg, 96%; Method F: 122 mg, 98%). ¹H NMR (700 MHz, CDCl₃) δ 7.51 (d, *J* = 8.1 Hz, 2H), 7.45 (s, 1H), 7.17 (d, *J* = 8.4 Hz, 2H), 7.05 (dd, *J* = 18.3, 8.2 Hz, 4H), 5.35 (s, 2H), 2.19 (s, 3H). ¹³C NMR (176 MHz, CDCl₃) δ 148.6, 138.2, 134.9, 133.3, 129.6, 129.4, 129.4, 127.6, 125.7, 119.2, 31.9, 53.5, 21.4.



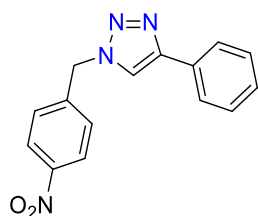
1-(4-(methylbenzyl)-4-(p-tolyl)-1H-1,2,3-triazole (B₃): Isolated as white solid (Method A: 131 mg, 100%; Method F: 130 mg, 92%). ¹H NMR (700 MHz, CDCl₃) δ 7.68 (d, *J* = 8.1 Hz, 2H), 7.59 (s, 1H), 7.20 (q, *J* = 7.9 Hz, 6H), 5.51 (s, 2H), 2.36 (s, 6H). ¹³C NMR (176 MHz, CDCl₃) δ 148.3, 138.8, 138.0, 131.8, 129.9, 129.5, 128.2, 127.8, 125.7, 119.1, 54.1, 21.3.



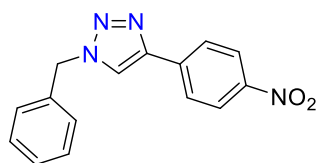
1-(4-methoxybenzyl)-4-phenyl-1H-1,2,3-triazole (B₄): Isolated as white solid (Method A: 126 mg, 95%; Method F: 129 mg, 97%). ¹H NMR (400 MHz, CDCl₃) δ 7.82 – 7.77 (m, 2H), 7.68 (s, 1H), 7.39 (t, *J* = 7.5 Hz, 2H), 7.33 – 7.27 (m, 2H), 6.89 (dd, *J* = 8.4, 2.6 Hz, 2H), 6.84 – 6.81 (m, 1H), 5.53 (s, 2H), 3.78 (s, 3H). ¹³C NMR (101 MHz, CDCl₃) δ 160.2, 136.2, 132.5, 130.6, 130.3, 128.9, 128.2, 125.8, 120.3, 114.3, 113.7, 55.4, 54.2.



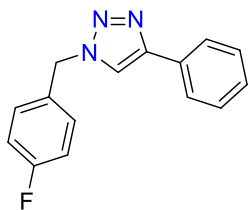
1-(4-methoxybenzyl)-4-p-tolyl-1H-1,2,3-triazole (B5): Isolated as white solid (Method A: 137 mg, 98%; Method F: 137 mg, 98%). ^1H NMR (400 MHz, CDCl_3) δ 7.60 (d, $J = 8.1$ Hz, 2H), 7.55 (s, 1H), 7.20 (dd, $J = 13.8, 5.8$ Hz, 1H), 7.12 (d, $J = 7.9$ Hz, 2H), 6.80 (dd, $J = 8.4, 2.5$ Hz, 2H), 6.76 – 6.73 (m, 1H), 5.43 (s, 2H), 3.69 (s, 3H), 2.27 (s, 3H). ^{13}C NMR (101 MHz, CDCl_3) δ 160.2, 148.3, 138.1, 136.2, 130.3, 129.5, 127.7, 125.7, 120.3, 119.3, 114.3, 113.7, 55.4, 54.2, 21.3.



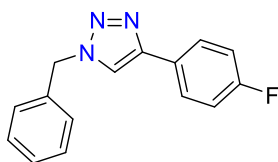
1-(4-nitrobenzyl)-4-phenyl-1H-1,2,3-triazole (C1): Isolated as light brown solid (Method A: 126 mg, 90%; Method F: 128 mg, 92%). ^1H NMR (400 MHz, CDCl_3) δ 8.28 – 8.21 (m, 2H), 7.99 – 7.92 (m, 2H), 7.81 (s, 1H), 7.42 – 7.38 (m, 3H), 7.35 – 7.31 (m, 2H), 5.61 (s, 2H). ^{13}C NMR (176 MHz, CDCl_3) δ 148.9, 148.2, 141.8, 130.2, 129.0, 128.7, 128.6, 125.9, 124.5, 119.8, 53.3.



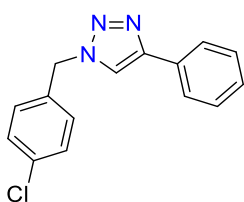
1-benzyl-4-(4-nitrophenyl)-1H-1,2,3-triazole (C2): Isolated as light brown solid (Method A: 126 mg, 90%; Method F: 126 mg, 90%). ^1H NMR (400 MHz, CDCl_3) δ 8.28 – 8.21 (m, 2H), 7.96 (d, $J = 8.9$ Hz, 2H), 7.80 (s, 1H), 7.40 (t, $J = 5.2$ Hz, 3H), 7.36 – 7.30 (m, 2H), 5.61 (s, 2H). ^{13}C NMR (101 MHz, CDCl_3) δ 147.4, 146.1, 136.9, 134.2, 129.4, 129.2, 128.3, 126.2, 124.4, 121.0, 54.6.



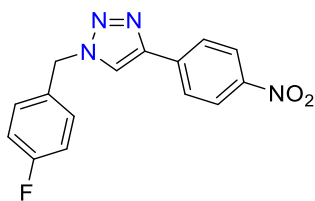
1-(4-fluorobenzyl)-4-phenyl-1H-1,2,3-triazole (C₃): Isolated as colour less solid (Method A: 118 mg, 93%; Method F: 120 mg, 95%). ¹H NMR (400 MHz, CDCl₃) δ 8.28 – 8.21 (m, 2H), 7.96 (d, *J* = 8.9 Hz, 2H), 7.80 (s, 1H), 7.40 (t, *J* = 5.2 Hz, 3H), 7.36 – 7.30 (m, 2H), 5.61 (s, 2H). ¹³C NMR (101 MHz, CDCl₃) δ 164.1, 161.6, 148.3, 132.5, 130.7, 129.9, 128.8, 128.5, 125.7, 119.5, 116.2, 116.0, 53.4.



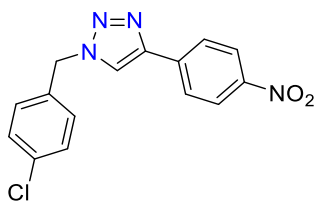
1-benzyl-4-(4-fluorophenyl)-1H-1,2,3-triazole (C₄): Isolated as off-white solid (Method A: 118 mg, 93%; Method F: 116 mg, 92%). ¹H NMR (700 MHz, CDCl₃) δ 7.79 (d, *J* = 7.6 Hz, 2H), 7.68 (s, 1H), 7.39 (t, *J* = 7.6 Hz, 2H), 7.33 (t, *J* = 8.3 Hz, 3H), 7.22 (d, *J* = 8.3 Hz, 2H), 5.51 (s, 2H). ¹³C NMR (101 MHz, CDCl₃) δ 163.9, 161.5, 147.4, 134.6, 129.2, 128.9, 128.1, 127.5, 127.4, 126.8, 126.8, 119.4, 115.9, 115.7, 54.3



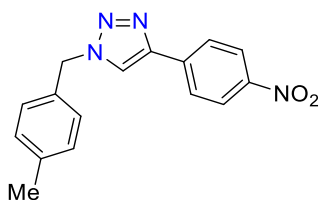
1-(4-chlorobenzyl)-4-phenyl-1H-1,2,3-triazole (C₅): Isolated as white solid (Method A: 128mg, 95%; Method F: 125 mg, 93%). ¹H NMR (400 MHz, CDCl₃) δ 7.76 (dd, *J* = 8.2, 5.4 Hz, 2H), 7.64 (s, 1H), 7.37 (d, *J* = 6.4 Hz, 3H), 7.30 (d, *J* = 7.4 Hz, 2H), 7.07 (t, *J* = 8.5 Hz, 2H), 5.55 (s, 2H). ¹³C NMR (101 MHz, CDCl₃) δ 148.4, 134.9, 133.3, 130.4, 129.4, 129.4, 128.9, 128.3, 125.8, 119.6, 53.5.



1-(4-fluorobenzyl)-4-(4-nitrophenyl)-1H-1,2,3-triazole (C₆): Isolated as white solid (Method A: 128 mg, 86%; Method F: 135 mg, 92%). ¹H NMR (700 MHz, CDCl₃) δ 7.79 (d, *J* = 7.6 Hz, 2H), 7.68 (s, 1H), 7.39 (t, *J* = 7.6 Hz, 2H), 7.33 (t, *J* = 8.3 Hz, 3H), 7.22 (d, *J* = 8.3 Hz, 2H), 5.51 (s, 2H). ¹³C NMR (176 MHz, CDCl₃) δ 163.8, 162.4, 147.4, 146.2, 136.7, 130.2, 130.2, 126.2, 124.4, 121.0, 116.5, 116.3, 53.8. HRMS (ESI-TOF) *m/z*: [M + H]⁺ calcd for C₁₅H₁₂FN₄O₂ 299.0944; Found 299.0944.

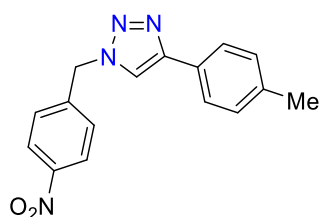


1-(4-chlorobenzyl)-4-(4-nitrophenyl)-1H-1,2,3-triazole (C₇): Isolated as white solid (Method A: 134 mg, 85%; Method F: 135 mg, 86%). ¹H NMR (400 MHz, CDCl₃) δ 7.81 – 7.76 (m, 2H), 7.67 (s, 1H), 7.39 (dd, *J* = 8.1, 6.8 Hz, 2H), 7.36–7.29 (m, 3H), 7.23 (d, *J* = 8.5 Hz, 2H), 5.52 (s, 2H). ¹³C NMR (101 MHz, CDCl₃) δ 148.4, 134.9, 133.3, 130.4, 129.4, 129.4, 128.9, 128.3, 125.8, 119.6, 53.5. HRMS (ESI-TOF) *m/z*: [M + H]⁺ calcd for C₁₅H₁₂ClN₄O₂ 315.0649; Found 315.0649.

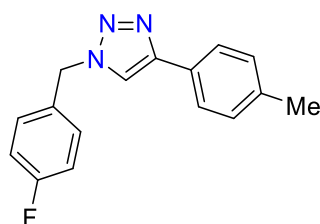


1-(4-methylbenzyl)-4-(4-nitrophenyl)-1H-1,2,3-triazole (D₁): Isolated as white solid (Method A: 134 mg, 91%; Method F: 134 mg, 91%). ¹H NMR (400 MHz, CDCl₃) δ 8.17 (d, *J* = 8.8 Hz, 2H), 7.89 (d, *J* = 8.8 Hz, 2H), 7.72 (s, 1H), 7.16 (d, *J* = 2.6 Hz, 4H), 5.49 (s, 2H), 2.30 (s, 3H). ¹³C NMR (101 MHz, CDCl₃) δ 147.4, 146.0, 139.2, 136.9, 131.2, 130.0, 128.4, 126.2, 124.3,

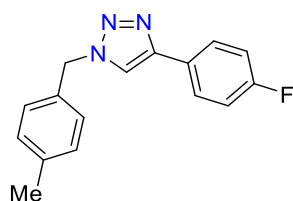
121.0, 54.4, 21.3. HRMS (ESI-TOF) m/z : $[M + H]^+$ calcd for $C_{15}H_{12}FN_4O_2$ 299.0944; Found 299.0944.



1-(4-nitrobenzyl)-4-(p-tolyl)-1H-1,2,3-triazole(D₂): Isolated as white solid (Method A: 136 mg, 93%; Method F: 138 mg, 94%). 1H NMR (400 MHz, $CDCl_3$) δ 8.20 (d, $J = 8.7$ Hz, 2H), 7.74 – 7.65 (m, 3H), 7.42 (d, $J = 8.7$ Hz, 2H), 7.21 (d, $J = 8.0$ Hz, 2H), 5.67 (s, 2H), 2.36 (s, 3H). ^{13}C NMR (101 MHz, $CDCl_3$) δ 148.8, 148.1, 141.9, 138.5, 129.6, 128.6, 127.3, 125.7, 124.4, 119.5, 53.2, 21.3.

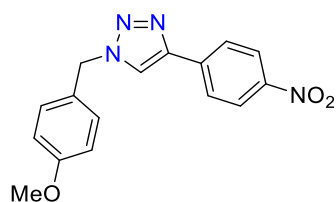


1-(4-fluorobenzyl)-4-(p-tolyl)-1H-1,2,3-triazole(D₃): Isolated as light brown solid (Method A: 128 mg, 96%; Method F: 127 mg, 95%). 1H NMR (400 MHz, $CDCl_3$) δ 7.69 – 7.47 (m, 3H), 7.19 (s, 2H), 7.11 (d, $J = 7.1$ Hz, 2H), 6.96 (s, 2H), 5.42 (s, 2H), 2.27 (s, 3H). ^{13}C NMR (101 MHz, $CDCl_3$) δ 164.1, 161.6, 148.4, 138.1, 132.4, 130.7, 130.7, 130.0, 129.9, 129.5, 129.3, 127.6, 125.6, 119.2, 116.2, 116.0, 53.4, 21.3.

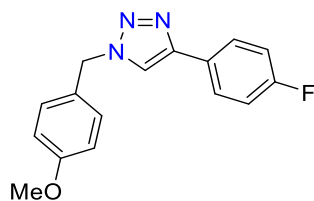


4-(4-fluorophenyl)-1-(4-methylbenzyl)-1H-1,2,3-triazole (D₄): Isolated as Light brown solid (Method A: 127 mg, 95%; Method F: 130 mg, 97%). 1H NMR (400 MHz, $CDCl_3$) δ 7.75 (dd, $J = 8.6, 5.4$ Hz, 2H), 7.60 (s, 1H), 7.20 (d, $J = 1.5$ Hz, 4H), 7.07 (t, $J = 8.6$ Hz, 2H), 5.51 (s,

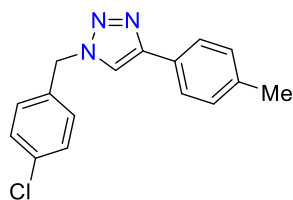
2H), 2.35 (s, 3H). ^{13}C NMR (101 MHz, CDCl_3) δ 163.9, 161.5, 147.3, 138.9, 134.6, 134.6, 131.6, 129.9, 128.2, 127.5, 127.4, 126.9, 126.8, 119.3, 115.9, 115.7, 54.1, 21.2.



1-(4-methoxybenzyl)-4-(4-nitrophenyl)-1H-1,2,3-triazole(D₅): Isolated as white solid (Method A: 140 mg, 90%; Method F: 141 mg, 91%). ^1H NMR (400 MHz, CDCl_3) δ 8.26 (d, $J = 8.9$ Hz, 2H), 7.97 (d, $J = 8.9$ Hz, 2H), 7.81 (s, 1H), 7.33 (t, $J = 7.9$ Hz, 1H), 6.92 (dd, $J = 8.3$, 2.6 Hz, 2H), 6.86 (d, $J = 1.8$ Hz, 1H), 5.57 (s, 2H), 3.80 (s, 3H). ^{13}C NMR (101 MHz, CDCl_3) δ 160.3, 147.7, 136.9, 135.7, 130.5, 126.2, 124.4, 121.1, 120.5, 114.4, 114.1, 55.5, 54.5.

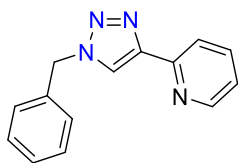


4-(4-fluorophenyl)-1-(4-methoxybenzyl)-1H-1,2,3-triazole(D₆): Isolated as a white solid (Method A: 135 mg, 95%; Method F: 135 mg, 95%). ^1H NMR (400 MHz, CDCl_3) δ 7.81 – 7.71 (m, 2H), 7.63 (s, 1H), 7.33 – 7.27 (m, 1H), 7.09 (t, $J = 8.7$ Hz, 2H), 6.95 – 6.86 (m, 2H), 6.84 (d, $J = 1.9$ Hz, 1H), 5.53 (s, 2H), 3.79 (s, 3H). ^{13}C NMR (101 MHz, CDCl_3) δ 160.3, 136.1, 130.4, 127.6, 127.5, 120.4, 116.0, 115.8, 114.3, 113.8, 55.4, 54.3.

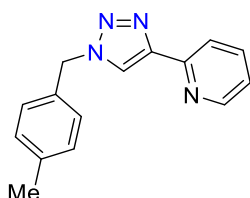


1-(4-chlorobenzyl)-4-(p-tolyl)-1H-1,2,3-triazole (D₇): Isolated as off-white solid (Method A: 136 mg, 96%; Method F: 135 mg, 95%). ^1H NMR (400 MHz, CDCl_3) δ 7.79 (dd, $J = 5.2$, 3.3 Hz, 2H), 7.63 (s, 1H), 7.39 (t, $J = 7.5$ Hz, 2H), 7.33 – 7.28 (m, 1H), 7.20 (d, $J = 2.1$ Hz, 3H),

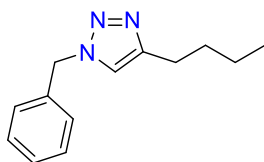
5.52 (s, 2H), 2.36 (s, 3H). ^{13}C NMR (101 MHz, CDCl_3) δ 148.2, 138.8, 131.7, 130.7, 129.9, 128.9, 128.2, 125.8, 119.5, 54.1, 21.2.



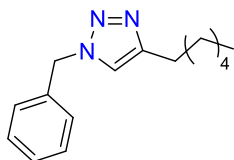
2-(1-benzyl-1H-1,2,3-triazol-4-yl)pyridine (E₁): Isolated as white solid (Method A: 110 mg, 93%; Method F: 109 mg, 92%). ^1H NMR (700 MHz, CDCl_3) δ 8.52 (d, $J = 4.6$ Hz, 1H), 8.16 (d, $J = 7.9$ Hz, 1H), 8.06 (s, 1H), 7.75 (td, $J = 7.8, 1.6$ Hz, 1H), 7.38 – 7.33 (m, 3H), 7.33 – 7.28 (m, 2H), 7.19 (dd, $J = 7.0, 5.1$ Hz, 1H), 5.57 (s, 2H). ^{13}C NMR (176 MHz, CDCl_3) δ 150.2, 149.3, 148.7, 137.0, 134.4, 129.2, 128.9, 128.4, 123.0, 122.0, 120.3, 54.5.



2-(1-(4-methylbenzyl)-1H-1,2,3-triazol-4-yl)pyridine (E₂): Isolated as white solid (Method A: 120 mg, 96%; Method F: 124 mg, 99%). ^1H NMR (700 MHz, CDCl_3) δ 8.50 (d, $J = 4.5$ Hz, 1H), 8.14 (d, $J = 8.0$ Hz, 1H), 8.03 (s, 1H), 7.72 (d, $J = 1.5$ Hz, 1H), 7.16 (dd, $J = 38.0, 8.0$ Hz, 5H), 5.49 (s, 2H), 2.30 (s, 3H). ^{13}C NMR (176 MHz, CDCl_3) δ 150.2, 149.2, 148.5, 138.7, 137.0, 131.3, 129.8, 128.3, 122.8, 121.9, 120.2, 54.1, 21.1.



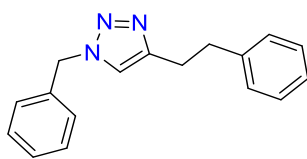
1-benzyl-4-butyl-1H-1,2,3-triazole (F₁): Isolated as off white solid (Method A: 110 mg, 93%; Method F: 108 mg, 92%). ^1H NMR (400 MHz, CDCl_3) δ 7.32 (q, $J = 5.3$ Hz, 3H), 7.21 (dd, $J = 10.4, 4.6$ Hz, 3H), 5.44 (s, 2H), 2.65 (t, $J = 7.7$ Hz, 2H), 1.65 – 1.52 (m, 2H), 1.32 (dd, $J = 14.9, 7.4$ Hz, 2H), 0.88 (t, $J = 7.3$ Hz, 3H). ^{13}C NMR (101 MHz, CDCl_3) δ 148.9, 135.0, 128.9, 128.5, 127.9, 120.6, 53.9, 31.4, 25.3, 22.2, 13.7.



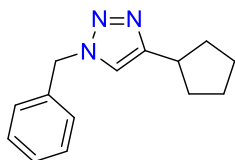
1-benzyl-4-hexyl-1H-1,2,3-triazole(F₂): Isolated as brown solid (Method A: 116 mg, 95%; Method F: 113.5 mg, 93%). ¹H NMR (700 MHz, CDCl₃) δ 7.32 (dd, *J* = 15.9, 8.5 Hz, 3H), 7.21 (d, *J* = 7.3 Hz, 2H), 7.18 (s, 1H), 5.45 (s, 2H), 2.65 (t, *J* = 7.7 Hz, 2H), 1.66 – 1.55 (m, 2H), 1.36 – 1.28 (m, 2H), 1.25 (d, *J* = 6.4 Hz, 4H), 0.83 (t, *J* = 6.5 Hz, 3H). ¹³C NMR (176 MHz, CDCl₃) δ 149.0, 135.0, 129.0, 128.5, 127.9, 120.6, 53.9, 31.5, 29.3, 28.8, 25.7, 22.5, 14.0.



1-benzyl-4-tetradecyl-1H-1,2,3-triazole(F₃): Isolated as brown solid (Method A: 161 mg, 90%; Method F: 156 mg, 87%). ¹H NMR (700 MHz, CDCl₃) δ 7.34 (t, *J* = 8.9 Hz, 3H), 7.24 (d, *J* = 7.2 Hz, 2H), 7.18 (s, 1H), 5.47 (s, 2H), 2.67 (t, *J* = 7.7 Hz, 2H), 1.67 – 1.57 (m, 2H), 1.31 – 1.19 (m, 22H), 0.87 (t, *J* = 7.0 Hz, 3H). ¹³C NMR (176 MHz, CDCl₃) δ 149.14, 135.1, 129.1, 128.6, 128.0, 120.6, 54.0, 32.0, 29.7, 29.7, 29.7, 29.7, 29.7, 29.6, 29.5, 29.4, 29.3, 25.8, 22.7, 14.2. HRMS (ESI-TOF) *m/z*: [M + H]⁺ calcd for C₂₃H₃₈N₃ 356.5780; Found 356.5780.



1-benzyl-4-phenethyl-1H-1,2,3-triazole(F₄): Isolated as white solid (Method A: 126.5 mg, 96%; Method F: 126.5 mg, 96%). ¹H NMR (700 MHz, CDCl₃) δ 7.35 (d, *J* = 7.2 Hz, 3H), 7.24 (t, *J* = 7.5 Hz, 2H), 7.21 – 7.16 (m, 3H), 7.14 (d, *J* = 7.7 Hz, 2H), 7.04 (s, 1H), 5.45 (s, 2H), 3.01 (d, *J* = 7.6 Hz, 2H), 2.98 (d, *J* = 7.7 Hz, 2H). ¹³C NMR (101 MHz, CDCl₃) δ 147.7, 141.1, 134.9, 129.0, 128.5, 128.4, 128.3, 127.8, 126.0, 121.1, 53.9, 35.5, 27.5.



1-benzyl-4-cyclopentyl-1H-1,2,3-triazole (F₅): Isolated as brown solid (Method A: 102 mg, 90%; Method F: 106 mg, 93%). ¹H NMR (400 MHz, CDCl₃) δ 7.34 – 7.24 (m, 3H), 7.19 (t, *J* = 3.8 Hz, 2H), 7.09 (s, 1H), 5.41 (s, 2H), 3.19 – 2.97 (m, 1H), 2.08 – 1.91 (m, 2H), 1.65 (d, *J* = 8.1 Hz, 2H), 1.62 – 1.51 (m, 4H). ¹³C NMR (101 MHz, CDCl₃) δ 135.1, 129.1, 128.7, 128.1, 119.6, 54.1, 36.9, 33.3, 25.2.

3.5.6 NMR spectra of the Products:

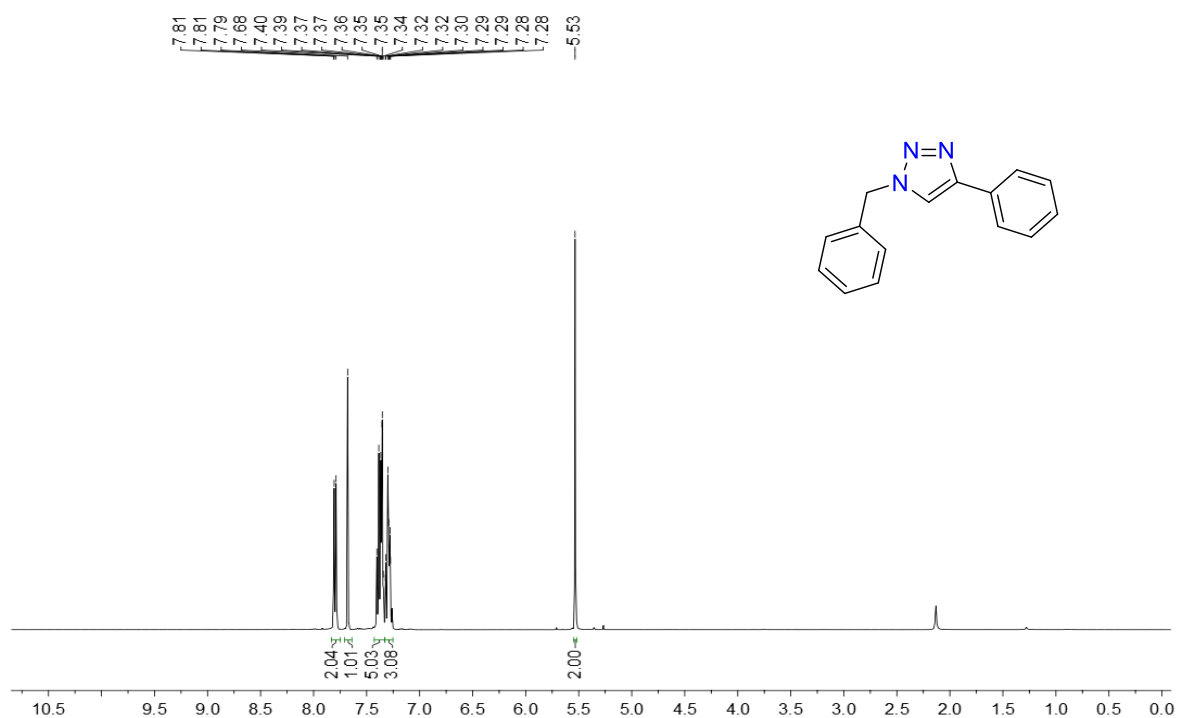


Figure 3.13. ¹H NMR (400 MHz) spectrum of 1-benzyl-4-phenyl-1H-1,2,3-triazole (A) in CDCl₃ at r.t.

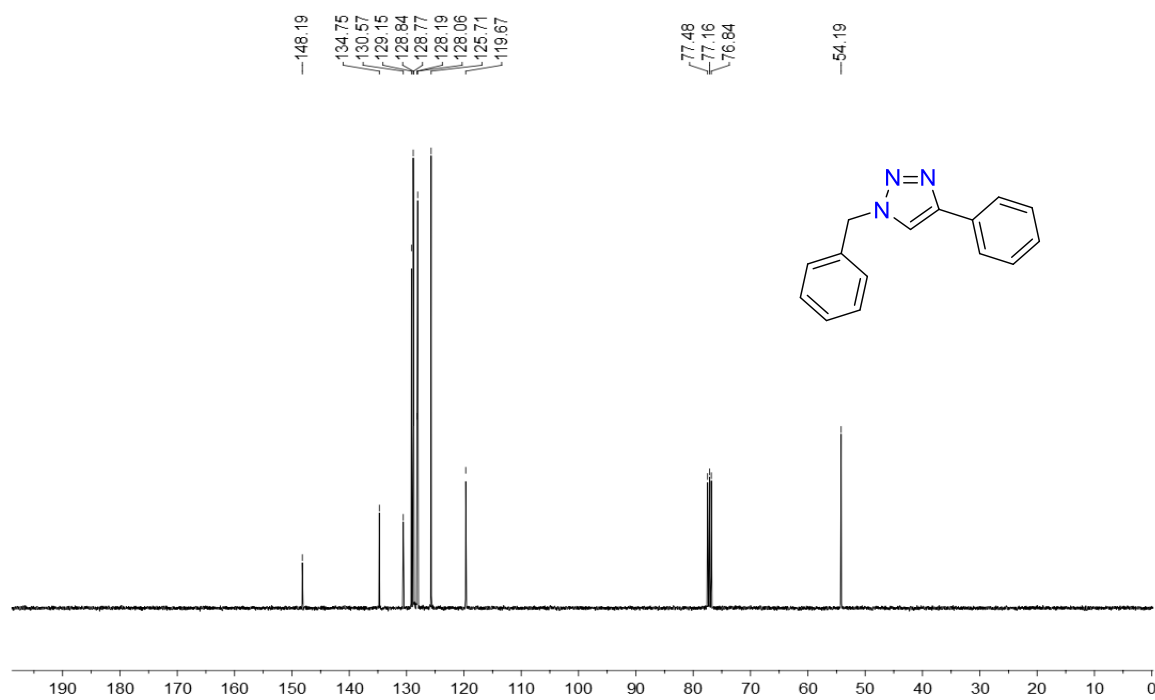


Figure 3.14. ¹³C NMR (101 MHz) spectrum of 1-benzyl-4-phenyl-1H-1,2,3-triazole (A) in CDCl₃ at r.t.

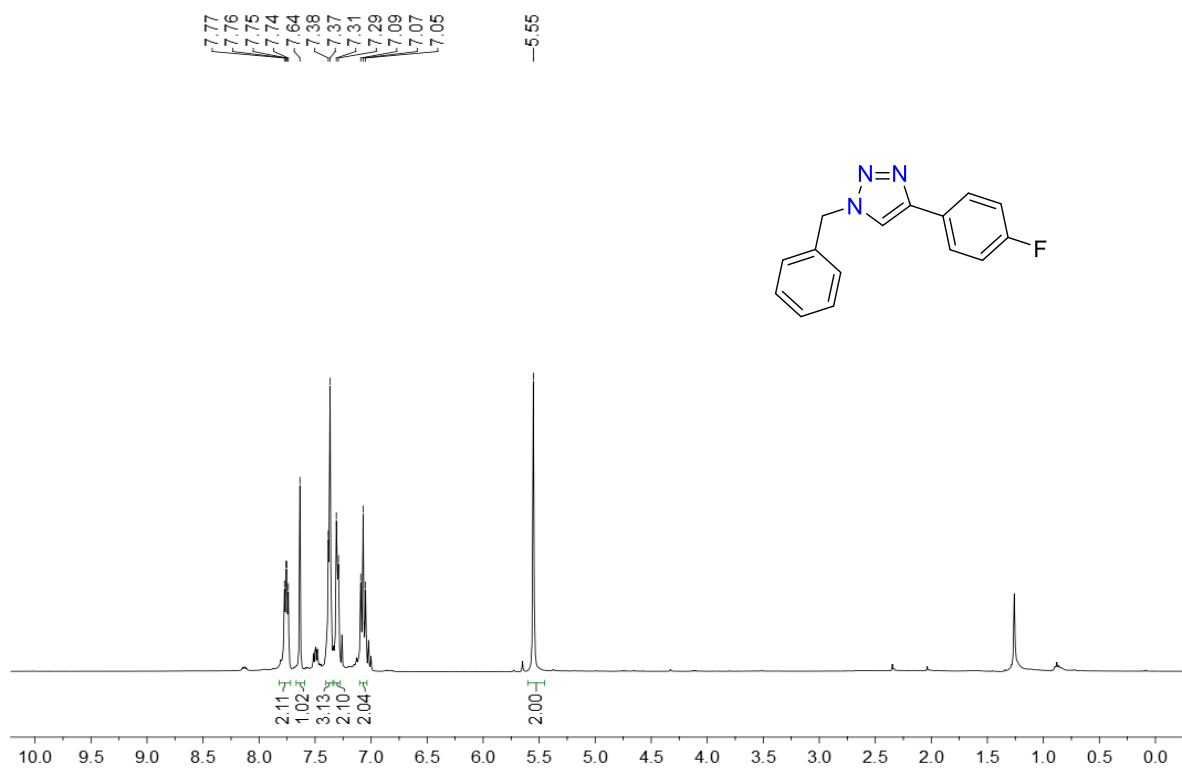


Figure 3.15. ¹H NMR (400 MHz) spectrum of 1-benzyl-4-(4-fluorophenyl)-1H-1,2,3-triazole (C₄) in CDCl₃ at r.t.

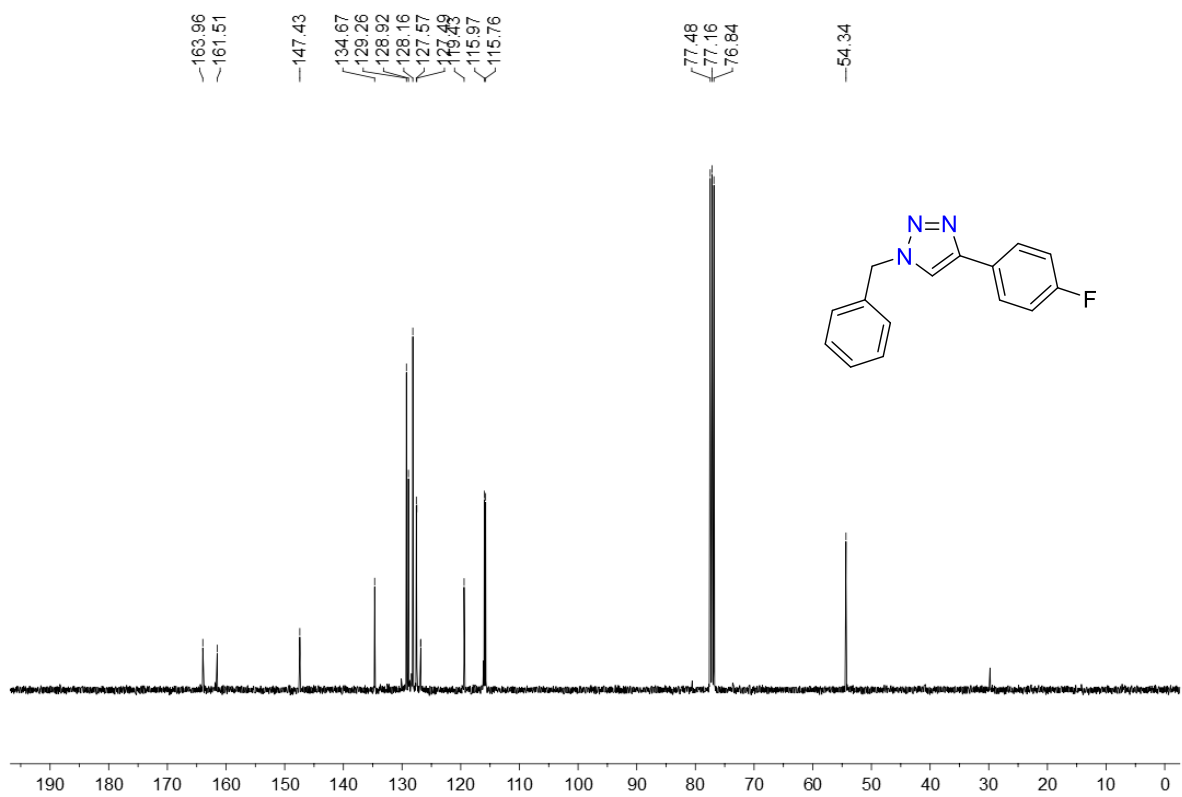


Figure 3.16. ¹³C NMR (101 MHz) spectrum of 1-benzyl-4-(4-fluorophenyl)-1H-1,2,3-triazole (C₄) in CDCl₃ at r.t.

3.5.7 Molecular structure determination by single crystal X-ray crystallography

A crystal of **complex 17** and **18** with accession code CCDC 2196025 and 2196026 respectively, were mounted under crystal oil coated at ambient conditions. All measurements were made on an *Oxford Diffraction SuperNova* area-detector diffractometer using an INCOATEC micro source (Mo-K α radiation, $\lambda = 0.71073$ Å, multilayer optics) and Al filtered.

Data reduction was performed using the *CrysAlisPro* program. The intensities were corrected for Lorentz and polarization effects, and an absorption correction based on the multi-scan method using SCALE3 ABSPACK in *CrysAlisPro*^l was applied. Data collection and refinement parameters are given in **Table 3.4**. OleX and refinement was carried out using least-square minimization implemented in ShelXL. All nonhydrogen atoms were refined with anisotropic displacement parameters. Hydrogen atom positions were fixed geometrically in idealized positions and were refined using a riding model.

Table 3.4. Crystallographic Data and Refinement Parameters for **17** and **18**.

	17	18
Empirical formula	C ₂₁ H ₂₀ ClCuN ₂ S	C ₃₂ H ₃₀ Br ₂ Cu ₂ N ₆ O ₂
Formula weight (g mol ⁻¹)	431.44	817.52
Temperature	100.00(10)	300(2)
Wavelength	1.54184	1.54184
Crystal system	Monoclinic	Triclinic
Space group	<i>P2₁/c</i>	<i>P1</i>
<i>a</i> (Å)	13.7190(6)	7.89294(11)
<i>b</i> (Å)	7.0406(4)	8.2012(3)
<i>c</i> (Å)	21.6694(14)	12.3243(6)
α (deg)	90	89.564(9)
β (deg)	97.637(5)	108.670(4)
γ (deg)	90	92.344(3)
volume (Å ³)	2074.5(2)	755.15(5)
Z	4	1
<i>D</i> _{calc} (g cm ⁻³)	1.381	1.798

μ (mm ⁻¹)	3.649	5.175
$F(000)$	888.0	408.0
Crystal Size (mm ³)	0.2 × 0.2 × 0.1	0.2 × 0.1 × 0.1
2 θ Range (deg)	8.234 to 152.274	7.572 to 151.138
Index Ranges	-17 ≤ h ≤ 17, -8 ≤ k ≤ 8, -26 ≤ l ≤ 17	-9 ≤ h ≤ 9, -10 ≤ k ≤ 10, -15 ≤ l ≤ 15
Reflections collected	22310	22035
Independent reflections (R_{int})	4230 (0.0523)	5561 (0.0533)
Completeness to theta	99.96	99.96
Refinement method	Full-matrix least-squares on F ²	Full-matrix least-squares on F ²
Data/Restraints/parameters	4230/0/235	5561/3/400
Goodness-of-fit on F ²	1.188	1.054
Final R indices [$I > 2\sigma(I)$]	$R_1 = 0.0758$, $wR_2 = 0.2011$	$R_1 = 0.0321$, $wR_2 = 0.0858$
R indices (all data)	$R_1 = 0.0849$, $wR_2 = 0.2082$	$R_1 = 0.0324$, $wR_2 = 0.0862$
Largest diff. peak/hole (e Å ⁻³)	0.94/-0.65	0.73/-0.61

Table 3.5. Selected bond lengths (Å) around the metal centre in Copper complexes **17** and **18**.

Complexes/Bonds	Bond lengths	
	17	18
Cu–N(pyridine)	2.095(4)	2.063(5) 2.066(5)
Cu–N(imine/pyrazole)	2.071(4)	2.258(5) 2.259(5)
Cu–X (X= Cl/Br/I)	2.2786(13)	2.4352(11) 2.4377(11) 2.5240(10) 2.5276(10)
Cu–S	2.2440(13)	

Table 3.6. Selected bond angles ($^{\circ}$) around the metal centre in Copper complexes **17** and **18**.

Bond angles			
17		18	
S1 ¹ -Cu1-CL5	103.683(16)	Br2-Cu2-Br1	114.07(4)
N1-Cu1-CL5	93.357(13)	N4-Cu2-Br1	101.88(13)
N1-Cu1-S1 ¹	100.095(16)	N4-Cu2-Br2	119.79(14)
N2-Cu1-CL5	163.38(5)	N4-Cu2-N6	93.56(18)
N2-Cu1-S1 ¹	96.24(5)	N6-Cu2-Br2	108.89(13)
N2-Cu1-N1	87.98(5)	N6-Cu2-Br1	117.36(13)
		Br1-Cu1-Br2 ²	114.18(4)
		N3-Cu1-Br2 ²	117.79(12)
		N3-Cu1-Br1	108.42(13)
		N1-Cu1-Br2 ²	101.48(13)
		N1-Cu1-Br1	120.36(13)
		N1-Cu1-N3	93.34(18)

Symmetry code: ¹ 1-X,-1/2+Y,1/2-Z; ² +X,-1+Y,+Z

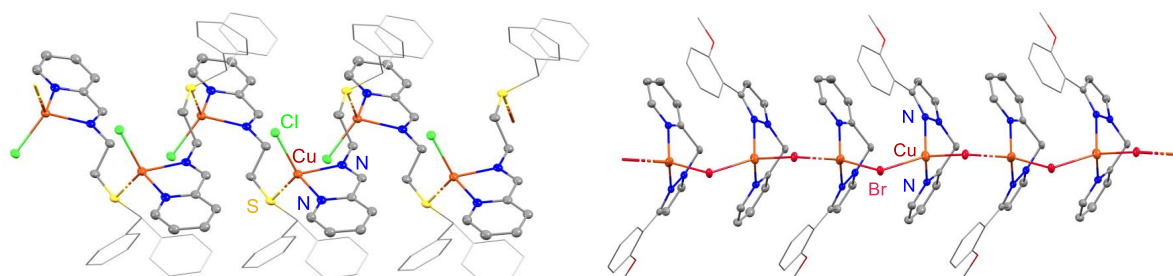


Figure 3.17. 1D Molecular chain of complex **17** and **18**

3.6 REFERENCES

- (1) Anastas, P. T.; Warner, J. C. Principles of Green Chemistry. *In Green Chemistry: Theory and Practice*; Oxford University Press, 1998; pp 29–56.
- (2) Anastas, P. T.; Heine, L. G.; Williamson, T. C. *Green Chemical Syntheses and Processes*; American Chemical Society: Washington, DC, 2000.
- (3) Anastas, P. T.; Kirchoff, M. M. Origins, Current Status, and Future Challenges of Green Chemistry. *Acc. Chem. Res.* **2002**, *35*, 686-694..
- (4) Anastas, P.; Eghbali, N. Green chemistry: Principles and practice. *Chem. Soc. Rev.* **2010**, *39*, 301–312.
- (5) Sheldon, R. A. Fundamentals of green chemistry: efficiency in reaction design. *Chem. Soc. Rev.* **2012**, *41*, 1437–1451.
- (6) Prat, D.; Hayler, J.; Wells, A. A survey of solvent selection guides. *Green Chem.* **2014**, *16*, 4546–4551.
- (7) Rodríguez-Padrón, D.; Puente-Santiago, A. R.; Balu, A. M.; Muñoz-Batista, M. J.; Luque, R. Environmental Catalysis: Present and Future. *ChemCatChem* **2019**, *11*, 18–38.
- (8) Polshettiwar, V.; Varma, R. S. Green chemistry by nano-catalysis. *Green Chem.* **2010**, *12*, 743–754.
- (9) Anilkumar, G.; Saranya, S. *Copper Catalysis in Organic Synthesis*; Wiley-VCH: Weinheim, Germany, 2020.
- (10) Evans, G.; Blanchard, N. *Copper-Mediated Cross-Coupling Reactions*; Wiley & Sons: New Jersey, USA, 2013.
- (11) Alexakis, A.; Krause, N.; Woodward, S. *Copper-Catalyzed Asymmetric Synthesis*; Wiley-VCH, 2014.

- (12) Bhunia, S.; Pawar, G. G.; Kumar, S. V.; Jiang, Y.; Ma, D. Selected Copper-Based Reactions for C–N, C–O, C–S, and C–C Bond Formation. *Angew. Chem., Int. Ed.* **2017**, *56*, 16136–16179.
- (13) Allen, S. E.; Walvoord, R. R.; Padilla-Salinas, R.; Kozlowski, M. C. Aerobic Copper-Catalyzed Organic Reactions. *Chem. Rev.* **2013**, *113*, 6234–6458.
- (14) Chen, S.-J.; Golden, D. L.; Krska, S. W.; Stahl, S. S. Copper-Catalyzed Cross Coupling of Benzylic C-H Bonds and Azoles with Controlled N-Site Selectivity. *J. Am. Chem. Soc.* **2021**, *143*, 14438–14444.
- (15) Müller, D. S.; Marek, I. Copper mediated carbometalation reactions. *Chem. Soc. Rev.* **2016**, *45*, 4552–4566.
- (16) Tang, X.; Wu, W.; Zeng, W.; Jiang, H. Copper-Catalyzed Oxidative Carbon-Carbon and/or Carbon-Heteroatom Bond Formation with O₂ or Internal Oxidants. *Acc. Chem. Res.* **2018**, *51*, 1092–1105.
- (17) Guan, X.; Zhu, H.; Driver, T. Cu-Catalyzed crosscoupling of nitroarenes with aryl boronic acids to construct diarylamines. *ACS Catal.* **2021**, *11*, 12417–12422.
- (18) Meldal, M.; Tornøe, C. W. Cu-Catalyzed Azide–Alkyne Cycloaddition. *Chem. Rev.* **2008**, *108*, 2952–3015.
- (19) Wang, P.-Z.; Wu, X.; Cheng, Y.; Jiang, M.; Xiao, W.-J.; Chen, J.-R. Photoinduced Copper-Catalyzed Asymmetric Three-Component Coupling of 1,3-Dienes: An Alternative to Kharasch–Sosnovsky Reaction. *Angew. Chem., Int. Ed.* **2021**, *60*, 22956–22962.
- (20) Liu, R. Y.; Buchwald, S. L. CuH-Catalyzed Olefin Functionalization: From Hydroamination to Carbonyl Addition. *Acc. Chem. Res.* **2020**, *53*, 1229–1243.
- (21) Geng, H. Q.; Meyer, T.; Franke R.; Wu, X. F. Copper-catalyzed hydroformylation and hydroxymethylation of styrenes. *Chem. Sci.* **2021**, *12*, 14937–14943.

- (22) Besalú-Sala, P.; Magallón, C.; Costas, M.; Company, A.; Luis, J. M. Mechanistic Insights into the *ortho*-Defluorination-Hydroxylation of 2-Halophenolates Promoted by a Bis(α -oxo)diCopper(III) Complex. *Inorg. Chem.* **2020**, *59*, 17018–17027.
- (23) Trammell, R.; Rajabimoghadam, K.; Garcia-Bosch, I. Copper Promoted Functionalization of Organic Molecules: from Biologically Relevant Cu/O₂ Model Systems to Organometallic Transformations. *Chem. Rev.* **2019**, *119*, 2954–3031.
- (24) Kolb, H. C.; Sharpless, K. B. The growing impact of click chemistry on drug discovery. *Drug Discovery Today* **2003**, *8*, 1128–1137.
- (25) Moses, J. E.; Moorhouse, A. D. The Growing Applications of Click Chemistry. *Chem. Soc. Rev.* **2007**, *36*, 1249–1262.
- (26) Thirumurugan, P.; Matosiuk, D.; Jozwiak, K. Click Chemistry for Drug Development and Diverse Chemical–Biology Applications. *Chem. Rev.* **2013**, *113*, 4905–4979.
- (27) Mamidyala, S. K.; Finn, M. G. In Situ Click Chemistry: Probing the Binding Landscapes of Biological Molecules. *Chem. Soc. Rev.* **2010**, *39*, 1252–1261.
- (28) Golas, P. L.; Matyjaszewski, K. Marrying Click Chemistry with Polymerization: Expanding the Scope of Polymeric Materials. *Chem. Soc. Rev.* **2010**, *39*, 1338–1354.
- (29) Qin, A.; Lamb, J. W. Y.; Tang, B. Z. Click Polymerization. *Chem. Soc. Rev.* **2009**, *39*, 2522–2544.
- (30) Nandivada, H.; Jiang, X.; Lahann, J. Click Chemistry: Versatility and Control in the Hands of Materials Scientists. *Adv. Mater.* **2007**, *19*, 2197–2208.
- (31) Aromí, G.; Barrios, L. A.; Roubeau, O.; Gamez, P. Triazoles and tetrazoles: prime ligands to generate remarkable coordination materials. *Coord. Chem. Rev.* **2011**, *255*, 485–546.

- (32) Crowley, J. D.; Gavey, E. L. Use of di-1,4-substituted-1,2,3-triazole “click” ligands to self-assemble dipalladium(II) coordinatively saturated, quadruply stranded helicate cages. *Dalton Trans.* **2010**, *39*, 4035–4037.
- (33) Ghosh, R.; Jana, N. C.; Panda, S.; Bagh, B. Transfer Hydrogenation of Aldehydes and Ketones in Air with Methanol and Ethanol by an Air-Stable Ruthenium–Triazole Complex. *ACS Sustainable Chem. Eng.* **2021**, *9*, 4903–4914.
- (34) Vivancos, Á.; Segarra, C.; Albrecht, M. Mesoionic and Related Less Heteroatom Stabilized N-Heterocyclic Carbene Complexes: Synthesis, Catalysis, and Other Applications. *Chem. Rev.* **2018**, *118*, 9493–9586.
- (35) Maity, R.; Sarkar, B. Chemistry of Compounds Based on 1,2,3-Triazolylidene-Type Mesoionic Carbenes. *JACS Au* **2022**, *2*, 22–57.
- (36) Bagh, B.; McKinty, A. M.; Lough, A. J.; Stephan, D. W. 1, 2, 3-Triazolylidene ruthenium (II) (η^6 -arene) complexes: synthesis, metallation and reactivity. *Dalton Trans.* **2014**, *43*, 12842–12850.
- (37) Bagh, B.; McKinty, A. M.; Lough, A. J.; Stephan, D. W. 1,2,3-Triazolylidene Ruthenium (II)-Cyclometalated Complexes and Olefin Selective Hydrogenation Catalysis. *Dalton Trans.* **2015**, *44*, 2712–2723.
- (38) Bagh, B.; Stephan, D. W. Half Sandwich ruthenium(II) Hydrides: Hydrogenation of Terminal, Internal, Cyclic and Functionalized Olefins. *Dalton Trans.* **2014**, *43*, 15638–15645.
- (39) Rostovtsev, V. V.; Green, L. G.; Fokin, V. V.; Sharpless, K. B. A Stepwise Huisgen Cycloaddition Process: Copper(I)-Catalyzed Regioselective Ligation of Azides and Terminal Alkynes. *Angew. Chem. Int. Ed.* **2002**, *41*, 2596–2599.

- (40) Khatua, M.; Goswami, B.; Kamal; Samanta, S. Azide–Alkyne “Click” Reaction in Water Using Parts-Per-Million Amine-Functionalized Azoaromatic Cu(I) Complex as Catalyst: Effect of the Amine Side Arm. *Inorg. Chem.* **2021**, *60*, 17537–17554.
- (41) Kolb, H. C.; Finn, M. G.; Sharpless, K. B. Click Chemistry: Diverse Chemical Function from a Few Good Reactions. *Angew. Chem., Int. Ed.* **2001**, *40*, 2004–2021.
- (42) Perez-Balderas, F.; Ortega-Munoz, M.; Morales-Sanfrutos, J.; Hernandez-Mateo, F.; Calvo-Flores, F. G.; Calvo-Asin, J. A.; Isac-Garcia, J.; Santoyo-Gonzalez, F. *Org. Lett.* **2003**, *5*, 1951–1954.
- (43) Lal, S.; Diez-Gonzalez, S. [CuBr(PPh₃)₃] for azide-alkyne cycloaddition reactions under strict click conditions. *J. Org. Chem.* **2011**, *76*, 2367–2373.
- (44) Shao, C.; Wang, X.; Zhang, Q.; Luo, S.; Zhao, J.; Hu, Y. Acid-base jointly promoted Copper(I)-catalyzed azide-alkyne cycloaddition. *J. Org. Chem.* **2011**, *76*, 6832–6836.
- (45) Worrell, B. T.; Malik, J. A.; Fokin, V. V. Direct Evidence of a Dinuclear Copper Intermediate in Cu(I)-Catalyzed Azide-Alkyne Cycloadditions. *Science* **2013**, *340*, 457–460.
- (46) Venderbosch, B.; Oudsen, J.–P. H.; van der Vlugt, J. I.; Korstanje, T. J.; Tromp, M. Cationic Copper Iminophosphorane Complexes as CuAAC Catalysts: A Mechanistic Study. *Organometallics* **2020**, *39*, 3480–3489.
- (47) Himo, F.; Lovell, T.; Hilgraf, R.; Rostovtsev, V. V.; Noodleman, L.; Sharpless, K. B.; Fokin, V. V. Copper(I)-Catalyzed Synthesis of Azoles. DFT Study Predicts Unprecedented Reactivity and Intermediates. *J. Am. Chem. Soc.* **2005**, *127*, 210–216.
- (48) Rodionov, V. O.; Fokin, V. V.; Finn, M. G. Mechanism of the ligand-free Cu^I-catalyzed azide alkyne cycloaddition reaction. *Angew. Chem., Int. Ed.* **2005**, *44*, 2210–2215.

- (49) Tornøe, C. W.; Christensen, C.; Meldal, M. Peptidotriazoles on Solid Phase: [1,2,3]-Triazoles by Regiospecific Copper(I)-Catalyzed 1,3-Dipolar Cycloadditions of Terminal Alkynes to Azides. *J. Org. Chem.* **2002**, *67*, 3057-3064.
- (50) Alonso, F.; Moglie, Y.; Radivoy, G. Copper nanoparticles in click chemistry. *Acc. Chem. Res.* **2015**, *48*, 2516-2528.
- (51) Patterson, M. R.; Dias, H. R. Tetranuclear and trinuclear Copper(i) pyrazolates as catalysts in Copper mediated azide-alkyne cycloadditions (CuAAC). *Dalton Trans.* **2022**, *51*, 375–383.
- (52) Zhang, X. F.; Zhi, S. J.; Wang, W.; Liu, S.; Jasinski, J. P.; Zhang, W. A pot-economical and diastereoselective synthesis involving catalyst-free click reaction for fused-triazolobenzodiazepines. *Green Chem.* **2016**, *18*, 2642–2646.
- (53) Chassaing, S.; Bénétteau, V.; Pale, P. When CuAAC “Click Chemistry” Goes Heterogeneous. *Catal. Sci. Technol.* **2016**, *6*, 923–957.
- (54) Haldón, E.; Nicasio, M. C.; Pérez, P. J. Copper-Catalysed Azide–Alkyne Cycloadditions (CuAAC): An Update. *Org. Biomol. Chem.* **2015**, *13* (37), 9528–9550.
- (55) Becer, C. R.; Hoogenboom, R.; Schubert, U. S. Click Chemistry beyond Metal-Catalyzed Cycloaddition. *Angew. Chem., Int. Ed.* **2009**, *48*, 4900–4908.
- (56) McElroy, C. R.; Constantinou, A.; Jones, L. C.; Summerton, L.; Clark, J. H. Towards a Holistic Approach to Metrics for the 21st Century Pharmaceutical Industry. *Green Chem.* **2015**, *17*, 3111–3121.
- (57) DeSimone, J. M. Practical Approaches to Green Solvents. *Science* **2002**, *297*, 799–803.
- (58) Curzons, A. D.; Constable, D. J. C.; Mortimer, D. N.; Cunningham, V. L. So, you think your process is green, how do you know? Using principles of sustainability to determine what is green—a corporate perspective. *Green Chem.* **2001**, *3*, 1–6.

- (59) Constable, D. J. C.; Curzons, A. D.; Cunningham, V. L. Metrics to 'green' chemistry- which are the best? *Green Chem.* **2002**, *4*, 521-527.
- (60) Sheldon, R. A. Green solvents for sustainable organic synthesis: state of the art. *Green Chem.* **2005**, *7*, 267-278.
- (61) Dyson, P. J.; Jessop, P. G. Solvent Effects in Catalysis: Rational Improvements of Catalysts via Manipulation of Solvent Interactions. *Catal. Sci. Technol.* **2016**, *6*, 3302-3316.
- (62) Winterton, N. The Green Solvent: A Critical Perspective. *Clean Technol. Environ. Policy* **2021**, *23*, 2499-2522.
- (63) Gandeepan, P.; Kaplaneris, N.; Santoro, S.; Vaccaro, L.; Ackermann, L. Biomass-Derived Solvents for Sustainable Transition Metal-Catalyzed C-H Activation. *ACS Sustainable Chem. Eng.* **2019**, *7*, 8023-8040.
- (64) Gu, Y.; Jérôme, F. Bio-based solvents: an emerging generation of fluids for the design of eco-efficient processes in catalysis and organic chemistry. *Chem. Soc. Rev.* **2013**, *42*, 9550-9570.
- (65) Tshibalonzaa, N. N.; Monbaliu, J.-C. M. The deoxy dehydration (DODH) reaction: a versatile technology for accessing olefins from bio-based polyols. *Green Chem.* **2020**, *22*, 4801-4848.
- (66) Vidal, C.; García-Álvarez, J. Glycerol: a bio renewable solvent for base-free Cu(I)-catalyzed 1,3-dipolar cycloaddition of azides with terminal and 1-iodoalkynes. Highly efficient transformations and catalyst recycling. *Green Chem.* **2014**, *16*, 3515-3521.
- (67) Zhao, J.; Li, P.; Xu, Y.; Shi, Y.; Li, F. Nickel-Catalyzed Transformation of Diazoacetates to Alkyl Radicals Using Alcohol as a Hydrogen Source. *Org. Lett.* **2019**, *21*, 9386-9390.

- (68) Xu, J.; Huang, W.; Bai, R.; Queneau, Y.; Jérôme, F.; Gu, Y. Utilization of bio-based glycolaldehyde aqueous solution in organic synthesis: application to the synthesis of 2,3-dihydrofurans. *Green Chem.* **2019**, *21*, 2061–2069.
- (69) García, N.; García-García, P.; Fernández-Rodríguez, M. A.; García, D.; Pedrosa, M. R.; Arnáiz, F. J.; Sanz, R. An unprecedented use for glycerol: chemo selective reducing agent for sulfoxides. *Green Chem.* **2013**, *15*, 999–1005.
- (70) Rasina, D.; Lombi, A.; Santoro, S.; Ferlin, F.; Vaccaro, L. Searching for novel reusable biomass-derived solvents: furfuryl alcohol/water azeotrope as a medium for waste-minimised Copper catalysed azide–alkyne cycloaddition. *Green Chem.* **2016**, *18*, 6380–6386.
- (71) Luciani, L.; Goff, E.; Lanari, D.; Santoro, S.; Vaccaro, L. Waste minimised Copper-catalysed azide-alkyne cycloaddition in Polar clean as a reusable and safe reaction medium. *Green Chem.* **2018**, *20*, 183–187.
- (72) Abbott, A. P.; Capper, G.; Davies, D. L.; Rasheed, R. K.; Tambyrajah, V. Novel solvent properties of choline chloride/urea mixtures. *Chem. Commun.* **2003**, 70–71.
- (73) Smith, E. L.; Abbott, A. P.; Ryder, K. S. Deep Eutectic Solvents (DESs) and Their Applications. *Chem. Rev.* **2014**, *114*, 11060–11082.
- (74) Nebra, N.; GarcíaÁlvarez, J. Recent Progress of Cu-Catalyzed Azide-Alkyne Cycloaddition Reactions (CuAAC) in Sustainable Solvents: Glycerol, Deep Eutectic Solvents, and Aqueous Media. *Molecules* **2020**, *25*, 2015–2032.
- (75) Giofre, S. V.; Tiecco, M.; Ferlazzo, A.; Romeo, R.; Ciancaleoni, G.; Germani, R.; Iannazzo, D. Base-Free Copper-Catalyzed Azide Alkyne Click Cycloadditions (CuAAC) in Natural Deep Eutectic Solvents as Green and Catalytic Reaction Media. *Eur. J. Org. Chem.* **2021**, *2021*, 4777–4789.

- (76) Kafle, A.; Handy, S. T. A one-pot, Copper-catalyzed azidation/click reaction of aryl and heteroaryl bromides in an environmentally friendly deep eutectic solvent. *Tetrahedron*. **2017**, *73*, 7024–7029.
- (77) Hansen, B. B.; Spittle, S.; Chen, B.; Poe, D.; Zhang, Y.; Klein, J. M.; Horton, A.; Adhikari, L.; Zelovich, T.; Doherty, B. W.; Gurkan, B.; Maginn, E. J.; Ragauskas, A.; Dadmun, M.; Zawodzinski, T. A.; Baker, G. A.; Tuckerman, M. E.; Savinell, R. F.; Sangoro, J. R. Deep Eutectic Solvents: A Review of Fundamentals and Applications. *Chem. Rev.* **2021**, *121*, 1232–1285.
- (78) Skopek, M. A.; Mohamoud, M. A.; Ryder, K. S.; Hillman, A. R. Nanogravimetric observation of unexpected ion exchange characteristics for polypyrrole film p-doping in a deep eutectic ionic liquid. *Chem. Commun.* **2009**, 935–937.
- (79) Abbott, A. P.; Barker, G. W.; Walter, A. J.; Kocovsky, P. Electrochemical recognition of analytes using quaternary ammonium binaphthyl salts. *Analyst*. **2003**, *128*, 245–248.
- (80) Lawes, S. D. A.; Hainsworth, S. V.; Blake, P.; Ryder, K. S.; Abbott, A. P. Lubrication of Steel/Steel Contacts by Choline Chloride Ionic Liquids. *Tribol. Lett.* **2010**, *37*, 103–110.
- (81) Gutiérrez, M. C.; Carriazo, D.; Tamayo, A.; Jiménez, R.; Picó, F.; Rojo, J. M.; Ferrer, M. L.; del Monte, F. Deep-Eutectic-Solvent Assisted Synthesis of Hierarchical Carbon Electrodes Exhibiting Capacitance Retention at High Current Densities. *Chem. Eur. J.* **2011**, *17*, 10533–10537.
- (82) Jhong, H. R.; Wong, S. H.; Wan, C. C.; Wang, Y. Y.; Wei, T. C. A novel deep eutectic solvent-based ionic liquid used as electrolyte for dye-sensitized solar cells. *Electrochem. Commun.* **2009**, *11*, 209–211.

- (83) Morrison, H. G.; Sun, C. C.; Neervannan, S. Characterization of thermal behavior of deep eutectic solvents and their potential as drug solubilization vehicles. *Int. J. Pharm.* **2009**, *378*, 136–139.
- (84) Serrano, M. C.; Gutiérrez, M. C.; Jiménez, R.; Ferrer, M. L.; Monte, F. d. Synthesis of Novel Lidocaine-Releasing Poly(Diol-CoCitrate) Elastomers by Using Deep Eutectic Solvents. *Chem. Commun.* **2012**, *48*, 579–581.
- (85) Deraedt, C.; Pinaud, N.; Astruc, D. Recyclable Catalytic Dendrimer Nanoreactor for Part-Per-Million Cu(I) Catalysis of "Click" Chemistry in Water. *J. Am. Chem. Soc.* **2014**, *136*, 12092–12098.
- (86) Díez-González, S.; Nolan, S. P. [(NHC)₂Cu]X Complexes as Efficient Catalysts for Azide-Alkyne Click Chemistry at Low Catalyst Loadings. *Angew. Chem., Int. Ed. Engl.* **2008**, *47*, 8881–8884.
- (87) Wang, C.; Wang, D.; Yu, S.; Cornilleau, T.; Ruiz, J.; Salmon, L.; Astruc, D. Design and applications of an efficient amphiphilic "click" CuI catalyst in water. *ACS Catal.* **2016**, *6*, 5424–5431.
- (88) Yamada, Y. M. A.; Sarkar, S. M.; Uozumi, Y. Amphiphilic Self Assembled Polymeric Copper Catalyst to Parts Per Million Levels: Click Chemistry. *J. Am. Chem. Soc.* **2012**, *134*, 9285–9290.
- (89) Bai, Y.; Feng, X.; Xing, H.; Xu, Y.; Kim, B. K.; Baig, N.; Zhou, T.; Gewirth, A. A.; Lu, Y.; Oldfield, E.; Zimmerman, S. C. A Highly Efficient Single-Chain Metal–Organic Nanoparticle Catalyst for Alkyne-Azide "Click" Reactions in Water and in Cells. *J. Am. Chem. Soc.* **2016**, *138*, 11077–11080.
- (90) Jana, N. C.; Sethi, S.; Saha, R.; Bagh, B. Aerobic oxidation of vanillyl alcohol to vanillin catalyzed by air-stable and recyclable Copper complex and TEMPO under base-free conditions. *Green Chem.* **2022**, *24*, 2542–2556.

- (91) Troyano, J.; Zapata, E.; Perles, J.; Amo-Ochoa, P.; FernándezMoreira, V.; Martínez, J. I.; Zamora, F.; Delgado, S. Multifunctional Copper(I) Coordination Polymers with Aromatic Mono- and Ditopic Thioamides. *Inorg. Chem.* **2019**, *58*, 3290–3301.
- (92) Liang, X.-Q.; Gupta, R.-K.; Li, Y.-W.; Ma, H.-Y.; Gao, L.-N.; Tung, C.-H.; Sun, D. Structural Diversity of Copper(I) Cluster-Based Coordination Polymers with Pyrazine-2-thiol Ligand. *Inorg. Chem.* **2020**, *59*, 2680–2688.
- (93) Pathaw, L.; Maheshwaran, D.; Nagendraraj, T.; Khamrang, T.; Velusamy, M.; Mayilmurugan, R. Tetrahedral Copper(I) complexes of novel N, N-bidentate ligands and photophysical properties. *Inorg. Chim. Acta.* **2021**, *514*, 119999–120008.
- (94) Ilgen, F.; Konig, B. Organic reactions in low melting mixtures based on carbohydrates and L-carnitine—a comparison. *Green Chem.* **2009**, *11*, 848–854.
- (95) Xiong, X.; Yi, C.; Liao, X.; Lai, S. A practical multigram-scale method for the green synthesis of 5-substituted-1H-tetrazoles in deep eutectic solvent. *Tetrahedron Lett.* **2019**, *60* 402–406.
- (96) Prat, D.; Wells, A.; Hayler, J.; Sneddon, H.; McElroy, C. R.; Abou-Shehada, S.; Dunn, P. J. CHEM21 Selection Guide of Classical and Less Classical-Solvents. *Green Chem.* **2016**, *18*, 288–296.
- (97) Allen, D. T.; Gathergood, N.; Licence, P.; Subramaniam, B. Expectations for Manuscripts Contributing to the Field of Solvents in ACS Sustainable Chemistry & Engineering. *ACS Sustainable Chem. Eng.* **2020**, *8*, 14627–14629.
- (98) Kuok (Mimi) Hii, K.; Moores, A.; Pradeep, T.; Sels, B.; Allen, D. T.; Licence, P.; Subramaniam, B. Expectations for Manuscripts on Catalysis in ACS Sustainable Chemistry & Engineering. *ACS Sustainable Chem. Eng.* **2020**, *8*, 4995–4996.
- (99) Allen, D. T.; Carrier, D. J.; Gong, J.; Hwang, B.-J.; Licence, P.; Moores, A.; Pradeep, T.; Sels, B.; Subramaniam, B.; Tam, M. K. C.; Zhang, L.; Williams, R. M. Advancing the

- Use of Sustainability Metrics in ACS Sustainable Chemistry & Engineering. *ACS Sustainable Chem. Eng.* **2018**, *6*, 1–1.
- (100) Droesbeke, M. A.; Du Prez, F. E. Sustainable Synthesis of Renewable Terpenoid-Based (Meth)acrylates Using the CHEM21 Green Metrics Toolkit. *ACS Sustainable Chem. Eng.* **2019**, *7*, 11633–11639.
- (101) Prieschl, M.; García-Lacuna, J.; Munday, R.; Leslie, K.; O’Kearney-McMullan, A.; Hone, C. A.; Kappe, C. O. Optimization and sustainability assessment of a continuous flow Ru-catalyzed ester hydrogenation for an important precursor of a β 2-adrenergic receptor agonist. *Green Chem.* **2020**, *22*, 5762–5770.
- (102) Dalidovich, T.; Mishra, K. A.; Shalima, T.; Kudrjasova, M.; Kananovich, D. G.; Aav, R. Mechanochemical Synthesis of Amides with Uronium-Based Coupling Reagents: A Method for Hexaamidation of Biotin[6]uril. *ACS Sustainable Chem. Eng.* **2020**, *8*, 15703–15715.
- (103) Zhu, Z.; Wang, Z.; Jian, Y.; Sun, H.; Zhang, G.; Lynam, J. M.; McElroy, C. R.; Burden, T. J.; Inight, R. L.; Fairlamb, I. J. S.; Zhang, W.; Gao, Z. Pd-Catalysed carbonylative Suzuki–Miyaura crosscouplings using $\text{Fe}(\text{CO})_5$ under mild conditions: generation of a highly active, recyclable and scalable ‘Pd–Fe’ nanocatalyst. *Green Chem.* **2021**, *23*, 920–926.
- (104) Sheldon, R. A. The E Factor: Fifteen Years On Green Chem. **2007**, *9*, 1273–1283.
- (105) Lam, C. H.; Escande, V.; Mellor, K. E.; Zimmerman, J. B.; Anastas, P. T. Teaching Atom Economy and E-Factor Concepts through a Green Laboratory Experiment: Aerobic Oxidative Cleavage of *meso*-Hydrobenzoin to Benzaldehyde Using a Heterogeneous Catalyst. *J. Chem. Educ.* **2019**, *96*, 761–765.

Chapter-4

Copper(I)-Catalyzed Click Chemistry in Deep Eutectic Solvent for the Syntheses of β -D-Glucopyranosyltriazoles

4.1 ABSTRACT

In the last two decades, click chemistry has progressed as a powerful tool in joining two different molecular units to generate fascinating structures with a widespread application in various branch of sciences. Copper(I)-catalyzed azide-alkyne cycloaddition (CuAAC) reaction, also known as click chemistry, has been extensively utilized as a versatile strategy for the rapid and selective formation of 1,4-disubstituted 1,2,3-triazoles. The successful use of CuAAC reaction for the preparation of biologically active triazole-attached carbohydrate-containing molecular architectures is an emerging area of glycoscience. In this regard, a well-defined Copper(I)-iodide complex (**19**) with a tridentate NNO ligand (**L7**) was synthesized and effectively utilized as an active catalyst. Instead of using potentially hazardous reaction media such as DCM or toluene, the use of deep eutectic solvent (DES), an emerging class of green solvent, is advantageous for the syntheses of triazole-glycohybrids. The present work shows, for the first time, the successful use of DES as a reaction medium to click various glycosides and terminal alkynes in the presence of sodium azide. Various 1,4-disubstituted 1,2,3-glucopyranosyltriazoles were synthesized and the pure products were isolated by using a very simple work-up process (filtration). The reaction media was recovered and recycled in five consecutive runs. The presented catalytic protocol generated very minimum waste as reflected by a low *E*-factor (2.21-3.12). Finally, the optimized reaction conditions were evaluated with the CHEM21 green metrics toolkit.

4.2 INTRODUCTION

In 2002, Karl B. Sharpless¹ and Morten P. Meldal² independently discovered Copper(I)-catalyzed 1,3-dipolar cycloaddition reaction between organic azides and terminal alkynes, commonly known as CuAAC or the “click reaction”. Later the reaction became popular to the scientific community because of its flexible and adaptable strategies for the easy syntheses of 1,4-disubstituted 1,2,3-triazoles which have widespread application in medicinal,^{3–5} pharmaceutical,^{6,7} biological,^{8–12} and material sciences,^{13–17} drug discoveries^{18–21} and catalysis.^{22–26} Indeed, the 2022 Nobel prize in Chemistry went to both Karl B. Sharpless and Morten P. Meldal along with Carolyn R. Bertozzi, for their seminal work on click and bioorthogonal chemistry. Unlike Huisgen's uncatalyzed thermal version,²⁷ the Copper(I) catalyzed version is absolutely regioselective and regiospecific. Not only that, the catalytic protocol is easy to perform under very mild conditions and provides high to excellent yields with a wide variety of substrate scope. Therefore, there is no doubt the CuAAC reaction is a novel discovery in the context of “click chemistry” as coined by Sharpless in 1999.²⁸

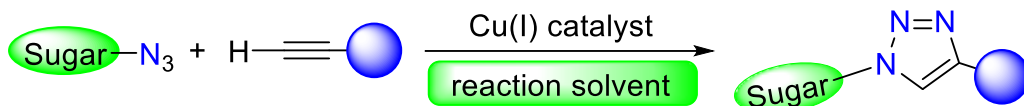
The impact of click chemistry has already been spread out in diverse fields of science.^{29–45} Along with the successful development of CuAAC reactions in various fields of chemistry, its application in carbohydrate chemistry has been parallelly explored.^{46–58} In this regard, Tiwari and co-workers elegantly illustrated the application of click chemistry in glycoscience.^{46,47} Carbohydrates are very common class of biomolecules and an integral part of living cells. They are significantly important in the construction of structural building blocks of genetic materials and serve as necessary energy source.⁵⁹ They play vital roles in different intracellular and intercellular activities in form of signal-transmitter, cell surface receptors and bacterial adhesives.^{60,61} Carbohydrate moieties are also boon for human use because of their hydrophilicity, minimum toxicity, biocompatibility and bioavailability.^{59–63} Due to all these superior properties, synthetic organic chemists showed an enormous interest in designing

carbohydrate scaffolds for easy access to the biologically active molecules.⁶³ In this context, an intriguing approach to click carbohydrate based alkyne and azide functionality is the CuAAC reaction. CuAAC reaction allow facile access to emerging class of triazole appended carbohydrate building blocks such as glycoconjugates,^{46,47} glycopolymers,⁶⁴ glycohybrids,⁶⁵ glycopeptides,⁶⁶ glycoproteins,⁶⁷ glycolipids,⁶⁸ glycoclusters,⁴⁸ and glycodendrimers.⁶⁹ These glycoproducts have widespread applications including medicinal science, material science, gelation, chelation, sensing, glycosylation, pharmacology and catalysis.⁴⁶⁻⁵⁸ However, sustainable synthetic approach of this modular and bio-orthogonal click carbohydrate chemistry is less explored. Many CuAAC reactions have been performed in conventional green solvents such as water, alcohols and their mixtures.⁷⁰⁻⁷³ However, various groups carried out CuAAC reactions in harmful organic solvents such as acetonitrile, DCM, toluene and THF.⁷⁴⁻⁷⁷ There is a recent trend to find alternative (non-hazardous) solvents. Vaccaro *et al.* used a mixture of water and biomass-derived furfuryl alcohol⁷⁸ and a mixture of water and Polarclean⁷⁹ as green media. Various groups used ionic liquids⁸⁰ and deep eutectic solvents (DESs)⁸¹⁻⁸³ as alternative reaction media. Very recently, we reported CuAAC reaction in presence of Copper(I) coordination polymer as effective catalyst in DES as sustainable solvent.⁸⁴ The selection of sustainable solvents in “click chemistry” for the syntheses of glucopyranosyltriazaoles is equally important. The catalytic protocols for the syntheses of 1,4-disubstituted 1,2,3-triazoles linked with glycoconjugates mostly used environmentally hazardous solvents like dichloromethane (DCM), toluene, dimethylformamide (DMF) and acetonitrile.^{46,47} In 2003, Santoyo-González have prepared multivalent neoglycoconjugates by using the organic-soluble Copper complexes (Ph₃P)₃CuBr and (EtO)₃PCuI as catalysts in toluene under microwave irradiation (Scheme 4.1).⁸⁵ Tiwari and co-workers reported elegant syntheses of various triazolyl glycoconjugates embedded with ethisterone,⁸⁶ o-

benzylquercetin,⁸⁷ noscapine,⁸⁸ bistriazolyl,⁸⁹ vanillin,⁹⁰ 1,3,4-oxadiazole,⁹¹ noscapine^{92,93} and glycodendrimers⁹⁴ in the presence of CuI and DIPEA in DCM (**Scheme 4.1**). However, a large amount of Copper and ligands was used. Very recently, Singh and co-workers also utilized DCM as reaction medium for the efficient syntheses of a variety of glycoconjugate triazoles in presence of mono or dinuclear Cu(I) complexes.^{95,96} We paid serious attention to perform CuAAC reactions for the syntheses of glucopyranosyltriazaoles, in which catalytic protocol does not require extra purification steps and can also be performed in environmentally benign solvents. In this context, Dondoni and co-workers validated the CuAAC reaction in 10 different ionic liquids which opens up a new perspective in glycol chemistry using this prototype click method.⁹⁷ However, a large majority of ionic liquids are expensive, very complex to prepare, highly toxic and non-biodegradable. In contrast, various synthetic research groups have considered DES (particularly, metal-free type-III DES) as an emerging class of green media with distinct properties which can balance the major disadvantages of ionic liquids.⁹⁸⁻¹⁰³ However in a very recent review, Marrucho and Guazzelli et al. expressed serious concerns for the general notion of considering DES as a much better alternative to ionic liquids.¹⁰⁴ Although, they concluded DESs (with wisely selected starting components) as a promising environmentally benign solvent to replace traditional volatile organic solvents. To the best of our literature search, the use of DES in click inspired syntheses of glycoconjugates have not been investigated so far. Hence, we studied the potential applicability of DES as sustainable reaction medium for the synthesis of important glycoconjugate triazoles for the first time *via* CuAAC reaction (**Scheme 4.1**). Herein, we report readily accessible and well-defined Copper(I)-iodide complex with NNO ligand framework as efficient catalyst for the syntheses of various glucopyranosyltriazaoles in DESs (**Scheme 4.1**).

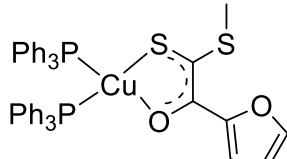
Scheme 4.1 CuAAC reaction in synthesis of triazolyl glycoconjugates and sustainable features of the present work.

Previous work:

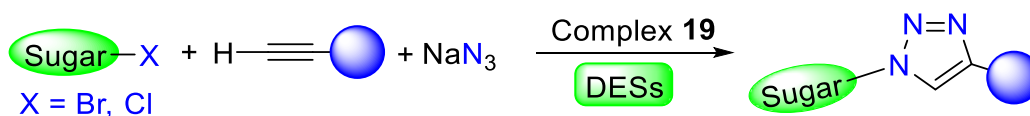


Santoyo-González et al.
[Cu]: (Ph₃P)₃CuBr or (EtO)₃PCuI (10-20 mol%)
Ligand: DIPEA or DBU (3 eqv)
Solvent: Toluene
Temp & time: r.t. MW (850W), 45 min
Org. Lett. 2003, 5, 1951

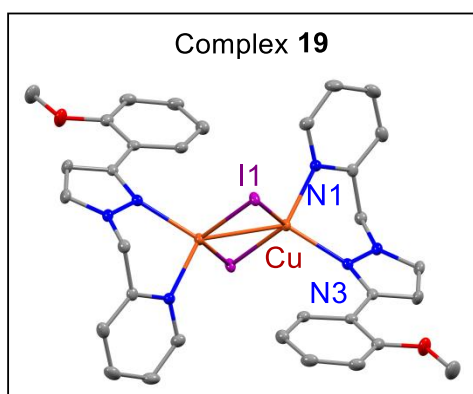
Tiwari et al.
[Cu]: CuI (2 eqv)
Ligand: DIPEA (3 eqv)
Solvent: DCM
Temp & time: r.t. 12h
New J. Chem. 2019, 43, 12475

Singh et al.
[Cu]: 1 mol%

Solvent: Dry DCM
Temp & time: r.t., 3 h
New J. Chem. 2019, 43, 1166

Present work:



Reaction condition : 19 (1.5 mol%), TBAB/glycerol (1:4), 70 °C, 12 h



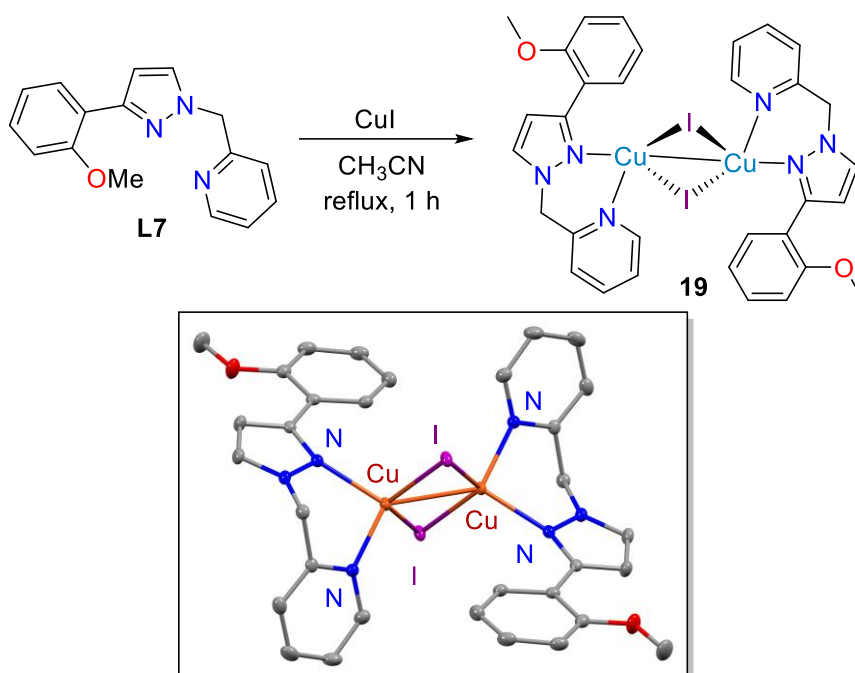
- ✓ Three component one pot reaction
- ✓ Stable well-defined Cu(I)-catalyst
- ✓ No use of reducing agent
- ✓ Green and sustainable medium
- ✓ Easy product isolation (filtration only)
- ✓ Reaction media recycled 5 times
- ✓ 2.15 < E-factor < 3.12
- ✓ Wide substrate scope
- ✓ Excellent isolated yields of products

4.3 RESULTS AND DISCUSSION

In the past two decades, various Copper(I) complexes have been extensively used as catalysts in CuAAC reactions.²⁹⁻⁴⁵ The active Copper(I) species required for this chemical transformation can also be generated *in situ* by the reaction of Copper(II) salt with a reducing agent such as sodium ascorbate. However, problem arises with the stability of the Copper(I) complexes during the course of reaction and poor solubility of Copper(I) salts in common organic solvents. Therefore, considerable attention has been paid in recent years to synthesize stable as well active Copper(I) complexes with appropriate ligand systems.¹⁰⁵ In this regard, majority of the developed Copper(I) systems are those with phosphines and *N*-heterocycle carbenes (NHCs).^{106,107} Phosphines and NHCs are the ligands with strong donor ability and resulting Copper(I) complexes showed good catalytic activity. Very recently, phosphine-based Copper(I) oxodithioester, dioxanthate and xanthate complexes are used for synthesis of triazolyl glyconjugates under homogeneous conditions.^{95,96} Complexes with N, O and S donor ligand systems also used for this CuAAC reaction.¹⁰⁸⁻¹¹⁰ Recently, our group reported an air-stable and well-defined Copper(I)-chloride coordination polymer with NNS ligand framework for sustainable synthesis of various triazoles in green solvents.⁸⁴ However, coordination of that NNS ligand with CuI resulted in insoluble solid and we could not reveal its identity. Similar tridentate NNO ligand system^{111,112} might also be effective to develop Copper(I) catalyst with high efficiency. Therefore, we have selected a NNO ligand **L7** and facile coordination of ligand **L7** with CuI resulted in the formation of a dinuclear Copper(I) **19** (Scheme 4.2). **19** was characterized by ¹H and ¹³C NMR spectroscopy, IR spectroscopy, mass analysis and elemental analysis. In the ¹H NMR spectrum of **19**, the methoxy methyl and methylene protons were appeared as singlet at 3.76 and 5.55 ppm, respectively. Aromatic protons were observed in the expected downfield region (6.70–8.52 ppm). In the IR spectrum of **19**, mixed stretching vibration of C=N and C=C bonds of the pyrazole ring was slightly shifted to 1515 cm⁻¹ in

comparison to the free ligand **L7** (1505 cm^{-1}). Symmetric and asymmetric vibrations due to $\text{C}(\text{sp}^3)\text{-H}$ bonds stretching was observed in the range of 3130 to 2740 cm^{-1} . The vibrational stretching bands in the range of 1400 to 1640 cm^{-1} were assigned for phenyl ($\text{C}=\text{C}$) and pyridyl ($\text{C}=\text{N}$) functionalities. Molecular ion peak was observed at 328.0517 in the mass spectrum of **19**.

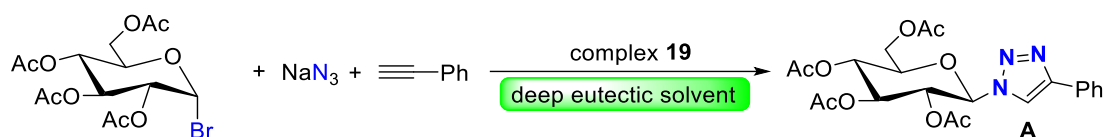
Scheme 4.2 Synthesis of Copper(I) iodide **19 (the molecular structure of **19** showing 30% ellipsoids and hydrogen atoms are omitted for clarity).**



We have further used single crystal X-ray diffraction analysis to know the geometrical identity of **19** (Scheme 4.2). Single crystal X-ray diffraction analysis revealed that **19** crystallized in monoclinic system with space group $P2_1/c$. The asymmetric unit of **19** consist of half of the centrosymmetric dimer in which the Copper centre is surrounded by two nitrogen atoms of the NNO ligand and one iodide. It is worth to mention that the hard oxygen donor ether moiety did not bind to the Copper centre and was moved away from the metal through the rotation of the C-C bond. Although, this NNO ligand has been reported as a tridentate ligand, **L7** behaves as a bidentate ligand with CuI . The coordination geometry of Cu(I) center in **19** can be best described as highly distorted tetrahedral due to the presence of large iodide donors.^{109,110} The

Cu...Cu distance in **19** is 2.6101(6) Å, which is in the range of Cu...Cu single bond distance (ideal Cu...Cu covalent bond distance is 2.64 Å while the corresponding van der Waals' distance is 2.80 Å).¹¹⁰ The Cu–N_{pyridyl}, Cu–N_{pyrazolyl} and Cu–I bond lengths are 2.091(5), 2.118 (5) and 2.627(13) Å, respectively. All these bond distances are in the expected range and are consistent with similar Cu(I) complexes having tetrahedral geometry.^{109,110} It is worth to mention that binuclear **Copper 19** is highly stable in solid state for weeks; however, it slowly decomposes upon long exposure in air in solution state.

A substantial amount of research effort has been devoted in search of better catalysts for click reaction and this can be considered as a general trend in different fields of catalysis. In contrast, traditionally research community has paid minor attentions in selecting sustainable reaction media. The click reaction in glycochemistry have already been explored and the reaction is performed in various hazardous organic solvents such as toluene, DCM, acetonitrile, DMF and THF.^{46–58,86–96} Herein, for the first time, we studied the use of deep eutectic solvents (DESs) as reaction media for the syntheses of triazolyl glycoconjugates. In our present work, a series of DESs were prepared through the combination of various hydrogen-bond acceptor such as choline chloride (ChCl), tetra butyl ammonium bromide (TBAB), tetramethyl ammonium chloride (TMAC) and methyl triphenyl phosphonium bromide (MTPB) and various hydrogen bond donors, namely urea, thiourea, glycerol and ethylene glycol. A literature ratio^{100,113} of this hydrogen-bond acceptor and hydrogen bond donors was used to prepared total ten DESs and all were screened for the syntheses of triazolyl glycoconjugates *via* prototype click reaction catalyzed by Cu(I) iodide **19** (**Table 4.1**). It is worth to mention that we used type III DESs as a class of metal-free green solvents.

Table 4.1 Catalytic activity of **19 for CuAAC reaction in various DESs^a**

Ent	Cat. 19 (mol %)	Solvent mixture (ratio)	Temp. (°C)	Time (h)	Yield ^b (%)
1	1.5	ChCl/glycerol (1:2)	r.t.	24	35
2	1.5	ChCl/glycerol (1:2)	70	24	97
3	1.5	ChCl/ethylene glycol (1:2)	70	24	83
4	1.5	ChCl/thiourea (1:2)	70	24	97
5	1.5	ChCl/urea (1:2)	70	24	70
6	1.5	TBAB/glycerol (1:4)	70	24	98
7	1.5	TBAB/ethylene glycol (1:4)	70	24	82
8	1.5	TMAC/glycerol (1:2)	70	24	56
9	1.5	TMAC/ethylene glycol (1:2)	70	24	60
10	1.5	MTPB/glycerol (1:3)	70	24	97
11	1.5	MTPB/ethylene glycol (1:3)	70	24	98
12	1.5	ChCl/glycerol (1:2)	70	12	94
13	1.5	ChCl/thiourea (1:2)	70	12	58
14	1.5	TBAB/glycerol (1:4)	70	12	98
15	1.5	MTPB/glycerol (1:3)	70	12	80
16	1.5	MTPB/ethylene glycol (1:3)	70	12	76
17	1.5	TBAB/glycerol (1:4)	70	10	87
18	1.5	TBAB/glycerol (1:4)	70	8	75
19	1	TBAB/glycerol (1:4)	70	12	76
20	1.5	TBAB/glycerol (1:4)	r.t.	12	31

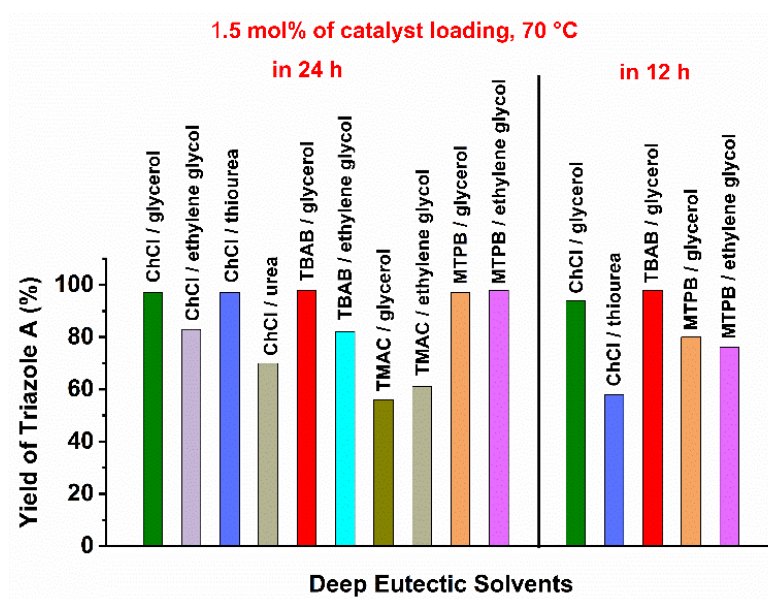
^a Reactions conducted in a vial (10 mL) with 0.25 mmol of acetobromo- α -D-glucose, 0.25 mmol of phenyl acetylene, 0.75 mmol of sodium azide, 1/1.5 mol% **19** (2/3 mol % [Cu]) in 2 mL of DES at r.t./70 °C. ^b Isolated yields of triazole product **A**.

With a readily available well-defined Copper(I) complex in hand, we investigated the catalytic efficiency of **19** for a three component CuAAC reaction with phenyl acetylene, sodium azide and acetobromo- α -D-glucose as standard substrates (**Table 4.1**). Instead of using expensive and

unstable organoazides, *in situ* generated organoazides by reacting sodium azide and halo-derivatives brings certain advantages. Thus, we focused on the three component CuAAC reaction to test the catalytic activity of **19** in various DESs (**Table 4.1** and **Fig. 4.1**). For the first set of experiments, a mixture of choline chloride (ChCl) and glycerol (1: 2), a heavily used and a very common DES, was used at r.t. Using 1.5 mol% catalyst loading (3 mol% [Cu]), we found only 34% yield of triazolyl glycoconjugate **A** in 24 h (entry 1). The triazole product **A** was analyzed by using ¹H-NMR spectroscopy. The starting α -D-glucose is converted into a β -isomer of glucopyranosyltriazole *via in situ* formation of stable acetoazido- β -D-glucose. This initial catalytic activity of **19** in ChCl/glycerol (1: 2) was found to be poor at r.t. Hence, the following CuAAC reactions were conducted at elevated temperature (70 °C). According to CHEM21 green metrics toolkit, 70 °C falls in the acceptable range of reaction temperature.¹¹⁴ To our satisfaction, quantitative yield of glucopyranosyltriazole **A** was obtained if the reaction was performed in ChCl/glycerol (1 : 2) at 70 °C in presence of 1.5 mol % of **19** (entry 2). Thereafter, we explored various hydrogen bond donors in DES preparation. ChCl/ethylene glycol (1: 2) and ChCl/thiourea (1: 2) as reaction medium resulted in 83% (entry 3) and quantitative (entry 4) yields of **A**, respectively. If we use a mixture of choline chloride and urea in 1: 2 ratios, we found roughly 70% yields of desired triazole **A** under (entry 5). Thus, combination of ChCl as a hydrogen-bond acceptor, and glycerol or thiourea as hydrogen bond donors displayed better catalytic performance as compared to other ChCl based DESs. Next, we explored various other well-known DESs by varying both hydrogen-bond donors and hydrogen-bond acceptors. We tested six other DESs namely TBAB/glycerol (1:4), TBAB/ethylene glycol (1:4), TMAC/glycerol (1:2), TMAC/ethylene glycol (1:2), MTPB/glycerol (1: 3), and MTPB/ethylene glycol (1: 3). Under unaltered reaction conditions except various solvents (as used in entry 2 to 5), we found quantitative yields in case of TBAB/glycerol (1: 4) (entry 6), MTPB/glycerol (1: 3) (entry 10), and MTPB/ethylene glycol

(1:3) (entry 11). In contrast, comparatively less catalytic efficiency was noted in TBAB/ethylene glycol (1:4) (80%, entry 7), TMAC/glycerol (1:2) (56%, entry 8) and TMAC/ethylene glycol (1:2) (60%, entry 9). Hence, it can be concluded that glycerol is an effective hydrogen-bond donor in the present CuAAC reaction. Thereafter, we turned our attention to those DESs which showed quantitative formation of **A** and explored the catalytic activity of **19** at reduced reaction time. We performed the reaction at 70 °C for 12 h in ChCl/glycerol (1:2), ChCl/thiourea (1:2), TBAB/glycerol (1:4), MTPB/glycerol (1:3) and MTPB/ethylene glycol (1:3) in presence of 1.5 mol % **19**. We observed almost quantitative formation of **A** only in ChCl/glycerol (1:2) (entry 12) and TBAB/glycerol (1:4) (entry 14). In all other cases, we found incomplete conversion of starting materials and roughly 60 to 80% yields of **A** were obtained (entry 13: 58%, entry 15: 80% and entry 16: 76%). Thus, we concluded that ChCl/glycerol (1:2) and TBAB/glycerol (1:4) were the best reaction media as full conversion of substrates and quantitative yield of **A** were observed. Further reduction of reaction time to 10 and 8 h in TBAB/glycerol (1:4) resulted in incomplete conversions with small amount of unreacted starting materials (entry 17: 87% and entry 18: 75%). The catalyst loading was also reduced to 1 mol % in TBAB/glycerol (1:4) and again we found less yield of **A** (entry 19: 76%). If the reaction was conducted with 1.5 mol% of catalyst loading at r.t. for 12 h in TBAB/glycerol (1:4), we observed poor yield (entry 20: 30%). From these reaction optimizations, the best conditions were concluded as the following: entry 12: 1.5 mol % of catalyst loading, ChCl/glycerol (1:4), 70 °C, 12 h; entry 14: 1.5 mol% of catalyst loading, TBAB/glycerol (1:4), 70 °C, 12 h (entry 12 and 14: depicted in bold and green)

Fig. 4.1 Comparative catalytic performance of 19 in various DESs.

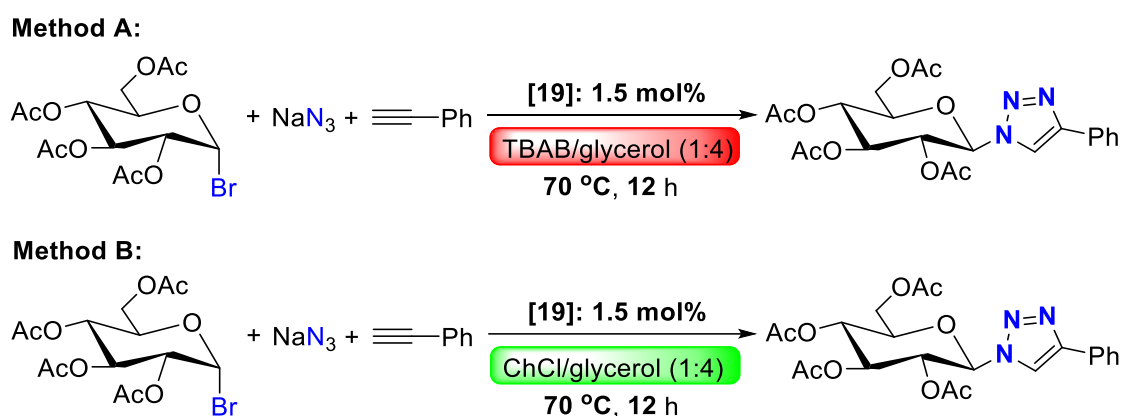


In this current work, we studied the possible use of DES as an emerging class of environmentally benign solvent for CuAAC reaction to synthesize glucopyranosyltriazole and we feel the necessity to evaluate the green and sustainable aspects of our optimized catalytic protocols with the help of “The 12 Principles of Green Chemistry”.^{115–120} In the present protocol for CuAAC reaction, we did not use any additive or reducing agent to stabilise or generate the Copper(I) oxidation state, thus no doubt this is an advantage. A readily available, stable, and well-defined Copper(I)-iodide complex is directly used for three component cycloaddition reaction between acetobromo- α -D-glucose and phenyl acetylene in presence of sodium azide. Thereafter, the best optimized reaction conditions (entry 12 and 14 in **Table 4.1**) were evaluated with the help of CHEM21 green metrics toolkit which is a reckonable extension of “The 12 Principles of Green Chemistry”.¹¹⁴ The results of these two methods (Method A and B) are summarized in **Table 4.2**. In past, several research groups (including us) utilized this toolkit to determine the green and sustainable aspects of various catalytic transformations.^{111,121–125} Herein, we examined the optimized CuAAC reaction protocols by utilizing zero pass and first pass of CHEM21 green metrics toolkit. This toolkit also has second and third pass, but these are considered as industrial toolkits and outside the scope of the present

study. The desirable and undesirable processes are highlighted by three different flags; green flag defines an acceptable process; amber flag stands for acceptable with concerns and red flag indicates undesirable process. First, we checked the metrics yield, conversion, and selectivity. As both optimized reaction conditions gave full conversion, almost quantitative yields and excellent regioselectivity, green flags were assigned for all three metrics yield, conversion (conv.) and selectivity. High atom economy (A.E.), reaction mass efficiency (M.E.), optimum efficiency and mass intensity demonstrated high efficiency of both catalytic processes. Solvent is a crucial metric and we have used TBAB/glycerol (1:4) and ChCl/glycerol (1:2) as a metal-free type-III DES in our optimized protocols. As TBAB has potential issues as reflected with amber and red H-codes, method A received red flag for solvent metric. As both ChCl and glycerol as associated with green H-codes, solvent metric for method B earned green flag. As our methods are catalytic, they received green flag. However, we were unable to recover the catalyst. Thus, catalyst recovery metric received red flags both Method A and B. After completion of CuAAC reaction, triazole product binds Copper center and the Copper catalyst are lost with the product. After product isolation, the reaction medium was free of Copper and thus, the catalyst could not be recycled. However, the reaction media were recovered successfully. The recovered DESs were reused and recycled five times to perform new sets of CuAAC reactions and hence, this metric earned green flag. Although Copper is very cheap and an earth-abundant base metal, worldwide availability of Copper is dependent on geo-political issues. In that sense, Copper as catalyst received amber flag in element metric. Next amber flag was assigned for reactor as we performed the reactions in batch. Generally, a reaction conducted in continuous flow process receives green flag. Then the work-up processes were analyzed. In our optimized catalytic protocols, we utilized very common and easy work up techniques. The desired triazole product was simply isolated by dilution of the reaction media followed by filtration and washing with aq. ammonia solution. The isolated product was pure

which does not require any further complex purification steps such as column chromatography. Thus, the present method is highly sustainable and assigned with green flag. Thereafter, the energy parameter of our catalytic protocol was considered. CHEM 21 green metrics toolkit also guided us in structuring a chemical process; an acceptable temperature range in terms of favourable energy is 0 to 70 °C. We have performed our reactions at 70 °C and hence, they earned green flag in energy metric. Overall, our catalytic protocols are sustainable as most of the metrics earn green flags. However, Method B with ChCl/glycerol (1: 2) can be considered as a better one (green flag for solvent metric). Most importantly use of DESs as environmentally benign reaction media opens a new pathway for the syntheses of important glycoconjugates.

Table 4.2 Calculation of different metrics of CuAAC reaction under optimized condition



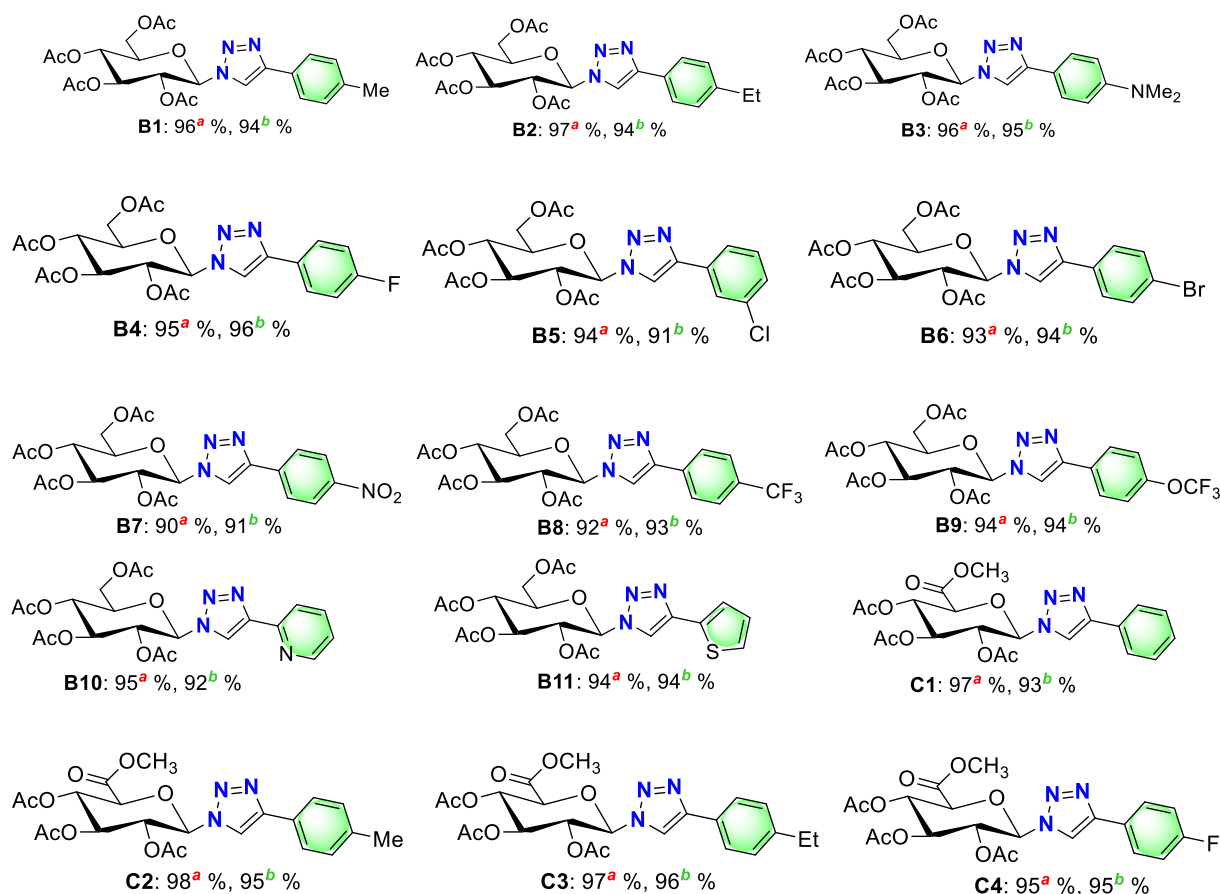
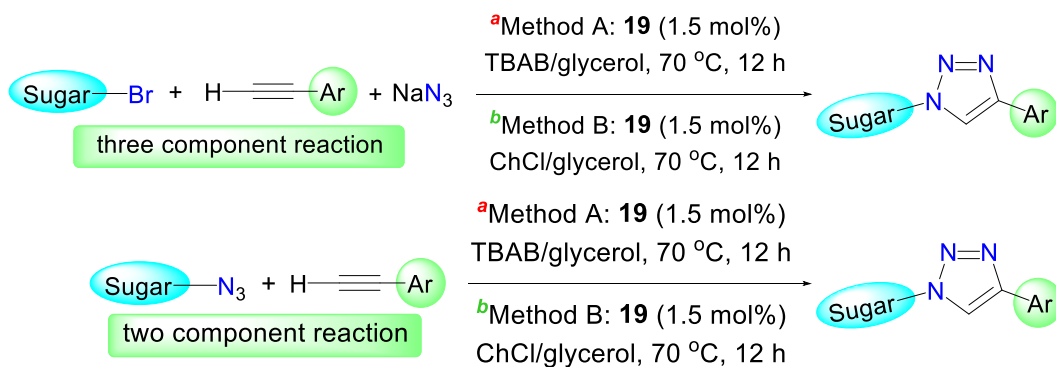
Meth.	Yield	Conv.	Selectivity	A.E.	M.E.
A	98 	100 	98 	82.2	69.0
B	94 	100 	94 	82.2	66.1
Meth.	Optimum Efficiency	Mass Intensity	Solvent	Catalyst	Catalyst Recovery
A	83.9	15.5	TBAB/glyc. 	Yes 	NO 
B	80.5	16.3	ChCl/glyc. 	Yes 	No 
Meth.	Media Recovery	Element	Reactor	Work up	Energy
A	Yes 	Cu 	Batch 	Filtration 	70 °C 
B	Yes 	Cu 	Batch 	Filtration 	70 °C 

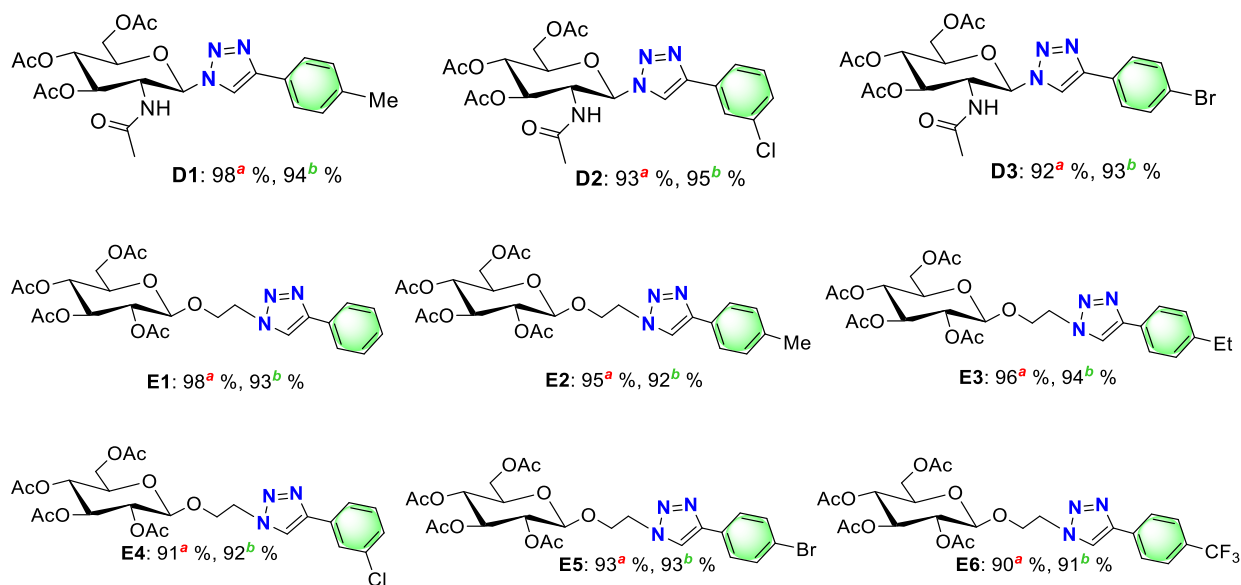
To achieve green and sustainable development, waste management (remaining starting materials, by-products, unrecovered catalysts, and solvent losses *etc.*) in chemical processes is a crucial factor. In this regard, *E*-factor gives us a general idea to estimate the quantity of waste generated for the production of one kilogram of desired product.^{126,127} Thus, calculation of *E*-factor is essential to evaluate real applicability and environmental acceptability of a chemical process. Usually, favourable *E*-factor should be in the range of 1 to 5. The calculated *E*-factors of present optimized catalytic processes of CuAAC reactions are in the range of 2 to 4 (Method A: 2.21-3.02, Method B: 2.38-3.12), which reflects the potential applicability of the present optimized protocol for the bulk production of important glycoconjugates. Additionally, two gram-scale reactions were also effectively conducted using 10 mmol acetobromo- α -D-glucose and phenyl acetylene in presence of sodium azide (25 mmol) and we observed close to quantitative yields of desired triazole **A**. Hence, these catalytic methodologies illustrate the possible use of DES as a reusable solvent for the syntheses of triazole equipped glycoderivatives (in contrast to the commonly use hazardous organic solvents) and this might also be realistic for probable industrial application.

To probe the practical applicability of our approach, we explored the substrate scope under both of the optimized reaction conditions (**Scheme 4.3**). For this purpose, we carried out CuAAC reactions with the combination of four different glycosides containing halide or azide functionality. Halide compounds were *in situ* converted to the corresponding azides by reacting with sodium azide. We did not use sodium azide when the starting glycosides had an azide functionality. We also tested various terminal alkynes. Primarily under the optimized reaction conditions, acetobromo- α -D-glucose (in presence of sodium azide) was successfully clicked with different terminal alkynes having electron donating and withdrawing functionalities and we found excellent yields of various 1,4-disubstituted 1,2,3-gluco-pyranosyltriazoles (**B1, B2, B3, B4, B5, B6, B7, B8, B9**). Therefore, good tolerance to various electronic environment of the functional groups was observed. It is noteworthy to mention that all these triazolyl glyco-products were isolated by simple dilution of reaction media followed filtration and washing with aqueous ammonia solution. Thereafter, the combination of acetobromo- α -D-glucose with terminal alkynes having five- or six-member heterocycles also gave excellent yields of desired triazole products (**B10, B11**). Then, we tested another glycoside acetobromo- α -D-glucuronic acid methyl ester (at C5 position). Acetobromo- α -D-glucuronic acid methyl ester was also effectively clicked with various terminal alkynes with electron donating as well electron withdrawing groups and expected triazole products were obtained in excellent yields (**C1, C2, C3, C4**). Thereafter, we tested a glycoside which has acetamide substitution at C2 instead of acetoxy group. 2-Acetamido-2-deoxy- α -D-gluco-pyranosyl chloride 3,4,6-triacetate was also combined smoothly with various terminal alkynes. Good tolerance to various electronic environment was noted with excellent yields of triazole products (**D1, D2, and D3**). Finally, 2-azidoethyl 2,3,4,6-tetra-*O*-acetyl- β -D-gluco-pyranoside was tested to click with various terminal alkynes and we observed excellent yields of the corresponding triazoles

(E1, E2, E3, E4, E5, E6). Thus, the electronic nature of the substituents has almost no effect in this CuAAC protocol catalyzed by **19** in DESs.

Scheme 4.3. CuAAC reactions of various glycosides and terminal alkynes using optimized methods.
 TBAB/glycerol (1: 4) and ChCl/glycerol (1: 2) using optimized methods.





4.4 CONCLUSION

Facile complexation of a tridentate NNO ligand **L7** with Copper iodide resulted in the formation of a dimeric Copper(I) **19**. **19** was characterised by standard techniques such as elemental analysis, mass spectrometry, IR and NMR spectroscopy and single crystal X-ray crystallography. **19** proved to be an effective catalyst for the synthesis of numerous triazole equipped glycoconjugates using CuAAC reaction. This 1,3-cycloaddition of azido-glycose and terminal alkyne was performed in eleven different DESs. Among those, TBAB/glycerol (1:4) and ChCl/glycerol (1:2) were found to be the best reaction media and almost quantitative yields of the desired 1,4-disubstituted 1,2,3-glucopyranosyltriazoles product were achieved in 12 h at 70 °C in presence of 1.5 mol % of catalyst loading. This study showed, for the first time, the straightforward use of reusable and environmentally benign type-III DES as reaction medium for the syntheses of various glucopyranosyltriazoles using click chemistry. Purification of product by using very simple work-up procedure (filtration) is also advantageous. Although used Copper catalyst could not be recovered, the used reaction media was reused several times. The sustainable features of the optimized reaction protocols were examined with the help of CHEM21 green metrics toolkit. Additionally, the catalytic protocols generated minimum waste as reflected by low *E*-factor of 2.21 < *E*-factor < 3.12. Thus, the present catalytic system is

highly sustainable and opens up a new perspective in successful use of DES as a reaction medium in glycochemistry inspired by prototype click reaction.

4.5 EXPERIMENTAL SECTION

4.5.1 Synthesis of ligand L7 and Copper(I) 19

Synthesis of ligand L7: Compound 3-(2-methoxyphenyl)-1H-pyrazole is a known compound and was synthesized using following procedure. A solution of 2-Methoxy acetophenone (1.50 g, 10.0 mmol) in a 1:1 mixture of DMF-DMA (15 mL) was reflux for 3 days under inert condition to give an orange brown solution. Removal of solvents under vacuum gave a brown oil. Thereafter, ethanol (20 mL) and hydrazine hydrate (1.28 g, 40.0 mmol) were added and the reaction mixture was refluxed for 2 hours. The resulting yellow solution was cooled to room temperature and cold water (15 mL) was added giving an off-white precipitate. The mixture was kept at 0-4 °C overnight to allow complete precipitation and the solid was collected after filtration. The solid was washed with cold water (3 x 20 mL) to give a white solid as pure product (1.67 g, 96%). ¹H NMR (CDCl₃): δ 12.50 (br, 1H), 7.73 (m, 1H), 7.69 (s, 1H), 7.09 (m, 2H), 6.67 (s, 1H), 4.02 (s, 3H).

In a pressure tube, 3-(2-methoxyphenyl)-1H-pyrazole (1.74 g, 10.0 mmol), 2-(chloromethyl) pyridine hydrochloride (1.64 g, 10.0 mmol), NaOH solution (40%, 5 mL) and toluene (15 mL) were added and the reaction mixture was stirred at r.t. for 15 mins. Then tert-butylammonium hydroxide (4 mL) was added and the reaction mixture was stirred at 130 °C temperature for 24 h. The resulting red mixture was cooled down to r.t. and extracted with ethyl acetate (3 x 50 mL). All volatiles were removed under high vacuum to give 2-((3-(2-methoxyphenyl)-1H-pyrazol-1-yl) methyl) pyridine as pure product (2.27 g, 73%). ¹H NMR (400 MHz, CDCl₃) δ 8.59 (s, 1H), 7.98 (dd, *J* = 7.7, 1H), 7.62–7.64 (m, *J* = 7.7, 1H), 7.56 (d, *J* = 2.3 Hz, 1H), 7.28–7.30 (m, *J* = 8.2, 1.7 Hz, 1H), 7.20 (dd, *J* = 7.0, Hz, 1H), 7.08–6.96 (m, 3H), 6.87 (d, *J* = 2.3 Hz, 1H), 5.53 (s, 2H), 3.91 (s, 3H). ¹³C NMR (101 MHz, CDCl₃) δ 157.13, 156.87, 149.34,

149.01, 137.20, 130.53, 128.87, 122.76, 122.45, 121.83, 120.91, 111.39, 107.79, 57.73, 55.57. HRMS (ESI-TOF) m/z : $[M + H]^+$ calcd for $C_{16}H_{16}N_3O$ 266.1293; found 266.1285. Anal. Calcd for $C_{16}H_{15}N_3O$ (265.12): C, 72.43; H, 5.70; N, 15.84. Found: C, 72.25; H, 5.56; N, 15.68. FTIR V_{max} (cm^{-1}): 2800–3100 (C–H), 1505 (N–N), 1410–1600 (C=N, py; C=C, ph).

Synthesis of Copper (I) 19

The ligand (0.066 g, 0.25 mmol) was dissolved in 5 mL CH_3CN in a Schlenk tube inside the glovebox. CuI (0.047 g, 0.25 mmol) suspension in acetonitrile was then added to the ligand solution with continuous stirring. The reaction mixture turned into whitish colour solution and the stirring was continued for 24 hours. The reaction mixture was then dried in high vacuum and the NMR of the crude solid was recorded in $DMSO-d_6$. The crude solid was then dissolved in DMF and taken into a 5 mL vial. The crystallization was carried out by diffusing with diethyl ether. Block shape white crystals suitable for X-ray crystallography were grown at the bottom of the vial after two days. Yield: (0.093 g, 82%). 1H NMR (700 MHz, $DMSO$) δ 8.51 (s, 1H), 8.03 (s, 1H), 7.95 (t, $J = 7.5$ Hz, 1H), 7.84 (d, $J = 6.5$ Hz, 1H), 7.57 (s, 1H), 7.44 (s, 1H), 7.30 (t, $J = 7.3$ Hz, 1H), 7.03 (d, $J = 8.3$ Hz, 1H), 6.88 (t, $J = 7.3$ Hz, 1H), 6.69 (s, 1H), 5.55 (s, 2H), 3.75 (s, 3H). ^{13}C NMR (101 MHz, $DMSO$) δ 156.47, 154.19, 149.78, 148.38, 138.51, 132.36, 129.62, 129.51, 124.14, 123.97, 120.89, 120.14, 111.49, 107.21, 55.42, 54.92. Anal. Calcd. for $C_{32}H_{30}Cu_2I_2N_6O_2$ (911.50): C, 47.17; H, 3.32; N, 9.22; Found: C, 47.03; H, 3.37; N, 9.10. HRMS (ESI-TOF) m/z : $[M]^+$ calcd for $C_{16}H_{15}CuN_3O$ 328.0511; found 328.0517. FTIR V_{max} (cm^{-1}): 2740–3130 (C–H), 1515 (N–N), 1400–1640 (C=N, py; C=C, ph).

4.5.2 Characteristic spectra of ligand L7 and Copper(I) 19

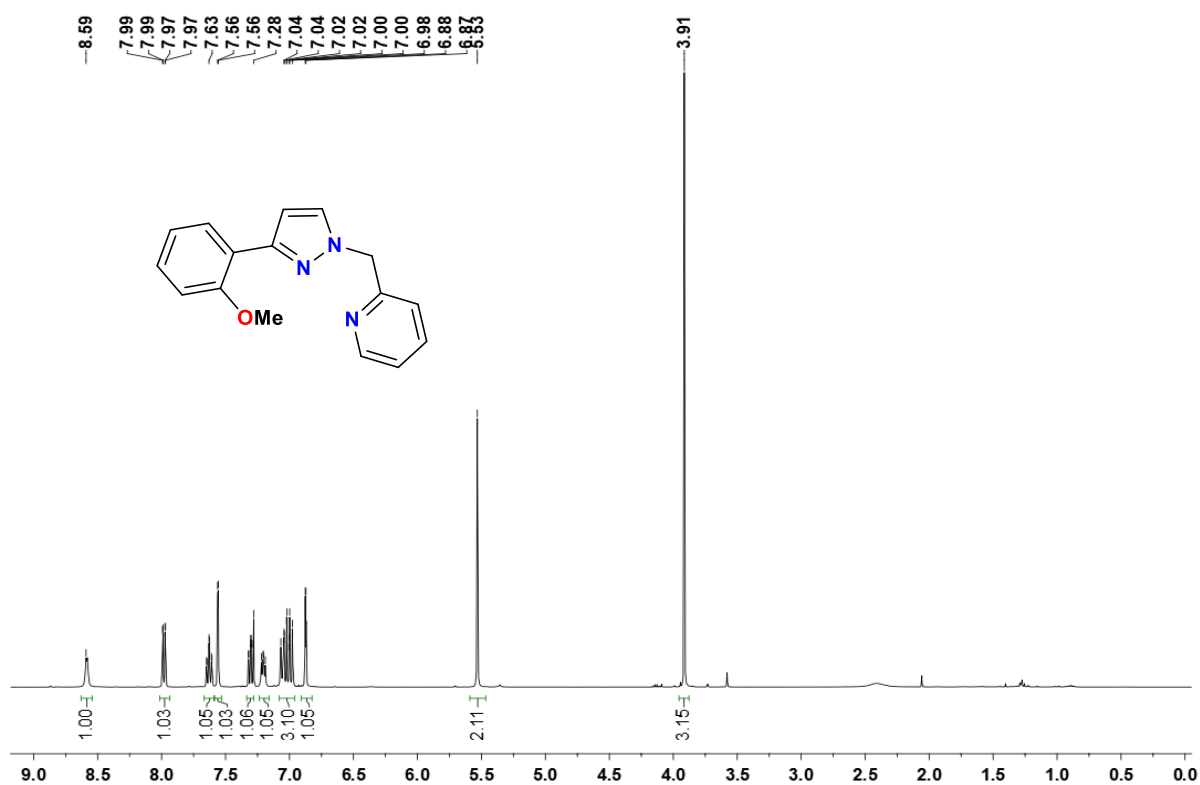


Figure 4.2. ^1H NMR of 2-((3-(2-methoxyphenyl)-1H-pyrazol-1-yl) methyl)pyridine (L7) in CDCl_3 at r.t.

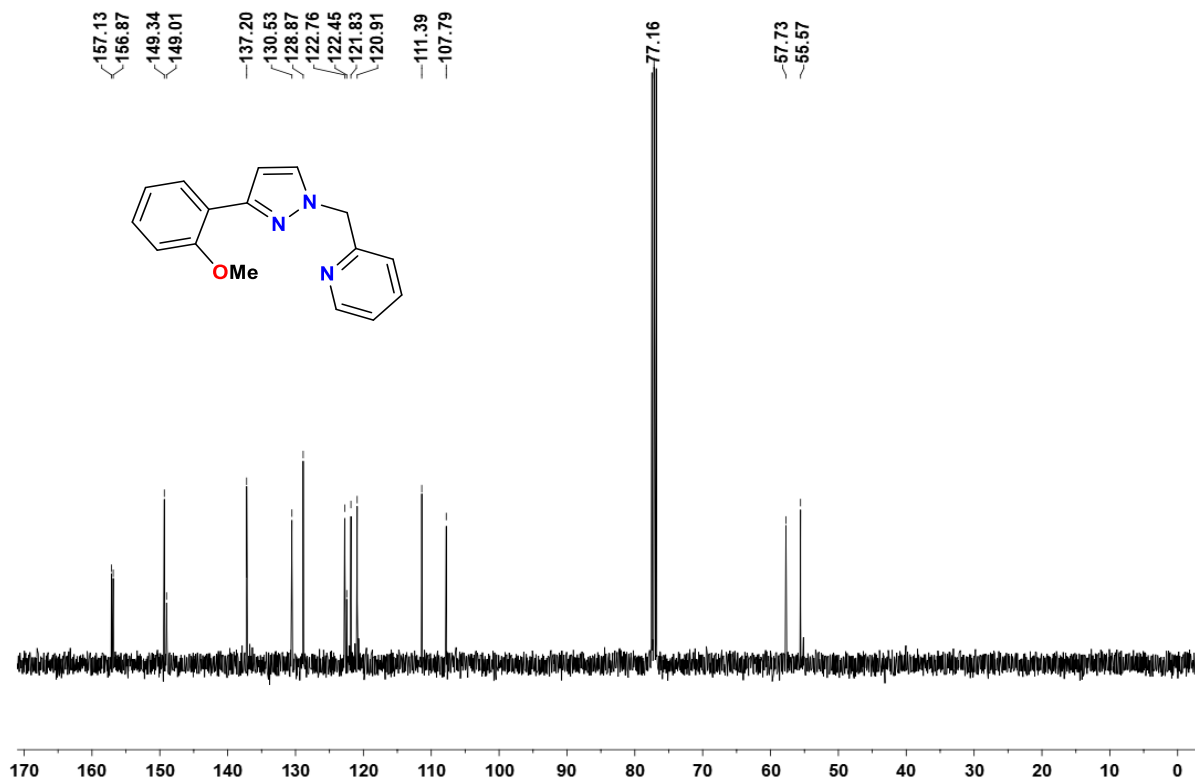


Figure 4.3. ^{13}C NMR of 2-((3-(2-methoxyphenyl)-1H-pyrazol-1-yl) methyl)pyridine (L7) in CDCl_3 at r.t.

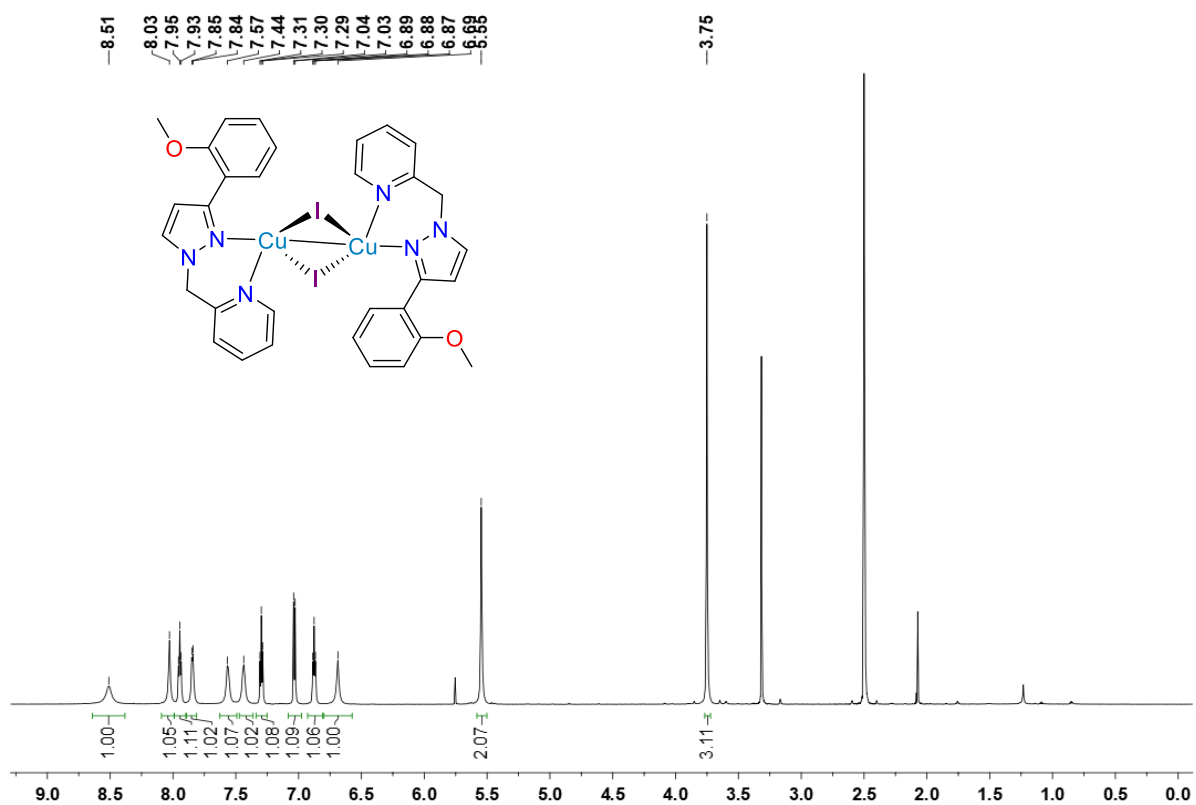


Figure 4.4: ^1H NMR of **19** in DMSO-d_6 .

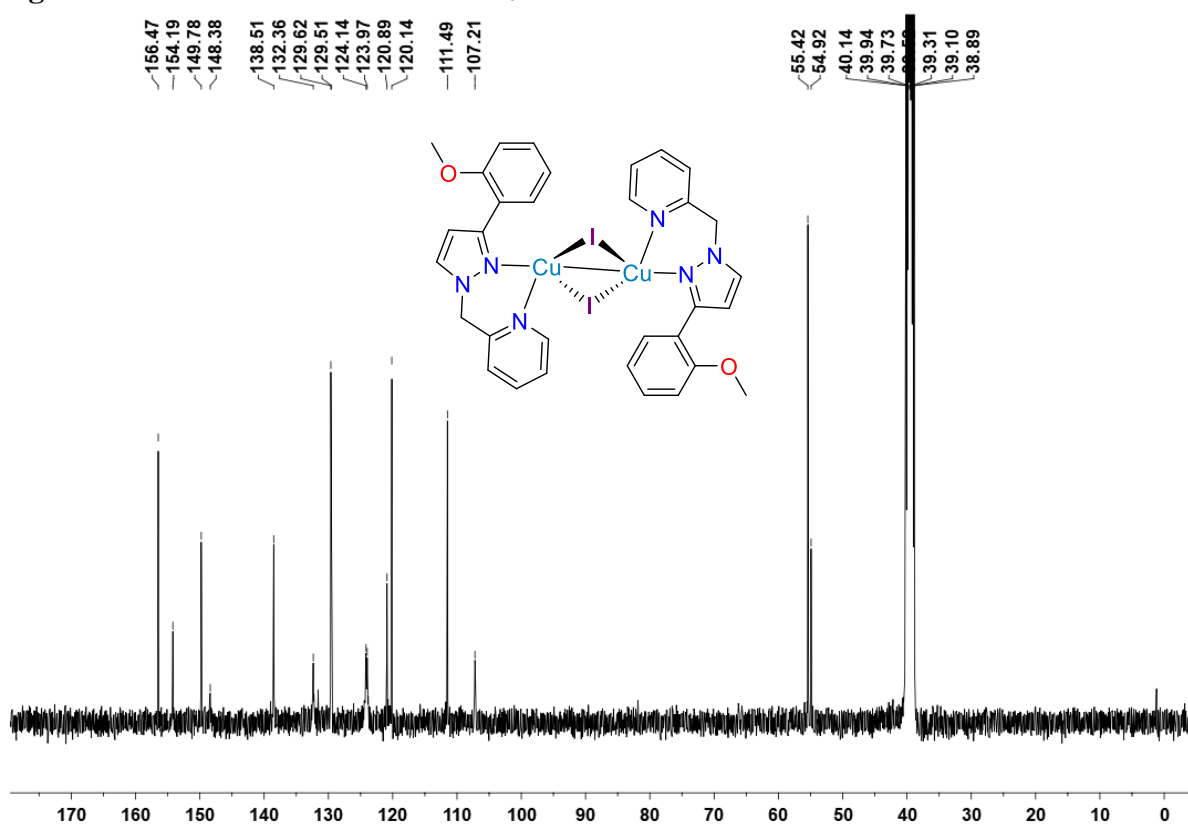


Figure 4.5: ^{13}C NMR of **19** in DMSO-d_6 .

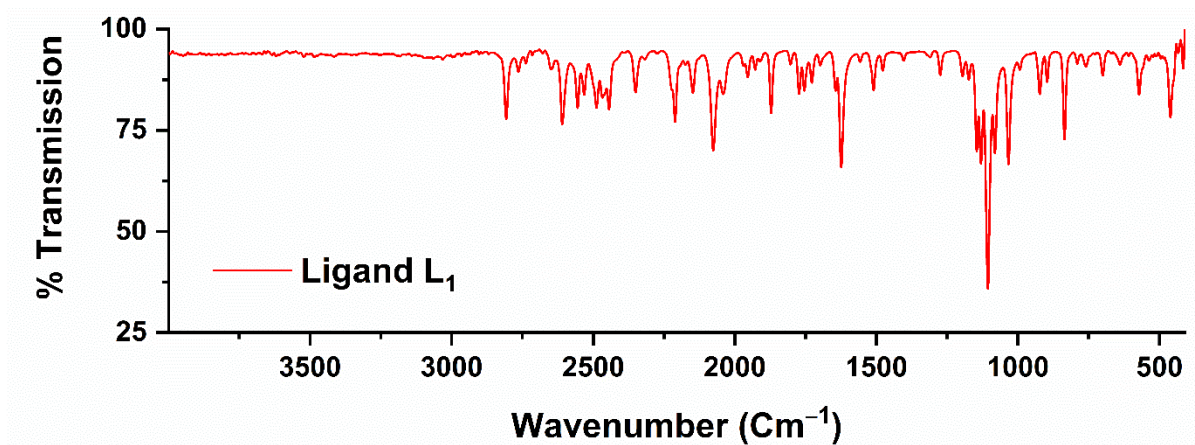


Figure 4.6: FTIR Spectrum of ligand L7.

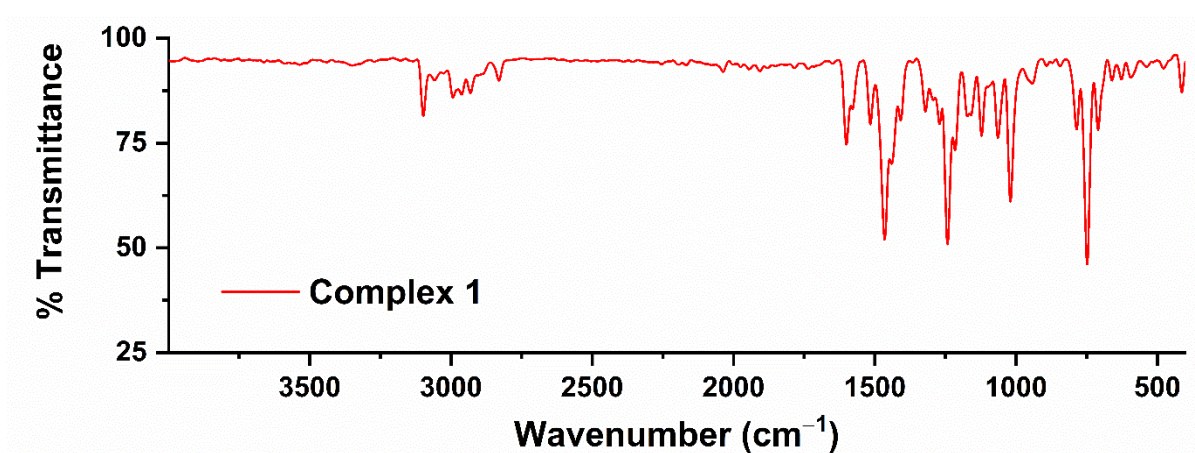


Figure 4.7: FTIR Spectrum of 19.

4.5.3 General procedure for CuAAC reactions (for reaction optimisation).

All the CuAAC reactions were performed under inert condition. 1-Bromo- α -D-glucose tetraacetate, 2,3,4,6-Tetra-O-acetyl- α -D-glucopyranosyl bromide (0.102 g, 0.25 mmol), phenyl acetylene (0.025 g, 0.25 mmol), NaN₃ (0.040 g, 0.625 mmol), and 1.5 mol % Copper 19 (3 mol % [Cu]), were weighed in a vial (10 mL). Thereafter, different deep eutectic solvent for different experiments was added to it. The resultant mixture was heated at appropriate temperature (r.t./ 70 °C) for an appropriate time with stirring. Formation of solid crude was observed after the desire reaction time. The crude solid product was then filtered and washed with additional 2 mL of 25 % ammonia solution to remove Copper from the triazole products. The compound was then dried under vacuum and white crude solid compound was isolated as pure form. The product was dissolved in CDCl₃ and ¹H NMR spectrum was recorded. The

anomeric configuration of the triazole was compared with reported compound from literature and the NMR data/spectra of our products are identical with the reported β -isomer of glucopyranosyltriazaoles. The NMR signature of the corresponding α -D-Glucopyranosyltriazole is different.

4.5.4 General procedure for gram-scale CuAAC reactions:

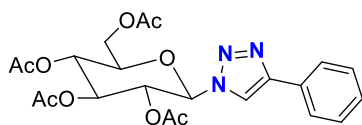
The optimised reaction conditions in TBAB/glycerol (Method A; 1.5 mol% of catalyst loading, ChCl/glycerol (1:2), 70 °C, 12 h) or in ChCl/glycerol (Method B; 1.5 mol% of catalyst loading, ChCl/glycerol (1:2), 70 °C, 12 h) was selected for gram-scale (10 mmol) CuAAC reactions as reaction medium. For this purpose, acetobromo- α -D-glucose (4.112 g, 10 mmol), phenyl acetylene (1.021 g, 10 mmol), NaN₃ (1.625 g, 25 mmol), and Copper 19 (1.5 mol%), were added in 40 mL of TBAB/glycerol (1:4) or ChCl/glycerol (1:2). After the desired reaction time the crude solid product was filtered and washed with additional 20 mL of 25% ammonia solution. The compound was then dried under vacuum and white crude solid compound was isolated as pure form. The product was then dissolved in CDCl₃ and ¹H NMR spectrum was recorded.

4.5.5 General procedure for substrate scope:

Both the optimised reaction conditions (Method A; 1.5 mol% of catalyst loading, TBAB/glycerol (1:4), 70 °C, 12 h; Method B; 1.5 mol% of catalyst loading, ChCl/glycerol (1:2), 70 °C, 12 h) were utilized for the synthesis of various β -D-glucopyranosyltriazaoles. In this regard, four different glucopyran-derivatives (0.25 mmol), and alkynes (0.25 mmol) were combined with sodium azide (0.62 mmol) and Copper 19 (1.5 mol%) in a vial (10 mL). It is important to mention that, we did not use sodium azide when the starting glycosides had an azide functionality i.e., the substrates scope with 2-azidoethyl 2,3,4,6-tetra-O-acetyl- β -D-glucopyranoside. Thereafter, DESs ChCl/glycerol or TBAB/glycerol (1:4) (2 mL) was added to it. The reaction mixture was placed under optimized reaction conditions. After that, the

reaction mixture was diluted with water followed by filtered and washed with 25% ammonia solution to get desire β -D-glucopyranosyltriazoles product. The compound was then dried under vacuum and crude solid compound was isolated as pure form. Occasionally the crude product was purified by column chromatography using silica as stationary phase and ethyl acetate-hexane mixture (1:9) as eluent. The product was then dissolved in CDCl_3 and NMR (^1H and ^{13}C) spectrum was recorded. Most of the products glucopyranosyltriazoles (β -isomer) are reported compounds and the NMR data/spectra of our products are identical with the reported compounds. The NMR signature of the corresponding α -D-Glucopyranosyltriazole is different.

4.5.6 NMR data of the products:



(2R,3R,4S,5R,6R)-2-(acetoxymethyl)-6-(4-phenyl-1H-1,2,3-triazol-1-yl)tetrahydro-2H-pyran-3,4,5-triyl triacetate (A): Isolated as white solid (46.5 mg, 98%). ^1H NMR (400 MHz, CDCl_3) δ 8.00 (s, 1H), 7.86 – 7.80 (m, 2H), 7.43 (t, $J = 7.5$ Hz, 2H), 7.36 (d, $J = 7.4$ Hz, 1H), 5.93 (d, $J = 9.3$ Hz, 1H), 5.52 (t, $J = 9.4$ Hz, 1H), 5.44 (t, $J = 9.4$ Hz, 1H), 5.27 (t, $J = 9.7$ Hz, 1H), 4.33 (dd, $J = 12.6, 5.1$ Hz, 1H), 4.16 (dd, $J = 12.6, 2.0$ Hz, 1H), 4.03 (ddd, $J = 10.1, 5.0, 2.1$ Hz, 1H), 2.08 (d, $J = 3.9$ Hz, 6H), 2.04 (s, 3H), 1.88 (s, 3H). ^{13}C NMR (101 MHz, CDCl_3) δ 170.65, 170.07, 169.53, 169.16, 148.65, 130.01, 129.02, 128.72, 126.05, 117.86, 85.94, 75.31, 72.87, 70.33, 67.88, 61.72, 20.82, 20.68, 20.66, 20.32.



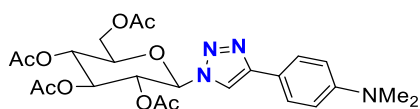
(2R,3R,4S,5R,6R)-2-(acetoxymethyl)-6-(4-(p-tolyl)-1H-1,2,3-triazol-1-yl)tetrahydro-2H-pyran-3,4,5-triyl triacetate (B₁): Isolated as off white solid (47 mg, 96%). ^1H NMR (700 MHz, CDCl_3) δ 7.96 (d, $J = 2.8$ Hz, 1H), 7.77 – 7.67 (m, 2H), 7.24 (d, $J = 4.5$ Hz, 2H), 5.93

(dd, $J = 9.3, 2.8$ Hz, 1H), 5.52 (td, $J = 9.4, 2.8$ Hz, 1H), 5.44 (dd, $J = 9.3, 2.8$ Hz, 1H), 5.27 (dd, $J = 9.7, 2.7$ Hz, 1H), 4.40 – 4.24 (m, 1H), 4.16 (d, $J = 12.6$ Hz, 1H), 4.03 (d, $J = 4.8$ Hz, 1H), 2.38 (d, $J = 2.4$ Hz, 3H), 2.08 (dd, $J = 6.4, 3.0$ Hz, 6H), 2.03 (d, $J = 2.8$ Hz, 3H), 1.88 (d, $J = 2.8$ Hz, 3H). ^{13}C NMR (176 MHz, CDCl_3) δ 170.66, 170.07, 169.53, 169.15, 148.72, 138.63, 129.68, 127.18, 125.95, 117.47, 85.90, 75.27, 72.91, 70.30, 67.88, 61.72, 21.43, 20.82, 20.67, 20.66, 20.31.



(2R,3R,4S,5R,6R)-2-(acetoxymethyl)-6-(4-(4-ethylphenyl)-1H-1,2,3-triazol-1-yl)tetrahydro-2H-pyran-3,4,5-triyl triacetate (B₂): Isolated as white solid (49 mg, 97%).

^1H NMR (400 MHz, CDCl_3) δ 7.96 (s, 1H), 7.76 (s, 1H), 7.74 (s, 1H), 7.27 (s, 1H), 7.25 (s, 1H), 5.93 (d, $J = 9.3$ Hz, 1H), 5.52 (t, $J = 9.4$ Hz, 1H), 5.44 (t, $J = 9.4$ Hz, 1H), 5.31 – 5.22 (m, 1H), 4.40 – 4.25 (m, 1H), 4.16 (dd, $J = 12.6, 2.1$ Hz, 1H), 4.03 (ddd, $J = 10.1, 5.0, 2.1$ Hz, 1H), 2.68 (q, $J = 7.6$ Hz, 2H), 2.09 (s, 3H), 2.07 (s, 3H), 2.03 (s, 3H), 1.87 (s, 3H), 1.25 (t, $J = 7.6$ Hz, 3H). ^{13}C NMR (101 MHz, CDCl_3) δ 170.66, 170.07, 169.53, 169.13, 148.74, 145.02, 128.51, 127.43, 126.05, 117.47 (s), 85.92, 75.29, 72.91, 70.31, 67.90, 61.73, 28.82, 20.83, 20.68, 20.65, 20.31, 15.64.



(2R,3R,4S,5R,6R)-2-(acetoxymethyl)-6-(4-(4-(dimethylamino)phenyl)-1H-1,2,3-triazol-1-yl)tetrahydro-2H-pyran-3,4,5-triyl triacetate (B₃): Isolated as white solid (50 mg, 97%). ^1H NMR (400 MHz, CDCl_3) δ 7.84 (s, 1H), 7.72–7.67 (m, 2H), 6.78–6.74 (m, 1H), 5.91 (d, $J = 9.4$ Hz), 5.53 (t, $J = 9.5$ Hz, 2H), 5.42 (t, $J = 9.4$ Hz, 1H), 5.32–5.19 (m, 1H), 4.32 (dd, $J = 12.6, 5.1$ Hz, 1H), 4.15 (dd, $J = 12.6, 2.1$ Hz, 1H), 4.01 (ddd, $J = 10.1, 5.0, 2.1$ Hz, 1H), 2.99 (s, 3H), 2.08 (s, 3H), 2.07 (s, 3H), 2.03 (s, 3H), 1.87 (s, 3H). ^{13}C NMR (101 MHz, CDCl_3) δ 170.67,

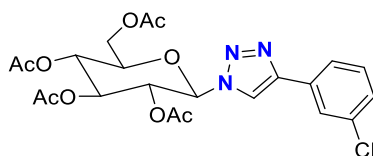
170.09, 169.53, 169.13, 150.80, 149.16, 127.00, 118.11, 116.11, 112.53, 85.85, 75.22, 73.03, 70.25, 67.93, 61.76, 40.56, 20.83, 20.68, 20.67, 20.33.



(2R,3R,4S,5R,6R)-2-(acetoxymethyl)-6-(4-(4-fluorophenyl)-1H-1,2,3-triazol-1-

yl)tetrahydro-2H-pyran-3,4,5-triyl triacetate (B₄): Isolated as white solid (46.8 mg, 95%).

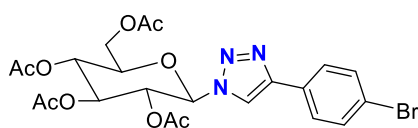
¹H NMR (400 MHz, CDCl₃) δ 8.01 (s, 1H), 7.71 (d, *J* = 8.4 Hz, 2H), 7.56 (d, *J* = 8.4 Hz, 2H), 5.93 (d, *J* = 9.0 Hz, 1H), 5.47 (dt, *J* = 24.7, 9.5 Hz, 2H), 5.26 (t, *J* = 9.6 Hz, 1H), 4.33 (dd, *J* = 12.7, 5.0 Hz, 1H), 4.15 (d, *J* = 12.6 Hz, 1H), 4.03 (dd, *J* = 10.1, 3.2 Hz, 1H), 2.08 (d, *J* = 3.4 Hz, 6H), 2.04 (s, 3H), 1.89 (s, 3H). ¹³C NMR (101 MHz, CDCl₃) δ 170.65, 170.06, 169.53, 169.20, 147.61, 132.18, 128.93, 127.55, 122.68, 118.01, 85.95, 77.48, 77.16, 76.84, 75.32, 72.75, 70.31, 67.78, 61.67, 20.83, 20.68, 20.66, 20.33.



(2R,3R,4S,5R,6R)-2-(acetoxymethyl)-6-(4-(3-chlorophenyl)-1H-1,2,3-triazol-1-yl)

tetrahydro-2H-pyran-3,4,5-triyl triacetate (B₅): Isolated as white solid (47.8 mg, 94%).

¹H NMR (400 MHz, CDCl₃) δ 8.03 (s, 1H), 7.83 (t, *J* = 1.6 Hz, 1H), 7.70 (dt, *J* = 7.4, 1.5 Hz, 1H), 7.32 (ddd, *J* = 11.0, 8.4, 4.9 Hz, 2H), 5.93 (d, *J* = 9.0 Hz, 1H), 5.47 (dt, *J* = 18.5, 9.5 Hz, 2H), 5.33 – 5.19 (m, 1H), 4.32 (dd, *J* = 12.7, 5.0 Hz, 1H), 4.15 (dd, *J* = 12.6, 2.0 Hz, 1H), 4.04 (ddd, *J* = 10.1, 5.0, 2.1 Hz, 1H), 2.07 (d, *J* = 3.6 Hz, 6H), 2.03 (s, 3H), 1.88 (s, 3H). ¹³C NMR (101 MHz, CDCl₃) δ 170.60, 170.01, 169.49, 169.13, 147.30, 134.96, 131.75, 130.28, 128.66, 126.07, 124.08, 118.39, 85.95, 75.30, 72.73, 70.38, 67.81, 61.66, 20.78, 20.64, 20.61, 20.27.



(2R,3R,4S,5R,6R)-2-(acetoxymethyl)-6-(4-(4-bromophenyl)-1H-1,2,3-triazol-1-

yl)tetrahydro-2H-pyran-3,4,5-triyl triacetate (B₆): Isolated as white solid (51.43 mg, 93%).

¹H NMR (400 MHz, CDCl₃) δ 8.01 (s, 1H), 7.71 (d, J = 8.4 Hz, 2H), 7.56 (d, J = 8.4 Hz, 2H), 5.93 (d, J = 9.0 Hz, 1H), 5.47 (dt, J = 25.0, 9.5 Hz, 2H), 5.26 (t, J = 9.6 Hz, 1H), 4.33 (dd, J = 12.7, 5.0 Hz, 1H), 4.15 (d, J = 12.6 Hz, 1H), 4.03 (dd, J = 10.1, 3.3 Hz, 1H), 2.08 (d, J = 3.7 Hz, 6H), 2.04 (s, 3H), 1.89 (s, 3H). ¹³C NMR (101 MHz, CDCl₃) δ 170.65, 170.06, 169.54, 169.20, 132.19, 128.97, 127.54, 122.69, 86.02, 75.34, 72.75, 70.31, 67.78, 61.67, 20.85, 20.70, 20.67, 20.35.



(2R,3R,4S,5R,6R)-2-(acetoxymethyl)-6-(4-(4-nitrophenyl)-1H-1,2,3-triazol-1-

yl)tetrahydro-2H-pyran-3,4,5-triyl triacetate (B₇): Isolated as yellow solid (46.8 mg, 90%).

¹H NMR (700 MHz, CDCl₃) δ 8.31 (d, J = 8.5 Hz, 2H), 8.16 (s, 1H), 8.02 (d, J = 8.5 Hz, 2H), 5.95 (d, J = 8.8 Hz, 1H), 5.48 (dq, J = 18.6, 9.5 Hz, 2H), 5.27 (t, J = 9.5 Hz, 1H), 4.35 (dd, J = 12.7, 5.0 Hz, 1H), 4.17 (d, J = 12.7 Hz, 1H), 4.05 (dd, J = 10.1, 4.9 Hz, 1H), 2.09 (d, J = 5.1 Hz, 6H), 2.05 (s, 3H), 1.90 (s, 3H). ¹³C NMR (101 MHz, CDCl₃) δ 170.60, 170.01, 169.52, 169.25, 147.80, 146.48, 136.23, 126.60, 124.48, 119.54, 86.13, 75.53, 72.64, 70.49, 67.81, 61.67, 20.83, 20.68, 20.66, 20.33.



(2R,3R,4S,5R,6R)-2-(acetoxymethyl)-6-(4-(4-(trifluoromethyl)phenyl)-1H-1,2,3-triazol-

1-yl)tetrahydro-2H-pyran-3,4,5-triyl triacetate (B₈): Isolated as off white solid (50 mg,

92%). ¹H NMR (400 MHz, CDCl₃) δ 8.10 (s, 1H), 7.96 (d, J = 8.1 Hz, 2H), 7.69 (d, J = 8.2 Hz, 2H), 5.95 (d, J = 9.0 Hz, 1H), 5.48 (dt, J = 18.4, 9.5 Hz, 2H), 5.32 – 5.22 (m, 1H), 4.34 (dd, J = 12.7, 5.1 Hz, 1H), 4.16 (dd, J = 12.6, 2.0 Hz, 1H), 4.05 (ddd, J = 10.1, 5.0, 2.0 Hz, 1H), 2.09

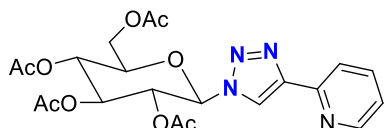
(s, 3H), 2.08 (s, 3H), 2.04 (s, 3H), 1.89 (s, 3H). ^{13}C NMR (101 MHz, CDCl_3) δ 170.64, 170.04, 169.54, 169.22, 147.26, 133.44, 130.75, 130.42, 126.22, 126.06, 126.02, 125.50, 122.80, 118.80, 86.03, 75.42, 72.73, 70.42, 67.83, 61.69, 20.82, 20.67, 20.64, 20.31.



(2R,3R,4S,5R,6R)-2-(acetoxymethyl)-6-(4-(4-(trifluoromethoxy)phenyl)-1H-1,2,3-

triazol-1-yl)tetrahydro-2H-pyran-3,4,5-triyl triacetate (B₉): Isolated as white solid (52.55

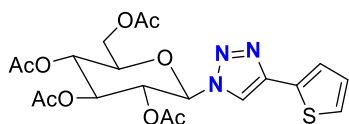
mg, 94%). ^1H NMR (700 MHz, CDCl_3) δ 8.01 (s, 1H), 7.86 (d, $J = 8.4$ Hz, 2H), 7.28 (d, $J = 8.2$ Hz, 2H), 5.93 (d, $J = 9.3$ Hz, 1H), 5.50 (t, $J = 9.4$ Hz, 1H), 5.45 (t, $J = 9.4$ Hz, 1H), 5.27 (t, $J = 9.7$ Hz, 1H), 4.33 (dd, $J = 12.7, 4.9$ Hz, 1H), 4.16 (d, $J = 12.5$ Hz, 1H), 4.04 (dd, $J = 9.5, 4.0$ Hz, 1H), 2.08 (d, $J = 5.6$ Hz, 6H), 2.04 (s, 3H), 1.89 (s, 3H). ^{13}C NMR (101 MHz, CDCl_3) δ 170.68, 170.08, 169.56, 169.22, 149.36, 147.37, 128.74, 127.46, 121.55, 118.10, 85.97, 75.33, 72.71, 70.31, 67.77, 61.66, 20.85, 20.70, 20.67, 20.33. HRMS (ESI-TOF) m/z : $[\text{M} + \text{H}]^+$ calcd for $\text{C}_{23}\text{H}_{25}\text{F}_3\text{N}_3\text{O}_{10}$ 560.1492; Found 560.1494.



(2R,3R,4S,5R,6R)-2-(acetoxymethyl)-6-(4-(pyridin-2-yl)-1H-1,2,3-triazol-1-

yl)tetrahydro-2H-pyran-3,4,5-triyl triacetate(B₁₀): Isolated as brown solid (45 mg, 95%).

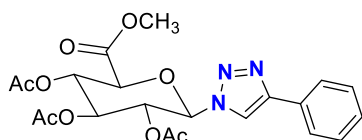
^1H NMR (700 MHz, CDCl_3) δ 8.60 (s, 1H), 8.40 (s, 1H), 8.14 (d, $J = 7.3$ Hz, 1H), 7.77 (d, $J = 6.8$ Hz, 1H), 7.25 (s, 1H), 5.92 (d, $J = 8.9$ Hz, 1H), 5.47 (dt, $J = 31.7, 8.3$ Hz, 2H), 5.33 – 5.23 (m, 2H), 4.31 (dd, $J = 12.5, 4.7$ Hz, 1H), 4.16 (d, $J = 12.5$ Hz, 1H), 4.02 (d, $J = 5.3$ Hz, 1H), 2.08 (d, $J = 12.7$ Hz, 6H), 2.04 (s, 3H), 1.89 (s, 3H). ^{13}C NMR (101 MHz, CDCl_3) δ 170.61, 170.06, 169.41, 168.93, 149.63, 149.05, 136.97, 123.27, 120.68, 120.47, 85.93, 75.18, 72.75, 70.56, 67.72, 61.58, 20.74, 20.61, 20.60, 20.26.



(2R,3R,4S,5R,6R)-2-(acetoxymethyl)-6-(4-(thiophen-2-yl)-1H-1,2,3-triazol-1-

yl)tetrahydro-2H-pyran-3,4,5-triyl triacetate(B₁₁): Isolated as off white solid (45 mg, 94%).

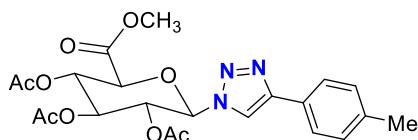
¹H NMR (400 MHz, CDCl₃) δ 7.91 (s, 1H), 7.41 (dd, *J* = 3.6, 1.0 Hz, 1H), 7.32 (dd, *J* = 5.0, 1.0 Hz, 1H), 7.08 (dd, *J* = 5.0, 3.6 Hz, 1H), 5.91 (d, *J* = 9.1 Hz, 1H), 5.46 (dt, *J* = 25.3, 9.5 Hz, 2H), 5.26 (t, *J* = 9.6 Hz, 1H), 4.33 (dd, *J* = 12.6, 5.1 Hz, 1H), 4.16 (dd, *J* = 12.6, 1.9 Hz, 1H), 4.02 (ddd, *J* = 10.0, 5.0, 2.0 Hz, 1H), 2.08 (d, *J* = 6.0 Hz, 6H), 2.03 (s, 3H), 1.89 (s, 3H). ¹³C NMR (101 MHz, CDCl₃) δ 170.65, 170.06, 169.51, 169.15, 143.77, 132.22, 127.82, 125.71, 124.96, 117.25, 85.98, 75.35, 72.83, 70.34, 67.83, 61.70, 20.83, 20.68, 20.65, 20.33.



(2S,3S,4S,5R,6R)-2-(methoxycarbonyl)-6-(4-phenyl-1H-1,2,3-triazol-1-yl)tetrahydro-

2H-pyran-3,4,5-triyl triacetate(C₁): Isolated as white solid (44 mg, 95%). ¹H NMR (400

MHz, DMSO) δ 9.05 (s, 1H), 7.84 (d, *J* = 7.3 Hz, 2H), 7.48 (t, *J* = 7.6 Hz, 2H), 7.38 (d, *J* = 7.4 Hz, 1H), 6.47 (d, *J* = 9.1 Hz, 1H), 5.77 (t, *J* = 9.3 Hz, 1H), 5.68 (t, *J* = 9.4 Hz, 1H), 5.24 (t, *J* = 9.8 Hz, 1H), 4.87 (d, *J* = 10.0 Hz, 1H), 3.64 (s, 3H), 2.04 (s, 3H), 2.00 (s, 3H), 1.81 (s, 3H). ¹³C NMR (101 MHz, DMSO) δ 169.52, 169.34, 168.53, 166.58, 147.02, 129.96, 129.04, 128.36, 125.22, 120.57, 83.84, 72.88, 71.42, 69.93, 68.47, 52.68, 23.05, 20.26, 20.22, 19.89.

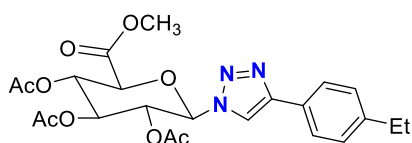


(2S,3S,4S,5R,6R)-2-(methoxycarbonyl)-6-(4-(p-tolyl)-1H-1,2,3-triazol-1-yl)tetrahydro-

2H-pyran-3,4,5-triyl triacetate(C₂): Isolated as off white solid (46.5 mg, 98%). ¹H NMR (400

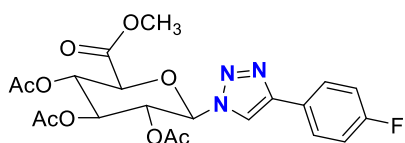
MHz, CDCl₃) δ 7.80 (s, 1H), 7.75 (d, *J* = 8.0 Hz, 2H), 7.23 (d, *J* = 7.9 Hz, 2H), 5.16 (t, *J* = 9.5

Hz, 1H), 5.11 – 4.99 (m, 2H), 4.68 (dd, $J = 11.3, 3.5$ Hz, 1H), 4.58 – 4.48 (m, 1H), 4.45 (d, $J = 7.9$ Hz, 1H), 4.31 – 4.23 (m, 2H), 4.12 (d, $J = 12.4$ Hz, 1H), 3.94 – 3.86 (m, 1H), 3.69 (dd, $J = 9.9, 2.4$ Hz, 1H), 2.37 (s, 3H), 2.08 (s, 3H), 2.02 (s, 3H), 1.98 (s, 3H), 1.71 (s, 3H). ^{13}C NMR (101 MHz, DMSO) δ 169.50, 169.31, 168.50, 166.57, 147.06, 137.71, 129.55, 127.19, 125.15, 120.09, 83.80, 72.85, 71.44, 69.90, 68.46, 52.65, 20.83, 20.25, 20.21, 19.89. HRMS (ESI-TOF) m/z : $[\text{M} + \text{H}]^+$ calcd for $\text{C}_{22}\text{H}_{26}\text{N}_3\text{O}_9$ 476.1669; Found 476.1689.



(2R,3R,4S,5S,6S)-2-(4-(4-ethylphenyl)-1H-1,2,3-triazol-1-yl)-6-

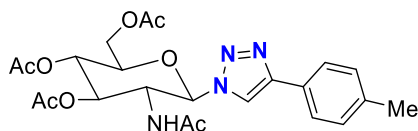
(methoxycarbonyl)tetrahydro-2H-pyran-3,4,5-triyl triacetate(C₃): Isolated as white solid (47.4 mg, 97%). ^1H NMR (400 MHz, CDCl_3) δ 8.00 (s, 1H), 7.73 (d, $J = 8.0$ Hz, 2H), 7.25 (s, 2H), 5.95 (d, $J = 8.9$ Hz, 1H), 5.50 (dd, $J = 11.8, 8.9$ Hz, 2H), 5.38 (s, 1H), 4.32 (d, $J = 9.8$ Hz, 1H), 3.74 (s, 3H), 2.66 (d, $J = 7.6$ Hz, 2H), 2.05 (d, $J = 9.4$ Hz, 6H), 1.86 (s, 3H), 1.24 (t, $J = 7.6$ Hz, 3H). ^{13}C NMR (101 MHz, CDCl_3) δ 169.91, 169.49, 169.06, 166.36, 148.85, 145.05, 128.53, 127.38, 126.06, 117.61, 85.64, 75.10, 72.16, 70.05, 69.18, 53.31, 28.84, 20.66, 20.60, 20.29, 15.64. HRMS(ESI-TOF) m/z : $[\text{M} + \text{H}]^+$ calcd for $\text{C}_{23}\text{H}_{28}\text{N}_3\text{O}_9$ 490.1826; Found 490.1811.



(2R,3R,4S,5S,6S)-2-(4-(4-fluorophenyl)-1H-1,2,3-triazol-1-yl)-6-

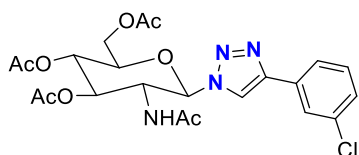
(methoxycarbonyl)tetrahydro-2H-pyran-3,4,5-triyl triacetate(C₄): Isolated as of white solid (45 mg, 94%). ^1H NMR (400 MHz, CDCl_3) δ 8.03 (s, 1H), 7.84 – 7.76 (m, 2H), 7.12 (dd, $J = 12.0, 5.4$ Hz, 2H), 6.01 – 5.93 (m, 1H), 5.56 – 5.46 (m, 2H), 5.39 (t, $J = 9.5$ Hz, 1H), 4.35 (d, $J = 9.8$ Hz, 1H), 3.75 (s, 3H), 2.07 (s, 3H), 2.05 (s, 3H), 1.89 (s, 3H). ^{13}C NMR (101 MHz,

CDCl₃) δ 169.87, 169.48, 169.10, 166.34, 161.83, 147.87, 127.85, 126.19, 117.81, 116.15, 115.94, 85.67, 75.07, 72.06, 70.11, 69.15, 53.32, 20.65, 20.58, 20.30. HRMS (ESI-TOF) m/z : [M + H]⁺ calcd for C₂₁H₂₃N₃O₉ 480.1418; Found 480.1389.



(2R,3S,6S)-5-acetamido-2-(acetoxymethyl)-6-(4-(p-tolyl)-1H-1,2,3-triazol-1-

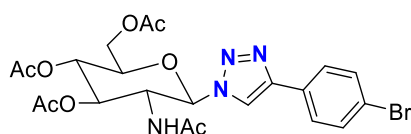
yl)tetrahydro-2H-pyran-3,4-diyl diacetate(D₁): Isolated as white solid (48.8 mg, 98%). ¹H NMR (400 MHz, DMSO) δ 8.79 (s, 1H), 8.13 (d, J = 9.2 Hz, 1H), 7.72 (d, J = 8.1 Hz, 2H), 7.28 (d, J = 8.0 Hz, 2H), 6.13 (d, J = 9.9 Hz, 1H), 5.39 (t, J = 9.9 Hz, 1H), 5.11 (t, J = 9.8 Hz, 1H), 4.65 (d, J = 9.7 Hz, 1H), 4.28 (ddd, J = 10.1, 5.0, 2.2 Hz, 1H), 4.17 (dd, J = 12.5, 5.1 Hz, 1H), 4.08 (dd, J = 12.4, 2.0 Hz, 1H), 2.33 (s, 3H), 2.02 (s, 3H), 2.00 (s, 3H), 1.96 (s, 3H), 1.59 (s, 3H). ¹³C NMR (101 MHz, DMSO) δ 169.50, 169.31, 168.50, 166.57, 147.06, 137.71, 129.55, 127.19, 125.15, 120.09, 83.80, 72.85, 71.44, 69.90, 68.46, 52.65, 20.83, 20.25, 20.21, 19.89. HRMS (ESI-TOF) m/z : [M + H]⁺ calcd for C₂₃H₂₉N₄O₈ 489.1985; Found 489.1937.



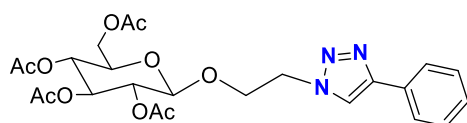
(2R,3S,6S)-5-acetamido-2-(acetoxymethyl)-6-(4-(3-chlorophenyl)-1H-1,2,3-triazol-1-

yl)tetrahydro-2H-pyran-3,4-diyl diacetate(D₂): Isolated as white solid (47.3 mg, 93%). ¹H NMR (400 MHz, DMSO) δ 9.01 (s, 1H), 8.15 (d, J = 9.1 Hz, 1H), 7.90 (s, 1H), 7.82 (d, J = 7.9 Hz, 1H), 7.52 (t, J = 7.9 Hz, 1H), 7.44 (d, J = 8.0 Hz, 1H), 6.16 (d, J = 9.9 Hz, 1H), 5.38 (d, J = 9.9 Hz, 1H), 5.10 (t, J = 9.8 Hz, 1H), 4.63 (d, J = 9.8 Hz, 1H), 4.32 (d, J = 7.3 Hz, 1H), 4.19 (dd, J = 12.6, 5.0 Hz, 1H), 4.09 (d, J = 10.7 Hz, 1H), 2.03 (s, J = 7.1 Hz, 3H), 2.02 (s, 3H), 1.97 (s, 3H), 1.60 (s, 3H). ¹³C NMR (101 MHz, DMSO) δ 170.03, 169.58, 169.50, 169.37, 145.49, 131.99, 129.48, 127.17, 121.18, 120.65, 84.95, 73.38, 72.25, 68.02, 61.74, 52.35,

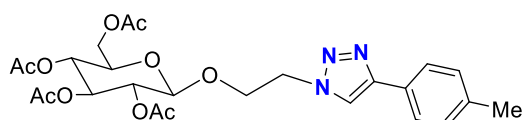
22.31, 20.52, 20.42, 20.28. HRMS (ESI-TOF) m/z : $[M + H]^+$ calcd for $C_{22}H_{26}ClN_4O_8$ 509.1439; Found 509.1446.



(2R,3S,6S)-5-acetamido-2-(acetoxymethyl)-6-(4-(3-bromophenyl)-1H-1,2,3-triazol-1-yl)tetrahydro-2H-pyran-3,4-diyl diacetate(D₃): Isolated as white solid (51.4 mg, 92%). ¹H NMR (400 MHz, DMSO) δ 8.92 (s, 1H), 8.11 (d, $J = 9.2$ Hz, 1H), 7.81–7.77 (m, 2H), 7.69 – 7.66 (m, 2H), 6.15 (d, $J = 9.9$ Hz, 1H), 5.39 (t, $J = 9.9$ Hz, 1H), 5.11 (t, $J = 9.8$ Hz, 1H), 4.64 (q, $J = 9.8$ Hz, 1H), 4.29 (ddd, $J = 10.1, 5.0, 2.2$ Hz, 1H), 4.18 (dd, $J = 12.5, 5.0$ Hz, 1H), 4.09 (dd, $J = 12.5, 2.1$ Hz, 1H), 2.02 (s, 3H), 2.01 (s, 3H), 1.96 (s, 3H), 1.59 (s, 3H). ¹³C NMR (101 MHz, DMSO) δ 170.03, 169.58, 169.50, 169.37, 145.49, 131.99, 129.48, 127.17, 121.18, 120.65, 84.95, 73.38, 72.25, 68.02, 61.74, 52.35, 22.31, 20.52, 20.42, 20.28.

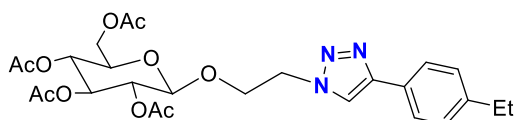


(2R,3R,4S,5R,6R)-2-(acetoxymethyl)-6-(2-(4-phenyl-1H-1,2,3-triazol-1-yl)ethoxy)tetrahydro-2H-pyran-3,4,5-triyl triacetate(E₁): Isolated as white solid (50.9 mg, 98%). ¹H NMR (400 MHz, CDCl₃) δ 7.88 (s, 1H), 7.86 (s, 2H), 7.42 (t, $J = 7.5$ Hz, 2H), 7.32 (t, $J = 7.3$ Hz, 1H), 5.16 (t, $J = 9.5$ Hz, 1H), 5.12 – 4.97 (m, 2H), 4.70 (d, $J = 14.7$ Hz, 1H), 4.54 (dd, $J = 12.1, 9.2$ Hz, 1H), 4.46 (d, $J = 7.9$ Hz, 1H), 4.33–4.21 (m, 2H), 4.12 (d, $J = 11.0$ Hz, 1H), 3.91 (t, $J = 8.6$ Hz, 1H), 3.75–3.64 (m, 1H), 2.07 (s, 3H), 2.01 (s, 3H), 1.97 (s, 3H), 1.71 (s, 3H). ¹³C NMR (101 MHz, CDCl₃) δ 170.76, 170.22, 169.65, 169.57, 130.54, 128.96, 128.30, 125.78, 121.67, 100.62, 72.49, 72.04, 70.96, 68.25, 68.00, 61.76, 50.19, 20.86, 20.71, 20.68, 20.49.



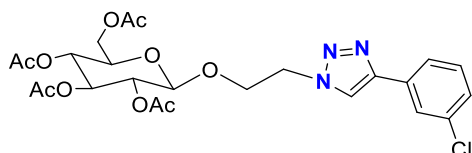
(2R,3R,4S,5R,6R)-2-(acetoxymethyl)-6-(2-(4-(p-tolyl)-1H-1,2,3-triazol-1-

yl)ethoxy)tetrahydro-2H-pyran-3,4,5-triyl triacetate(E₂) : Isolated as off white solid (50.6 mg, 95%). ¹H NMR (400 MHz, CDCl₃) δ 7.80 (s, 1H), 7.75 (d, *J* = 8.0 Hz, 2H), 7.23 (d, *J* = 7.9 Hz, 2H), 5.16 (t, *J* = 9.5 Hz, 1H), 5.11–4.99 (m, 2H), 4.68 (dd, *J* = 11.3, 3.5 Hz, 1H), 4.58 – 4.48 (m, 1H), 4.45 (d, *J* = 7.9 Hz, 1H), 4.31–4.23 (m, 2H), 4.12 (d, *J* = 12.4 Hz, 1H), 3.94 – 3.86 (m, 1H), 3.69 (dd, *J* = 9.9, 2.4 Hz, 1H), 2.37 (s, 3H), 2.08 (s, 3H), 2.02 (s, 3H), 1.98 (s, 3H), 1.71 (s, 3H). ¹³C NMR (101 MHz, CDCl₃) δ 170.76, 170.23, 169.65, 169.58, 130.59, 128.96, 128.28, 125.77, 121.60, 100.63, 72.50, 72.04, 70.97, 68.25, 68.01, 61.76, 50.17, 20.86, 20.71, 20.68, 20.49.



(2R,3R,4S,5R,6R)-2-(acetoxymethyl)-6-(2-(4-(4-ethylphenyl)-1H-1,2,3-triazol-1-

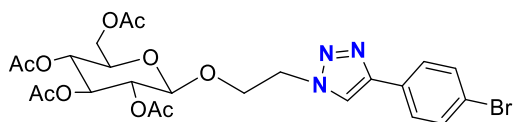
yl)ethoxy)tetrahydro-2H-pyran-3,4,5-triyl triacetate(E₃) : Isolated as white solid (52.5 mg, 96%). ¹H NMR (400 MHz, CDCl₃) δ 7.80 (s, 1H), 7.76 (d, *J* = 8.0 Hz, 2H), 7.24 (d, *J* = 8.0 Hz, 2H), 5.15 (t, *J* = 9.5 Hz, 1H), 5.08–4.98 (m, 2H), 4.71–4.60 (m, 1H), 4.55–4.48 (m, 1H), 4.45 (d, *J* = 7.9 Hz, 1H), 4.29 – 4.20 (m, 2H), 4.11 (dd, *J* = 12.3, 2.0 Hz, 1H), 3.90 (td, *J* = 9.7, 2.7 Hz, 1H), 3.68 (ddd, *J* = 9.8, 4.6, 2.3 Hz, 1H), 2.65 (q, *J* = 7.6 Hz, 2H), 2.05 (s, 3H), 2.00 (s, 3H), 1.96 (s, 3H), 1.71 (s, 3H), 1.23 (t, *J* = 7.6 Hz, 3H). ¹³C NMR (101 MHz, CDCl₃) δ 170.68, 170.14, 169.58, 169.51, 147.82, 144.43, 128.39, 128.01, 125.75, 121.16, 100.62, 72.54, 72.03, 70.99, 68.31, 68.00, 61.78, 50.11, 28.73, 20.78, 20.64, 20.62, 20.46, 15.56.



(2R,3R,4S,5R,6R)-2-(acetoxymethyl)-6-(2-(4-(3-chlorophenyl)-1H-1,2,3-triazol-1-

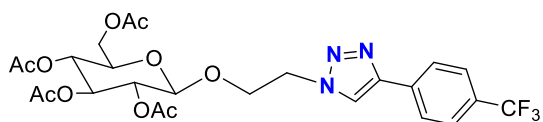
yl)ethoxy)tetrahydro-2H-pyran-3,4,5-triyl triacetate (E₄)): Isolated as white solid (51.5

mg, 93%). ¹H NMR (400 MHz, CDCl₃) δ 7.85 (s, 1H), 7.75 (d, *J* = 8.3 Hz, 2H), 7.54 (d, *J* = 8.3 Hz, 2H), 5.16 (t, *J* = 9.5 Hz, 1H), 5.11–4.96 (m, 2H), 4.68 (d, *J* = 14.5 Hz, 1H), 4.59–4.48 (m, 1H), 4.46 (d, *J* = 7.8 Hz, 1H), 4.25 (dd, *J* = 12.1, 4.6 Hz, 2H), 4.12 (d, *J* = 11.2 Hz, 1H), 3.90 (t, *J* = 8.4 Hz, 1H), 3.69 (d, *J* = 7.6 Hz, 1H), 2.06 (s, 3H), 2.01 (s, 3H), 1.98 (s, 3H), 1.73 (s, 3H). ¹³C NMR (101 MHz, CDCl₃) δ 170.58, 170.07, 169.49, 169.43, 146.60, 131.99, 129.52, 127.22, 122.02, 121.64, 100.50, 72.37, 71.99, 70.94, 68.21, 67.76, 61.69, 50.13, 20.71, 20.56, 20.54, 20.43. HRMS (ESI-TOF) *m/z*: [M + H]⁺ calcd for C₂₄H₂₉ClN₃O₁₀ 554.1389; Found 554.1542.



(2R,3R,4S,5R,6R)-2-(acetoxymethyl)-6-(2-(4-(4-bromophenyl)-1H-1,2,3-triazol-1-

yl)ethoxy)tetrahydro-2H-pyran-3,4,5-triyl triacetate(E₅): Isolated as white solid (54.4 mg, 91%). ¹H NMR (400 MHz, CDCl₃) δ 7.85 (s, 1H), 7.75 (d, *J* = 8.3 Hz, 2H), 7.54 (d, *J* = 8.3 Hz, 2H), 5.16 (t, *J* = 9.5 Hz, 1H), 5.11–4.96 (m, 2H), 4.68 (d, *J* = 14.5 Hz, 1H), 4.59–4.48 (m, 1H), 4.46 (d, *J* = 7.8 Hz, 1H), 4.25 (dd, *J* = 12.1, 4.6 Hz, 2H), 4.12 (d, *J* = 11.2 Hz, 1H), 3.90 (t, *J* = 8.4 Hz, 1H), 3.69 (d, *J* = 7.6 Hz, 1H), 2.06 (s, 3H), 2.01 (s, 3H), 1.98 (s, 3H), 1.73 (s, 3H). ¹³C NMR (101 MHz, CDCl₃) δ 170.58, 170.07, 169.49, 169.43, 146.60, 131.99, 129.52, 127.22, 122.02, 121.64, 100.50, 72.37, 71.99, 70.94, 68.21, 67.76, 61.69, 50.13, 20.71, 20.56, 20.54, 20.43. HRMS (ESI-TOF) *m/z*: [M + H]⁺ calcd for C₂₄H₂₈BrN₃O₁₀ 598.1036; Found 598.1036.



(2R,3R,4S,5R,6R)-2-(acetoxymethyl)-6-(2-(4-(4-(trifluoromethyl)phenyl)-1H-1,2,3-

triazol-1-yl)ethoxy)tetrahydro-2H-pyran-3,4,5-triyl triacetate(E₆): Isolated as white solid (52.8 mg, 90%). ¹H NMR (400 MHz, CDCl₃) δ 8.00 (d, *J* = 8.1 Hz, 2H), 7.95 (s, 1H), 7.68 (d, *J* = 8.2 Hz, 2H), 5.17 (t, *J* = 9.5 Hz, 1H), 5.10–4.98 (m, 2H), 4.75–4.64 (m, 1H), 4.60–4.51 (m,

1H), 4.47 (d, $J = 7.9$ Hz, 1H), 4.31–4.22 (m, 2H), 4.13 (dd, $J = 12.3, 2.0$ Hz, 1H), 3.92 (td, $J = 10.0, 2.5$ Hz, 1H), 3.70 (ddd, $J = 9.7, 4.4, 2.1$ Hz, 1H), 2.06 (s, 3H), 2.01 (s, 3H), 1.98 (s, 3H), 1.73 (s, 3H). ^{13}C NMR (101 MHz, CDCl_3) δ 170.69, 170.18, 169.59, 169.55, 146.38, 134.14, 130.25, 129.92, 125.97, 125.76, 122.51, 100.62, 72.47, 72.14, 71.09, 68.34, 67.79, 61.82, 50.33, 20.81, 20.67, 20.65, 20.54. HRMS (ESI-TOF) m/z : $[\text{M} + \text{H}]^+$ calcd for $\text{C}_{25}\text{H}_{29}\text{F}_3\text{N}_3\text{O}_{10}$ 588.1805; Found 588.2238.

4.5.7 NMR spectra of the products:

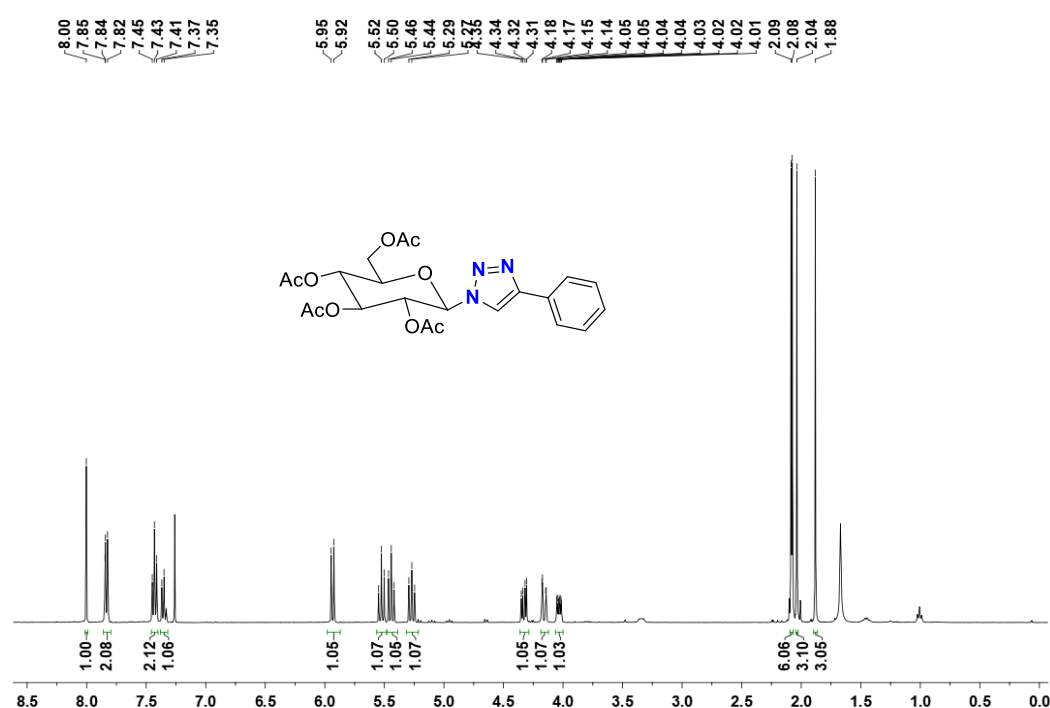


Figure 4.8. ^1H NMR (400 MHz) spectrum of (2R,3R,4S,5R,6R)-2-(acetoxymethyl)-6-(4-phenyl-1H-1,2,3-triazol-1-yl) tetrahydro-2H-pyran-3,4,5-triyl triacetate (**A**) CDCl_3 at r.t.

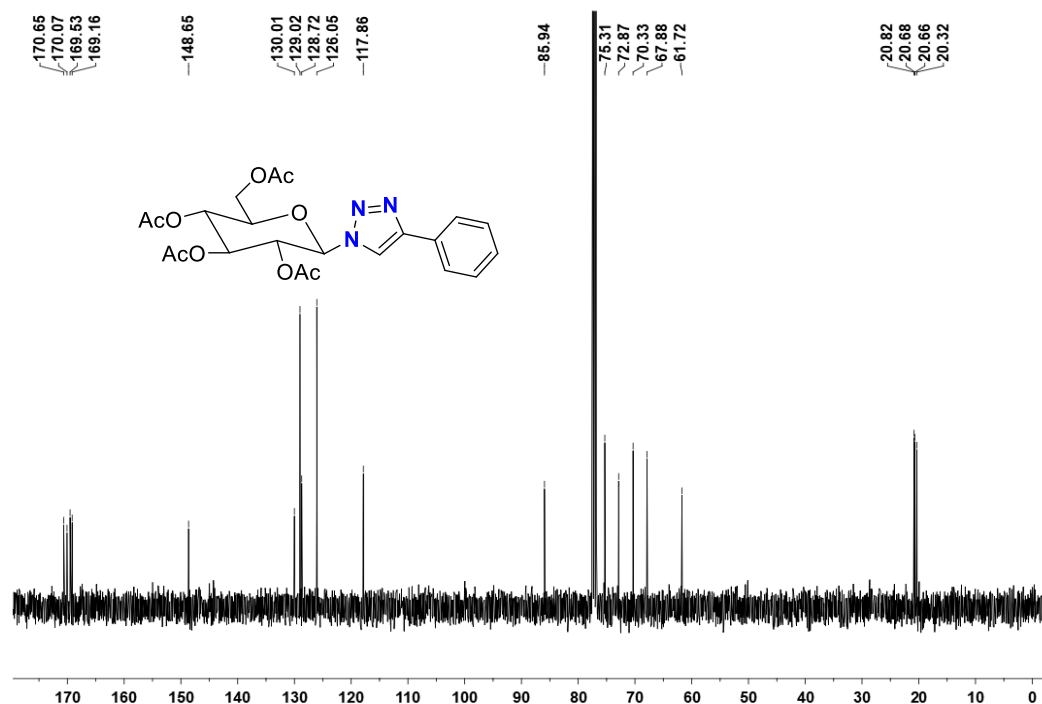


Figure 4.9. ^{13}C NMR (101 MHz) spectrum of (2R,3R,4S,5R,6R)-2-(acetoxymethyl)-6-(4-phenyl-1H-1,2,3-triazol-1-yl)tetrahydro-2H-pyran-3,4,5-triyl triacetate (**A**) in CDCl_3 at r.t.

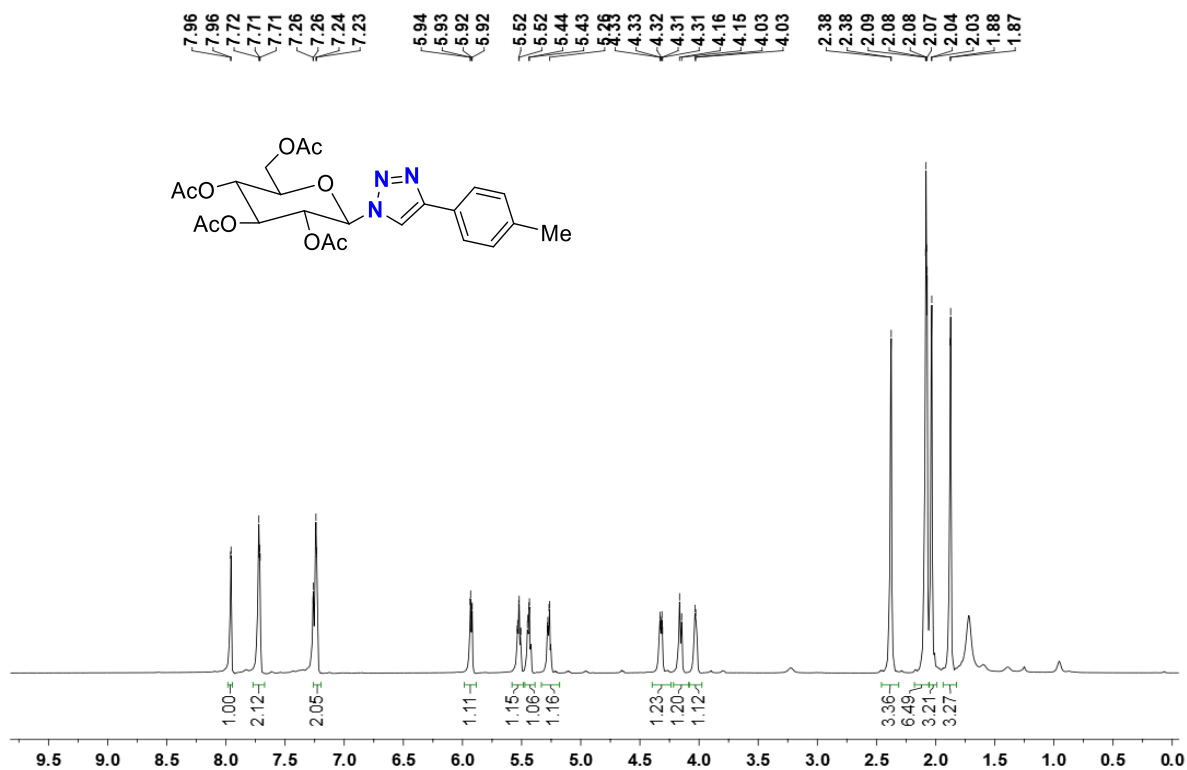


Figure 4.10. ^1H NMR (400 MHz) spectrum of (2R,3R,4S,5R,6R)-2-(acetoxymethyl)-6-(4-(p-tolyl)-1H-1,2,3-triazol-1-yl)tetrahydro-2H-pyran-3,4,5-triyl triacetate (**B₁**) CDCl_3 at r.t.

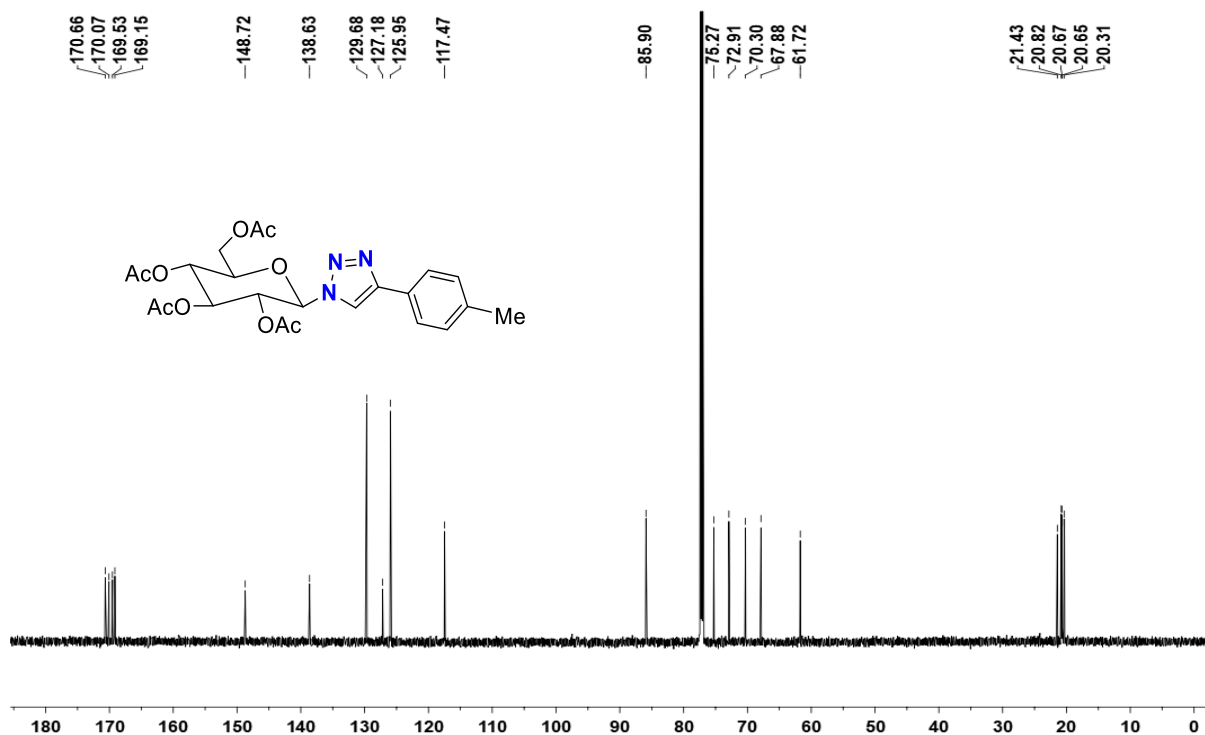


Figure 4.11. ^{13}C NMR (101 MHz) spectrum of (2R,3R,4S,5R,6R)-2-(acetoxymethyl)-6-(4-(p-tolyl)-1H-1,2,3-triazol-1-yl)tetrahydro-2H-pyran-3,4,5-triyl triacetate (**B**₁) in CDCl_3 at

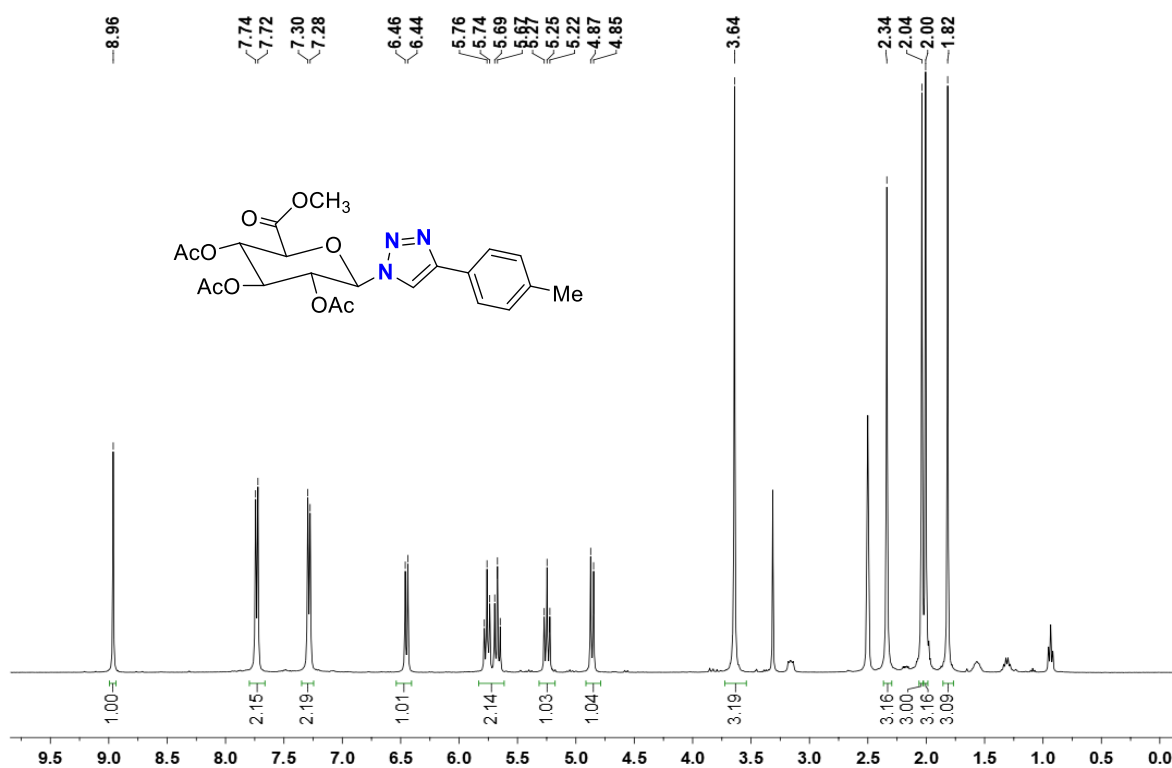


Figure 4.12 ^1H NMR (400 MHz) spectrum of (2S,3S,4S,5R,6R)-2-(methoxycarbonyl)-6-(4-(p-tolyl)-1H-1,2,3-triazol-1-yl)tetrahydro-2H-pyran-3,4,5-triyl triacetate (**C**₂) DMSO at r.t.

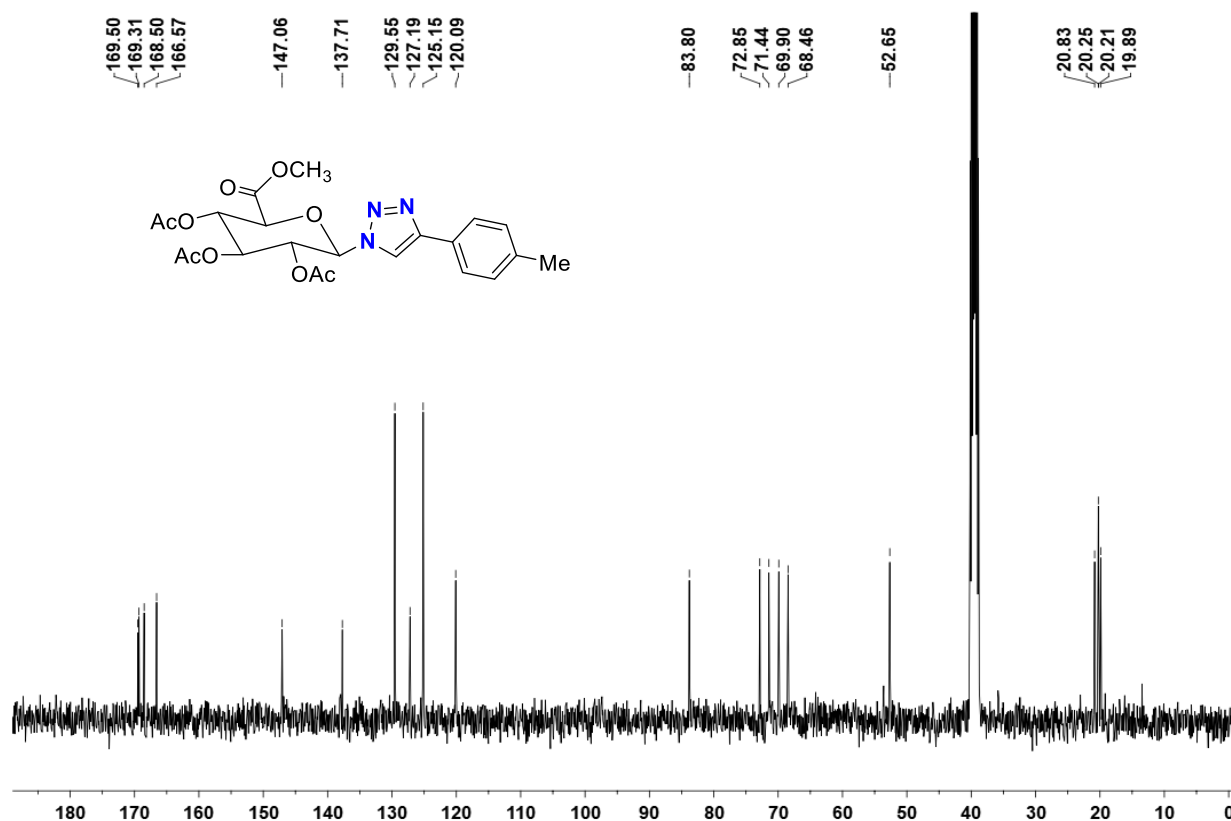


Figure 4.13. ^{13}C NMR (101 MHz) spectrum of (2*S*,3*S*,4*S*,5*R*,6*R*)-2-(methoxycarbonyl)-6-(4-(*p*-tolyl)-1*H*-1,2,3-triazol-1-yl)tetrahydro-2*H*-pyran-3,4,5-triyl triacetate (**C**₂) in DMSO at r.t.

4.5.8 Molecular structure determination by single crystal X-ray crystallography

A crystal of **19** with accession code CCDC 2240116 was mounted under crystal oil coated at ambient conditions. All measurements were made on an Oxford Diffraction SuperNova area-detector diffractometer using an INCOATEC micro source (Mo- $K\alpha$ radiation, $\lambda = 0.71073 \text{ \AA}$, multilayer optics) and Al filtered. Data reduction was performed using the CrysAlisPro program. The intensities were corrected for Lorentz and polarization effects, and an absorption correction based on the multi-scan method using SCALE3 ABSPACK in CrysAlisPro was applied. Data collection and refinement parameters are given in Table 4.3. OleX and refinement was carried out using least-square minimization implemented in ShelXL. All nonhydrogen atoms were refined with anisotropic displacement parameters. Hydrogen atom positions were fixed geometrically in idealized positions and were refined using a riding model.

Table 4.3. Crystallographic Data and Refinement Parameters for **19**.

Complex	19
Empirical formula	C ₁₆ H ₁₅ CuIN ₃ O
Formula weight (g mol ⁻¹)	455.75
Temperature	100.00(10)
Radiation	MoK α ($\lambda = 0.71073$)
Crystal system	Monoclinic
Space group	<i>P</i> 2 ₁ / <i>c</i>
<i>a</i> (Å)	12.2982(5)
<i>b</i> (Å)	8.7867(3)
<i>c</i> (Å)	15.5899(6)
α (deg)	90
β (deg)	109.228(4)
γ (deg)	90
volume (Å ³)	1590.68(11)
<i>Z</i>	4
<i>D</i> _{calc} (g cm ⁻³)	1.381
μ (mm ⁻¹)	1.903
<i>F</i> (000)	888.0
Crystal Size (mm ³)	0.2 × 0.1 × 0.1
2 θ Range (deg)	6.92 to 60.878
Index Ranges	-15 ≤ <i>h</i> ≤ 16, -11 ≤ <i>k</i> ≤ 11, -21 ≤ <i>l</i> ≤ 19
Reflections collected	15069
Independent reflections	3809 [<i>R</i> _{int} = 0.0476, <i>R</i> _{sigma} = 0.0397]
Completeness to theta	99.96
Refinement method	Full-matrix least-squares on <i>F</i> ²
Data/Restraints/parameters	3809/0/200
Goodness-of-fit on <i>F</i> ²	1.038
Final <i>R</i> indices [<i>I</i> > 2 σ (<i>I</i>)]	<i>R</i> ₁ = 0.0271, <i>wR</i> ₂ = 0.0623
<i>R</i> indices (all data)	<i>R</i> ₁ = 0.0322, <i>wR</i> ₂ = 0.0644
Largest diff. peak/hole (e Å ⁻³)	0.69/-0.69

Table 4.4. Selected bond lengths (Å) around the metal centre in Copper complexes **19** and **20**.

	Bond lengths
Complexes/Bonds	1
Cu–N(pyridine)	2.091(2)
Cu–N(pyrazole)	2.118(2)
Cu–I	2.6250(4)
Cu ¹ –I	2.6271(3)

Cu–Cu ^a	2.6101(6)
--------------------	-----------

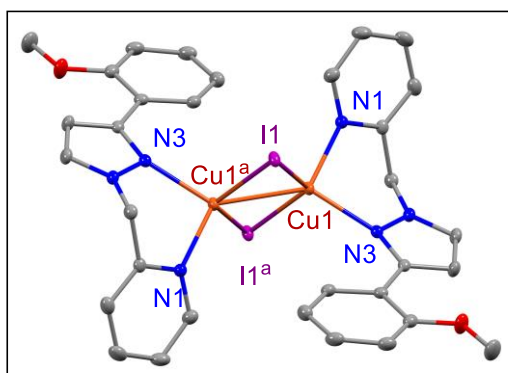
Symmetry code: ^a1-X,1-Y,1-Z

Table 4.5. Selected bond angles (°) around the metal centre in Copper complexes 19 and 20.

Bond angles	
Cu1–I1–Cu1 ^a	59.599(11)
I1–Cu1–I1 ^a	120.401(11)
Cu1 ^a –Cu1–I1	60.240(12)
Cu1 ^a –Cu1–I1 ^a	60.161(12)
N3–Cu1–I1 ^a	104.02(6)
N3–Cu1–I1	119.32(6)
N3–Cu1–Cu1 ^a	137.42(6)
N1–Cu1–I1	103.51(6)
N1–Cu1–I1 ^a	112.20(6)
N1–Cu1–Cu1 ^a	127.96(6)
N1–Cu1–N3	94.44(8)

Symmetry code: ^a 1-X,1-Y,1-Z

Figure 4.14. Molecular structure of 19



4.6 REFERENCES

- (1) Rostovtsev, V.V.; Green, L.G.; Fokin, V.V.; Sharpless, K.B. A Stepwise Huisgen Cycloaddition Process: Copper(I)-Catalyzed Regioselective “Ligation” of Azides and Terminal Alkynes. *Angew. Chem. Int. Ed.* **2002**, *41*, 2596-2599.
- (2) Tornøe, C. W.; Christensen, C.; Meldal, M. Peptidotriazoles on Solid Phase: [1,2,3]-Triazoles by Regiospecific Copper(I)-Catalyzed 1,3-Dipolar Cycloadditions of Terminal Alkynes to Azides. *J. Org. Chem.* **2002**, *67*, 3057–3064.

- (3) B. Zhang, Comprehensive review on the anti-bacterial activity of 1,2,3-triazole hybrids. *Eur. J. Med. Chem.* **2019**, *168*, 357-372.
- (4) Prasher, P.; Sharma, M. Tailored Therapeutics Based on 1,2,3-1H-Triazoles: A Mini Review. *Medchemcomm.* **2019**, *10*, 1302-1328.
- (5) Bonandi, E.; Christodoulou, M. S.; Fumagalli, G.; Perdicchia, D.; Rastelli, G.; Passarella, D. The 1,2,3-Triazole Ring as a Bioisostere in Medicinal Chemistry. *Drug Discov. Today.* **2017**, *22*, 1572-1581.
- (6) Kluba, C. A.; Mindt, T. L. Click-to-Chelate: Development of Technetium and Rhenium-Tricarbonyl Labeled Radiopharmaceuticals. *Molecules.* **2013**, *18*, 3206-3226.
- (7) Moses, J. E.; Moorhouse, A. D. The Growing Applications of Click Chemistry. *Chem. Soc. Rev.* **2007**, *36*, 1249-1262.
- (8) Amblard, F.; Cho, J. H.; Schinazi, R. F. Cu(I)-Catalyzed Huisgen Azide-Alkyne 1,3-Dipolar Cycloaddition Reaction in Nucleoside, Nucleotide, and Oligonucleotide Chemistry. *Chem. Rev.* **2009**, *109*, 4207-4220.
- (9) Angell, Y. L.; Burgess, K. Peptidomimetics via Copper-Catalyzed Azide-Alkyne Cycloadditions. *Chem. Soc. Rev.* **2007**, *36*, 1674-1689.
- (10) El-Sagheer, A. H.; Brown, T. Click Chemistry with DNA. *Chem. Soc. Rev.* **2010**, *39*, 1388-1405.
- (11) Saha, P.; Panda, D.; Dash, J. The Application of Click Chemistry for Targeting Quadruplex Nucleic Acids. *Chem. Commun.* **2019**, *55*, 731-750.
- (12) El-Sagheer, A. H.; Brown, T. Click Nucleic Acid Ligation: Applications in Biology and Nanotechnology. *Acc. Chem. Res.* **2012**, *45*, 1258-1267.
- (13) Akter, M.; Rupa, K.; Anbarasan, P. 1,2,3-Triazole and Its Analogues: New Surrogates for Diazo Compounds. *Chem. Rev.* **2022**, *122*, 13108-13205.

- (14) Golas, P. L.; Matyjaszewski, K. Marrying Click Chemistry with Polymerization: Expanding the Scope of Polymeric Materials. *Chem. Soc. Rev.* **2010**, *39*, 1338-1354.
- (15) Qin, A.; Lam, J. W. Y.; Tang, B. Z. Click Polymerization. *Chem. Soc. Rev.* **2010**, *39*, 2522–2544.
- (16) Nandivada, H.; Jiang, X.; Lahann, J. Click Chemistry: Versatility and Control in the Hands of Materials Scientists. *Adv. Mater.* **2007**, *19*, 2197–2208.
- (17) Aromí, G.; Barrios, L. A.; Roubeau, O.; Gamez, P. Triazoles and Tetrazoles: Prime Ligands to Generate Remarkable Coordination Materials. *Coord. Chem. Rev.* **2011**, *255*, 485–546.
- (18) Kolb, H. C.; Sharpless, K. B. The Growing Impact of Click Chemistry on Drug Discovery. *Drug Discov. Today.* **2003**, *8*, 1128-1137.
- (19) Sharpless, K. B.; Manetsch, R. In Situ Click Chemistry: A Powerful Means for Lead Discovery. *Expert Opin. Drug Discov.* **2006**, *1*, 525–538.
- (20) Thirumurugan, P.; Matosiuk, D.; Jozwiak, K. Click Chemistry for Drug Development and Diverse Chemical-Biology Applications. *Chem. Rev.* **2013**, *113*, 4905-4979.
- (21) Rani, A.; Singh, G.; Singh, A.; Maqbool, U.; Kaur, G.; Singh, J. CuAAC-Ensembled 1,2,3-Triazole-Linked Isosteres as Pharmacophores in Drug Discovery: Review. *RSC Adv.* **2020**, *10*, 5610–5635.
- (22) Huang, D.; Zhao, P.; Astruc, D. Catalysis by 1,2,3-Triazole- and Related Transition-Metal Complexes. *Coord. Chem. Rev.* **2014**, *272*, 145–165.
- (23) Ghosh, R.; Jana, N. C.; Panda, S.; Bagh, B. Transfer Hydrogenation of Aldehydes and Ketones in Air with Methanol and Ethanol by an Air-Stable Ruthenium–Triazole Complex. *ACS Sustain. Chem. Eng.* **2021**, *9*, 4903–4914.

- (24) Bagh, B.; McKinty, A. M.; Lough, A. J.; Stephan, D. W. 1,2,3-Triazolylidene Ruthenium(II)(H⁶-Arene) Complexes: Synthesis, Metallation and Reactivity. *Dalton Trans.* **2014**, *43*, 12842–12850.
- (25) Bagh, B.; McKinty, A. M.; Lough, A. J.; Stephan, D. W. 1,2,3-Triazolylidene Ruthenium(II)-Cyclometalated Complexes and Olefin Selective Hydrogenation Catalysis. *Dalton Trans.* **2015**, *44*, 2712–2723.
- (26) Bagh, B.; Stephan, D. W. Half Sandwich Ruthenium(II) Hydrides: Hydrogenation of Terminal, Internal, Cyclic and Functionalized Olefins. *Dalton Trans.* **2014**, *43*, 15638–15645.
- (27) Huisgen, R. 1,3-Dipolar Cycloadditions. Past and Future. *Angew. Chem. Int. Ed.* **1963**, *2*, 565–598.
- (28) Kolb, H. C.; Finn, M. G.; Sharpless, K. B. Click Chemistry: Diverse Chemical Function from a Few Good Reactions. *Angew. Chem. Int. Ed.* **2001**, *40*, 2004–2021.
- (29) Meldal, M.; Tornøe, C. W. Cu-Catalyzed Azide-Alkyne Cycloaddition. *Chem. Rev.* **2008**, *108*, 2952–3015.
- (30) Kowalski, K. A Brief Survey on the Application of Metal-Catalyzed Azide–Alkyne Cycloaddition Reactions to the Synthesis of Ferrocenyl-x-1,2,3-Triazolyl-R (x = None or a Linker and R = Organic Entity) Compounds with Anticancer Activity. *Coord. Chem. Rev.* **2023**, *479*, 214996.
- (31) Vivancos, A.; Segarra, C.; Albrecht, M. Mesoionic and Related Less Heteroatom-Stabilized N-Heterocyclic Carbene Complexes: Synthesis, Catalysis, and Other Applications. *Chem. Rev.* **2018**, *118*, 9493–9586.
- (32) Alonso, F.; Moglie, Y.; Radivoy, G. Copper Nanoparticles in Click Chemistry. *Acc. Chem. Res.* **2015**, *48*, 2516–2528.

- (33) Hein, J. E.; Fokin, V. V. Copper-Catalyzed Azide-Alkyne Cycloaddition (CuAAC) and beyond: New Reactivity of Copper(I) Acetylides. *Chem. Soc. Rev.* **2010**, *39*, 1302–1315.
- (34) Liang, L.; Astruc, D. The Copper(I)-Catalyzed Alkyne-Azide Cycloaddition (CuAAC) “Click” Reaction and Its Applications. An Overview. *Coord. Chem. Rev.* **2011**, *255*, 2933–2945.
- (35) Ladomenou, K.; Nikolaou, V.; Charalambidis, G.; Coutsolelos, A. G. “Click”-Reaction: An Alternative Tool for New Architectures of Porphyrin Based Derivatives. *Coord. Chem. Rev.* **2016**, *306*, 1–42.
- (36) Meldal, M. Polymer “Clicking” by CuAAC Reactions. *Macromol. Rapid Commun.* **2008**, *29*, 1016–1051
- (37) Kappe, C. O.; Van der Eycken, E. Click Chemistry under Non-Classical Reaction Conditions. *Chem. Soc. Rev.* **2010**, *39*, 1280–1290.
- (38) Rinaldi, L.; Martina, K.; Baricco, F.; Rotolo, L.; Cravotto, G. Solvent-Free Copper-Catalyzed Azide-Alkyne Cycloaddition under Mechanochemical Activation. *Molecules.* **2015**, *20*, 2837–2849.
- (39) Gopalan, B.; Balasubramanian, K. K. Applications of Click Chemistry in Drug Discovery and Development. In *Click Reactions in Organic Synthesis*; Wiley-VCH Verlag GmbH & Co. KGaA: Weinheim, Germany, 2016; pp 25–76.
- (40) Wang, C.; Ikhlef, D.; Kahlal, S.; Saillard, J.-Y.; Astruc, D. Metal-Catalyzed Azide-Alkyne “Click” Reactions: Mechanistic Overview and Recent Trends. *Coord. Chem. Rev.* **2016**, *316*, 1–20.
- (41) Hema, K.; Sureshan, K. M. Topochemical Azide-Alkyne Cycloaddition Reaction. *Acc. Chem. Res.* **2019**, *52*, 3149–3163.
- (42) Mandoli, A. Recent Advances in Recoverable Systems for the Copper-Catalyzed Azide-Alkyne Cycloaddition Reaction (CuAAC). *Molecules* **2016**, *21*, 1174.

- (43) Li, P.-Z.; Wang, X.-J.; Zhao, Y. Click Chemistry as a Versatile Reaction for Construction and Modification of Metal-Organic Frameworks. *Coord. Chem. Rev.* **2019**, *380*, 484–518.
- (44) Chandrasekaran, S. *Click Reactions in Organic Synthesis*; Chandrasekaran, S., Ed.; Wiley-VCH Verlag: Weinheim, Germany, 2016.
- (45) Kumar, G. S.; Lin, Q. Light-Triggered Click Chemistry. *Chem. Rev.* **2021**, *121*, 6991–7031.
- (46) Tiwari, V. K.; Mishra, B. B.; Mishra, K. B.; Mishra, N.; Singh, A. S.; Chen, X. Cu-Catalyzed Click Reaction in Carbohydrate Chemistry. *Chem. Rev.* **2016**, *116*, 3086–3240.
- (47) Agrahari, A. K.; Bose, P.; Jaiswal, M. K.; Rajkhowa, S.; Singh, A. S.; Hotha, S.; Mishra, N.; Tiwari, V. K. Cu(I)-Catalyzed Click Chemistry in Glycoscience and Their Diverse Applications. *Chem. Rev.* **2021**, *121*, 7638–7956.
- (48) Dondoni, A.; Marra, A. Calixarene and Calixresorcarene Glycosides: Their Synthesis and Biological Applications. *Chem. Rev.* **2010**, *110*, 4949–4977.
- (49) Chandrasekaran, V.; Lindhorst, T. K. Sweet Switches: Azobenzene Glycoconjugates Synthesized by Click Chemistry. *Chem. Commun.* **2012**, *48*, 7519–7521.
- (50) Kufleitner, M.; Haiber, L. M.; Wittmann, V. Metabolic Glycoengineering - Exploring Glycosylation with Bioorthogonal Chemistry. *Chem. Soc. Rev.* **2023**, *52*, 510–535.
- (51) Kushwaaha, D.; Pandey, P.; Kale, R. R.; Tiwari, V. K. Cu(acac)₂ Mediated Azide-Alkyne Cycloaddition for easy access of Regioselective Triazolyl Glycoconjugates. *Trends Carbohydr. Res.* **2012**, *4*, 45–53.
- (52) Cecioni, S.; Imberty, A.; Vidal, S. Glycomimetics versus Multivalent Glycoconjugates for the Design of High Affinity Lectin Ligands. *Chem. Rev.* **2015**, *115*, 525–561.

- (53) García-Oliva, C.; Merchán, A.; Perona, A.; Hoyos, P.; Rumbero, Á.; Hernáiz, M. J. Development of Sustainable Synthesis of Glucuronic Acid Glycodendrimers Using Ball Milling and Microwave-Assisted CuAAC Reaction. *New J Chem.* **2022**, *46*, 6389–6393.
- (54) Mishra, A.; Tiwari, V. K. One-Pot Synthesis of Glycosyl- β -Azido Ester via Diazotransfer Reaction toward Access of Glycosyl- β -Triazolyl Ester. *J. Org. Chem.* **2015**, *80*, 4869–4881.
- (55) Kuijpers, B. H. M.; Groothuys, S.; Keereweer, A. B. R.; Quaedflieg, P. J. L. M.; Blaauw, R. H.; van Delft, F. L.; Rutjes, F. P. J. T. Expedient Synthesis of Triazole-Linked Glycosyl Amino Acids and Peptides. *Org. Lett.* **2004**, *6*, 3123–3126.
- (56) Dondoni, A.; Marra, A. C-Glycoside Clustering on Calix [4] Arene, Adamantane, and Benzene Scaffolds through 1,2,3-Triazole Linkers. *J. Org. Chem.* **2006**, *71*, 7546–7557.
- (57) Potopnyk, M. A.; Jarosz, S. “Sweet” Sucrose Macrocycles via a “Click Chemistry” Route. In *Click Chemistry in Glycoscience*; John Wiley & Sons, Inc.: Hoboken, NJ, USA, 2013; pp 235–250.
- (58) Isobe, H.; Cho, K.; Solin, N.; Werz, D. B.; Seeberger, P. H.; Nakamura, E. Synthesis of Fullerene Glycoconjugates via a Copper-Catalyzed Huisgen Cycloaddition Reaction. *Org. Lett.* **2007**, *9*, 4611–4614.
- (59) Varki, A. Biological Roles of Oligosaccharides: All of the Theories Are Correct. *Glycobiology* **1993**, *3*, 97–130.
- (60) Bertozzi, C. R.; Kiessling, L. L. Chemical Glycobiology. *Science* **2001**, *291*, 2357–2364.
- (61) Angata, T.; Varki, A. Chemical Diversity in the Sialic Acids and Related Alpha-Keto Acids: An Evolutionary Perspective. *Chem. Rev.* **2002**, *102*, 439–469.
- (62) Schmidt, R. R.; Kinzy, W. Anomeric-Oxygen Activation for Glycoside Synthesis: The Trichloroacetimidate Method. *Adv. Carbohydr. Chem. Biochem.* **1994**, *50*, 21–123.

- (63) Tiwari, V. K.; Mishra, R. C.; Sharma, A.; Tripathi, R. P. Carbohydrate Based Potential Chemotherapeutic Agents: Recent Developments and Their Scope in Future Drug Discovery. *Mini Rev. Med. Chem.* **2012**, *12*, 1497–1519.
- (64) Kempe, K.; Krieg, A.; Becer, C. R.; Schubert, U. S. “Clicking” on/with Polymers: A Rapidly Expanding Field for the Straightforward Preparation of Novel Macromolecular Architectures. *Chem. Soc. Rev.* **2012**, *41*, 176-191.
- (65) Kuijpers, B. H. M.; Groothuys, S.; Hawner, C.; Dam, J. T.; Quaedflieg, P. J. L. M.; Schoemaker, H. E.; van Delft, F. L.; Rutjes, F. P. J. T. Cu-Catalyzed Formation of Triazole-Linked Glycoamino Acids and Application in Chemoenzymatic Peptide Synthesis. *Org. Process Res. Dev.* **2008**, *12*, 503–511.
- (66) Lee, D. J.; Mandal, K.; Harris, P. W. R.; Brimble, M. A.; Kent, S. B. H. A One-Pot Approach to Neoglycopeptides Using Orthogonal Native Chemical Ligation and Click Chemistry. *Org. Lett.* **2009**, *11*, 5270–5273.
- (67) Rabuka, D.; Hubbard, S. C.; Laughlin, S. T.; Argade, S. P.; Bertozzi, C. R. A Chemical Reporter Strategy to Probe Glycoprotein Fucosylation. *J. Am. Chem. Soc.* **2006**, *128*, 12078–12079.
- (68) Tang, S.; Wang, Q.; Guo, Z. Synthesis of a Monophosphoryl Derivative of Escherichia Coli Lipid A and Its Efficient Coupling to a Tumor-Associated Carbohydrate Antigen. *Chemistry* **2010**, *16*, 1319–1325.
- (69) Joosten, J. A. F.; Tholen, N. T. H.; Ait El Maate, F.; Brouwer, A. J.; van Esse, G. W.; Rijkers, D. T. S.; Liskamp, R. M. J.; Pieters, R. J. High-Yielding Microwave-Assisted Synthesis of Triazole-Linked Glycodendrimers by Copper-Catalyzed [3+2] Cycloaddition. *European J. Org. Chem.* **2005**, *2005*, 3182–3185.

- (70) Deraedt, C.; Pinaud, N.; Astruc, D. Recyclable Catalytic Dendrimer Nanoreactor for Part-per-Million Cu(I) Catalysis of “Click” Chemistry in Water. *J. Am. Chem. Soc.* **2014**, *136*, 12092–12098.
- (71) Tasca, E.; La Sorella, G.; Sperti, L.; Strukul, G.; Scarso, A. Micellar Promoted Multi-Component Synthesis of 1,2,3-Triazoles in Water at Room Temperature. *Green Chem.* **2015**, *17*, 1414–1422.
- (72) Brotherton, W. S.; Michaels, H. A.; Simmons, J. T.; Clark, R. J.; Dalal, N. S.; Zhu, L. Apparent Copper(II)-Accelerated Azide-Alkyne Cycloaddition. *Org. Lett.* **2009**, *11*, 4954–4957.
- (73) Pachón, L. D.; van Maarseveen, J. H.; Rothenberg, G. Click Chemistry: Copper Clusters Catalyse the Cycloaddition of Azides with Terminal Alkynes. *Adv. Synth. Catal.* **2005**, *347*, 811–815.
- (74) Kamata, K.; Nakagawa, Y.; Yamaguchi, K.; Mizuno, N. 1,3-Dipolar Cycloaddition of Organic Azides to Alkynes by a DiCopper-Substituted Silicotungstate. *J. Am. Chem. Soc.* **2008**, *130*, 15304–15310.
- (75) Meng, J.-C.; Fokin, V. V.; Finn, M. G. Kinetic Resolution by Copper-Catalyzed Azide–Alkyne Cycloaddition. *Tetrahedron Lett.* **2005**, *46*, 4543–4546.
- (76) Nallagangula, M.; Namitharan, K. Copper-Catalyzed Sulfonyl Azide–Alkyne Cycloaddition Reactions: Simultaneous Generation and Trapping of Copper Triazoles and Ketenimines for the Synthesis of Triazolopyrimidines. *Org. Lett.* **2017**, *19*, 3536–3539.
- (77) Hein, J. E.; Tripp, J. C.; Krasnova, L. B.; Sharpless, K. B.; Fokin, V. V. Copper(I)-Catalyzed Cycloaddition of Organic Azides and 1-Iodoalkynes. *Angew. Chem. Int. Ed.* **2009**, *48*, 8018–8021.
- (78) Rasina, D.; Lombi, A.; Santoro, S.; Ferlin, F.; Vaccaro, L. Searching for Novel Reusable Biomass-Derived Solvents: Furfuryl Alcohol/Water Azeotrope as a Medium for

- Waste-Minimised Copper-Catalysed Azide–Alkyne Cycloaddition. *Green Chem.* **2016**, *18*, 6380–6386.
- (79) Luciani, L.; Goff, E.; Lanari, D.; Santoro, S.; Vaccaro, L. Waste-Minimised Copper-Catalysed Azide–Alkyne Cycloaddition in Polarclean as a Reusable and Safe Reaction Medium. *Green Chem.* **2018**, *20*, 183–187.
- (80) Ahmady, A. Z.; Heidarizadeh, F.; Keshavarz, M. Ionic Liquid Containing Copper(I): A New, Green, Homogeneous, and Reusable Catalyst for Click Cyclization. *Synth. Commun.* **2013**, *43*, 2100–2109.
- (81) Martins, M. A. P.; Paveglio, G. C.; Rodrigues, L. V.; Frizzo, C. P.; Zanatta, N.; Bonacorso, H. G. Promotion of 1,3-Dipolar Cycloaddition between Azides and β -Enaminones by Deep Eutectic Solvents. *New J. Chem.* **2016**, *40*, 5989–5992.
- (82) Nolan, M. D.; Mezzetta, A.; Guazzelli, L.; Scanlan, E. M. Radical-Mediated Thiol–Ene ‘Click’ Reactions in Deep Eutectic Solvents for Bioconjugation. *Green Chem.* **2022**, *24*, 1456–1462.
- (83) Giofrè, S. V.; Tiecco, M.; Ferlazzo, A.; Romeo, R.; Ciancaleoni, G.; Germani, R.; Iannazzo, D. Base-free Copper-catalyzed Azide-alkyne Click Cycloadditions (CuAAc) in Natural Deep Eutectic Solvents as Green and Catalytic Reaction Media. *European J. Org. Chem.* **2021**, *2021*, 4777–4789.
- (84) Sethi, S.; Jana, N. C.; Behera, S.; Behera, R. R.; Bagh, B. Azide-Alkyne Cycloaddition Catalyzed by Copper(I) Coordination Polymers in PPM Levels Using Deep Eutectic Solvents as Reusable Reaction Media: A Waste-Minimized Sustainable Approach. *ACS Omega* **2023**, *8*, 868–878.
- (85) Pérez-Balderas, F.; Ortega-Muñoz, M.; Morales-Sanfrutos, J.; Hernández-Mateo, F.; Calvo-Flores, F. G.; Calvo-Asín, J. A.; Isac-García, J.; Santoyo-González, F. Multivalent

- Neoglycoconjugates by Regiospecific Cycloaddition of Alkynes and Azides Using Organic-Soluble Copper Catalysts. *Org. Lett.* **2003**, *5*, 1951-1954.
- (86) Kumar, D.; Mishra, K. B.; Mishra, B. B.; Mondal, S.; Tiwari, V. K. Click Chemistry Inspired Highly Facile Synthesis of Triazolyl Ethisterone Glycoconjugates. *Steroids*. **2014**, *80*, 71-79.
- (87) Dwivedi, P.; Mishra, K. B.; Mishra, B. B.; Singh, N.; Singh, R. K.; Tiwari, V. K. Click Inspired Synthesis of Antileishmanial Triazolyl O-Benzylquercetin Glycoconjugates. *Glycoconj. J.* **2015**, *32*, 127–140.
- (88) Mishra K. B.; Shashi S.; and Tiwari V. K. Click-inspired facile synthesis of novel bis-triazolyl glycoconjugates. *Trends Carbohydr. Res.* **2016**, *9*, 53-58.
- (89) Mishra, A.; Tiwari, V. K. Synthesis of Novel Bis-Triazolyl Glycoconjugates via Dual Click Reaction for the Selective Recognition of Cu(II) Ions. *ChemistrySelect.* **2017**, *2*, 9466–9471.
- (90) Dwivedi, P.; Mishra, K. B.; Pritika; Mishra, B. B.; Tiwari, V. K. Click Inspired Synthesis of Triazole-Linked Vanillin Glycoconjugates. *Glycoconj. J.* **2017**, *34*, 61-70.
- (91) Kushwaha, D.; Tiwari, V. K. Click Inspired Synthesis of 1,2,3-Triazole-Linked 1,3,4-Oxadiazole Glycoconjugates: Synthesis of Triazole-Linked 1,3,4-Oxadiazole Glycoconjugates. *J. Heterocycl. Chem.* **2017**, *54*, 2454–2462.
- (92) Mishra, K. B.; Mishra, R. C.; Tiwari, V. K. First Noscapine Glycoconjugates Inspired by Click Chemistry. *RSC Adv.* **2015**, *5*, 51779–51789.
- (93) Mishra, K. B.; Tiwari, N.; Bose, P.; Singh, R.; Rawat, A. K.; Singh, S. K.; Mishra, R. C.; Singh, R. K.; Tiwari, V. K. Design, Synthesis and Pharmacological Evaluation of Noscapine Glycoconjugates. *ChemistrySelect.* **2019**, *4*, 2644–2648.
- (94) Agrahari, A. K.; Singh, A. S.; Singh, A. K.; Mishra, N.; Singh, M.; Prakash, P.; Tiwari, V. K. Click Inspired Synthesis of Hexa and Octadecavalent Peripheral Galactosylated

- Glycodendrimers and Their Possible Therapeutic Applications. *New J Chem.* **2019**, *43*, 12475–12482.
- (95) Kumari, K.; Singh, A. S.; Manar, K. K.; Yadav, C. L.; Tiwari, V. K.; Drew, M. G. B.; Singh, N. Catalytic Activity of New Heteroleptic [Cu(PPh₃)₂(β-Oxodithioester)] Complexes: Click Derived Triazolyl Glycoconjugates. *New J Chem* **2019**, *43*, 1166–1176.
- (96) Anamika, A.; Agrahari, A. K.; Manar, K. K.; Yadav, C. L.; Tiwari, V. K.; Drew, M. G. B.; Singh, N. Highly Efficient Structurally Characterised Novel Precatalysts: Di- and Mononuclear Heteroleptic Cu(I) Dixanthate/Xanthate–Phosphine Complexes for Azide-Alkyne Cycloadditions. *New J Chem.* **2019**, *43*, 8939–8949.
- (97) Marra, A.; Vecchi, A.; Chiappe, C.; Melai, B.; Dondoni, A. Validation of the Copper(I)-Catalyzed Azide-Alkyne Coupling in Ionic Liquids. Synthesis of a Triazole-Linked C-Disaccharide as a Case Study. *J. Org. Chem.* **2008**, *73*, 2458-2461.
- (98) Alonso, D. A.; Baeza, A.; Chinchilla, R.; Guillena, G.; Pastor, I. M.; Ramón, D. J. Deep Eutectic Solvents: The Organic Reaction Medium of the Century. *European J. Org. Chem.* **2016**, *2016*, 612–632.
- (99) Abbott, A.P.; Capper G.; Davies D. L.; Rasheed R. K and Tambyrajah. V. *Chem. Commun.* **2003**, 70-71.
- (100) Smith, E. L.; Abbott, A. P.; Ryder, K. S. Deep Eutectic Solvents (DESs) and Their Applications. *Chem. Rev.* **2014**, *114*, 11060–11082.
- (101) Nebra, N.; García-Álvarez, J. Recent Progress of Cu-Catalyzed Azide-Alkyne Cycloaddition Reactions (CuAAC) in Sustainable Solvents: Glycerol, Deep Eutectic Solvents, and Aqueous Media. *Molecules.* **2020**, *25*, 2015.

- (102) Xiong, X.; Yi, C.; Liao, X.; Lai, S. A Practical Multigram-Scale Method for the Green Synthesis of 5-Substituted-1H-Tetrazoles in Deep Eutectic Solvent. *Tetrahedron Lett.* **2019**, *60*, 402–406.
- (103) Kafle, A.; Handy, S. T. A One-Pot, Copper-Catalyzed Azidation/Click Reaction of Aryl and Heteroaryl Bromides in an Environmentally Friendly Deep Eutectic Solvent. *Tetrahedron.* **2017**, *73*, 7024-7029.
- (104) Afonso, J.; Mezzetta, A.; Marrucho, I. M.; Guazzelli, L. History Repeats Itself Again: Will the Mistakes of the Past for ILs Be Repeated for DESs? From Being Considered Ionic Liquids to Becoming Their Alternative: The Unbalanced Turn of Deep Eutectic Solvents. *Green Chem.* **2023**, *25*, 59–105.
- (105) Díez-González, S. Well-Defined Copper(i) Complexes for Click Azide–Alkyne Cycloaddition Reactions: One Click Beyond. *Catal. Sci. Technol.* **2011**, *1*, 166.
- (106) Díez-González, S.; Nolan, S. P. [(NHC)₂Cu]X Complexes as Efficient Catalysts for Azide-Alkyne Click Chemistry at Low Catalyst Loadings. *Angew. Chem. Int. Ed.* **2008**, *47*, 8881–8884.
- (107) Collinson, J.-M.; Wilton-Ely, J. D. E. T.; Díez-González, S. Reusable and Highly Active Supported Copper(I)-NHC Catalysts for Click Chemistry. *Chem. Commun.* **2013**, *49*, 11358–11360.
- (108) Rodionov, V. O.; Presolski, S. I.; Gardinier, S.; Lim, Y.-H.; Finn, M. G. Benzimidazole and Related Ligands for Cu-Catalyzed Azide-Alkyne Cycloaddition. *J. Am. Chem. Soc.* **2007**, *129*, 12696–12704.
- (109) Sareen, N.; Singh, A. S.; Tiwari, V. K.; Kant, R.; Bhattacharya, S. A Dinuclear Copper(I) Thiodiacetate Complex as an Efficient and Reusable “click” Catalyst for the Synthesis of Glycoconjugates. *Dalton Trans.* **2017**, *46*, 12705–12710.

- (110) Joshi, D. K.; Mishra, K. B.; Tiwari, V. K.; Bhattacharya, S. Synthesis, Structure, and Catalytic Activities of New Cu(I) Thiocarboxylate Complexes. *RSC Adv.* **2014**, *4*, 39790–39797.
- (111) Ghosh, R.; Behera, R. R.; Panda, S.; Behera, S. K.; Jana, N. C.; Bagh, B. Catalytic Transfer Hydrogenation of Lignocellulosic Biomass Model Compounds Furfural and Vanillin with Ethanol by an Air-stable Iron(II) Complex. *ChemCatChem.* **2022**.
- (112) Behera, R. R.; Ghosh, R.; Panda, S.; Khamari, S.; Bagh, B. Hydrosilylation of Esters Catalyzed by Bisphosphine Manganese(I) Complex: Selective Transformation of Esters to Alcohols. *Org. Lett.* **2020**, *22*, 3642–3648.
- (113) Hansen, B. B.; Spittle, S.; Chen, B.; Poe, D.; Zhang, Y.; Klein, J. M.; Horton, A.; Adhikari, L.; Zelovich, T.; Doherty, B. W.; Gurkan, B.; Maginn, E. J.; Ragauskas, A.; Dadmun, M.; Zawodzinski, T. A.; Baker, G. A.; Tuckerman, M. E.; Savinell, R. F.; Sangoro, J. R. Deep Eutectic Solvents: A Review of Fundamentals and Applications. *Chem. Rev.* **2021**, *121*, 1232–1285.
- (114) McElroy, C. R.; Constantinou, A.; Jones, L. C.; Summerton, L.; Clark, J. H. Towards a Holistic Approach to Metrics for the 21st Century Pharmaceutical Industry. *Green Chem.* **2015**, *17*, 3111–3121.
- (115) Anastas, P.; and J Warner, J. C.; *Green Chemistry: Theory and Practice*, Oxford University Press, Oxford, **1998**.
- (116) Anastas, P.; Eghbali, N. Green Chemistry: Principles and Practice. *Chem. Soc. Rev.* **2010**, *39*, 301–312.
- (117) Sheldon, R. A. Fundamentals of Green Chemistry: Efficiency in Reaction Design. *Chem. Soc. Rev.* **2012**, *41*, 1437–1451.

- (118) Prat, D.; Wells, A.; Hayler, J.; Sneddon, H.; McElroy, C. R.; Abou-Shehada, S.; Dunn, P. J. CHEM21 Selection Guide of Classical- and Less Classical-Solvents. *Green Chem.* **2016**, *18*, 288–296.
- (119) Allen, D. T.; Gathergood, N.; Licence, P.; Subramaniam, B. Expectations for Manuscripts Contributing to the Field of Solvents in ACS Sustainable Chemistry & Engineering. *ACS Sustain. Chem. Eng.* **2020**, *8*, 14627–14629.
- (120) Kuok (Mimi) Hii, K.; Moores, A.; Pradeep, T.; Sels, B.; Allen, D. T.; Licence, P.; Subramaniam, B. Expectations for Manuscripts on Catalysis in ACS Sustainable Chemistry & Engineering. *ACS Sustain. Chem. Eng.* **2020**, *8*, 4995–4996.
- (121) Jana, N. C.; Sethi, S.; Saha, R.; Bagh, B. Aerobic Oxidation of Vanillyl Alcohol to Vanillin Catalyzed by Air-Stable and Recyclable Copper Complex and TEMPO under Base-Free Conditions. *Green Chem.* **2022**, *24*, 2542–2556.
- (122) Allen, D. T.; Carrier, D. J.; Gong, J.; Hwang, B.-J.; Licence, P.; Moores, A.; Pradeep, T.; Sels, B.; Subramaniam, B.; Tam, M. K. C.; Zhang, L.; Williams, R. M. Advancing the Use of Sustainability Metrics in ACS Sustainable Chemistry & Engineering. *ACS Sustain. Chem. Eng.* **2018**, *6*, 1–1.
- (123) Droesbeke, M. A.; Du Prez, F. E. Sustainable Synthesis of Renewable Terpenoid-Based (Meth)Acrylates Using the CHEM21 Green Metrics Toolkit. *ACS Sustain. Chem. Eng.* **2019**, *7*, 11633–11639.
- (124) Prieschl, M.; García-Lacuna, J.; Munday, R.; Leslie, K.; O’Kearney-McMullan, A.; Hone, C. A.; Kappe, C. O. Optimization and Sustainability Assessment of a Continuous Flow Ru-Catalyzed Ester Hydrogenation for an Important Precursor of a B₂-Adrenergic Receptor Agonist. *Green Chem.* **2020**, *22*, 5762–5770.
- (125) Dalidovich, T.; Mishra, K. A.; Shalima, T.; Kudrjašova, M.; Kananovich, D. G.; Aav, R. Mechanochemical Synthesis of Amides with Uronium-Based Coupling Reagents: A

Method for Hexa-Amidation of Biotin [6]Uril. *ACS Sustain. Chem. Eng.* **2020**, *8*, 15703–15715.

(126) Sheldon, R. A. The E Factor: Fifteen Years On. *Green Chem.* **2007**, *9*, 1273.

(127) Lam, C. H.; Escande, V.; Mellor, K. E.; Zimmerman, J. B.; Anastas, P. T. Teaching Atom Economy and E-Factor Concepts through a Green Laboratory Experiment: Aerobic Oxidative Cleavage of *Meso*-Hydrobenzoin to Benzaldehyde Using a Heterogeneous Catalyst. *J. Chem. Educ.* **2019**, *96*, 761–765.

Chapter 5

SUMMARY

Design, synthesis, and characterization of first row transition metal complexes and development of their catalytic applications in diverse organic transformations are challenging. Highly selective chemical reactions in catalysis can be performed by steric and electronic modification of ligands in transition metal complexes. Transition metal catalysis has emerged as a topic of attention over traditional synthetic techniques in recent decades due to its waste-free, cost-effective, and environmentally friendly approach to chemical transformations. The development of sustainable catalytic systems based on less toxic, accessible, and inexpensive base metals has emerged as a focus in homogeneous metal catalysis. In this direction Simple and readily accessible tridentate NNO and NNS ligands were designed, synthesized and utilized for the preparation of Copper(I) and Copper(II) complexes which were tested as catalysts in two basic organic transformations, oxidation and click reaction.

Chapter 1 describes why we chose first row transition metal over novel metal. It also explains the general introduction of Copper catalysed reactions which includes oxidation of primary and secondary alcohol to corresponding carbonyl compounds and azide-alkyne cycloadditions (click chemistry).

Chapter 2 demonstrates Aerobic oxidation of vanillyl alcohol to vanillin catalyzed by air-stable and recyclable Copper complex and TEMPO under base-free conditions. These reactions are catalyzed by a NNS Copper (II) complex developed in our laboratory. The aerobic oxidation of lignin-derived monomeric phenolics to produce diverse value-added compounds has piqued the scientific community's interest. Particularly, the aerobic oxidation of vanillyl alcohol to vanillin, a significant fragrance molecule with several uses, has drawn a great deal

of attention in study. For this, four Copper(II) complexes were created. The aerobic conversion of vanillyl alcohol to vanillin at ambient temperatures in the presence of a catalytic quantity of the TEMPO radical was examined for all four air stable complexes. With the use of the CHEM21 green metrics tools, the green and sustainable credentials of several catalytic methods under diverse reaction circumstances were evaluated. Based on the results of experimental studies and published papers, a likely catalytic route is suggested.

Chapter 3 describes the azide-alkyne cycloaddition catalyzed by Copper(I) coordination polymers in PPM levels using deep eutectic solvents as reusable reaction media: a waste-minimized sustainable approach. Two air-stable Copper(I)-halide coordination polymers NNS and NNO ligand frameworks were developed and effectively employed as successful catalysts in organic reactions. The azide-alkyne “click” reaction was successfully conducted in pure water at r.t. under aerobic conditions. Other green solvents, including ethanol and glycerol, were also effectively used. Finally, deep eutectic solvents as green and sustainable reaction media were successfully utilized. In deep eutectic solvents, complete conversion with excellent isolated yield was achieved in a short period of time (1 h) with low catalyst loading (1 mol %) at r.t.

Chapter 4 describes the Copper(I)-catalyzed click chemistry in deep eutectic solvent for the syntheses of β -D-glucopyranosyltriazaoles. The successful use of CuAAC reaction for the preparation of biologically active triazole-attached carbohydrate-containing molecular architectures is an emerging area of glycoscience. In this regard, a well-defined Copper(I)-iodide complex with a tridentate NNO ligand was synthesized and effectively utilized as an active catalyst. Instead of using potentially hazardous reaction media such as DCM or toluene, the use of deep eutectic solvent (DES), an emerging class of green solvent, is advantageous for the syntheses of triazole-glycohybrids. For the first time, the successful use of DES as a

reaction medium to click various glycosides and terminal alkynes in the presence of sodium azide. Various 1,4-disubstituted 1,2,3-glucopyranosyltriazoles were synthesized and the pure products were isolated by using a very simple work-up process (filtration). The reaction media was recovered and recycled in five consecutive runs. The presented catalytic protocol generated very minimum waste as reflected by a low *E*-factor (2.21–3.12).

Overall, a simple and readily accessible NNO and NNS ligands were designed and prepared, and its catalytic applications in different transformations have been developed. Copper(II) complexes were used as effective catalysts for the sustainable aerobic oxidation of lignin-derived vanillyl alcohol to vanillin, a widely used aroma molecule. In addition, Copper(I) catalyzed azide-alkyne cycloaddition was effectively performed in presence of ppm level catalyst loading. Various glucopyranosyltriazoles were also synthesized using this click chemistry. These reactions were performed in environmentally benign solvents like water, ethanol, glycerol, and deep eutectic solvents. Low *E*-factors in all these processes showed very limited waste production.

